INTERACTIONS BETWEEN WOOD
AND COATINGS WITH
LOW ORGANIC SOLVENT CONTENT

Mari de Meijer

INTERACTIONS BETWEEN WOOD
AND COATINGS WITH
LOW ORGANIC SOLVENT CONTENT

Erratum

Page 37   *Equation 2.2* should be *equation 3.2*

Page 39   *Figure 3.1*: "shear-stress" should be "shear-rate"

Page 110   In *Table 6.6* the heading of the columns "elastic strain energy" and "interfacial work of adhesion" has been changed. The right combination is given below:

Coating:	Interfacial work of adhesion $W^a{}_{cw}$	Elastic strain Energy (β)
Ac1	0.087	28
Ac2	0.096	12341
Ac3	0.094	7415
WBA	0.098	25
HSA	0.093	74
SBA	0.093	96

Interactions between wood and coatings with low organic solvent content

Mari de Meijer

Stellingen

I.   Het gegeven dat coatings evenals hout kunnen zwellen, biedt nieuwe inzichten in de oorzaak van mogelijk falen van coatings op hout.
Dit proefschrift.

II. De lage viscositeit van watergedragen dispersies of emulsies bij hoge afschuifsnelheden maakt de toepassing van verdikkers noodzakelijk. Dit heeft een negatieve invloed op de indringing in het hout en impliceert derhalve dat bij toepassing van dergelijke grondstoffen, applicatietechnieken met lage afschuifsnelheden de voorkeur verdienen.
Dit proefschrift.

III. De huidige theorieën voor het berekenen van de hechtingsarbeid aan een grensvlak, kunnen de waargenomen verschillen in hechting tussen coatings en hout niet verklaren.
Dit proefschrift.

IV. Na analyse van het beschikbare contactoppervlak in plaats van de oppervlakteruwheid van hout blijkt, in tegenstelling tot wat Allen beweert, mechanische verankering wel een bijdrage te leveren aan de hechting.
Allen, K.W., Journal of Adhesion, 21, 1987, 261-277.

V.   De conclusie van Nussbaum *et al.* dat oplosmiddelhoudende en watergedragen alkydharsen met vergelijkbare viscositeit in gelijke mate het hout kunnen penetreren, gaat voorbij aan de grote verschillen in rheologisch gedrag van oplossingen en emulsies bij toenemend vaste-stof-gehalte.
Nussbaum, R.M., Sutcliffe, E.J. and Hellgren, A.-C., Journal of Coatings Technology, 70, 1998, 49-57.

VI. De wijze waarop Fakhouri *et al.* diffusiecoëfficiënten en concentratieprofielen berekenen uit experimenten waarbij het hout in water wordt ondergedompeld, houdt ten onrechte geen rekening met de effecten van capillaire wateropname in de lumina van het hout.
Fakhouri, B., Mounji, H. and Vergnaud, J.M., Holzforschung, 47, 1993, 271-277.

VII.   Voor het staven van theorieën over transportprocessen in hout met in situ metingen is het noodzakelijk analysetechnieken te ontwikkelen met een oplossend vermogen op celniveau.

VIII.   Het feit dat de engelstalige begrippen *durable* en *sustainable* in het nederlands beide met het woord *duurzaam* worden vertaald, leidt gemakkelijk tot begripsverwarring.

IX.   Door de sterk toegenomen mogelijkheden op het gebied van houtmodificatie is hout niet langer een traditioneel maar een innovatief materiaal.

X.   Het begrip kennisdiffusie suggereert ten onrechte dat kennis sneller kan worden overgedragen naarmate het verschil in kennis groter is.

XI.   Stellingen die niet van een proefschrift zijn afgeleid leiden slechts af.

Stellingen behorend bij het proefschrift "Interactions between wood and coatings with low organic solvent content" van Mari de Meijer.

Wageningen, 5 November 1999.

CONTENTS

VOORWOORD

SUMMARY

The aim of the work described in this thesis is to improve the knowledge on the fundamental interactions between low VOC-coatings and wood, in particular in relation to wood protection in exterior use. To avoid environmental damage and dangerous conditions in the workplace, low-VOC paints have gained increasing importance by the use of waterborne and so called high solids paints. These low-VOC coatings are more and more being used on wood species with: a reduced natural durability against biological decay, higher fluctuations in wood moisture content and reduced dimensional stability. To maintain a good competitive position for wood in the joinery market a longer product lifetime and lower maintenance demands are needed. This will also contribute to a reduction of the total environmental impact during the life cycle of finished wood. Knowledge on the interactions between wood and low-VOC coatings might contribute to the development of technologies that will enlarge the lifetime and protective capacities of wood coatings.

This research has focused on understanding three main aspects of the interaction between coatings and wood. The first one deals with the penetration and wetting of low-VOC coatings, in particular waterborne, coatings. The second aspect deals with the adhesion mechanism of a coating on wood. The third part of the research looks into the sorption of moisture and the related dimensional changes of coated wood. In this respect, special attention has been given to the processes occurring at the surface. The research described in *chapter 2* to *7* was carried with model paint systems, based on commercially available raw materials. Both pigmented and unpigmented coatings based on acrylic dispersions, acrylic emulsions, alkyd emulsions, solventborne or high solid alkyd resins were used. The research in *chapter 8* and *9* was done with commercially available waterborne and solventborne paints. The majority of the work was done on the wood species: spruce *(Picea abies)*, pine sapwood *(Pinus sylvestris)* and meranti *(Shorea spp.)*.

Chapter 1 gives an introduction to this thesis and an overview of the background, the protective capacities and the performance of wood coatings.

Chapter 2 describes the microscopic investigations of the penetration of coatings in wood. The degree of penetration is determined by the possibility of the flow of a coating into the wood capillaries. This depends both on the structure of the wood and the properties of the coating. For softwoods, three potential penetration routes exist: flow in the axial direction from open ends of capillaries, flow into rays ending at the surface and flow from rays through cross-field pits into adjacent axial tracheids. The permeability of the wood only has an influence on the degree of penetration if the penetration depth exceeds the maximum length of a single cell element. In the case of meranti the penetration is limited to the vessels and rays.

In *chapter 3* two quantitative techniques for the measurement of penetration are given. The first one measures the maximum depth of penetration into axial direction on a microscopic scale. The second one determines the penetration rate from the volumetric uptake from the axial surface. The maximum penetration depth can be partially related to the diameter of the axial tracheids but both negative and positive correlations exist. Large differences in the maximum penetration depth between coatings were observed. Generally, acrylic dispersion showed the lowest penetration followed by alkyd emulsions, solventborne and high solid alkyd resins. Addition of pigment has a negative influence on the penetration. The viscosity proved to be an important factor to explain differences between coatings. An increasing wood moisture content (2 to 28 %) caused a deeper penetration.

The dynamics of capillary flow into wood are further studied in *chapter 4* using the Washburn-model. Accordingly, the penetration rate is proportional to the capillary radius, the liquid surface tension times the cosine of the contact angle and inversely proportional to the viscosity and the height of capillary rise. During the capillary uptake, water or solvent is

selectively taken up into the wood. This causes an increasing solid matter content and hence also increasing viscosity and a decreasing capillary pressure. The waterborne coatings showed a very rapid increase of viscosity with increasing mass fraction of binder. At a mass fraction of about 0.45 to 0.55 the viscosity reaches extremely high values, in particular at low shear rates (< 1 s^{-1}). With solventborne binders this increase is less pronounced. The rapid increase of the viscosity limits the capillary penetration in most cases. The increase in mass fraction of the binder during capillary uptake was calculated from the analysis of evaporation rates on glass and wood. These showed that at least half of the water or solvent was taken up into the wood on first instance. The addition of a thickener decreased the total capillary uptake and enhanced the selective uptake of water. The Washburn-equation can predict the penetration process fairly well in qualitative terms. To obtain quantitative predictions, a correction for the increase in viscosity is needed because in reality the viscosity increase happens faster than is predicted by the model calculations. Additional research showed that capillary uptake was reduced with decreasing surface tension as long as the wetting is complete, this is in agreement with the Washburn equation.

The surface free energy of wood was determined from the acid-base and Lifshitz-van der Waals components based on contact angle measurements with water, diiodomethane and formamide as described in *chapter 5*. Different measuring techniques for the contact angle were compared. The obtained angle was shown to be highly dependent on the way the measurement was performed. This is due to the adsorption of liquids onto the wood, the surface roughness and the chemical heterogeneity of the wood. The surface free energy of wood ranged between 40 and 50 mJ m^{-2} with a dominant Lifshitz-van der Waals component. The acid and base parameters were strongly dependent on the measuring conditions.

Chapter 6 describes a newly developed method to measure the adhesion quantitatively. The method is based on measuring the force need to peel the coating from the wood by means of a pressure sensitive tape. This method has the advantage of showing differences in adhesion between early- and latewood zones, corresponding to differences in penetration. A disadvantage is the limited maximum measurable force which restricts its application to measurement under wet conditions (wood moisture content over 25 %) where adhesion is lower. The lower adhesion at higher moisture content can partly be explained by the internal stress due the higher expansion of some coatings in comparison to wood. The interfacial of work of adhesion as it was calculated from the surface free energy of coating and wood was positive under both dry and wet conditions.

The influence of the penetrated coating on the moisture sorption and dimensional change of pine sapwood is described in *chapter 7*. If compared to a coating present as a film on the surface, the penetrated coating had a very limited influence on the equilibrium moisture content, the water vapour diffusion rate and the dimensional changes. Only the capillary uptake of water was reduced depending on the type of coating. The small influence of the penetrated coating upon the wood moisture content, can partly be explained by the swelling of the coating itself and the relative low void filling due to shrinkage of the coating after drying.

How a coating can influence the moisture distribution in spruce is given in *chapter 8*. During long term measurements of the uptake of water, the moisture distribution was determined experimentally and compared with calculated profiles from the apparent diffusioncoefficient. The most realistic prediction was found if the apparent diffusioncoefficient of unfinished wood was used, taking the impact of a coating into account by a reduced moisture content at the surface. Moisture diffuison is the dominant transport mechanism; it is only close to the surface that capillary water uptake is noticeable, in particular with unfinished wood.

Chapter 9 studies the adsorption and desorption of water and the dimensional change in spruce and meranti as a function of coating type, film thickness, temperature and relative

humidity of the environment. The apparent moisture diffusion coefficients are dependent on all these factors and also on the initial and final wood moisture content. The dimensional change can be described as a function of time by a two-parameter regression model. The rate constant in this model is directly related to the apparent diffusion coefficient, as long as the influence of capillary water uptake is small.

The general conclusions of this research are given in *chapter 10*. A certain amount of coating penetration into the wood improves adhesion and prevents rapid capillary water uptake. It was shown that coatings, like wood, can adsorb water and swell. Therefore it is recommended to consider the moisture-related aspects of wood coatings in terms of the differences between both materials. To achieve a good wet adhesion, the dimensional change of the coating and the wood should be in the same range. The surface free energy and the work of adhesion between a coating and wood can not explain the observed differences in adhesion between different coatings. The penetration is mainly controlled by the viscosity of the coating as a function of the solid matter content and the shear rate. In this respect the influence of the carrier medium (water or organic solvent) is more important than the chemical composition of the binder. A positive capillary pressure is, however, a necessity to enable the penetration of a coating into wood. If a coating is present as a film on the surface, the moisture sorption and dimensional change of wood is strongly reduced. The strongest fluctuations in wood moisture content take place directly under the surface. Both waterborne and solventborne coatings largely prevent the rapid capillary uptake of moisture. The moisture uptake into coated wood is a lot slower than in unfinished wood. Therefore in practice a permanent reduction of wood moisture content for both water- and solventborne can be expected.

SAMENVATTING

Het doel van het in dit proefschrift beschreven onderzoek, is het vergroten van de kennis over de fundamentele wisselwerkingen tussen oplosmiddelarme verven en hout, in het bijzonder in relatie tot de bescherming van hout in exterieure toepassingen. Om schadelijke effecten aan het milieu en de arbeidsomstandigheden te voorkomen hebben oplosmiddelarme verven, zowel watergedragen als de zogeheten high solid producten, sterk aan betekenis gewonnen. Deze oplosmiddelarme verven worden in toenemende mate toegepast op houtsoorten met een beperkte natuurlijke duurzaamheid tegen biologische aantasting en een sterkere wisseling in houtvochtgehalte en dimensies. Om een goede concurrentiepositie van hout als grondstof voor geveltimmerwerk en aanverwante toepassingen te waarborgen is het van belang om de levensduur te verlengen en de onderhoudsbehoefte te verlagen. Dit draagt tevens bij aan een geringere integrale milieubelasting gedurende de gehele levensduur van afgewerkt hout. Kennis over de wisselwerkingen tussen hout en oplosmiddelarme verven vormt de basis voor de ontwikkeling van technologieën die de levensduur en beschermende werking van coatings op hout kunnen verbeteren.

Dit onderzoek richt zich op drie aspecten die van groot belang zijn bij het begrijpen van de wisselwerkingen tussen verf en hout. Het eerste aspect betreft de bevochtiging en indringing van oplosmiddelarme, in het bijzonder watergedragen, coatings. Ten tweede is het hechtingmechanisme van verf op het hout onderzocht. Ten derde is onderzoek verricht naar de opname en de afgifte van water en de bijbehorende dimensieverandering in hout dat van een coating was voorzien. Hierbij is bijzondere aandacht besteed aan de processen die zich aan het oppervlak afspelen. Het in *hoofdstuk 2* tot *7* beschreven onderzoek is uitgevoerd met model verfsystemen gebaseerd op commercieel verkrijgbare grondstoffen. In het onderzoek zijn zowel gepigmenteerde als niet gepigmenteerde coatings toegepast die waren gebaseerd op acrylaatdispersies, acrylaatemulsies, alkydemulsies en oplosmiddelhoudende of high solid alkydharsen. Het onderzoek uit *hoofdstuk 8* en *9* is uitgevoerd met commercieel verkrijgbare watergedragen en oplosmiddelhoudende verven. Het merendeel van de experimenten is uitgevoerd met de houtsoorten vuren *(Picea abies)*, grenen spinthout *(Pinus sylvestris)* en meranti *(Shorea spp.)*.

Hoofdstuk 1 vormt de inleiding tot dit proefschrift en geeft een overzicht van de achterliggende ontwikkelingen, de beschermende werking en de prestaties van coatings op hout.

Hoofdstuk 2 beschrijft het microscopisch onderzoek naar de indringing van coatings in hout. De mate van penetratie wordt bepaald door de mogelijkheid tot indringing van de verf in de capillairen van het hout. Dit hangt zowel af van de structuur van het hout als van de eigenschappen van de coating. Voor naaldhout blijken drie mogelijke penetratieroutes te bestaan: indringing in axiale richting via open einden van tracheïden aan het oppervlak, indringing in stralen eindigend aan het oppervlak en via stralen door de kruisingsvelden naar de aanliggende langstracheïden. De permeabiliteit van een houtsoort heeft slechts invloed op de mate van indringing indien de indringdiepte groter is dan de maximale lengte van het desbetreffende celelement. Voor meranti is de indringing beperkt tot de vaten en de stralen.

In *hoofdstuk 3* worden twee technieken beschreven om de mate van indringing te kwantificeren. De eerste methode is gebaseerd op de microscopische bepaling van de maximale indringdiepte in axiale richting. De tweede methode meet de indringsnelheid aan de hand van de volumetrische opname van een vloeistof vanaf het axiale vlak. De maximale indringing hangt onder andere af van de diameter van de langstracheïden. Afhankelijk van het type bindmiddel is de indringing zowel positief als negatief gecorreleerd aan de diameter van het capillair. Tussen de diverse typen coating en bindmiddel zijn zeer grote verschillen in maximale indringing waargenomen. Over het algemeen vertonen acrylaatdispersies de

geringste mate van indringing, gevolgd door coatings gebaseerd op alkydemulsies, oplosmiddelhoudende en high solid alkydharsen. Het toevoegen van pigment heeft een negatieve invloed op de penetratie. De viscositeit van de coating blijkt een belangrijke factor te zijn bij het verklaren van verschillen tussen bindmiddelen. Een toenemend houtvochtgehalte (in de range van 2 tot 28 %) leidt tot een diepere indringing.

De dynamiek van het indringingsmechanisme wordt in *hoofdstuk 4* nader bestudeerd aan de hand van het capillaire stromingsmodel van Washburn. Volgens dit model is de penetratiesnelheid evenredig met de capillair diameter, de oppervlaktespanning van de vloeistof maal de cosinus van de contacthoek van de vloeistof in het capillair en omgekeerd evenredig met de viscositeit en de indringdiepte. Tijdens de capillaire opname wordt water of oplosmiddel selectief in de celwand opgenomen. Als gevolg hiervan stijgt de vaste stof concentratie en daarmee ook de viscositeit en daalt de capillaire druk. De watergedragen bindmiddelen vertonen een zeer sterke stijging van de viscositeit met toenemende massafractie bindmiddel. Rond een massafractie van 0.45 tot 0.55 bereikt de viscositeit zeer hoge waarden, in het bijzonder bij lage afschuifsnelheden (<1 s^{-1}). Bij oplosmiddelhoudende bindmiddelen is dit effect aanzienlijk geringer. De sterke stijging van de viscositeit tijdens de capillaire indringing is doorgaans de beperkende factor bij de penetratie. De toenemende massafractie bindmiddel tijdens de capillaire indringing is berekend aan de hand van analyses van verdampingsnelheden op hout en glas. Hieruit blijkt dat ten minste de helft van het water of oplosmiddel uit de verf in eerste instantie in het hout wordt opgenomen. Het toevoegen van een verdikker verlaagt de capillaire opname en versterkt de selectieve opname van water in het hout. De Washburn vergelijking kan de capillaire opname in kwalitatieve zin doorgaans goed voorspellen. Voor een kwantitatieve voorspelling blijkt een correctie van de viscositeit noodzakelijk omdat deze in werkelijkheid sneller stijgt dan door de modelberekeningen wordt voorspeld. Uit aanvullend onderzoek met oppervlakteactieve stoffen volgt dat, conform de Washburn vergelijking, de capillaire opname minder wordt bij een daling van de oppervlaktespanning mits de bevochtiging van het hout volledig is.

De oppervlakte energie van hout is bepaald aan de hand van berekening van de zuur-base en Lifshitz- van der Waals componenten op basis van randhoek metingen met water, diiodomethaan en formamide zoals beschreven in *hoofdstuk 5*. Verschillende meetmethoden voor de bepaling van de randhoek zijn vergeleken. Het blijkt dat de randhoek sterk afhankelijk is van de wijze waarop de meting wordt uitgevoerd. Dit is het gevolg van de adsorptie van vloeistoffen aan het hout, de oppervlakteruwheid en de chemische heterogeniteit van het hout. De totale oppervlakte energie van hout ligt tussen de 40 en 50 mJ m^{-2} met een sterke Lifshitz- van der Waals component. De zure en basische parameters zijn sterk afhankelijk van de meetcondities.

Voor een kwantitatieve bepaling van de hechtsterkte wordt in *hoofdstuk 6* een nieuw ontwikkelde methode beschreven. Deze methode is gebaseerd op de meting van de kracht benodigd voor het afpellen van een coating van het hout met behulp van een zelfklevende tape. Deze methode heeft als voordeel dat verschillen in hechtingskracht tussen vroeg- en laathoutzones, die corresponderen met verschillen in penetratie, bepaald kunnen worden. Een nadeel is van deze methode is de beperking in de maximaal meetbare kracht, met als gevolg dat alleen de zwakkere hechting onder natte condities (houtvochtgehalte boven de 25%) meetbaar is. Coatings met een diepere penetratie en een groter contactoppervlak met het hout beschikken over een aanzienlijk betere hechting. De lagere hechting bij verhoogd vochtgehalte laat zich deels verklaren uit de opgebouwde interne spanning door de sterkere zwelling van sommige coatings ten opzichte van het hout. De oppervlakte energie van zowel hout als coating is gemeten. Aan de hand van de oppervlakte energie van de coating en het hout is de onderlinge hechtingsarbeid berekend. Deze blijkt onder zowel natte als droge omstandigheden positief te zijn.

De invloed van de ingedrongen coating op de wateropname en -afgifte en de dimensieverandering van grenen spinthout is beschreven in *hoofdstuk 7*. Het blijkt dat de in het hout ingedrongen coating maar een zeer beperkt effect heeft op het evenwichtsvochtgehalte, de waterdampdiffusiesnelheid en de dimensieverandering in vergelijking met een coating die als een film op het houtoppervlak ligt. Afhankelijk van het type coating, wordt de capillaire opname van vloeibaar water wel verminderd. De geringe invloed van de ingedrongen coating laat zich deels verklaren door wateropname en de zwelling van de coating zelf en de relatief geringe mate van porievulling door krimp van de coating tijdens droging.

De invloed van een coating op de verdeling van het houtvochtgehalte in vurenhout wordt beschreven in *hoofdstuk 8*. Tijdens langdurige metingen van de wateropname is de houtvochtverdeling experimenteel bepaald en vergeleken met berekende profielen aan de hand van de klaarblijkelijke diffusiecoëfficiënt. Het blijkt dat de houtvochtverdeling het best kan worden voorspeld aan de hand van de klaarblijkelijk diffusiecoëfficiënt van onafgewerkt hout. De invloed van de coating laat zich het meest realistisch uitdrukken in de vorm van een lagere concentratie van het water aan het oppervlak. Diffusie van water is het overheersende transport mechanisme, alleen direct onder het oppervlak heeft de capillaire wateropname een merkbare invloed, in het bijzonder bij niet afgewerkt hout.

In *hoofdstuk 9* wordt de wateropname en -afgifte en de dimensieverandering in vuren en meranti bestudeerd als functie van het type coating, de laagdikte, de temperatuur en de relatieve luchtvochtigheid van de omgeving. De klaarblijkelijke diffusiecoëfficiënt is afhankelijk van al deze factoren en het aanvangs- en eindvochtgehalte. De dimensieverandering als functie van de tijd, kan beschreven worden met een twee-parameter asymptotisch regressiemodel. De snelheidsafhankelijke constante in dit model is direct gekoppeld aan de klaarblijkelijke diffusiecoëfficiënt zolang de capillaire wateropname een geringe invloed heeft.

De algemene conclusies van dit onderzoek staan weergegeven in *hoofdstuk 10*. Een zekere mate van penetratie van de coating in het hout is zinvol om de hechting te verbeteren en een snelle capillaire opname van water tegen te gaan. Veel coatings blijken, evenals hout, water te adsorberen en te zwellen. Het is daarom aan te bevelen om aan vocht gerelateerde aspecten van coatings op hout te beschouwen als verschillen tussen beide materialen. Voor een goede natte hechting is het van groot belang dat de dimensieverandering van de coating niet te sterk van die van het hout verschilt. De oppervlakte-energie en de hechtingsarbeid van hout en coating levert geen verklaring voor de waargenomen verschillen in hechting tussen diverse coatings. De mate van penetratie wordt vooral beïnvloed door de viscositeit van de coating *als functie van het vaste stof gehalte en de afschuifsnelheid*. In dit opzicht is de aard van het medium (water of organisch oplosmiddel) van groter belang dan de chemische samenstelling van het bindmiddel. De aanwezigheid van een capillaire druk is echter wel een noodzakelijke voorwaarde om penetratie in het hout mogelijk te maken. Wanneer een coating als een film op het oppervlak van het hout aanwezig is wordt de wateropname en de dimensieverandering van het hout zeer sterk gereduceerd. De sterkste schommelingen in houtvochtgehalte treden direct onder het oppervlak op, maar zowel watergedragen als oplosmiddelhoudende coatings voorkomen grotendeels de snelle capillaire opname van water. De opname van water in afgewerkt hout verloopt zeer veel trager dan in onafgewerkt hout. Daarom is in de praktijk voor zowel watergedragen als oplosmiddelhoudende coatings een permanente verlaging van het houtvochtgehalte te verwachten.

1. GENERAL INTRODUCTION

1.1 Background to this thesis

Coatings, here used as a generic name for all types of paints, varnishes, lacquers etc., are an essential part of the majority of products based on solid wood or wood based materials. Coatings can provide wooden materials with the desired aesthetical properties like colour and gloss, but are mostly also of vital importance in the protection of wood against environmental influences like moisture, radiation, biological deterioration or damage from mechanical or chemical origin. This applies to both interior uses (like e.g. furniture) and exterior applications like wooden joinery, claddings or fences. The interactions between coating, substrate and external factors are quite different for interior and exterior uses. Therefore, the work in this thesis is in principal limited to the latter.

More than 95 % of exterior wood coatings are applied as liquid coatings with either an organic solvent or water as the carrier for the other coatings ingredients. The use and subsequent emission of volatile organic compounds (VOC) to the environment has been increasingly considered as a problem during the last 20 years from both an air-pollution and a health and safety point of view. VOC's (mainly those containing chlorofluorocarbons) are considered to contribute to ozone depletion in the stratosphere (the so-called hole in the ozone layer), ozone formation in the troposphere causing smog and global warming by CO_2 production [1].

Although the majority of VOC's are from natural sources, it is the change in the total concentration balance of these materials and the synergistic effects with antropogenic NO_x emissions that has let to various legislative actions to reduce the emission of VOC to improve air quality. Examples of those are United Nations VOC protocol, USA Clean Air Act, the German TA-Luft and the Dutch KWS 2000 [1]. The latter is a voluntary agreement between the Dutch government and VOC-emitting industries to reduce the VOC-emission levels of 1981 by 50 % in the year 2000. Nowadays a European directive is under preparation to reduce VOC-emissions, which defines VOC's as all materials with a vapour pressure of 0.01 kPa or more at a temperature of 293.15 K [3]. VOC emission from coatings is covered under all of these rules. Apart from solvent recovery or end-of-pipe destruction, the general strategy of the paint industry is to replace solventborne paints by low-VOC alternatives. Long term exposure to organic solvents might also induce neuropsychiatric symptoms like memory impairment, concentrating difficulties, fatigue, headache or personality changes [4]. This is often referred to as organic-psycho syndrome (OPS) or chronic toxic encephalopathy [5]. This potential danger has been recognised by the responsible authorities in many countries (including the Netherlands) which have lead to restrictions in the use of solvent rich coatings.

In the last 5 years, the use of wood species for exterior joinery in the Netherlands has shifted from mainly tropical hardwoods like meranti *(Shorea spp.)* to a position were softwoods (mainly spruce: *Picea abies*) have regained a substantial market share. This is mainly due to an increasing desire of end-users to use woods from sustainable managed forests as recommended by Dutch guidelines for sustainable building practice [6,80]. Within the scope of minimising the environmental impact of buildings, it is of great importance to prevent maintenance as much as possible by extending the service life of coated wood. Various life-cycle analysis studies have shown that the environmental impact of a piece of coated wooden joinery is proportional to its maintenance demands [7,9].

1.2   Performance and protective properties of exterior wood coatings

The performance of a coating on wood during outdoor exposure is controlled by various stressing factors like: photoirradiation, thermal radiation, mechanical impact, the presence of moisture and microorganisms causing different weathering effects like: photochemical degradation, loss of surface integrity (cracking, flaking or erosion) and discoloration. The type and intensity of the degradation is also strongly influenced by factors such as: time and conditions during weathering, wood properties, the quality of design of the wooden structure, the physical and chemical properties of the coating itself, the method of application, the film thickness, the colour of the coating and the way the maintenance has been carried out. How these factors mutually interact is schematically shown in *fig. 1.1* [10]. The most important findings from the literature of the past decades are summarised in the next sections.
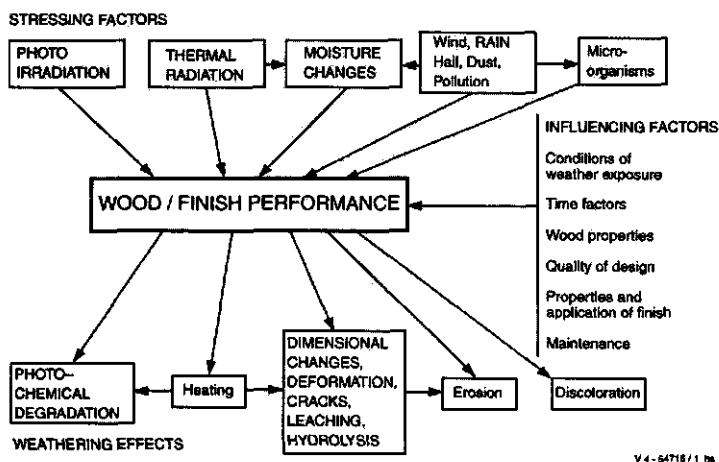
Figure 1.1 Schematic illustration of the weathering of finished wood, from [10]

1.2.1   Degradation of wood surfaces by photoirradiation

Numerous studies on the weathering behaviour of wooden surfaces [11,12,13,14,15,16] have shown that the colour change and subsequent weathering process of transparently coated wood is a stepwise degradation process. It starts with the absorption of energy from light in the UV and visible region followed by radical formation at phenolic or excited α-carbonyl units in the lignin and radical induced cleavage or chain scission in cellulose. This is followed by the formation of subsequent radicals, which causes further oxidation, chromophore formation and depolymerisation [17,18,19,20]. Finally the degradation products become water-soluble and are leached out resulting in erosion of the wood surface. The photochemical degradation also causes cracking and splitting of the wood, both on a microscopic level inside the cell walls and as visible cracks on the surface [12,21,22,23,24, 25]. Although light can only penetrate the coating and the outer layer of the wood to a depth of 200 μm, chain-reactions involved in secondary reaction steps can lead to degradation up to 2500 μm [26]. Although light is the initiator of the weathering process other factors like: the amount of liquid water at the wood surface [27.28], the wood moisture content [29], the oxygen concentration [13], the temperature [30,31,32] and type or chemical composition of the wood have an influence as well [33,34].

The photochemical degradation process described above, in principal applies to its full extent only to unfinished wood surfaces. Notwithstanding some experimental developments like acetylation [35], grafting of UV-absorbers [36, 37,38] or the fixation of complexing metals [39,40] the main way of protecting wood to weathering is by the application of a coating. The most effective protection against photoirradiation is given by completely opaque pigmented coatings, which neither transmit UV nor visible light. Under these coatings, no photochemical degradation takes place [41,42]. However, in those applications where the wood surface has to remain visible, light will reach the wood surface and induce photochemical degradation [43]. It has been shown that direct photolysis of chemical bonds can only be caused by wavelengths up to 340 nm but secondary degradation mechanisms can be influenced by wavelengths up to 400 nm [24]. This means that not only UV but also light from the visible region influences photochemical degradation. Current technologies to make transparent wood less sensitive to photochemical degradation involves the use of UV-absorbers, radical scavengers [44, 45] and more recently also transparent titanium dioxide [46]. Apart from direct protection to photoirradiation, a coating also decreases the weathering of a wood surface by reducing its moisture content and preventing leaching. Dark coloured coatings might increase the weathering of wood by increasing surface temperature, which cause in increase in the rate of moisture desorption and photochemical degradation.

1.2.2 Influence of coatings on wood moisture content

The strong influence of coating systems on the changes in wood moisture content during service have been recognised for a long time and hence have been subject to numerous studies which has been reviewed by Sell [11] and Graystone [47]. The interest in this subject has gained importance with the introduction of waterborne paints, which have higher moisture permeability in comparison to solventborne alternatives [48]. To understand the influence of coatings on the wood moisture content, several approaches have been used. This included permeability measurements of free coating films or coated wood samples [49, 50, 51, 52, 53, 54, 55, 56, 57], moisture content monitoring in practice on panels [58, 59, 60, 61] or full scale wooden constructions [62, 63, 64, 65] and computer simulations [66, 67]. In these studies, the permeability of a coating was found to depend on several factors like its build, degree and type of pigmentation and the type of binder. Within the same category of coatings, waterborne coatings usually show a higher permeability towards moisture. The permeability of the coating can both decrease and increase during weathering [68]. Micro-cracks might increase the permeability whereas leaching of hydrophilic components or ongoing film formation might decrease the permeability of the coating. Dark coloured coatings reduce the wood moisture considerably due to the heating of the surface [69, 70, 71]. Measurements at different depths of coated wooden samples reveal that at the surface rapid fluctuation takes place, which are superimposed on more long-term fluctuations in wood moisture content. The influence of the wood itself on the permeability is dependent on the type of coating. For zero or low build products the influence of the wood species might be considerable, whereas for high build coatings with sufficient film thickness over the entire wood surface the permeability of the wood is of only minor importance. Nevertheless, the wood species will remain to have an influence on dimensional change for a given change in wood moisture content.

Coatings reduce the rate of uptake of water into the wood by its barrier function against both liquid water (precipitation or dew) and water vapour diffusion. It also reduces the drying rates of wood by the same water vapour diffusion barrier. This has immediately raised the question of what is the optimum moisture permeability of a coating. Low permeability coatings might give a good protection against external moisture but at the same time there is a risk of fast moisture entry through a crack, open end grain or open corner joint in window frames [63,72] which can cause favourable conditions for decay. On the other hand a very

permeable coating might cause rapid moisture content changes and dimensional movements, which can give rise to jamming of windows and doors, cracking in the coating or the wood and excessive stresses on glued wood constructions. This means that the optimum moisture permeability is largely dependent on the type of wood and the structure it is applied on, as is also reflected in current European standards for exterior wood coatings which differentiate between stable, semi-stable or non-stable end uses [73]. For wooden joinery and doors, the coating has to be sufficiently impermeable to avoid excessive movement of the wood but, as a consequence the water desorption will be rather slow. This means that excessive moisture uptake through end grains has to be prevented by proper protection (end-grain sealing) and gluing of window corner joints [74, 75, 76, 77]. For uses that require less restriction of dimensional movement, a coating with higher moisture permeability is generally acceptable.

1.2.3   Microbiological degradation of coated wood surfaces

Coated wooden surfaces can be attacked by various types of microorganisms often referred to as mould, mildew or blue-stain. Additionally, waterborne coatings can be degraded by bacteria during their production and storage in their liquid state. This aspect is however beyond the scope of this thesis since this phenomenon is not related to microbiological failure in service. Microbiological degradation can be classified into the following categories [78, 79].

Mould fungi colonise wood and coating surfaces only superficially and cause only aesthetical problems. The most common species of mould fungi are *Aspergillus, Penicillium, Alternaria* and *Cladosporium*. The conditions controlling the growth of mould fungi are described in detail by Viitanen [80]. Recent studies with waterborne wood coatings have shown that mould growth is influenced by the wood material, type and concentration of film fungicides, leaching of preservative, the paint formulation and the exposure time or conditions. [81, 82, 83].

Blue stain fungi that grow on coated wood surfaces are mainly of the species *Aureobasidium pullulans* and to a lesser extent *Sclerophoma pityophila* [84]. Blue stain in service is considered not to originate from spores already present in the wood but from penetration through defects in the paint film or insufficiently protected end-grains [41, 78, 85]. Although blue stain fungi can not decay wood, they can damage the wood surface and increase its permeability due to perforation of the coating and the cell walls by the hyphae and fruiting bodies of the fungus [41,79,86, 87]. Protection against blue-stain fungi can be achieved by the use of fungicides in the coating, physical protection against moisture and prevention of photochemical degradation since the latter seems to support fungal growth. Recent findings suggest that the paint formulation itself might also affect the growth of blue stain [88].

The influence of a coating on **wood decay fungi** is mainly through its influence in wood moisture content. If the total moisture protection by the coating is sufficient decay will be prevented by maintaining sufficiently low wood moisture content. If rapid moisture entry is possible, the coating might favour decay because of the reduced drying rate. However, in several European countries other than the Netherlands it is common practice to include fungicides in joinery primers to create a superficial protection against decay fungi. The formulation of the coating (apart from the fungicidal effects) and the extent of weathering might also have an influence on the colonisation by brown rot fungi [89].

1.2. 4   Outdoor weathering performance

The results of several comparative outdoor weathering trials have been reported in the literature. The trials have included various climates, coatings types, wood species and substrate design [90, 91, 92, 93, 94, 95, 96, 97, 98, 99]. In general, these studies give fairly consistent results with respect to the main differences in performance of coatings on wood in

exterior applications. Opaque, high build paints have the longest durability and if failure occurs it is mainly related to cracking, chalking or surfaces mould growth. Latex paints based on waterborne acrylics generally perform better in preventing cracking in long term weathering, although some studies showed that acrylic coatings are not always resistant to cracking. Solid colour stains, or medium build opaque paints perform slightly worse with respect to crack resistance. Semitransparent stains, both medium and high build products, fail more rapidly because of cracking, flaking or peeling, erosion, blue-stain or moulds and photochemical degradation of the wood surface. Penetrating stains, which form no film at all, have the lowest durability and fail mainly by erosion of the surface. Increased amounts of pigments in these coatings directly decreased the erosion rate [100]. Repainting seems, however, to be easier because no peeling or flaking of the coating can occur. Pre-treatment of the wood with a water-repellent preservatives containing a small amount of binder improved the durability of the coating [101, 102]. The wood species had a clear influence on the durability of the coating. High permeable wood species like pine sapwood show more rapid coating failure if compared to softwoods with low water permeability or tropical hardwoods [91,101]. Rough sawn wood surfaces gave improved performance over smooth planed surface, which is mainly the result of higher spreading rates on rough sawn wood [92]. Many comparisons on the influence of the climate within Europe showed only a minor impact of climatic differences [98, 99, 103].

At present there are no well-established theories about the relationships between failure mode of exterior wood coatings and the formulation of the coating or the properties of the polymeric binder. In general a coating should adhere well to the wood under both dry and wet conditions and should be able to follow the dimensional movements of the wood [97, 104]. Furthermore, in film forming coatings the coating has to maintain its integrity to avoid cracking and chalking. One theory assumes that crack propagation due to differential expansion inside the wood, causes high stresses in the coating. The stress will then concentrate around inclusions in the paint like pigments and defects, followed by crack propagation in the coating itself. Hence, the rate of crack initiation is proportional to the water permeability of the coating and the crack propagation of the coating is proportional to its fracture energy [105]. Other studies have shown that the glass-transition temperature increases significantly during weathering [106, 107, 108] and suggest that on wood it should ideally remain between 0 to 10 °C for a period of 10 to 20 years to maintain flexible coatings [109]. Systematic studies on elongation of paint films showed clear reduction of flexibility with both decreasing temperatures and ongoing exposure which might be related to chemical changes in the binder observed by infrared analysis [110]. The impact of the difference in dimensional change between early- and latewood zones [111] on flaking of a coating has been addressed by Bodner et al [112]. It was stated that in order to avoid flaking, the ratio of the square root of the percentage density difference (in wood) times the coating thickness and the absolute density times the elasticity should be at least a factor 20. Unfortunately, a theoretical validation of this statement was not given. In an outdoor weathering test, the same authors found good correlation between the type of weathering, the pigmentation and the moisture content for both alkyd and acrylic coatings but a similar correlation with elasticity was only observed for alkyd coatings. In another study, correlations between cracking and moisture content fluctuations were observed for both alkyd and acrylic coatings but a similar correlation with flaking was only found for alkyd based coatings [113].

1.3   Developments with respect to VOC reduction in paints

1.3.1   Market developments
The market for (exterior) wood coatings is usually divided in two sectors:
- **Industrial wood coatings** applied by spraying, dipping, flow- or curtain coating in the production facilities of the wood working industry. This sector covers both primers and topcoats, the latter are used for completely factory finished joinery. The main technology to comply with VOC-limits is the use of waterborne coatings.
- **Architectural or decorative coatings** used for brush applications by professional painters or for do-it-yourself purposes. This market can be further divided in interior and exterior finishes for woodwork. Primers are mainly used for repainting of wood in existing buildings whereas the topcoats are used both for finishing of factory primed joinery and maintenance. Low VOC-coatings for interior use will increasingly be based on waterborne technologies to comply with health and safety requirements. Low VOC-coatings for exterior use might both be based on high solid and waterborne formulations.

The amounts of VOC's used in coatings in the Netherlands from 1990 to 1997 are given in *fig. 1.2. Table 1.1* shows the total sales volumes, amount of VOC's used, the market shares and average VOC-content of both low and high VOC paints in coatings for different market areas.

1.3.2   Coating technologies
Coatings for the protection of wood in exterior use generally contain the following categories of components:
- Binders: polymeric material to bind together the other ingredients, to form a film and to protect against external influences like moisture.
- Pigments and extenders (except in clear coatings): mainly to provide colour, hiding powder, protection of the wood against photodegradation and to modify the mechanical and adhesion properties of the film.
- Additives: a general name of various components that can provide: pigment stabilisation, control of rheology, substrate wetting, film formation and protection of the dry film (like fungicides or UV-absorbers).
- Carrier solvents: water or organic solvents with the purpose to transfer the other ingredients to the substrate and to allow the formation of a film.

Within the scope of this thesis, the composition and production of these materials will not be further discussed except for the binder, which plays a very important role in categorising low-VOC paints.

Binders are mostly classified with respect to the chemical composition of the polymer. The main binders in exterior wood coatings are nowadays based on acrylics or fatty acid containing alkyd-polyesters. The acrylic binders are generally produced by emulsion co-polymerisation of various monomers to form colloidal stabilised solid particles in water (latex). Core-shell polymerisation techniques are introduced in wood coatings to combine different properties more easily [114, 115]. The film formation of acrylic dispersions consists of evaporation of water, followed by coalescence and finally by interdiffusion of the polymers particles (autohesion) [116]. Apart from acrylic dispersions, emulsions or water-soluble acrylics can also be prepared [117]. Alkyd resins are traditionally used as solutes in organic solvent but waterborne alkyds also exist. They can be used either as water-soluble polymers or as emulsions. Waterborne alkyds are used in combination with acrylic dispersions (hybrids) [118] or as the sole type of binder [119]. Film formation of waterborne alkyd resins starts with the evaporation of water followed by phase-inversion into an oil-in-water emulsion and finally by the oxidative cross-linking to form a polymeric network [120].

Table 1.1 Data on VOC's produced by Dutch coating industry used within the Netherlands.

Sector	Type **	Sales (tons)	VOC (tons)	Market Share	Average*** VOC-content
Joinery	Low VOC	1,199	71	20 %	6 %
	High VOC	4,663	1,640	78 %	35 %
	Diluents	136	136	2 %	100 %
	Total	5,997	1,846	100 %	31 %
Decorative	Low VOC	5,095	493	26 %	10 %
Professional *	High VOC	14,183	4,822	72 %	34 %
	Diluents	313	297	2 %	95 %
	Total	19,591	5,612	100 %	29 %
Do-it-yourself *	Low VOC	6,727	710	33 %	11 %
	High VOC	13,910	4,739	67 %	34 %
	Diluents	41	40	0 %	98 %
	Total	20,678	5,489	100 %	27 %

*: All types of coatings except wall paints.
**: Low VOC-paint is defined as containing less then 250 g VOC / kg paint, excluding water.
***: In the paint.
Source: VVVF statistics 1997.
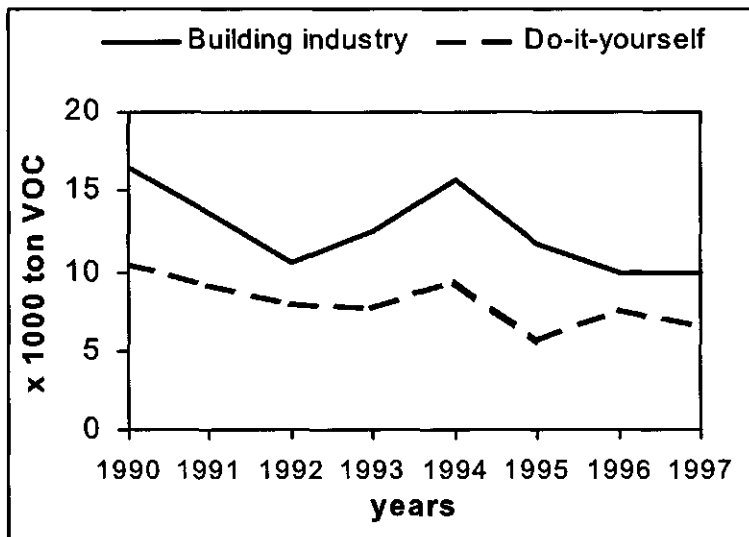
Fig. 1.2 Quantity of VOC in paints in the Netherlands for the segments building industry and do-it-yourself, including wall paints. Source: VVVF statistics 1997.

High solid coatings for wood are also based on fatty acid containing alkyd-polyesters. An acceptable application viscosity, at a reduced concentration of organic solvent, can be achieved by using polymers with a narrow molecular weight distribution, increased oil-length, or with highly branched polymer structures. Additionally, reactive diluents reduce the viscosity during the wet stage but do not contribute to solvent emissions because they are incorporated in the polymer network during the crosslinking [121, 122, 123, 124].

1.4   Outline of this thesis

To reduce the VOC-content, coatings are subject to major changes with respect to their chemical composition, formulation, physical and protective properties. In addition to that, the use of wood species in joinery has shifted towards the use of species with a lower natural durability and higher dimensional changes. Reduction of maintenance costs is required to maintain the competitive position of wood towards competing materials like plastic and aluminium. These three developments require a more fundamental knowledge about the interactions between wood and coatings for exterior applications. The aim of this thesis is to contribute to this by studying the interfacial aspects of substrate wetting and penetration, its influence on adhesion and the moisture related aspects of coatings on wood. How these aspects were studied in the different parts of this thesis is outlined below.

Chapter 2 describes the influence of wood anatomy and surface structure on the possible penetration pathways of different coatings. In *chapter 3*, the maximum depth of coating penetration into pine and spruce is quantitatively related to both wood and coating properties. The dynamics of the capillary penetration of polymeric binders as a function of viscosity and surface tension taking into account the changes in solid matter content due to solvent evaporation and selective uptake in the wood is studied in *chapter 4*. This is followed by an evaluation of the different techniques to determine the surface free energy of wood surfaces in *chapter 5*. The surface energy of wood was studied separately because of its potential influence on both wetting and adhesion of particularly waterborne coatings. The wet adhesion properties of primers on wood are analysed quantitatively in *chapter 6* by a newly developed method that can correlate substrate penetration and adhesion strength. Existing adhesion theories are evaluated within the framework of the adhesion of coatings to wood. The impact of coating penetration on moisture uptake and dimensional changes is described in *chapter 7*. *Chapters 8* and *9* deal with the transport of moisture into wood a through a coating, present as a film on the surface. In *chapter 8* the moisture profiles are measured and analysed by diffusion models. In *chapter 9* the kinetics of sorption and dimensional change are described in relation to coating type, film thickness, wood species, temperature and moisture gradient. *Chapter 10* discusses the impact of the previous findings on the potential influence on the exterior durability and the consequences for the formulation of exterior wood coatings.

With the exception of the work described in *chapters 8* and *9*, all studies were made with simplified and known coating formulations based on commercially available binders and other raw materials. The formulation of the coatings is given in Annex II. In the work of *chapters 8* and *9* commercially available coatings have been used.

References

[1] **Wigglesworth, D.J.**; Volatile organics – legislation and the drive to compliance, In: The chemistry and physics of coatings, Ed. A. R. Marrion, RCS, Cambridge, 1994, pp. 8-20.

[2] **Willemse, F.R.J.**; Groene verf= natuurverf=duurzame milieuconservering, Materialen, Jan./Feb.,1999,10-13.

[3] **Community preparatory acts**; Proposal for a council directive on limitation of emissions of volatile organic compounds due to the use of organic solvents in certain industrial activities, Document 596PC0538, 1997.

[4] **Bleecker, M.L.; Bolla, K.I.; Agnew, J.; Schwartz, B.S.; Ford, D.F.**; Dose-related subclinical neurobehavioral effects of chronic exposure to low levels of organic solvent, American Journal of , Industrial Medicine, 19, 1991, 715-728.

[5] **Gregersen, P.; Klausen, H.; Elsnab, C.U.**; Chronic toxic encephalopathy in solvent-exposed painters in Denmark 1976-1980: clinical cases and social consequences after a 5-year follow-up, American Journal of Industrial Medicine, 11, 1987, 399-417.

[6] **de Groot, H.**; Hout heeft de toekomst (in Dutch), Het Houtblad, June, 1997, 34-39.

[7] **Geurink, P.J.A.**; A total picture of the environmental aspects of the new generation decorative paints, 21 th Fatipec Congress, Amsterdam, 1992

[8] **Anonymous**; Handleiding Duurzaam Bouwen, Stuurgroep Experimenten Volkhuisvesting, (In Dutch) 1995.

[9] **Häkkinen, T.; Ahola, P.; Vanhato, L.**; Environmental impact of painted exterior wooden cladding, PRA conference Advances in exterior wood coatings and CEN standardisation, Brussels, 1998, paper 4.

[10] **Sell, J.; Feist, W.C.**; U.S. and European finishes for weather-exposed wood – a comparison, Forest Products Journal, 36 (4), 1986, 37-41.

[11] **Sell, J.**; Basic requirements for the surface treatment of exterior wood surfaces, Holz als Roh- und Werkstoff 33, 1975, 336-340.

[12] **Sell, J.; Leukens, U.**; Weathering phenomena of unprotected wood species, Holz als Roh- und Werkstoff 29, 1971, 23-31.

[13] **Feist, W.C.; Hon, D.S.-S.**; Chemistry of weathering and protection. In: Chemistry of solid wood, R.M. Rowell Ed.. Advances in Chemistry Ser. No. 207, ACS, Washington, pp. 401-451.

[14] **Hon, D.S.-S; Feist, W.C.**; Weathering characteristics of hardwood surfaces, Wood Science and Technology, 20, 1986, 169-183.

[15] **Evans, P.D.; Michell, A.J.; Schmalzl, K.J.**; Studies of the degradation and protection of wood surfaces, Wood Science and Technology, 26, 1992, 151-163.

[16] **Hon, D.S.-S; Shiraishi, N.**; Wood and cellulosic chemistry, Photochemistry of wood, New York, 1991, pp. 525.

[17] **Leary, G.J.**; The yellowing of wood by light: part II, Tappi, 51 (6), 1968, 257-260.

[18] **Gierer, J.; Lin, S.Y.**; Photodegradation of lignin, Svensk Papperstidning, 75 (7), 1972, 233-239.

[19] **Gellerstedt, G.; Pettersson, E-L.**; Light-induced oxidation of lignin, part 2. The oxidative degradation of aromatic rings. Svensk Papperstidning, 81 (1), 1977, 15-21.

[20] **Fengel, D.; Wegener, G.**; Degradation by light and ionising rays, In: Wood Chemistry, Ultrastructure, Reactions, Walter de Gruyter, Berlin New York, 1989, 345-372.

[21] **Minutti, V.P.**; Contraction in softwood surfaces during ultraviolet irradiation and weathering, Journal of paint technology, 45 (577), 1973, 27-34.

[22]   **Minutti, V.P.;** Microscale changes in cell structure at softwood surfaces during weathering, Forest Products Journal, 14 (12), 571-576.
[23]   **Evans, P.D.;** Structural changes in pinus radiata during weathering, Journal Institute of wood science, 11(5), 1989, 172-181.
[24]   **Derbyshire, H.; Miller, E.R.;** The photodegradation of wood during solar irradation, Holz als Roh- und Werkstoff, 39, 1989, 341-350.

[25]   **Kuo, M.; Hu, N.;** Ultrastructural changes of photodegradation of wood surfaces exposed to UV, Holzforschung, 45, 1991, 347-353.
[26]   **Feist, W.C.;** Outdoor wood weathering and protection, In: Archaeological wood: properties, chemistry, and preservation, Rowell, R.M., James, B.R. Ed., Advances in Chemistry Ser. No. 225, ACS. Washington, pp. 263-298.
[27]   **Evans, P.D.; Banks, W.B.;** Degradation of wood surfaces by water. Changes in mechanical properties of thin wood strips, Holz als Roh- und Werkstoff, 1988,46, 427-435.
[28]   **Anderson, E.L.; Pawlak, Z.; Owen, N.L.; Feist, W.C.;** Infrared studies of wood weathering. Part I: Softwoods, Applied Spectroscopy, 45 (4), 1991, 641-647.
[29]   **Hon, D.N.-S.; Feist, W.C.;** Free radical formation in wood: the role of water, Wood Science, 14 (1), 1981, 41-48.
[30]   **Derbyshire, H.; Miller, E.R.; Turkulin, H.;** Investigations into the photodegradation of wood using microtensile testing, Part 3: The influence of temperature on photodegradation rates, Holz als Roh- und Werkstoff, 1997,55, 287-291.
[31]   **Futó, L.P.;** Einfluss der Temperatuur auf den photochemischen Holzabbau, 1. Mitteilung: experimentelle Darstellung, Holz als Roh- und Werkstoff, 1976, 34, 31-36.
[32]   **Futó, L.P.;** Einfluss der Temperatuur auf den photochemischen Holzabbau, 2. Mitteilung: Rasterelektronenmikroskopische Darstellung, Holz als Roh- und Werkstoff, 1976, 34, 49-54.
[33]   **Sandermann, W.; Schlumbom, F.;** On the effect of filtered ultraviolet light on wood, Part I. Holz als Roh- und Werkstoff, 1962, 20, 245-252.
[34]   **Derbyshire, H.; Miller, E.R.; Turkulin, H.;** Investigations into the photodegradation of wood using microtensile testing, Part 2: An investigation of the changes in tensile strength of different wood species during natural weathering, Holz als Roh- und Werkstoff, 1996,54, 1-6.
[35]   **Becker, E.P.J.; Stevens, M.; Meijer, M. de; Militz, H.;** The effect of chemical modification of wood by acetylation on paintability, Journal of Coating Technology, 70 (878), 1998, 59-67.
[36]   **Williams, R.S.;** Effect of grafted UV stabilizers on wood surface erosion and clear coating performance, Journal of Applied Polymer Science, 28, 1983, 2093-2103.
[37]   **Grelier, S.; Castellan, A.; Desrousseaux, S.; Nourmamode, A.; Podgorski, L.;** Attempt to protect wood colour against UV/visible light by using antioxidants bearing isocyanate groups and grafted to the material with microwave, Holzforschung, 51, 1997, 511-518.
[38]   **Kiguchi, M.; Evans, P.D.;** Photostabilisation of wood surfaces using a grafted benzophenone UV absorber, Polymer Degradation and Stability, 61, 1998, 33-45.
[39]   **Evans, P.D.; Schmalzl, K.J.;** A Quantitative weathering study of wood surfaces. modified by chromiumVI and Iron III compounds, Holzforschung, 43, 1989, 289-292.
[40]   **Lange, P.J. de; de Kreek A.K.; van Linden, A.; Coenjaarts, N.J.;** Weathering of wood and protection by chromium studied by XPS, Surface and Interface Analysis, 19, 1992, 397-402.

[41] **Böttcher, P.;** Improving long term behaviour of exterior wood structures made from domestic wood species by renewal paint coating, Holz als Roh- und Werkstoff, 42, 1984, 85-91.

[42] **Turkulin, H.; Arnold, M.; Sell, J.; Derbyshire, H.;** Structural and fractographic SEM analysis of exterior coated wood, PRA conference Advances in exterior wood coatings and CEN standardisation, Brussels, 1998, paper 18.

[43] **Macleod, I.T.; Scully, A.D.; Ghiggino, K.P.; Ritchie, P.J.A.; Paravagna, O.M.; Leary, B.;** Photodegradation at the wood-clearcoat interface, Wood Science and Technology, 29, 1993, 183-189.

[44] **Hon, D.N.-S.; Chang, S-T.; Feist, W.C.;** Protection of Wood Surfaces against Photooxidation, Journal of Applied Polymer Science, 30, 1985, 1429-1448

[45] **Valet, A.;** Light stabilizers for paints, Hanover, 1997.

[46] **Hocken, J.; Pipplies, K.; Schulte, K.;** The advantageous use of ultra fine titanium dioxide in wood coatings, 5th Nürnberg Congress Creative Advances in Coatings Technology, 1999, paper 40.

[47] **Graystone, J.;** Moisture transport through wood coatings: the unanswered questions, , PRA conference Advances in exterior wood coatings and CEN standardisation, Brussels, 1998, paper 6.

[48] **Ahola, P.; Derbyshire, H.; Hora, G.; de Meijer, M;** Water protection of wooden window joinery painted with low organic solvent content paints with known composition. Part 1. Results of inter-laboratory test, Holz als Roh- und Werkstoff, 1999, 57, 45-50.

[49] **Wassipaul, F.; Janotta, O.;** Die Wasserdampfdurchlässigkeit von Anstrichmitteln, Teil 1, Holzforschung und Holzverwertung, 24 (4), 1972, 74-80.

[50] **Schneider, A.;** Investigations on the asymmetry of water vapour permeability of unilaterally coated wood, Holz als Roh- und Werkstoff, 33, 1975, 427-433.

[51] **Ahola, P.;** Moisture transport in wood coated with joinery paints. Holz als Roh- und Werkstoff 49,1991, 428-432.

[52] **Hora, G., Böttcher, P.;** Beurteilung des Feuchteschutzes von Holzaußenanstrichen, Vergleich von dynamischer Randwinkelmessung und Bestimmung des Wasseraufnahmekoeffizienten, Farbe und Lack, 11,1993, 924-928.

[53] **Hora, G., Böttcher, P.;** Einfluss eines Anstrichsystems auf den Feuchtehaushalt von Fachwerkholz, Bautenschutz und Bausanierung, 4, 1994, 37-41.

[54] **Hora, G., Böttcher, P.;** Feuchtephysikalische Eigenschaften von fachwerkspezifischen Dispersionen, Farbe und Lack, 3, 1995, 296-300.

[55] **Linden, J.A. van; Oort, P.;** Water permeability: comparison of methods and paint systems. XXII Fatipec Conference Budapest,1994, 135-148.

[56] **Derbyshire, H., Miller, E.R.;** Moisture conditions in coated exterior wood, Part 2: The relationship between coating permeability and timber moisture content, Journal of the Institute of Wood Science, 14 (4), 1997,162-168.

[57] **Ekstedt, J.;** Moisture dynamic assessment of coatings for exterior wood, Licentiate thesis Kungliga Tekniska Högskolan, Stockholm, 1995.

[58] **Teichgräber, R.;** Measurement and Evaluation of the Interactions between Paint Systems, Wood Species and Climate. Holz als Roh- und Werkstoff ,31,1973,127-132.

[59] **Derbyshire, H.; Miller, E.R.;** Moisture conditions in coated exterior wood, Part 3: Moisture content during natural weathering, Journal of the Institute of Wood Science, 14 (4), 1997,169-174.

[60] **Sell, J.;** Investigations for optimising the surface treatment of timber construction elements Part 1: Outdoor weathering test with window frame specimens, Holz als Roh- und Werkstoff, 40,1982, 225-232.

[61] **Meierhofer, U.;** Investigations for optimising the surface treatment of timber construction elements Part 2: Weathering tests on glulam segments, Holz als Roh- und Werkstoff, 41,1983, 197-202.

[62] **Taras, M.A.;** Moisture content variation of finished and partially finished wood homes in the southeast, Forest Products Journal, 17 (8), 1967, 60-63.

[63] **Eikenaar, J.J.;** Zur Regulierung des Feuchtigkeitshaushalts in Fenstern, Holz-Zentralblatt, 104 (18/30), 1978.

[64] **Sell, J.;** Physical phenomena in timber construction elements to weathering window joinery, Holz als Roh- und Werkstoff, 43, 1985, 259-267.

[65] **Hjort, S.;** Moisture balance in painted wood panelling, PhD thesis, Chalmers University, Göteborg, 1997.

[66] **Gard, W.F.; Castenmiller, C.J.J; Hoeflaak, M.;** Accelerated weathering of wood coatings in conjunction with moisture modelling, Eurowood Technical Workshop Coatings / Finishes for Wood Products, Oporto, 1998.

[67] **Bancken, E.L.J.; Frencken, M.;** Modelling and measurement of moisture transport in coating-protected wood, PRA 7th Asia Pacific Conference, paper 19, 1997.

[68] **Derbyshire, H.; Miller, E.R.;** Moisture conditions in coated exterior wood, Part 1:An investigation on the moisture transmission characteristics of exterior wood coatings and the effect on weathering on coating permeability, Journal of the Institute of Wood Science, 14 (1), 1996, 40-47.

[69] **Seifert, E.; Schmid, J.;** Thermal behaviour of wood and wood based materials in relation to coloring, Holz als Roh- und Werkstoff 28, 1970, 178-182.

[70] **Schultz, H.; Böttcher, P.; Neigenfind, W.;** Effect of some paints and colours on the moisture conditions of naturally weathered wood specimens, Holz als Roh- und Werkstoff, 31,1973,132-137.

[71] **Janotta, O.;** Der Einfluss des Farbtones und der Wasserdampfdurchlässigkeit von Anstrichmitteln auf die Feuchtigkeitsverteilung im Holz. Auswirkungen auf die Kondenswasserbildung an Holzverbundfenstern, Holzforschung und Holzverwertung, 31, 1979, 45-59.

[72] **Janotta, O.;** Die Wasserdampfdurchlässigkeit von Anstrichmitteln, Teil 3, Holzforschung und Holzverwertung, 26 (1), 1974, 10-18.

[73] **EN 927-1;** Paints and varnishes: Coating materials and coating systems for exterior wood, Part 1: classification and selection, 1998.

[74] **Miller, E. R.; Boxall, J.;** The effectiveness of end-grain sealers in improving paint performance on softwood joinery, Holz als Roh- und Werkstoff, 42, 1984, 27-34.

[75] **Miller, E. R.; Boxall, J.;** The effectiveness of end-grain sealers in improving paint performance on softwood joinery. L-joint results after 4-year natural weathering, Holz als Roh- und Werkstoff, 45, 1987, 69-74.

[76] **Boxall, J.; Carey, J.K.; Miller, E.R.;** The effectiveness of end-grain sealers in improving paint performance on softwood joinery, Part 3: Influence of coating type and wood species on moisture content and fungal colonisation, Holz als Roh- und Werkstoff, 50, 1992, 227-232.

[77] **Blom, C.W.;** Een kwart eeuw (primitieve) relatieve vochtafsluiting -- theorie en praktijk (In Dutch), Eisma's Schildersblad, 84, (31/32), 1982, 1-8.

[78] **Skinner, C.E.;** Microbiological problems in the paint industry, Paint, Oil and Colour Journal, 30, 1970, 177-180.

[79]   **Bravery, A.F.; Miller, E.R.;** The role of pre-treatment in the finishing of exterior softwood, BWPA Annual Convention, 1980.

[80]   **Viitanen, H.;** Factors affecting the development of mould and brown rot decay in wooden material and wooden structures. Effect of humidity, temperature and exposure time. PhD thesis Swedish University of Agricultural Sciences, Uppsala, 1996.

[81]   **Viitanen, H.; Ahola, P.;** Resistance of painted pine sapwood to mould fungi, Part 1: The effect of waterborne paints and fungicides on mould growth, The Int. Res. Group on Wood Preserv., Stockholm, Doc. No. IRG/WP 97-10233, 1997.

[82]   **Viitanen, H.;** Ahola, P. Resistance of painted pine sapwood to mould fungi, Part 2: The effect of wood substrate and acrylate paints systems on mould growth, The Int. Res. Group on Wood Preserv., Stockholm, Doc. No. IRG/WP 97-10234, 1997.

[83]   **Lindner, W.;** Filmkonservierungsmittel – Verhalten in Aussenbewitterung und im Laborexperiment, XXIV. Fatipec Congress, Interlaken, 1998.

[84]   **Valcke, A.;** Vergelijkend onderzoek naar de efficiëntie van beschermings-, afwerkings-, en onderhoudssystemen voor houten buitenschrijnwerk onder natuurlijke weersomstandigheden (In Dutch), PhD Thesis University Ghent, 1985.

[85]   **Butin, J.;** Investigations on the formation of blue-stain on lacquered wood surfaces, Holz als Roh- und Werkstoff, 19, 1961, 337-340.

[86]   **Sell, J.;** Investigations on the infestation of untreated and surface treated wood by blue stain fungi, Holz als Roh- und Werkstoff, 26, 1968, 215-222.

[87]   **Kühne, H.; Leukens, U.; Sell, J.; Wälchli. O.;** Investigations on weathered wood surfaces, Part 1: Scanning electron-microscope observations on mould-fungi causing grey stain, Holz als Roh- und Werkstoff, 28, 1970, 223-229.

[88]   **van Acker, J.; Stevens, M.; Brauwers, C.; Rijckaert, V., Mol, E.;** Laboratory blue stain testing of low VOC paints, PRA conference Advances in exterior wood coatings and CEN standardisation, Brussels, 1998, paper 15.

[89]   **Bjurman, J.;** The protective effect of 23 paint systems on wood against attack by decay fungi, Holz als Roh- und Werkstoff, 50, 1992, 201-206.

[90]   **Feist, W.C.;** Weathering performance of finished southern pine plywood siding, Forest Products Journal, 38 (3), 1988, 22-28.

[91]   **Roux, M.L.; Wozniak, E.; Miller, E.R.; Boxall, J.; Böttcher, P.; Kropf, F., Sell, J.;** Natural weathering of various surface coatings on five species at four European sites, Holz als Roh- und Werkstoff, 46, 1988, 165-170.

[92]   **Feist, W.C.;** Weathering performance of finished aspen siding, Forest Products Journal, 44 (6), 1994, 15-23.

[93]   **Boxall, J.;** Exterior wood finishes: performance testing by accelerated natural weathering, JOCCA, 72 (2) 1984, 40-44.

[94]   **Carll, C.G.; Feist, W.C.;** Long-term weathering of finished aspen waferboard, Forest Products Journal, 39 (10), 1989, 25-30.

[95]   **Alblas, B.P.; van London, A.M.;** Comperative testing of the performance of several types of coating for the protection of wooden window frames, Surface Coatings International, 79 (12), 1996, 555-573.

[96]   **Jansen, M.L.;** Performance testing of exterior wood primers, JOCCA 74 (5), 1986, 117-128.

[97]   **Boxall, J.;** Factory-applied finishes for timber joinery; an evaluation, JOCCA, 80 (8), 1992, 40-44.

[98]   **Abrahams, I.L.; Graystone, J.A.;** Natural weathering of exterior wood coatings: a comparison of performance at five European sites, XXIII Fatipec Conference, Brussels, 1996.

[99]   **Hora, G.; Kruse, D.**; European round-robin natural exposure test of exterior wood coatings, 5th Nürnberg Congress Creative Advances in Coatings Technology, 1999, paper 42.

[100] **Feist, W., C.**; Role pigment concentration on the weathering of semitransparent stains, Forest Products Journal, 38 (2), 1988, 41-44.

[101] **Feist, W., C.**; Weathering performance of painted wood pretreated with water-repellent preservatives, Forest Products Journal, 40 (7/8), 1990, 21-26.

[102] **de Meijer, M.; Creemers, J.; Cobben, W.; Ahola, P.**; Influence of a dipping preservative treatment on the performance of wood finished with waterborne coatings, The Int. Res. Group on Wood Preserv., Stockholm, Doc. No. IRG/WP 98-40121, 1998.

[103] **Creemers, J.; de Meijer, M.; Sell, J.**; Influence of climatic factors on the weathering of coated wood, PRA conference Advances in exterior wood coatings and CEN standardisation, Brussels, 1998, paper 14.

[104] **Ashton, H.E.**; Flexibility and its retention in clear coatings exposed to weathering, Journal of Coating Technology, 51 (653), 1979, 41-52.

[105] **Floyd, F.L.**; Predictive model for cracking of latex paints applied on exterior wood surfaces, Journal of Coating Technology, 55 (696), 1983, 73-80.

[106] **Podgorski L.; Merlin A.; Déglise X.**; Analysis of the natural and artificial weathering of a wood coating by measurement of the glass transition temperature, Holzforschung, 50, 1996, 282-287.

[107] **Schmid, E.V.**; Risse und Abblätterungen bei alternden Anstrichen, Farbe und Lack, 94 (8), 1988, 616-620.

[108] **Schmid, E.V.**; Glasumwandlungtemperatur und Wasseraufnahme von bewitterten Holzlasuren, Farbe und Lack, 94 (8), 1988, 616-620.

[109] **Schmid, E.V.**; Exterior wood coatings and the glass-transition temperature, Polymers Paint Colour, 178 (4216), 1988, 460-468.

[110] **Ahola, P.**; Chemical and physical changes in paints or painted wood due to ageing, VTT Publication 155, Espoo, 1993.

[111] **Browne, F.L.**; Swelling of springwood and summerwood in softwood, Forest Products Journal 7, 416-424.

[112] **Bodner, J.; Janotta, O.; Indome, G.H.**; Physikalische Abbauvorgänge bei Aussenanstrichen auf Wasser und Lösungsmittelbasis, Holzforschung und Holzverwertung, 4, 1989, 59-62.

[113] **Meijer, M., de; Creemers. J.; Cobben, W.**; Interrelationships between the performance of low-VOC wood coatings and the dimensional changes of the wooden substrate, accepted for Surface Coatings International, 1999.

[114] **Désor, U.; Krieger, S.**; Water borne acrylic dispersions: an alternative to solventborne resins for the coating of wooden surfaces, XXIII Fatipec Conference, Brussels, 1996.

[115] **Bosschaart-Thurich, K.; Pathak U.; Berkhout, L.**; Advances in waterborne coatings for joinery, In: Advances in exterior wood coatings and CEN-standardisation, PRA conference Advances in exterior wood coatings and CEN standardisation, Brussels, 1998, paper 26.

[116] **Eckersley, S.T.; Rudin, A.**; Drying behaviour of acrylic latexes, Progress in Organic Coatings 23, 1994, 384-402.

[117] **Bufkin, B.G.; Wildman, G.C.**; Environmentally acceptable coatings for the wood industry, Forest Products Journal, 30 (10), 37-44.

[118] **Nakayama, Y.**; Polymer blend systems for water-borne systems, Progress in Organic Coatings, 33, 1998, 108-116.

[119] **Hofland A.**; Water-borne coatings for decorative and protective coatings: a comparative survey, Surface Coatings International 7, 1994, 270-281.

[120] **Beetsma, J.**; Alkyd paints: from the ease of organic solvents to the difficulties of water, XXII. Fatipec Conference Budapest Vol 2, 1984, 157-167.

[121] **Beetsma, J.; Santing, A.; Hofland, A.; Grootoonk, L.**; Combining High Quality with High Solids, XXIV. Fatipec Conference, Interlaken, 1998, A-175.

[122] **Weijnen, J.G.J.; Kemp, J.A.G.; van der Kolk, C.E.M.**; Architectural high solids alkyd lacquers; more then just solvent reduction, XXIV. Fatipec Conference, Interlaken, 1998, A-287.

[123] **Lindeboom, J.**; Air-drying high solids alkyd paints for decorative paints, Progress in Organic Coatings, 34, 1998, 147-151.

[124] **Boekee, D.; Klaasen, R.; van Dongen, J.; Bakker, P.**; Development and performance of a new generation stains, In: Advances in exterior wood coatings and CEN-standardisation, PRA conference Advances in exterior wood coatings and CEN standardisation, Brussels, 1998, paper 24.

2. Comparative Study on Penetration Characteristics of Modern Wood Coatings[*]

Summary

The penetration characteristics of five modern wood coatings (three waterborne, one high solid and one solvent borne) into pine sapwood, spruce and dark red meranti have been systematically compared. The degree of coating penetration is mainly determined by the ability of the coating to flow into wood capillaries. Binder type, pigmentation, solid matter content and drying speed appeared to influence this ability. In softwoods the following different coating penetration routes are observed: the flow into open ends of longitudinal early- and latewood tracheids, the flow into ray cells and the transport from rays through the cross-field into longitudinal tracheids adjacent to rays. The possibility for the coating to follow the latter route is strongly influenced by the existing type of cross-field pitting and to a lesser degree by the pigmentation of the paint. Clear differences between pine and spruce have been found with respect to the flow into ray parenchym and ray tracheids. The flow into open ends of longitudinal tracheids is strongly influenced by the grain angle of tracheids. Penetration into dark red meranti is mainly limited to vessels and rays. Tylose membranes can prevent the complete filling of vessels. The impact on penetration of the removal of extractives and of sanding of the surface has also been studied but appears to be of only minor importance.

[*]   **Mari de Meijer , Katharina Thurich, Holger Militz**
    Published in Wood Science and Technology 32, 1998, 347-365

2.1   Introduction

In the joinery industry of Western Europe a combination of two new developments has become increasingly important. The first is the protection of the wood by different types of waterborne and high solid coatings instead of the traditionally used solvent borne alkyd paints and stains. This development is mainly encouraged by the need to avoid the emission of air polluting volatile organic compounds used as solvents. The second development taking place is the replacement of tropical hardwoods by softwoods, which are more sensitive to water, less durable and less dimensionally stable. For these reasons a more fundamental understanding of the interaction between wood and modern coatings is needed to improve their durability and performance. The penetration of a primer into the wood can be important for several reasons. Firstly the penetration of coatings can improve water repellency and dimensional stability and reduce wood cracking, as was shown in several studies on the impregnation of wood with waterborne resins comparable to those used in coatings [1-3]. Secondly it seems to be very likely that the adhesion of the coating to the wood will benefit from a certain degree of penetration as well. Modern theories on adhesion [4,5] have distinguished several mechanisms like mechanical entanglement or interlocking, adsorption interactions by polar and dispersive forces and intermolecular diffusion. Mechanical entanglement is directly related to penetration, but the other mechanisms will benefit from penetration as well due to the increase in contact area between coatings and the cell walls. Thirdly coatings containing fungicides might have improved penetration of the fungicide because it penetrates together with the binder vehicles [6].

In the past the microscopic penetration patterns of solvent borne alkyd and linseed oil paints into wood have been intensively studied by several authors [7-14]. More recently studies have been made on the penetration of waterborne alkyd emulsions [6,14,15]. Rødsrud and Sutcliff [6] have compared the penetration of coatings based on waterborne acrylic dispersions, waterborne alkyd emulsions and solvent borne alkyds. In these studies the most commonly used techniques to study the microscopic distribution of binders and pigmented paints within the wood cells are: scanning electron microscopy of normal [13] and replica samples [3,12], fluorescence microscopy [9-11], autoradiography with ^{14}C labelled coatings [15] and scanning electron microscopy with X-ray analysis (SEM-EDAX) of brominated alkyds [15].

The observed gross penetration patterns in softwoods are: filling of the outer layers of tracheids and radial penetration into the rays. In hardwoods the penetration mainly consists of filling the capillaries of the vessels and ray cells. Penetration of the cell walls by the coating is subject to many discussions in literature but have not been proven unambiguously. Penetration of the coating into the cell wall might be limited to the solvent [11] or to small amounts of linseed oil [13,16].

The objective of the present study is to systematically compare the penetration of five different types of coatings (three waterborne, one high solid and one reference solvent borne alkyd) with and without the addition of pigments. The mechanisms of penetration are studied qualitatively by fluorescence and electron microscopy on spruce, pine sapwood and dark red dark red meranti. The influence of drying speed, surface preparation and extractive removal has been included in this study as well.

2.2   Materials and methods

2.2.1   Coating Materials

Five types of binders were used in this study: two waterborne acrylic dispersions with different particle sizes (WAD100 and WAD300), one alkydemulsion (WBA), one alkyd-

based high solid (HSA) and one traditional solventborne alkyd resin (SBA). The different types of binders were used in opaque model paints and as unpigmented solutions of binders. The opaque model paints were pigmented white with titanium-dioxide at a pigment volume concentration of 17 % and formulated in the simplest possible manner. The binder solutions contained only the binder, water or organic solvent and about 1 weight % coalescent which improves film formation of the acrylic dispersions or about 2 to 4 weight % cobalt-siccative which catalyses the oxidative drying of the alkyd resin. The most relevant properties of the coatings are given in *table 2.1*.

Additionally binder solutions without coalescent or drier were tested to study the influence of the drying-speed. Part of the binder solution was also tested at a solid matter content of 10-20 % below the standard amount of solids. All binders contained about one weight-percent anthracene dye to allow detection by fluorescence microscopy. The dye is chemically bonded to the binder molecules and is equally distributed over the molecular weight distribution of the binder polymer, which was proven by gel-permeation-chromatographic measurements where binder and dye could be detected separately.

Table 2.1   Properties of binders and coatings used in the experiments.

Type of Binder	Solvent type	Molecular weight		Particle size nm	Solid content weight %		
		Mn g/mol (number average)	Mw g/mol (weight average)		Pigmented coating	Not pigmented	Diluted and not pigmented
WAD 100 Acrylic Dispersion	water	approximately 500,000		100	56	31	23
WAD 300 Acrylic Dispersion	water	approximately 500,000		300	61	32	19
WBA Alkyd emulsion	water	1,800	50,000	500	55	37	21
HSA High solid Alkyd	white spirit + reactive diluent	3,000	7,000	solution	90	85	61
SBA Solvent Borne alkyd	white spirit	4,000	109,000	solution	59	45	29

2.2.2   Wood species and sample preparation

Industrially pre-dried pine sapwood *(Pinus sylvestris)*, spruce heartwood *(Picea abies)* and dark red meranti heartwood *(Shorea spp.)* were used. All the wood was straight grained, free from defects and was stored at 65 % RH and 22 °C before coating application. To study the penetration into radial and tangential direction for every combination of coating and wood species, three planed blocks of 70 x 70 mm (height x width) were used for spruce and pine, and three blocks of 45 x 45 mm for dark red meranti. Spruce and pine had one pure radial and one pure tangential surface, on the other two surfaces the growth-ring angle was between 20° and 40°. Growth-ring width was between 0.5 and 2.5 mm for pine and around 1 mm for spruce. The dark red meranti had growth-rings purely parallel to the surface on two sides, radial to the surface on the other two sides.

The influence of extractives was studied by comparing the penetration in normal and extractive-free cubic wood blocks of 10 mm with the coating applied on the radial and tangential surface, taking care to avoid longitudinal penetration. Extractive-free wood was

prepared by 16 hours of soxhlet-extraction with successively cyclohexane-ethanol, ethanol and water (according to ASTM-standard D1105).

Samples with a controlled angle between the length-axis of the tracheids and the surface were prepared as follows: pine panels were cut and hand-planed with the grain exactly parallel to the outer surface. Parts of the panels were further planed to an angle of 5 and 10°, see also *fig. 2.1*. The angle between surface and tracheids was checked on microscope slides taken from the samples. In this case only the pigmented solvent borne alkyd paint (SBA) was applied because it has the highest penetrating capacity.,
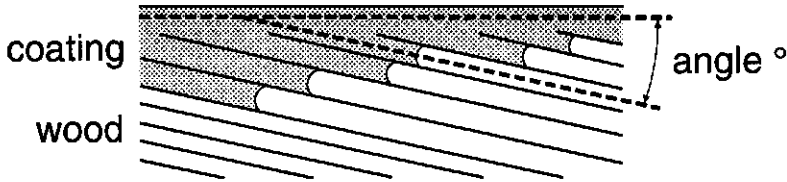
Figure 2.1   Angle between length axis of the longitudinal tracheids and the surface.

All coatings were applied in one or two layers by brush without prior sanding. The average spreading rate was approximately between 120 and 200 $g.m^{-2}$. Additionally the influence of surface preparation was studied by comparing the penetration into spruce panels with the following pre-treatments: only planing, planing followed by sanding with coarse (120) sandpaper, planing followed by sanding with coarse and fine (180) sandpaper and coarse and fine sanding followed by intensive cleaning by air-blowing. These four treatments were studied in combination with the pigmented coatings WAD300, WBA and SBA.

2.2.3 Microscopic analysis

For every combination of coating and wood seven radial and seven axial samples were cut out of the blocks and prepared to study the penetration into the wood. All samples were flattened on a microtome and examined with incident light fluorescence microscopy. The fluorescent light-source was a 50 W Mercury or 100 W Halogen lamp with a 300-400 nm exciting filter. Additionally, transmitted light microscopy was used to study penetration into sliced samples of coated wood. Scanning electron microscopic studies were made with a Hitachi S-520 SEM on gold-coated samples. The SEM was equipped with a Kevex 7100 X-ray analyser (EDAX) operated at 4.35-4.68 keV to detect titanium presence in the pigment.

2.3   Results and discussion

2.3.1 Penetration of pigmented paint into pine and spruce

The planed softwood surfaces all basically showed the following structure as it was observed on axial cross-sectional surfaces. On the wood surface the thick-walled latewood cells are mainly intact although sometimes slightly compressed whereas the thin-walled earlywood cells are cut open during planing. The latter implies that there is an open connection between the lumina and the surface on which the coating is applied. When rays end on the surface there is also an open connection with the ray cells, both to ray-tracheids and ray-parenchyma. The extent of coating penetration is firstly controlled by the ability of the liquid coating to flow into the open ends of the cells and secondly by the possibility of coating transport from cell to cell through the interconnecting pits. In the following text the penetration patterns observed are described in more detail for the coatings studied on both pine sapwood and spruce heartwood. An overview of the penetration patterns is given in *table 2.2*.

The pigmented WAD300 and WAD100 hardly show any penetration into either pine or spruce. Only the outer earlywood cells that are cut open over the full length are filled. Occasionally paint is found one cell layer below the surface in the earlywood. Here the paint flows over a short distance into the open end of a longitudinal tracheid (see *fig. 2.2*). The degree of this type of axial penetration of WAD100 is slightly less than with the WAD300. If the paint flows axially into the lumen only a thin layer covering the cell wall is present. Penetration in ray cells is limited to 10 μm with a preference to the ray parenchym cells. Although penetration in terms of transport from cell to cell is absent the increase in contact area between coating and cell wall in the early wood is considerable. Air bubbles entrapped in the coating were observed at the interface with the wood. The very limited penetration of the two acrylic coatings is in reasonable agreement with the findings of Rødsrud and Sutcliffe [6] who reported no penetration for the acrylic coatings used in their study.

The pigmented alkyd emulsion WBA fills a major part of the first cell layer under the surface by paint flow into the lumina of the earlywood; latewood cells are not filled with paint. The WBA penetrates into the rays with a limited penetration into the ray tracheids. Penetration into the parenchyma cells is limited to about 40 μm for spruce but much deeper for pine where the coating penetrates to a depth of 150 μm. In pine some longitudinal earlywood tracheids adjacent to the rays are filled with paints showing that the paint flows from rays to longitudinal tracheids. The HSA and SBA paints fill the outer first and second layer of earlywood cells in spruce and the first three layers in pine although often empty cells are found in between (see *fig. 2.7*). Penetration into the rays can be divided into penetration into ray tracheids, which is limited to the length of a single tracheid and into penetration into ray parenchyma cells. The latter depends very much on wood species. In spruce the coating never penetrates from one parenchyma cell into another. This however does happen frequently in pine where the coating can penetrate to a depth of 1000 μm.

The HSA and SBA paints were also found in pine latewood cells adjacent to rays (*fig. 2.8*) up to a distance of one growth ring away from the surface. In a radial cross-section (*fig. 2.3*) it can be seen that the paint flows from the ray parenchym through the fenestriform pits into the longitudinal tracheids. A similar type of penetration from rays into latewood tracheids was found [17] for wood-preservatives applied on pine by brush and by [15]) for alkyd paints. That this phenomenon is only found in pine and not in spruce might be explained by differences in cross field pitting and the degree of pit aspiration. The fenestriform pine pits are much larger (pit diameter of 10 to 25 μm) than the piceoid and cupressoid pits in spruce (pit diameter of about 2 to 5 μm). The latter can be more easily clogged with agglomerates of pigment particles, which have a single size of about 0.25 μm in case of the titanium dioxide used. Studies on alkyd resins penetrating eastern white pine [3] also showed that fenestriform pits can be filled with resin. Why the paints only penetrate the longitudinal latewood tracheids is not fully clear. Although it is known that bordered pits in normal tracheids are less frequently aspirated in latewood compared to earlywood [18] it is not certain whether this is a good explanation here, because the half bordered pits between rays and longitudinal tracheids might not be aspirated in both early and latewood. At least pits between rays tracheids were found not to be aspirated [18]. Another explanation for the differences in longitudinal penetration of early- and latewood adjacent to rays might be, that there are differences in capillary forces due to different sizes of the lumina in the longitudinal tracheids.

Table 2.2   Overview of the observed penetration patterns

Pigmented coating		Type of binder WAD300 acrylic dispersion	WAD100 acrylic dispersion	WBA alkyd emulsion	HSA high solid alkyd	SBA solventborne alkyd
pine	outer tracheids in earlywood	only filling outer cells seldom one cell row below surface	only filling outer cells very seldom one cell row below surface	filling outer cells and often first cell row below the surface	filling outer cells and up to three cell rows below surface	filling outer cells and first (sometimes second) cell row below surface
	outer tracheids in latewood	no filling lumina coating only on surface	no filling lumina coating only on surface	no filling lumina coating only on surface	occasionally also some filling of latewood cells	no filling lumina coating only on surface
	ray parenchyma	limited to depth of 10 μm	no penetration	penetration up to 150 μm	deep penetration to depth of 1000 μm	deep penetration to depth of 1000 μm
	tracheids	limited to depth of 10 μm	no penetration	limited penetration	penetration up to length of 1 tracheid	penetration up to length of 1 tracheid
	longitudinal tracheids adjacent to rays	no coating present	no coating present	some filling of latewood cells	frequent filling of latewood tracheids	frequent filling of latewood tracheids
spruce	outer tracheids in earlywood	only filling outer cells seldom one cell row below surface	only filling outer cells very seldom one cell row below surface	filling outer cells and often first cell row below surface	filling outer cells and up to three cell rows below surface	filling outer cells and first (sometimes second) cell row below surface
	outer tracheids in latewood	no filling lumina coating only on surface	no filling lumina coating only on surface	no filling lumina coating only on surface	occasionally also some filling of latewood cells	no filling lumina coating only on surface
	ray parenchyma	limited to depth of 10 μm	no penetration	penetration up to depth of 40 μm	penetration of the first cell	penetration of the first cell
	tracheids	limited to depth of 10 μm	no penetration	limited penetration	penetration up to length of 1 tracheid	penetration up to length of 1 tracheid
	longitudinal tracheids adjacent to rays	no coating present	no coating present	no coating present	no coating present	no coating present
dark red meranti	filling of vessels	yes, if not limited by tyloses	yes, if not limited by tyloses	yes, if not limited by tyloses	yes, also under tyloses	yes, if not limited by tyloses
	rays	no coating present	no coating present	very limited penetration	penetration up to length of 1 ray cell	penetration up to length of 1 ray cell
	axial parenchym and sklerenchym fibres	no coating present	no coating present	no coating present	penetration of cells close to surface	no coating present

unpigmented coating		wad300	wad100	wba	hsa	sba
pine	outer tracheids in earlywood	filling outer cells and 2-3 cell rows below surface	filling outer cells and often first cell row below surface	filling outer cells and 1-5 cell rows below surface	filling outer cells and 1-3 cell rows below surface	filling outer cells and 1-2 cell rows below surface
	outer tracheids in latewood	no coating present	only filling outer cells very seldom one cell row below surface	filling outer cells and limited filling 1-3 cell rows below surface	filling outer cells and 1-6 cell rows below surface	only filling outer cells very seldom one cell row below surface
	ray parenchyma	no coating present	no coating present	penetration up to depth of 150-500 µm	very deep penetration up to 2000 µm	very deep penetration up to 2000 µm
	tracheids	no coating present	no coating present	penetration up to length of 1 tracheid	penetration up to length of 1 tracheid	penetration up to length of 1 tracheid
	longitudinal tracheids adjacent to rays	no coating present	no coating present	frequent filling of latewood tracheids	completely filling latewood up to 2 mm away from surface	frequent filling of latewood up to 2 mm away from surface
spruce	outer tracheids in earlywood	filling 2-3 cell rows below surface	filling outer cells and often first cell row below surface	filling outer cells and 1-3 cell rows below surface	filling outer cells and 1-3 cell rows below surface	filling outer cells and 1-2 cell rows below surface
	outer tracheids in latewood	no coating present	no filling lumina coating only on surface	limited filling 1-3 cell rows below surface	filling 1-6 cell rows below surface	no filling lumina coating only on surface
	ray parenchyma	no coating present	no coating present	penetration up to depth of 40 µm	penetration up to depth of 140-200 µm	penetration of the first cell
	tracheids	no coating present	no coating present	limited penetration	penetration up to depth of 1000 µm	penetration up to length of 1 tracheid
	longitudinal tracheids adjacent to rays	no coating present	no coating present	no coating present	frequent filling of latewood tracheids	no coating present

Figure 2.2
Flow of pigmented WAD300 coating (dark blue) from the surface layer in open end of longitudinal tracheid in spruce. Microphotograph of radial cross section with incident fluorescent light (200 x).
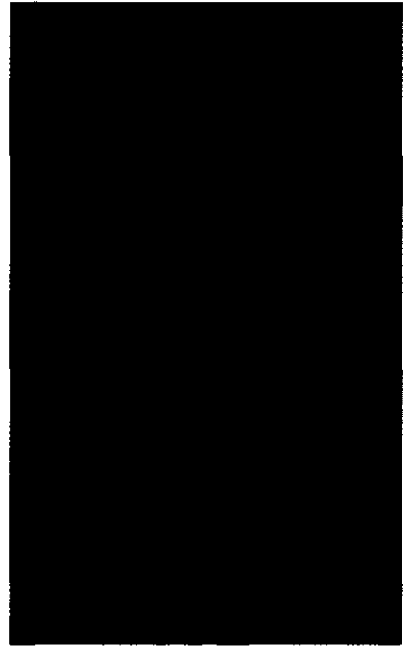
Figure 2.3
Transmitted normal light microphotograph showing how the HSA coating (dark area) penetrates from the ray parenchyma cells into the longitudinal tracheids through the fenestriform pits (200 x). The actual ray filled with the coating is out of the plane of the slide.
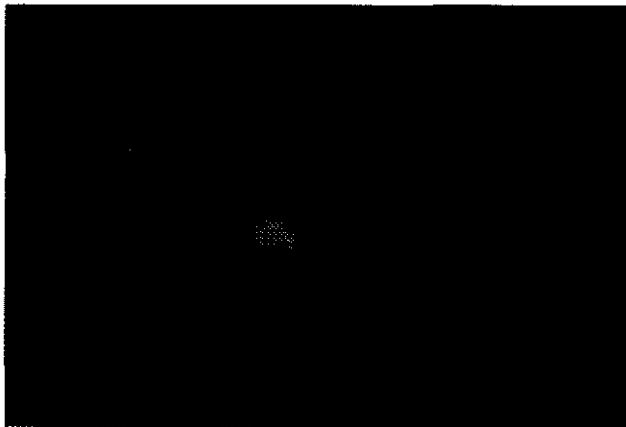
Figure 2.4   Axial cross-section showing penetration of SBA coating into dark red meranti (incident fluorescent light 100 x). Note the incomplete filling of the vessel in the middle because of tylose membrane and completely filled vessel at the left, ray cell are also penetrated. Bright white spots are natural resin channels.
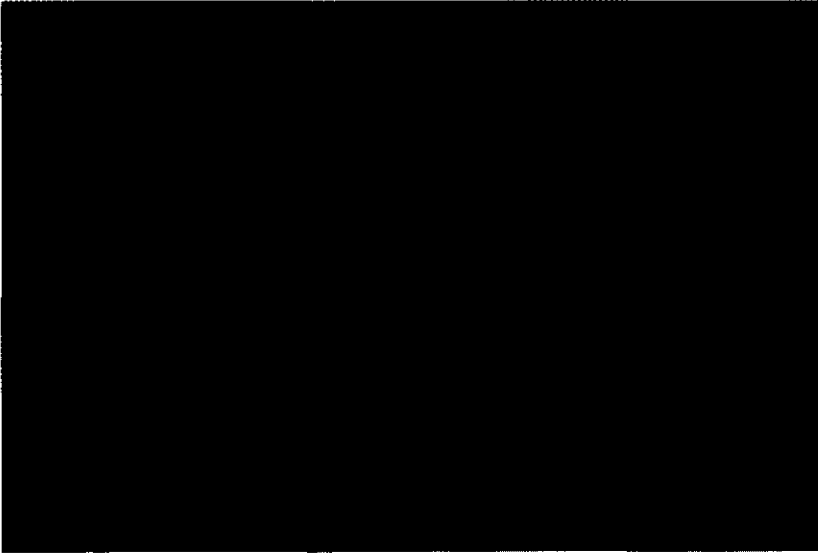
Figure 2.5   Fluorescence microphotograph of axial cross-section (40 x) showing the penetration of HSA binder (white colour) in pine. Note the filling of latewood bands four growth-rings away from the surface and the penetration into rays.
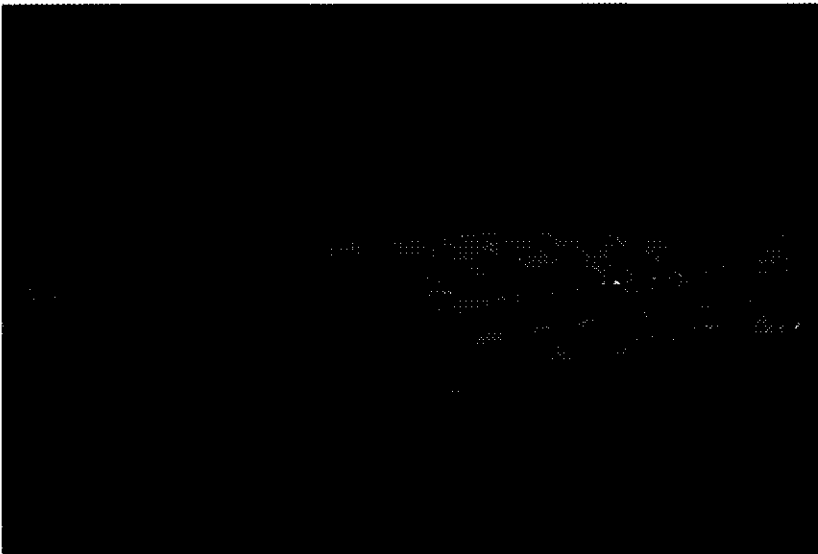
Figure 2.6   Fluorescence microphotograph of axial cross-section (100 x) showing the penetration of SBA coating (white colour) in pine with a controlled 10 ° angle between surface and length axis of longitudinal tracheids.
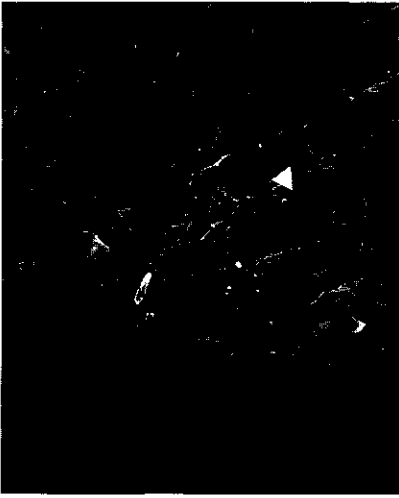
Figure 2.7
SEM-microphotograph (350 x) of pigmented HSA coating filling the outer earlywood tracheids. Note the fact that first, second and fourth tracheids are filled but that third one is empty (see arrow).

Figure 2.8
SEM-microphotograph (710 x) of pigmented HSA coating in a ray and in longitudinal tracheids adjacent to the ray which are filled through the half bordered pits (indicated by arrows).

Figure 2.9
SEM-microphotograph (200 x) showing how the SBA coating is resting on the membrane of a tylose (arrow) in a half open cut vessel in meranti.
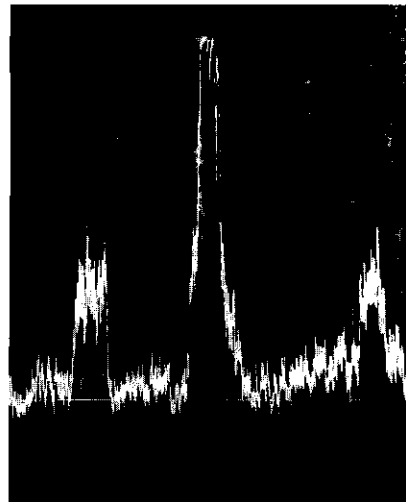
Figure 2.10
SEM-microphotograph (100 x) with EDAX line-scan on titanium of HSA coating showing that the pigment penetrates into a ray cell. X-ray peak is strongly increased at the ray; smaller peaks at left and right are artefacts due to crossing of a cell wall.

A remarkable observation in case of the HSA and SBA paint is the difference in colour of the paint penetrated into the wood. On the surface the colour is dark blue (typical for pigment and binder), whereas in the wood different shades of blue and white (typical for pure pigment) were observed. SEM-EDAX analysis of paint penetrated into the rays (see *fig.2.10*) proved that the pigment was present at depths of 180 μm but with fluorescence microscopy pigment was even observed at a depth of 1000 μm. A possible reason for the separation of pigment and binder could be the variation in molecular weight with a higher mobility of the lower weight fractions, or the fact that binder not adsorbed to the pigment surface can penetrate more deeply into the wood than the binder that is used to wet the pigment particles.

As the flow from open ends into the longitudinal tracheids seems to be a very important factor in filling the outer cells, the following experiment was performed to prove the importance of this mechanism in more detail. For the combination of pine sapwood and SBA coating the number of cell layers filled with coating was measured as a function of the angle between the surface and the length-axis of the longitudinal tracheids. As shown by the results presented in *table 2.3* no tracheids are filled at an angle of zero degrees. At a 5 ° angle already 5 cells or more are filled, whereas at a 10 ° angle a very large number of cells are filled in both early- and latewood (see *fig.2.6*). From these data it can be estimated that in normally prepared samples the angle was between zero and five degrees. The variation in angle between surface and length-axis of a tracheid can also explain why the penetration for one type of coating often varies from sample to sample.

Table 2.3   Number of tracheid-rows filled with coating, as a function angle between surface and length-axis of the longitudinal tracheids in pine sapwood measured perpendicular to the surface from axial cross-section. Coating type: pigmented solvent borne alkyd (SBA).

Angle between surface and length axis of tracheid	Number of cell rows filled with coating	
	earlywood	latewood
0 °	0-1	0-1
5 °	6-9	5-6
10 °	12-20	12-15

2.3.2   Penetration of unpigmented binders into pine and spruce

In general the unpigmented binder solutions show the same basic penetration pattern as the pigmented coatings however, in general penetration is deeper. On the surface often no clear film is present, in particular if the coating has penetrated deeply. *Table 2.2* gives an overview of the penetration pattern observed for each coating on both pine and spruce. In the following text the penetration is discussed in more detail including the influence of dilution and the presence of dryer or coalescent. The acrylic dispersion WAD300 forms a thin film on the latewood of pine and spruce and partially fills lumina in the earlywood up to 2 or 3 cell rows away from the surface. No differences were found between binder with and without coalescent. The diluted binder is very difficult to detect but is occasionally found in the lumina of earlywood tracheids. The acrylic dispersion WAD100 is found on the surface, in the first row of earlywood tracheids of pine and spruce and very seldom in latewood tracheids of pine, but not in spruce. The binder without the coalescent has a more irregular film formation on the surface, which is consistent with the fact that the coalescent improves the film formation. For both the WAD100 and WAD300 no binder was found in the rays, neither in ray parenchyma nor in ray tracheids. The diluted WAD100 clearly shows a deeper penetration compared to the diluted WAD300. The diluted binder WAD100 fills up to 5 cell

surfaces only planed and planed plus sanded coated with the SBA paint. Most likely the ends of ray cells are deformed and clogged with dust, which prevents paint from flowing into the rays. The reduced coating penetration after sanding supports the finding that sanded surfaces require less paint to obtain full coverage of the surface compared to planed ones [24].

Figure 2.11   SEM-microphotograph (350 x) showing the WAD300 coating on spruce planed and sanded with fine (180) sandpaper. Note that the outer cell walls are deformed by the sanding process.

2.4   Conclusions

Penetration of a coating into wood is first of all determined by the ability of the paint to flow into the open ends of the cell capillaries. The coatings studied showed very strong differences in penetration capacity. The type of binder has the biggest influence with the following increasing order in penetration: acrylic dispersions, alkyd emulsions, solventborne alkyds and high solid alkyds. Additionally the penetration is influenced by: drying speed of the coating, the ratio of solid to liquid material and the presence of pigments. The latter was also found by Nussbaum [16]. Very likely, paint properties like viscosity, surface tension and the rate of transfer of solvent from liquid coating to cell wall determine the penetrating capacity of a coating. This will be studied in future research where the maximum depth of penetration in the cells will be measured as a function of the paint properties mentioned.

If the paint is able to flow into the wood cells, three different ways of penetration in softwood can be distinguished as is schematically shown in *fig. 2.12*. Firstly the outer longitudinal tracheids are filled directly by coating flowing from the open ends on the surface. This predominantly occurs in the earlywood. The angle between length axis of the tracheid and the surface has a strong influence on the importance of this mechanism. A second way of penetration is through the rays, starting also at the open cut ends of the ray cells. In which way transport in the rays proceeds is strongly dependent on the wood species. In pine the major part of the coating flows through the parenchyma cells, transport from cell to cell must therefore be possible. In spruce the coating almost solely penetrates the ray tracheids. Studies on other wood species showed similar differences. Wardrop and Davies [25] reported preferential penetration in ray parenchym in the case of *Pinus radiata,* whereas Erickson and Balatinecz [22] found the ray tracheids to be most important for penetration in the case of Douglas fir. A third way of penetration is from ray cells to adjacent longitudinal tracheids in the latewood. By means of this mechanism unpigmented binder can reach longitudinal

tracheids up to a distance of 2 mm away from the surface. The extent of transport from rays to tracheids is strongly dependent on permeability of the cross-field pits and within the scope of this study it was found to be almost totally limited to pine sapwood. The importance of the three penetration mechanisms mentioned above implicates that penetration of the coating can strongly be influenced by the way in which boards are sawn out of a log. This because of the impact on differences in flat and standing growth rings, orientation of grain to the surface, width of early and latewood bands and the number of rays ending in radial and tangential surfaces. The origin of the wood might influence penetration because of differences in early- and latewood portions, conditions of the pits, number of rays and length of longitudinal tracheids. Drying conditions of the wood might also have some influence on coating penetration because of its impact on pit aspiration.
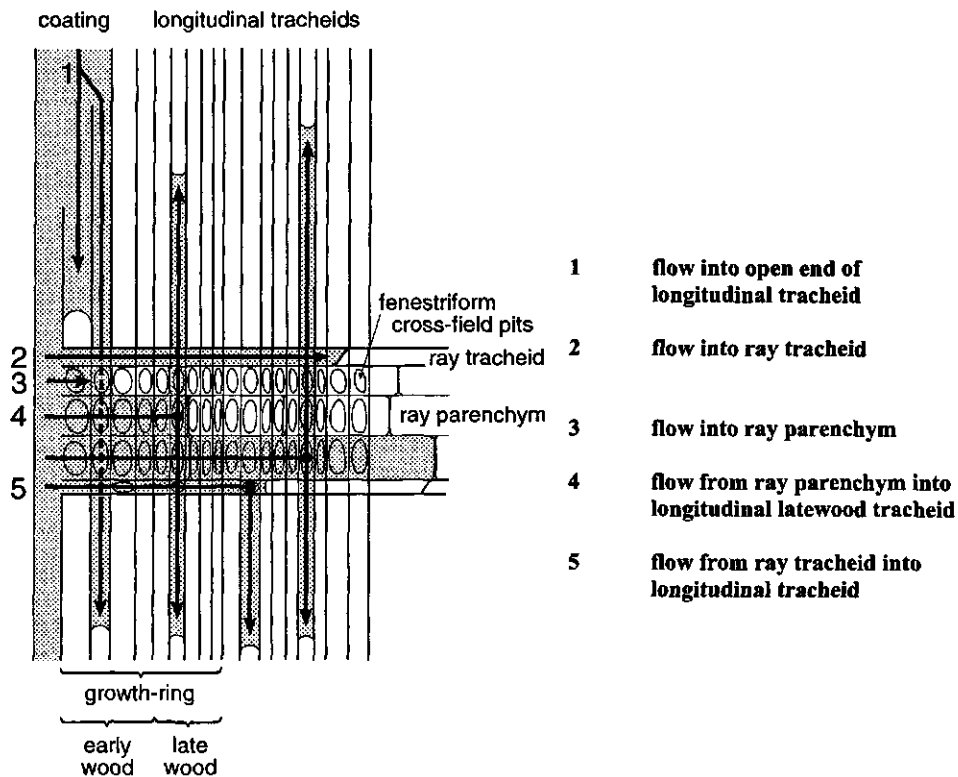
Figure 2.12 Schematic presentation of the different ways of possible coating penetration in softwoods seen from the radial cross-section.

Penetration in dark red meranti is mainly restricted to the filling of vessels and the first cells of rays and very occasionally axial parenchym and sklerenchym. The filling of a vessel by the coating is strongly reduced if tyloses are present. Extractives appeared to have none or only a very minor influence on the penetration in all tree wood species studied. Therefore negative influences of high extractive content on adhesion of a coating are probably not caused by reduced penetration, but are more likely the result of differences in chemical composition of the surface. Surface preparation can have some influence on coating

penetration because sanding reduces the number of open cell capillaries in which paint can flow. This means that sanding reduces the contact area between coating and wood and the possibilities for mechanical entanglement. This might reduce the adhesion of the coating if it is applied on a surface, which is sanded before the application of the first coating layer.

Acknowledgements:

References

[1]   **Militz, H.; Peek, R-D**; Möglichkeiten der Verbesserung einiger Eigenschaften von Pappelholz durch Tränken mit wasserlöslichen Harzen, Material und Organismen, 1993/1994 (1), 1994, 55-73.

[2]   **Kabir, A.F.R.; Nicholas, D.D.; Vasishth, R.C.; Barnes, H.M.**; Laboratory methods to predict the weathering characteristics of wood, Holzforschung, 46 (5), 1992, 395-401.

[3]   **Smulski, S.; Côté, W.A.**; Penetration of wood by a water-borne alkyd resin, Wood Science and Technology, 18, 1984, 59-75.

[4]   **Allen, K.W.**; A review of contemporary views of theories of adhesion, Journal of Adhesion, 21, 1987, 261-277.

[5]   **Pizzi, A.**; Non-mathematical review of adhesion theories as regards their applicability to wood, Holzforschung und Holzverwertung 44, 1992, 62-67.

[6]   **Rødsrud, G.; Sutcliffe, J.E.**; Alkyd emulsions - properties and application. Results from comparative investigations of penetration and ageing of alkyds, alkyd emulsions and acrylic dispersions. Presentation held at the 14th Congress of the Federation of Scandinavian Paint & Varnish Technologists - Copenhagen, 1993.

[7]   **Haslam, J.H.; Werthan, S.**; Studies in the Painting of Wood, Industrial and engineering chemistry, 23 (2), 1931, 226-233.

[8]   **Wallenfang, W.O.**; Zur Frage der Eindringtiefe von Ölen und Harzlösungen, Farbe und Lack, 70 (8), 1964, 258-263.

[9]   **Loon, J. van**; The interaction between paint and substrate, Journal of the Oil and Color Chemists Association, 49 (10), 1966, 844-867.

[10]   **Schneider, M.H.**; Cote W.A.; Studies of wood and coating interactions using fluorescence microscopy and pyrolysis gas-liquid chromatography, Journal of Paint Technology, 39 (511), 1067, 465-471.

[11]   **Côté, W.A.; Robison, R.G.**; A comparative study of wood, Journal of Paint Technology, 40 (525), 1968, 427-432.

[12]   **Schneider, M.H.**; Coating penetration into wood substance studied with electron microscopy using replica techniques, Journal of Paint Technology, 42 (547), 1970, 457-460.

[13]   **Schneider, M.H.**; Scanning electron microscope study of a coating component deposited from solution into wood, Journal of the Oil and Color Chemists Association, 62, 1979, 441-444.

[14]   **Schneider, M.H.**; Microscopic distribution of linseed oil after application to wood surface, Journal of Coatings Technology, 52 (665), 1980, 64-67.

[15]   **Nussbaum, R.M.**; Penetration of water-borne alkyd emulsions and solvent-borne alkyds into wood, Holz als Roh- und Werkstoff, 52, 1994, 389-393.

[16]   **Schneider, M.H.; Sharp, A.R.**; A model for the uptake of linseed oil by wood, Journal of Coatings Technology, 54 (693), 1982 91-96.

[17] **Schulze, B.; Theden, G.**; Das Eindringen aufgestrichener Holzschutzmittel in Kiefernsplintholz, Holz als Roh- und Werkstoff, 5 (7), 1942, 239-247.

[18] **Liese, W.; Bauch, J.**; On the closure of bordered pits in conifers, Wood Science and Technology, 1, 1967, 1-13.

[19] **Hofland, A.**; Water-borne coatings for decorative and protective coatings: a comparative survey, Surface Coatings International, 7, 1994, 270-281.

[20] **Courtois, H.**; Über den Einfluss einiger holzanatomischer Unterschiede auf die Tränkbarkeit von Mittelgebirgs- und Küstenfichtenholz, Holzforschung und Holzverwertung, 16, 1964, 61-66.

[21] **Laming, P.B.**; On intercellular spaces in the xylem ray parenchyma of picea abies, Acta Botanica Neerlandica, 23 (3), 1974, 217-223.

[22] **Erickson, H.D.; Balatinecz J.J.**; Liquid flow paths into wood using polymerisation techniques Douglas-Fir and styrene, Forest Products Journal, 1964, 293-299.

[23] **Murmanis, L.; River, B.H.; Stewart H.A.**; Surface and subsurface characteristics related to abrasive-planing conditions, Wood and fiber Science, 18 (1), 1986, 107-117.

[24] **Richter, K.; Feist, W.C.; Knaebe, M.T.**; The effect of surface roughness on the performance of finishes. Part 1. Roughness characterisation and stain performance, Forest Products Journal, 45 (7/8), 1995, 91-97.

[25] **Wardrop, A.B.; Davies, G.W.**; Morphological factors relating to the penetration of liquids into wood, Holzforschung, 15 (5), 1961, 129-141.

3. Quantitative measurements of capillary coating penetration in relation to wood and coating properties[*]

Summary

In order to study quantitatively the relations between the properties of waterborne coatings and their penetration, two techniques have been developed and applied to five different pigmented paints and unpigmented binders. The first technique measures the depth of penetration into the axial direction, the second one measures the change of contact-angle and volume of a coating droplet as a function of time. The low-shear viscosity of the pigmented paint has a strong influence on the degree of penetration; surface tension seems to be less important as long as the coating wets the cell capillary fairly well. The diameter of the wood cell has also an influence on the degree of penetration although both negative and positive correlations were found depending on the coating type. From the impact of wood moisture content and the differences between binders with comparable viscosities it can be assumed that the rate of transfer of water from liquid coating to cell wall and the subsequent increase in viscosity has a strong impact on penetration. Experimental results have been compared with calculations based on theoretical models for capillary penetration. In some cases the predictions were fairly adequate, but strong deviations were observed as well.

3.1 Introduction

The protection of softwoods by coatings with low organic solvent content like waterborne or high solid coatings has become increasingly important in the European joinery industry in recent years. Because the properties of waterborne and high solid coatings are different from the traditional solventborne coatings in many ways, a more fundamental understanding of the interactions between wood and waterborne coatings is desirable. One of the aspects in which waterborne coatings differ is the degree of penetration into the wood. In general the penetration of waterborne coatings is less compared to solventborne coatings, although large differences between waterborne coatings exist, depending on the type of formulation [1,2,3]. In contrast to this, high solid coatings show an increased penetration into the wood compared to normal solventborne alkyd paints.

In a previous study [1] it was shown that, apart from the anatomical structure of the wood, coating penetration is mainly determined by the ability of the coating to flow into the lumina of either tracheids or ray-cells. Most likely the flow of a coating through the wood capillaries will be influenced by many variables like viscosity, surface tension, drying rate of the coating and the diameter of the wood capillaries [4].

To study these factors in a more systematic way, the development of a quantitative technique of measuring coating penetration is needed. In existing literature only two quantitative studies on coating penetration into wood were found. Schneider and Sharp[5] developed a model for the uptake of linseed oil based on gravimetric measurements and Rødsrud and Sutcliffe [3] measured the concentration of bromine labelled alkyd-resins as a function of penetration depth.

In this study two quantitative techniques for the measurement of coating penetration into the longitudinal direction of the wood are presented. The first one is a static method, which measures the maximum depth of axial penetration of a coating on a microscopic level. The second method is based on the dynamic measurement of coating penetration by analysing the contact angle, shape and volume of a droplet on a smoothed axial surface. The measured differences in coating penetration are related to capillary diameter, wood species, binder type, pigmentation, viscosity, surface tension and wood moisture content. Finally the measured penetration depths are compared with existing physical models for capillary penetration.

3.2 Physicals model for penetration of liquids into capillaries

The flow of a liquid through a cylinder can generally be described with the Hagen-Poiseuille law:

$$\frac{V}{t} = \frac{\pi P r^4}{8 \eta L} \tag{3.1}$$

With the volume (V), time (t), capillary radius (r), length of the capillary (L) and liquid viscosity (η). Neglecting effects of gravity and counter pressure induced by compressed air inside the capillary, the driving pressure (P) for the liquid flow is equal to the capillary pressure (P_c) [6, 7]:

$$P_c = \frac{2 \gamma_L \cos \theta}{r} \tag{3.2}$$

With liquid surface tension (γ_L) and cosine of the contact angle (θ) of wetting liquid.
Because V/t = A u with A is area of the capillary (πr^2) and u is the velocity of the penetrating liquid (dL/dt) the *equations 3.1* and *3.2* can be rewritten to [6]:

$$L \, dL = \left(\frac{\gamma_L \cos \theta}{\eta} \right) \left(\frac{r}{4} \right) dt \tag{3.3}$$

Integrating the *equation 3.3* to L (penetration depth) and t (time) gives the following equation, which is generally known as the Washburn-equation [8]:

$$L = \sqrt{\frac{\gamma_L \cos\theta\, r\, t}{2\eta}}$$

(3.4)

This equation states that the depth of capillary penetration is proportional to the square root of: liquid surface tension, cosine of the contact angle between liquid and capillary wall, diameter of the capillary and the reciprocal liquid viscosity. Alternatively, and neglecting the effect of viscosity, the height of capillary rise can also be derived from *equation 2.2* by assuming that the capillary pressure is balanced by the weight of the liquid [9]. This gives the following relationship:

$$L = \frac{2\cos\theta\,\gamma_L}{r\,\rho_L g}$$

(3.5)

Equation 3.5 states that the depth of capillary penetration is proportional to the reciprocal radius of the capillary, the acceleration of gravity g ($9.8\ m\ s^{-2}$) and the density of the liquid ρ_L ($kg\ m^{-3}$).

3.3 Materials and methods

3.3.1 Wood samples and coating materials
In this study five different binders were used: two waterborne acrylic dispersions with a weight averaged molecular weight of approximately 500,000 $g.mol^{-1}$ and particle sizes of ± 100 nm (WAD100) and ± 300 nm (WAD300), one waterborne alkyd-emulsion (WBA) with a Mw of 50,000 $g.mol^{-1}$ and a particle size of ± 500 nm, one alkyd-based high solid (HSA) with a Mw of 7,000 $g.mol^{-1}$ and one traditional solventborne alkyd resin (SBA) with a Mw of 109,000 $g.mol^{-1}$. The different types of binders were used in simply formulated model paints pigmented with titanium dioxide to a pigment volume concentration of 17 % and in unpigmented solutions of binders. The latter contained only the binder, water or organic solvent and approximately 1 weight % coalescent which improves film formation of the acrylic dispersions or 2 to 4 weight % of a cobalt-siccative solution which catalyses the oxidative drying of the alkyd resins. All binders were labelled with an anthracene group for detection with fluorescence light-microscopy.

To include a highly permeable and impermeable softwood species, pine sapwood *(Pinus sylvestris)* with a density of $515 \pm 9\ kg.m^{-3}$ and spruce heartwood *(Picea abies)* with a density of $370 \pm 13\ kg.m^{-3}$ were used in this experiment. The wood was industrially pre-dried and stored at 65 % RH and 23 °C to obtain a wood moisture content of 14 % in case of pine and 12 % in case of spruce. For the study on the influence of wood moisture content samples were also dried at 60 °C or stored at 98 % RH to obtain wood moisture contents of respectively around 2 % and 28 %. Samples of 40 x 20 x 25 - 70 mm (width x thickness x length) were taken out of one board and were free from defects, cracks or compression wood. The axial surface, to which the paints were applied, was carefully planed with a microtome to avoid damage to the cell structure. The coatings were applied in two ways, by brushing the surface in an upright position until no more coating was absorbed and by dipping the samples in the paint for about 5 to 10 seconds. The uptake of coating material is given in *table 3.1*.

The viscosities and shear-stresses of the coatings were measured with a Bohlin controlled stress rheometer at a temperature of 23 °C with shear-rates in the range of 0.01 to 1000 s^{-1}. The viscosity of the unpigmented binder solutions was hardly influenced by the applied shear rate. The pigmented coatings, however, showed a strong non-Newtonian behaviour, which means that the viscosity can only be expressed as a function of the shear-

rate and shear stress. The rheology of non-Newtonian fluids is often described with the following two relationships [10]:

$$\tau = \tau_0 + k \gamma'^n \tag{3.6}$$

$$\eta(\gamma') = \frac{d\tau}{d\gamma'} \tag{3.7}$$

τ	:	shear-stress at given shear-rate	(Pa)
τ_0	:	shear-stress at zero shear-rate (yield-stress)	(Pa)
γ'	:	applied shear-rate	(s^{-1})
$\eta(\gamma')$	:	viscosity at given shear-rate	$(Pa\ s^{-1})$
k, n	:	fit parameters	

Fig. 3.1 shows the viscosities of the pigmented paints as a function of the shear-rate according to *equation 3.6*. Yield-stress values, viscosities at 0.01 and 1000 s^{-1}, surface tension, density and volume-percentage solids are given in *table 3.2* for both pigmented paints and unpigmented binder. Surface tension of the liquid coating was measured with the ring method according to DIN-standard 53914.

Table 3.1 Spreading rate in g wet paint m^{-2}.

		pine sapwood		spruce	
		brushing	dipping	brushing	dipping
paint	WAD100	350	-	350	525
	WAD300	313	275	225	313
	WBA	575	575	500	438
	HSA	1263	962	1438	775
	SBA	1088	750	1000	538
binder	WAD100	975	638	1063	675
	WAD300	837	713	1000	600
	WBA	925	612	1063	462
	HSA	1194	762	1088	763
	SBA	762	613	850	637
pigmentpaste		-	-	438	925

Table 3.2 Physical properties of paints and binder solutions.

		Surface tension mNm^{-1}	Viscosity Pa.s 0.01 s^{-1}	Viscosity Pa.s 1000 s^{-1}	Yield-stress Pa	Density g ml^{-1}	Weight % solids
paint	WAD100	42.85	214.30	0.54	0.43	1.25	61
	WAD300	47.80	29.33	0.31	3.13	1.26	56
	WBA	38.15	21.88	0.07	0.32	1.24	55
	HSA	32.75	1.05	0.79	0.02	1.40	90
	SBA	28.40	3.46	1.19	0.05	1.11	59
binder	WAD100	42.65	0.01	0.01	0.00	1.06	31
	WAD300	43.10	0.01	0.01	0.00	1.06	32
	WBA	34.45	0.01	0.01	0.00	1.03	37
	HSA	31.10	0.20	0.20	0.00	0.98	85
	SBA	27.60	1.36	0.78	0.00	0.91	45
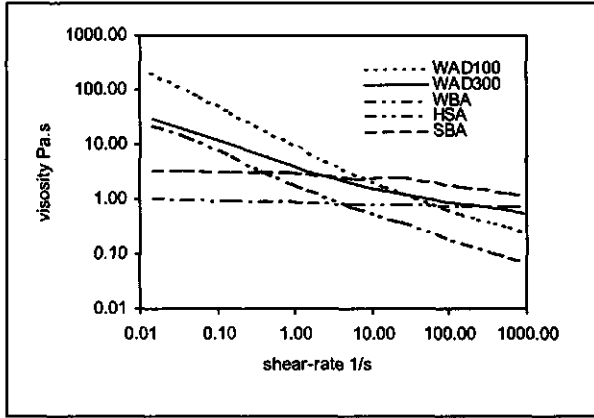
Figure 3.1. Viscosity of the pigmented paints as a function of applied shear-stress.

3.3.2 Measurement of maximum depth of axial penetration

The samples with the coating applied to the axial surface were cut along the grain into three to four different sub-samples. Each sub-sample was smoothed on the radial surface with a microtome and examined with an incident fluorescent light microscope. For each sample the depth of penetration into the axial direction and the diameter of the cell-lumen was measured for 80 to 150 individual tracheids with the micrometer in the eyepiece of the microscope. *Fig.3.2* shows a graphical presentation of the measuring principal. In those cases where the depth of axial penetration exceeded the length of a single tracheid, the measurement was taken along two cells that were lying in one line. The measurements have been divided over the sub-samples in groups of 10 to 15 adjacent tracheids alternatingly located in early- and latewood bands.
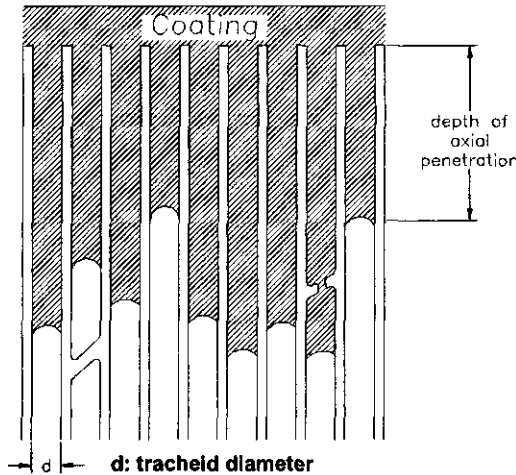
Figure 3.2 Measurement of depth of axial penetration.

3.3.3 Dynamic measurement of contact angle and droplet volume

Droplets with a volume of 20 ± 5 µl were placed with a pipette on a microtome flattened axial wood surface. The changes in diameter and height of the droplet and the contact angle on both sides were recorded with a video microscope over a period of 50 to 280 seconds. Five measurements were made for every combination of coating and wood species. De-ionised water and white spirit were also included in this experiment as reference liquids.
The volume of the droplet was calculated according to two different models. The first model (*equation 3.8*) which was given by Liptáková and Kúdela [11] uses the height (h) and diameter (d) to calculate the volume V_d. The second model (*equation 3.9*), given by Denesuk *et al.* [8], uses the diameter and the contact-angle (θ) for computation of the droplet-volume.

$$\text{Model 1:} \quad V_d = \tfrac{\pi}{6} h \left[3 \frac{d^2}{4} + h^2 \right] \tag{3.8}$$

$$\text{Model 2:} \quad V_d = \tfrac{\pi}{3}(0.5d)^3 \frac{(1 - \cos\theta)(\cos\theta + 2)}{\sin\theta(\cos\theta + 1)} \tag{3.9}$$

3.4 Results and discussions

3.4.1 Axial penetration of pigmented paints

The measured axial depths of coating penetration have been summarised in box-plots in *fig.3.3* according to the different experimental variables used in this study. Because the variation in the results within one set of variables is fairly large and the penetration-depths are not normally distributed, median and percentile (25% and 75%) values are calculated instead of means and standard deviations. This is done to prevent the results from being incorrectly interpreted because of some extreme values, which disproportionally influence the mean values.

The pigmented, more viscous paints do show a much lower degree of penetration compared to the non-pigmented and less viscous binder solutions. Differences between the pigmented paint types are also more pronounced than for the unpigmented ones. For this reason the logarithmic depth of penetration is given in *fig. 3.3* for the pigmented paint. The acrylic dispersion paints penetrate sometimes 30 to 100 µm into the cell lumina but very often there is no flow into the lumen at all. Although the WAD100 penetrated slightly better than the WAD300 this does not seem to be a relevant difference. The penetration depth of the pigment paste used to prepare the acrylic paints, was in the same range as the paints themselves. This indicates that the pigment particles are not limiting the penetration. The alkyd-emulsion paint (WBA) penetrated clearly better with a median depth of penetration ranging from 100 to 300 µm. The solvent borne SBA and HSA paints have the deepest penetration, roughly between 1500 and 3000 µm.

The viscosity at very low shear-rate appeared to have a very strong influence on the measured depth of penetration of the pigmented paints. In *fig.3.4* the logarithmic median depth of coating penetration is plotted against the logarithm of the viscosity at 0.01 s^{-1}. Even in this double-logarithmic plot an almost exponential relationship exists between the variables plotted. Looking at the flow-curves given in *fig.3.1* it becomes clear that it is the change in viscosity as a function of shear-rate that controls the penetration of the paints. At a shear-rate of 100 to 1000 s^{-1}, which is considered to control brush and spray properties [6], the best penetrating HSA and SBA paints have the highest viscosities. At a shear rate of 0.01 s^{-1} the viscosity ranking of the paints is completely different and corresponding to the differences found in penetration. The thickeners, which have to be used to give the waterborne dispersions and emulsion a sufficiently high enough application viscosity, have a strongly

limiting effect on the penetration. In this respect it should also be mentioned that the HSA and SBA paints did not contain an additional thickener.
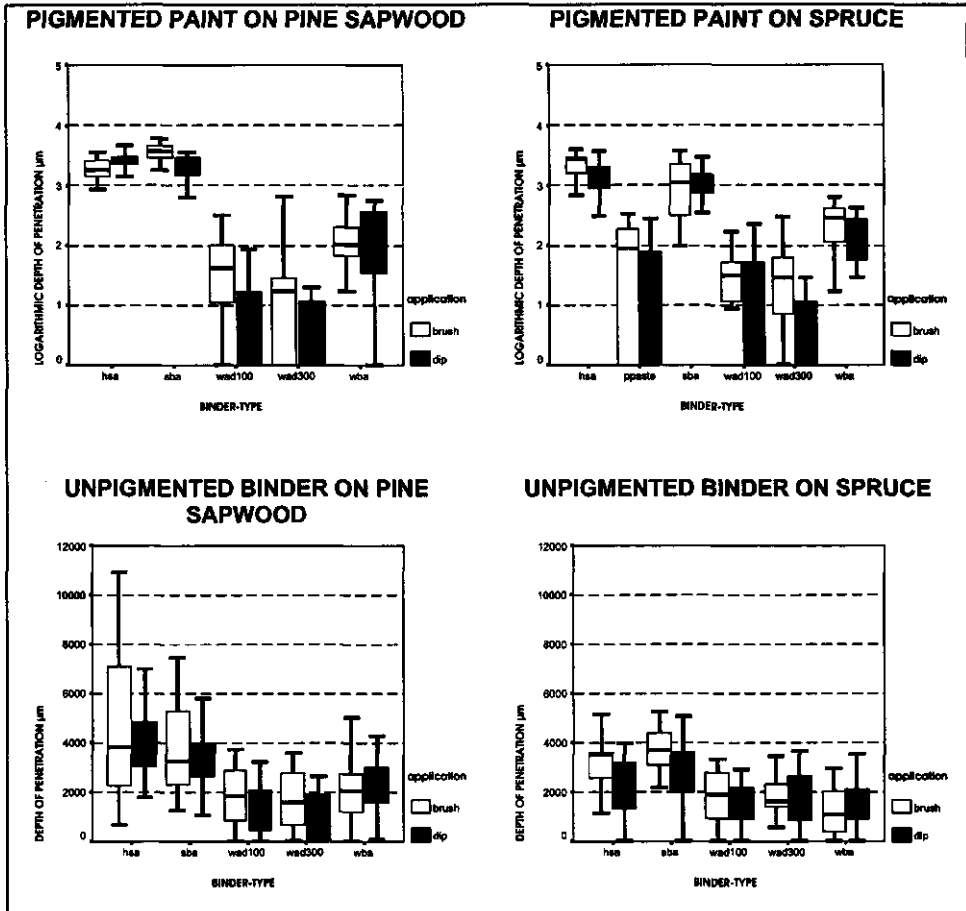
Figure 3.3   Box-plots showing the penetration as a function of binder type, pigmentation, wood species and application type. Boxes indicate 25 % and 75 % percentiles with the median-line in between. The line indicates upper and lower extreme values.

The influence of either brush or dip application on penetration is fairly consistent with differences in rheological behaviour of the pigmented paints. The WAD300, WAD100 and WBA paints and the pigment paste showed an increased penetration when they are brush-applied if compared to the dipped samples. This corresponds with the lower viscosity at a shear-rate of 100 s^{-1} ,which is typical for brushing, compared to the higher viscosity at a shear rate of 10 s^{-1} which is typical for dipping [6]. The penetration of the SBA paint also showed a small difference between brushed and dipped coatings which might be caused by the slight non-Newtonian behaviour in the shear-rate range of 10 to 100 s^{-1}. The penetration of the perfectly Newtonian HSA paint was hardly influenced by the type of application. The presence of a yield-stress in the relationship between shear-rate and shear stress does not influence the penetration. The WAD100, which is the only paint having a considerable yield -

stress, did not penetrate less deeply compared to the WAD300 paint which had hardly any yield-stress. All other paints or unpigmented binders had very low yield-stress values which can not be expected to influence penetration.
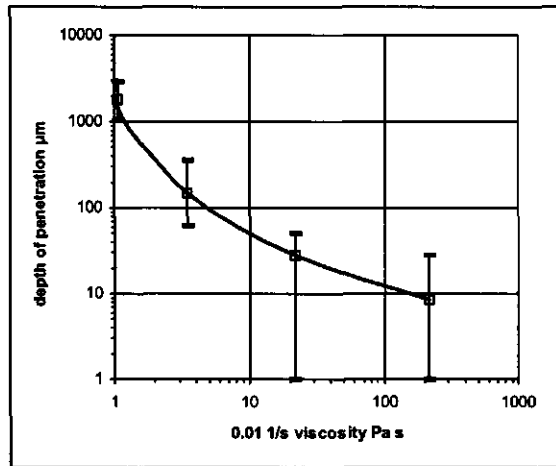
Figure 3.4   Dependence of penetration of the pigmented coating on viscosity at a shear-rate of $0,01s^{-1}$.

3.4.2 Axial penetration of unpigmented binder

The depth of axial penetration of the unpigmented binders is much higher than for the pigmented ones. The acrylic dispersion WAD100 and WAD 300 and the alkyd emulsion WBA mostly penetrate within the range of 800 to 2500 μm. Remarkably, the differences between the alkyd emulsion and the acrylic paint are not found with the unpigmented binders. The equal penetration of the three waterborne binders also shows that within the studied range of particle sizes (100 to 400 nm) there is no direct relationship with penetration depth. The penetration of the HSA and SBA binder is also strongly increased in the absence of pigments.

The increase in penetration of the latter two binder types is particularly strong in pine sapwood in which the binders can penetrate to a depth of 7000 μm (SBA) or 10.000 μm (HSA). Also for the alkyd emulsion binder (WBA) the penetration is slightly increased in case of pine sapwood. In all the other cases no relevant differences between pine sapwood and spruce heartwood were observed. Apparently, only if the median value of penetration exceeds the 3000 μm higher penetration depths are found in pine sapwood. Because this value corresponds with the average length of a pine or spruce tracheid it shows that longitudinal coating transport can be limited by transport from tracheid to tracheid through bordered pits, which are less permeable in spruce than in pine sapwood [12].

The penetration of the unpigmented binders does not seem to be influenced by the viscosity of the binder solution. The waterborne coatings, which have a much lower viscosity than the HSA and SBA binder, penetrate less deeply. The SBA alkyd resin had a seven times higher low-shear viscosity than the HSA binder, but both binder types did not differ much in depth of penetration except for the extreme values in pine sapwood. Surprisingly, there is a slight tendency to deeper binder penetration for the brush applied HSA and SBA samples, although the viscosity is hardly changing with the shear-rate. Gravity effects may have caused these differences because the paint was flowing upward during dipping and downward during brushing.

The surface tension of the binder solutions might have some influence on the axial penetration. The surface tension of the less penetrating water borne binders is clearly higher

than the surface tension of the HSA and SBA binder. On the other hand, the difference in surface tension of 9 mN.m^{-1} between the WAD300 and the WBA binder did not cause a very large difference in penetration. Therefore additional research in which the surface tension is varied within one binder type is required to further clarify the influence of the surface tension. The contact angle of the dry paint on the cell wall inside the lumina was also measured. This showed that the wetting of the cell wall can not be a limiting factor in penetration because the contact-angle was between the 3 and 10 degrees for all different binder types.

3.4.3 Influence of capillary diameter

The measured depths of axial penetration vary largely within a sample of given treatment conditions. A large part of this variation is however not a random thing, but can be explained by the influence of the cell lumen diameter. In order to understand the influence of the lumen diameter in more detail, this value was measured together with the maximum depth of axial penetration. In *fig.3.5* two typical examples of the relation between depth of penetration and lumen diameter are shown. Because the relationship between the lumen diameter and the depth of penetration is often not linear and the data are not normally distributed normal linear regression was not used. Instead Spearman rank correlation coefficients were used to evaluate the correlation between lumen diameter and the depth of penetration. This statistical technique has the advantage that it does not require normal data distribution or a linear association between the data to be correlated [13].

Table 3.3   Spearman rank correlation coefficients between depth of penetration and cell-diameter.

		wood species and application type						
	bindertype	pine sapwood				spruce heartwood		
		brushed		dipped		brushed		dipped	
		cc	n	cc	n	cc	n	cc	n
pigmented	WAD300	0.359**	117	0.562**	104	0.438**	147	0.549**	81
	WAD100	0.461**	126	0.658**	102	0.595**	117	0.687**	119
	WBA	0.602**	119	0.587**	126	0.858**	148	0.782**	109
	HSA	0.418**	87	-0.503**	116	0.463**	98	0.314**	112
	SBA	-0.628**	94	n.s.	95	0.507**	102	0.486**	103
pigment paste	none	-	-	-	-	0.790**	134	0.319**	126
not-pigmented	WAD300	0.749**	90	0.461**	95	0.658**	92	0.326**	71
	WAD100	0.719**	126	0.482**	97	0.705**	87	0.758**	78
	WBA	0.612**	113	0.517**	85	0.542**	113	0.226**	87
	HSA	-0.665**	91	-0.607**	83	-0.245*	77	0.245*	92
	SBA	-0.454**	84	-0.480**	83	-0.347**	55	0.504**	90

cc: correlation coefficient   n.s: not significant
n: number of measurements   *: significant at 95% confidence level
-: not measured   **: significant at 99 % confidence level
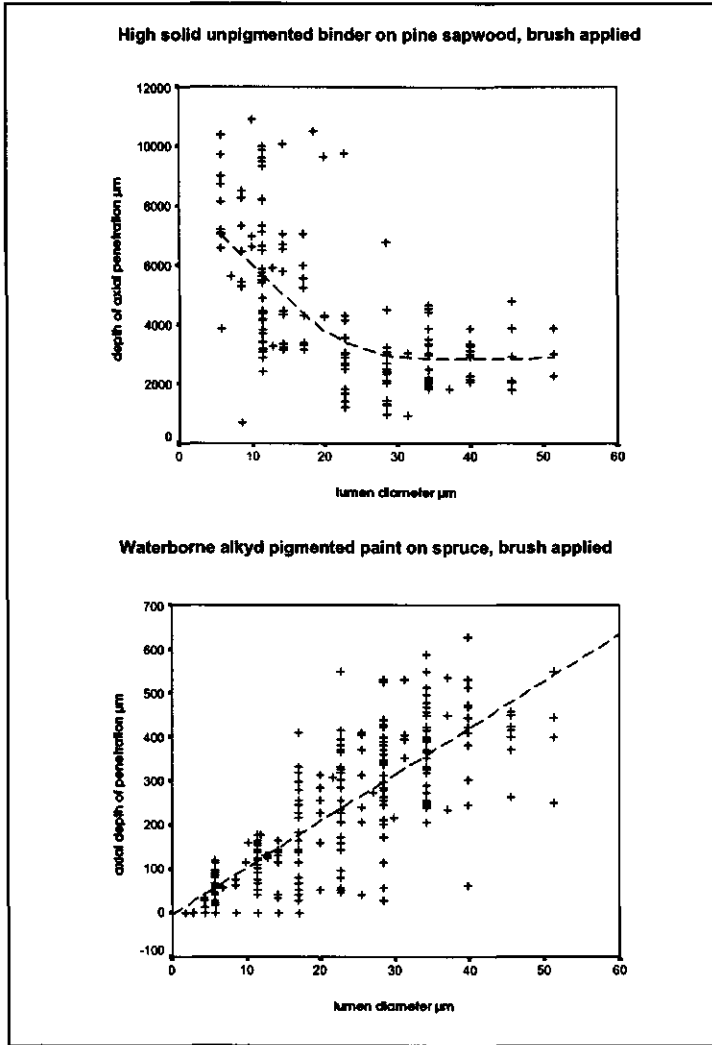
Figure 3.5   Two typical examples of correlation between tracheid diameter and depth of penetration.

Table 3.3 shows the Spearman rank correlation coefficients and the number of measurements. For all the waterborne pigmented paints and unpigmented binder solutions there is a highly significant positive correlation between the size of the lumina and the degree of axial penetration. For the HSA and SBA paints and binder the correlations are more complex. For the pigmented HSA paint there is a positive correlation between lumen diameter and penetration except for the sapwood samples which were dipped. For the pigmented SBA on pine sapwood there is a negative correlation if the paint is brushed or no correlation if the paint is dipped, but on spruce there is a positive correlation for both application types. The unpigmented HSA and SBA binders are penetrating more deeply if the lumen is smaller except if the coating is dipped on spruce wood.

3.4.4 Influence of wood moisture content

The influence of the wood moisture content on penetration was studied for the pigmented paint WAD300, WBA and SBA at the following three moisture contents: 2 %, 13 % and 28 %. The change in median depth of penetration with increasing wood moisture content is shown in *fig. 3.6*. Although for all three types of paint the penetration is deeper in case of higher wood moisture content, the effect is the strongest for the WAD300 paint. The effect of wood moisture shows that during the capillary penetration, transport of water or organic solvent from liquid paint to cell wall is influencing the penetration. With increasing wood moisture content the wood cell wall is less capable of absorbing water or organic solvent from the liquid paint. This will reduce the rate at which the solid matter content of the paint increases during the flow through the lumina. Because paint viscosity increases with solid matter content [6], the decrease of the capillary flow rate, which is directly dependent on viscosity, will be slower at higher wood moisture content.
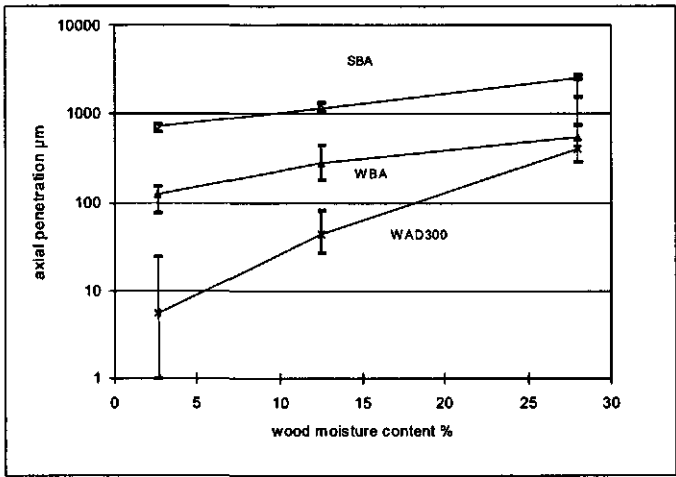
Figure 3.6.   Influence of wood moisture content on the median logarithmic depth of penetration of the pigmented WAD 300, WBA and SBA coating. Error bars indicate 25 % and 75 % percentiles.

3.4.5 Dynamic measurement of contact angle and droplet volume

The change of the contact angle, droplet diameter and droplet height was measured over a period of 200 to 300 seconds after the application of the coating or binder solution to the axial wood surface. The change in the contact angle for the pigmented paints on spruce is given in *fig. 3.7*. Both acrylic paints WAD100 and WAD300 have an initial contact angle of about 100 °, which is an indication of incomplete wetting. The contact angle hardly decreases during the measurements and after a day, when the coating has completely dried, the coating is still present as a droplet that has poorly wetted the substrate. The alkyd emulsion paint (WBA) has an initial contact angle of about 65 ° which decreases rapidly in the first 50 seconds but at a later stage the decrease is very slowly. The HSA and SBA coating also show a very fast initial decrease in contact angle in the first 50 seconds but this stage is followed by an ongoing decrease in contact angle. The HSA droplet even penetrates the wood completely within 175 seconds after application. The wood species did not influence the rate of change of contact angles or volume of the paint droplets.
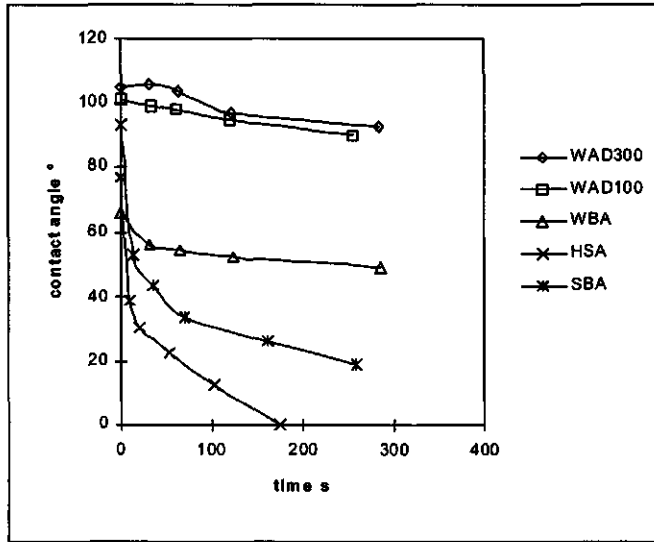
Figure 3.7 Change of the contact angle as a function of time for pigmented paint on spruce.
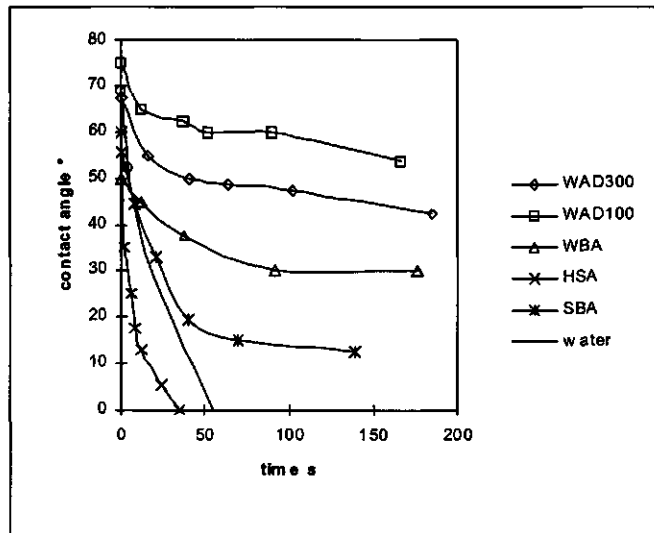
Figure 3.8   Change of the contact angle as a function of time for unpigmented binder on pine sapwood.

The change of the contact angle of the unpigmented binder solutions with time is shown in *fig. 3.8* for the pine samples. On spruce very similar results were obtained. The initial contact angles are much lower than for the pigmented paints for all types of coatings. The waterborne binders have a decreasing contact angle during the first 100 seconds but later on an equilibrium contact angle is reached. Unlike the pigmented paints there is now a clear difference between the two types of acrylic binders WAD100 and WAD300. The unpigmented solventborne alkyd (SBA) shows a more rapid change in contact angle, very

much comparable to the results of the pigmented coating. The HSA binder has a very rapid change in contact angle and the droplet fully penetrates the substrate within 40 seconds. Water and white spirit were also measured as reference liquids. Water shows a very rapid change in contact angle and the droplet disappears within 50 seconds. The white spirit penetrates the wood immediately, therefore no contact angles could be measured.

From existing literature [14, 11, 15] it is known that the contact angle of a liquid on a porous substrate is not only determined by interfacial forces but also by capillary penetration. In this study the degree of capillary penetration of the coatings is evaluated in two ways: firstly by the measurement of droplet height and diameter as a function of time and secondly by calculation of the droplet volume according to the two models described in *equations 3.8* and *3.9*.
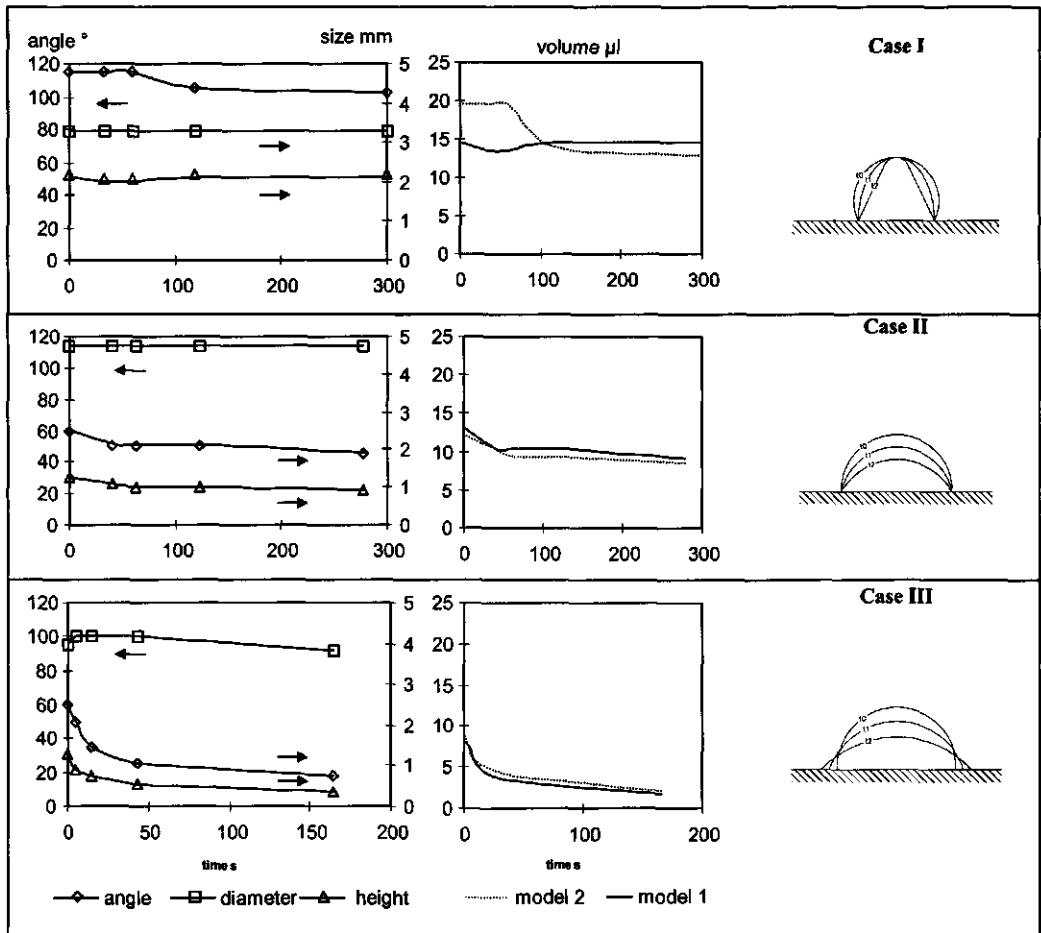
Figure 3.9   Three cases of the change of droplet shape, contact angle and volume as a function of time.

By simultaneous analysis of droplet height, droplet diameter and contact angle, the following three different cases of combined wetting and capillary penetration have been found (also illustrated in *fig. 3.9*):

Case I: Diameter and height of the droplet remains constant over the entire measuring period, in other words, the droplet does not spread over the wood. The contact angle is constant during the first 80 seconds but between 80 and 100 seconds there is a small decrease in contact angle. The change in contact angle must be the effect of a decrease in droplet volume, which is caused by the transition from a spherical to a conical shape. During this transition the height of the droplet does not change. This type of droplet volume change is observed for the acrylic paints, which have both the highest viscosity and the highest surface tension. Whether the change in volume is an effect of substrate penetration is not sure; it could also be caused by evaporation of water into the surrounding air. Because model 1 [11] calculates the volume from the height and the diameter, which are not changing, it fails to predict the decrease of the droplet volume. Model 2 [8] uses the changing contact angle to calculate the volume. This gives an accurate description of the volumetric change.

Case II: Droplet diameter remains constant during the wetting, which means that spreading of the liquid does not occur, but height and contact angle are decreasing. This type of wetting is mainly found for the alkyd emulsion paints (WBA) which combines a relatively high surface tension with a relatively low viscosity when compared to the acrylic paints. Both models predict almost identical volumetric changes.

Case III: In this case the contact angle and height of the droplet decrease during the first 50 seconds. The droplet diameter is not stable. Initially often an increase in diameter is observed, which indicates spreading of the liquid. Later on the diameter remains constant or a slight decrease is found, the latter is due to the ongoing penetration of the liquid into the wood. This case is identical with the description of the wetting of beech by water described by Liptáková and Kúdela [11]. Both model 1 and 2 give an adequate description of the volumetric changes of the droplet as a function of time. The case III wetting process is found for the HSA and SBA paints and all the binder solutions. This indicates that this type of wetting is typical for liquid with a low viscosity, the surface tension seems to be of less importance here.

Because model 2 is the one, which is most generally applicable, it was used to calculate the volumetric changes of the droplets as a function of time. The rate of volumetric capillary uptake of the coating is calculated according the following formula:

$$\frac{V_p}{V_o} = \frac{V_o - V_t}{V_o} = b\sqrt{t} \quad \text{and} \quad V_0 = V_t + V_p \tag{3.10}$$

V_p	:	volume of coating penetrated into the wood	(μl)
V_t	:	droplet volume at given time t	(μl)
V_0	:	droplet volume at given t = 0	(μl)
t	:	time	(s)
b	:	rate constant	($s^{-1/2}$)

For most of the samples there is fairly good linear relationship between the square root of time and the fractional penetrated coating volume (V_p / V_o) with r^2 values of 0.75 or higher. Because the rate constants are not normally distributed, medians instead of means are calculated. They are given in *table 3.4.*

The rate of capillary uptake varies with the binder type and the pigmentation. The rate of uptake is higher for the unpigmented binder, which can be easily explained by the lower viscosity of these liquids. The waterborne products show a lower rate of uptake, also for the unpigmented binders. This is remarkable because the viscosity of the unpigmented waterborne binders is not higher than of the solventborne ones. This result supports the idea that viscosity during penetration is rapidly increasing because of the absorption of water into the cell walls, which causes an increase in solid matter content. The HSA binder and pigmented coating has the highest rate of uptake, for the unpigmented binder even higher than the rate of uptake of water. Because the HSA binder has the lowest molecular weight it can be

expected that viscosity increase will be slower than for the other products. No significant differences between pine sapwood and spruce have been found. This indicates that during the initial capillary uptake the penetration is not limited by the permeability of the wood.

Table 3.4   Median rate of capillary uptake $(s^{-1/2})$

	pine sapwood		spruce	
	paint	binder	paint	binder
WAD100	-0.019	-0.036	-0.026	-0.022
WAD300	-0.024	-0.022	-0.016	-0.051
WBA	-0.016	-0.036	-0.016	-0.042
HSA	-0.079	-0.230	-0.078	-0.139
SBA	-0.054	-0.092	-0.052	-0.109
water	-0.162		-0.136	

3.4.6 Comparison of the measured data with the theoretical models

Knowing all the variables used in *equation 3.4* and *3.5*, it is possible to calculate depths of penetration and compare them with the measured ones. *Table 3.5* shows both measured and calculated depths of penetration. In this case the time for capillary penetration is assumed to be equal to the dipping or brushing time (approximately 7.5 seconds) and the median tracheid diameter is 23 μm. The contact angle in equation 4 is actually the contact angle of the liquid wetting the inside of the capillary. Because this value can not be measured directly during penetration, the equilibrium contact angle of the liquid droplet on top of the axial surface is used instead. For the waterborne coatings the contact angle reaches an equilibrium value. For the HSA and SBA coatings the angle is continuously decreasing, therefore complete wetting (zero contact angle) is assumed. Comparing the contact angles on the surface with the contact angles between cell wall and liquid inside the wood measured after drying the latter ones are smaller. This effect may be caused by drying effects.

Table 3.5   Comparison of measured and calculated data

	pigmented paint			unpigmented binder		
Bindertype:	contact angle°	calculated depth μm	measured depth μm	contact angle°	calculated depth μm	measured depth μm
WAD100	90	0	28	60	9185	1718
WAD300	90	0	10	48	11755	1594
WBA	50	220	148	30	14894	1786
HSA	0	1160	2156	0	2590	3280
SBA	0	595	1812	0	925	3115

tracheid diameter: 23 μm   contact-time: 7.5 s

As can be seen from *table 3.5* the Washburn-equation predicts the penetration of the waterborne coatings rather well. The almost zero penetration of the waterborne coatings is a combined effect of high viscosity and incomplete wetting of the cell capillary. The calculated depths of penetration for the waterborne binders are 5 to 8 times higher than the measured ones. This once again indicates that the viscosity during penetration can not be considered as

constant, due to increasing solid matter content and therefore increasing viscosity. By comparing measured and calculated data, it can be estimated that the actual average viscosity during penetration must be a hundred times higher than that of the starting liquid.

The Washburn-equation (*equation 3.4*) underestimates the penetration of both the pigmented and unpigmented HSA and SBA coating. Sometimes a negative correlation between depth of penetration and capillary radius is observed (see *table 3.3*). Therefore *equation 3.5* for capillary rise may seem to be a more appropriate one for these coatings. Fitting the data into *equation 3.5*, the depths of penetration become much too high, about 40,000 μm for the pigmented paints and 60,000 μm for the unpigmented binders. This shows that the effect of the viscosity can not be excluded from a model for capillary penetration. Future research has to clarify why the physical models for capillary penetration fail to describe all experimental cases.

3.5 Conclusions

Two new methods for quantitative measurements of coating penetration have been developed and successfully applied to compare the behaviour of different pigmented and unpigmented coatings. Both methods give complementary rather than interchangeable information on coating penetration. The static measurement of axial depth of penetration shows how deep a coating can penetrate in axial direction into the wood. The results show a large degree of variation, but differences between paints and binders can nevertheless be identified. Waterborne acrylic coatings show the lowest penetration. The deepest penetration is found for the high solid and solventborne coatings. The waterborne alkyd emulsion is in between these two classes of coatings. These findings are in very good agreement with qualitative descriptions of coating penetration found in a previous study [1]. Apart of the variation in penetration depth within a sample can be explained by the radius of the cell capillary. In most cases the coating penetration increases with capillary radius, but some exceptions to this are found for the HSA and SBA coating. The permeability of the wood plays a part in the case of coatings that penetrate very deeply.

The dynamic measurement of contact angle, droplet shape and volume gives information about the initial stage of coating penetration. The wetting process is strongly influenced by capillary penetration, which means that the viscosity is of importance for the wetting process as well. Three different cases of wetting were identified and explained by differences in viscosity and surface tension of the paint. The waterborne paints and binders show incomplete wetting of the wood with contact angles between 40 and 90 °. From droplet diameter and height or droplet diameter and contact angle the volume of the droplet can be calculated. The model which includes radius and contact angle [8].

The viscosity of the paint can explain most of the differences in penetration of the pigmented paints as long as the low-shear viscosity values of the non-Newtonian paints are used. The penetration capacity of a waterborne dispersion or emulsion is controlled by the thickeners, used to give the coating an acceptable application viscosity. Increasing the viscosity for this purpose reduces the penetration of the paint into the wood cells. In general brushing a paint gives deeper penetration than dipping the same paint. This can to a great extent be explained by the rheological behaviour of the coating. The surface tension appears to be of only minor importance. Differences in molecular weight and particle size between the binders studied cannot be related to differences in penetration. Increasing penetration with increasing wood moisture content shows that the viscosity of a waterborne coating is not constant during the penetration. Most likely the viscosity strongly increases due to a rise in solid matter content caused by migration of water into the cell wall. This can also explain differences in penetration of unpigmented binders, which do not differ much in starting viscosity.

The capillary penetration of pigmented waterborne coatings can be reasonably well described with the Washburn equation but for other types of coatings large deviations are found. For waterborne binders the overestimation of penetration depth is due to not incorporating the increasing viscosity in the model. The penetration of the solventborne coatings is underestimated by this model. The reason for that phenomenon is not yet completely understood. In general the outcome of this study can explain many of the differences in degree of penetration between the different coatings and binders. But for the development of a general physical model for capillary penetration of coatings into wood additional research is needed.

Acknowledgements

References

[1]   **Meijer, M. de; Thurich, K.; Militz, H.**;Comparative Study on Penetration Characteristics of Modern Wood Coatings, Wood Science and Technology, 32, 1998, 347-365.

[2]   **Nussbaum, R.M.**; Penetration of water-borne alkyd emulsions and solvent-borne alkyds into wood, Holz als Roh- und Werkstoff, 52, 1994, 389-393.

[3]   **Rødsrud, G.; Sutcliffe, J.E.**; Alkyd emulsions - properties and application. Results from comparative investigations of penetration and ageing of alkyds, alkyd emulsions and acrylic dispersions, Presentation held at the 14th Congress of the Federation of Scandinavian Paint & Varnish Technologists – Copenhagen, 1993.

[4]   **Meijer, M. de; Militz, H.; Thurich, K.**; Surface interactions between low VOC-coatings and wooden substrates, Proceedings of the XXIII Fatipec Congress Brussels, Volume C, 1996, 191-214.

[5]   **Schneider, M.H., Sharp, A.R.**; A model for the uptake of linseed oil by wood, Journal of Coatings Technology, 54 (693), 1982, 91-96.

[6]   **Patton, T.C.**; Paint Flow and Pigment Dispersion: A Rheological Approach to Coating and Ink Technology, 2nd edition. John Wiley and Sons, New York, Chichester, Brisbane, Toronto, Singapore, 1979.

[7]   **Banks, W.B.**; Addressing the Problem of Non-Steady Liquid Flow in Wood, Wood Science and Technology, 15, 1981, 171-177.

[8]   **Denesuk, M.;,Smith, G.L.; Zelinski, B.J.J.; Kreidl, N.J.; Uhlmann, D.R.**; Capillary Penetration of Liquid Droplets into Porous Materials, Journal of Colloid and Interface Science, 158, 1993, 114-120.

[9]   **Siau, J.F.**; Transport Processes in Wood, Springer Series in Wood Science, Berlin, Heidelberg, New York ,Tokyo, 1984.

[10] **Blom, C.; Jongschaap, R.J.J.; Mellema, J.**; Inleiding in de Reologie; Reometrie, Dispersiereologie, Polymeerreologie, Universiteit Twente - Kluwer Technische Boeken, Deventer, 1991.

[11] **Liptáková, E.; Kúdela J.**; Analysis of the Wood-Wetting Process, Holzforschung, 48, 1994, 139-144.

[12] **Liese, W.; Bauch, J.**;On the closure of bordered pits in conifers, Wood Science and Technology, 1, 1967, 1-13.

[13] **SPSS**; SPSS® Base 7.5 Applications Guide. SPSS Inc. Chicago, 1997.

[14] **Borhan, A.; Rungta, K.K.**; An Experimental Study of the Radial Penetration of Liquids in Thin Porous Substrates, Journal of Colloid and Interface Science, 158, 1993, 403-411.

[15] **Scheikl, M.,; Dunky, M.**; Softwareunterstüzte statische und dynamische Kontaktwinkelmeßmethoden bei der Benetzung von Holz, Holz als Roh- und Werkstoff, 54, 1996, 113-117.

4. A rheological approach to the capillary penetration of coatings into wood[*]

Summary

The capillary penetration of coatings into wood and the drying behaviour of unpigmented coatings on wood were studied and discussed with four different polymeric binder types including waterborne dispersions, emulsions and solventborne solutions. The influence of thickeners and surfactants was also taken into account. The rate of capillary penetration of a coating into wood can be described by the Washburn-equation. Accordingly, the rate of capillary penetration is proportional to the capillary radius, the liquid surface tension and the cosine of the contact angle and inversely proportional to the viscosity and the height of rise of the liquid in the capillary.

During drying and penetration of a coating that is applied on wood, a large amount of either the water or the solvent is selectively taken up by the cell wall. Hence, the solid matter content of the coating will increase during penetration into the wooden capillary. To estimate the amount of water taken up by the wood, the evaporation of a coating on wood and glass was compared. From the period during which the evaporation rate was constant and the mass fraction polymer at the end of the constant drying period, the evaporation rate to the wood was estimated. The magnitude of the evaporation rate to the wood depended on the type of binder and was at least as large as the evaporation rate to the air. This means that the mass fraction polymer, and subsequently the viscosity, will increase more rapidly on wood in comparison to an inert substrate.

The viscosity of the binders was measured at increasing mass fractions from 0.33 to 0.55 at shear rates between 0.1 and 100 s^{-1}. In particular the waterborne binders showed a very rapid increase in viscosity at higher mass fractions, especially at lower shear rates. The rapid increase in viscosity appeared to be the limiting factor in the penetration in most cases. However, the liquid surface tension and wetting also changed with increasing mass fraction polymer and might limit the penetration as well. Studies with increasing levels of thickener at the same mass fraction of binder showed a decrease in capillary uptake into the wood. At higher levels of thickener the selective uptake of water increased and the amount of binder that penetrated the wood was reduced.

The capillary penetration of various binders was determined experimentally and considerable differences between binder types were observed. Comparison of the experimental data with the model calculations, showed that the viscosity was actually more rapidly increasing than it was predicted from model calculation based on independent evaporation rate, surface tension and viscosity measurements.

Studies with solutions of surfactant in water showed decreasing penetration with increasing surfactant concentration if the wetting of the wood was complete. This was even observed above the critical micelle concentration, which might be explained by the fact that surfactants were adsorbed on the wood surface. Surfactant adsorption will deplete the surfactant solution inside the capillary, which will increase the actual surface tension of the liquid during penetration.

[*] **Mari de Meijer, Barend van de Velde and Holger Militz**
To be submitted to Journal of Coatings Technology

4.1   Introduction and theoretical background

The flow of polymeric liquids into the capillary pore structure of wood takes place in many practical situations. The penetration of a coating into a wooden substrate is one important example [1] but it also applies to the wetting and spreading of glues on wood [2] and the treatment of wood with polymer containing preservatives or water repellents [3,4]. The need to avoid the use of volatile organic compounds has caused a substantial change from solvent-based solution polymers to polymers that are dispersed or emulsified in water. The water based polymeric liquids generally contain a large amount of smaller surface active molecules which are used during manufacture of the polymer, to stabilise the product or to improve wetting by reducing liquid surface tension.

Previous research on the penetration of coatings into wood focused on: the morphological or anatomical aspects of the wooden substrate [1,5], the influence of binder type [6] or on the impact of the particle size or molecular weight within one category of polymer [7,8]. In numerous publications [9,10,11,12] the principle of capillary penetration is based on the Washburn-equation [13] which is derived from Poiseuille flow (*equation 4.1*) with the capillary pressure (P_c) minus the counter pressure due to gravity (P_g) as driving force for the flow [14]. Frequently, the influence of gravity has been neglected. If penetration depth is small this gives only a minor error, but at the equilibrium height of rise considerable deviations will occur.

For a cylindrical capillary this gives:

$$\frac{V}{t} = \frac{\pi P r^4}{8 \eta h} \tag{4.1}$$

$$P = P_c - P_g \qquad P_c = \frac{2 \gamma_L \cos \theta}{r} \qquad \text{and} \quad P_g = \rho g h \tag{4.2}$$

V	:	volume	(m³)
P	:	pressure	(Pa)
r	:	capillary radius	(m)
h	:	height (or distance) of capillary rise	(m)
A	:	area	(m²)
t	:	time	(s)
g	:	acceleration of gravity constant	(9.8 m s⁻²)
η	:	viscosity of the liquid	(Pa s)
γ_L	:	liquid surface tension	(mN m⁻¹)
θ	:	contact angle between liquid and wood	(°)
ρ	:	density of the liquid	(kg m⁻³)

With V= A h and A= πr^2 the following expression for the rate of capillary rise is obtained:

$$\frac{dh}{dt} = \frac{2 \gamma_L \cos \theta \, r - \rho g \pi h r^2}{8 \eta h} \qquad \text{if } \cos \theta > 0 \ (\theta < 90°) \tag{4.3}$$

The relationship between liquid surface tension and contact angle is given by the Young's equation:

$$\gamma_L \cos \theta = \gamma_S - \gamma_{SL} \qquad \text{if } \cos \theta < 1 \ (\theta > 0°) \tag{4.4}$$

The term $\gamma_L \cos \theta$ is determined by the difference between the surface tension of the solid (in equilibrium with air) (γ_S) and the interfacial tension (γ_{SL}) between the wood (solid) and the coating (liquid). If the wetting by the liquid is complete ($\theta = 0$; $\cos \theta = 1$), *equation 4.4* no longer applies and a decrease of the liquid surface tension will lower the capillary pressure. The rate of capillary rise is positively influenced by the capillary radius and negatively by the

viscosity and the height of rise. The maximum depth of capillary penetration is reached for the point where dh/dt approaches zero.

For a polymer containing liquid that penetrates the capillary cell structure of wood, none of the variables in *equation 4.3* can be considered constant with respect to either time or height of rise. In softwoods the capillary radius will vary between 3 and 30 μm [15] with the position of the cell in the wood (earlywood with wider and latewood with narrower cells) and with the length of the individual cell because the diameter decreases at the taper end of a tracheid [16]. Previous studies have shown that the penetration of a coating varies with capillary radius [17,18]. The micro-pores in the cell wall of the wood capillaries, with a size of 0.1- 1 nm [19], will only allow the lower molecular weight materials (Mw approximately below 3000 g mol^{-1}) [20,21,22,23] to enter the cell wall. The larger polymeric molecules will remain inside the capillary. The above mentioned process is visualised schematically in *fig.4.1*.The selective removal of solvent or water during the penetration process will increase the polymer fraction in the liquid and hence the viscosity of the solution. The wetting and the liquid surface tension might also be influenced by the increasing polymer concentration.
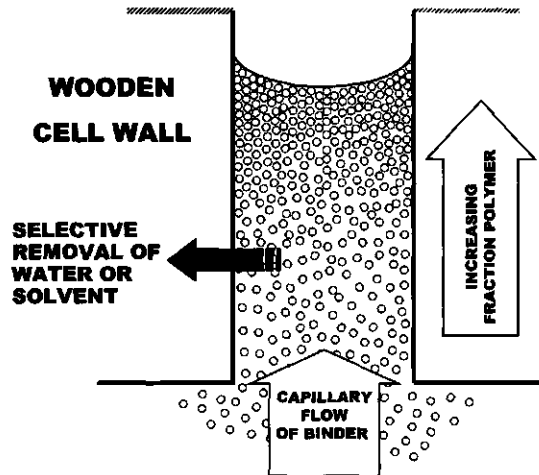
Figure 4.1 Schematic overview of the transport processes during penetration of a liquid containing polymeric material into a wood cell capillary.

The increase in polymer concentration during the capillary penetration into a wood pore can not be measured directly, since this would require an in situ measurement of water or solvent transport from liquid to cell wall, which is not possible with existing measurement techniques. The rate of transfer of water or solvent from a coating to the wooden substrate might however be estimated from a comparison of the evaporation rates on wood and an inert substrate like glass. This can be explained as follows, using existing theories for the drying of waterborne latex [24,25,26,27].

During the initial drying of a waterborne dispersion coating the rate of evaporation is constant and depends only on the environmental conditions. The polymer particles are assumed to be mobile in the water phase, evaporation takes place directly from the liquid water reservoir and the dry layer of polymer on the surface is not limiting the evaporation rate. During the initial stage, evaporation is independent of the coating thickness. The mass fraction polymer in the coating during the first drying stage is given by:

$$\phi_m(t) = \frac{m_p}{m_p + m_o - qAt} \quad \text{and} \quad \frac{dm}{dt} = -qA \tag{4.5}$$

ϕ_m (t)	:	mass fraction of polymer at time t	(-)
m	:	mass of coating	(kg)
m_o	:	mass of water or solvent at t=0	(kg)
m_p	:	mass of polymer	(kg)
A	:	surface area	(m^2)
q	:	evaporation rate of water or solvent	(kg m^{-2} s^{-1})

After the first drying stage, the evaporation rate is no longer constant because the agglomeration and the coalescence of polymer particles reduce the evaporation of water. At this stage, the evaporation rate becomes dependent on film thickness. In a plot of cumulative mass loss against drying-time the end of the first drying stage can be recognised by a deviation from the initial straight line. The time at which this occurs is here indicated by t_1 and the corresponding mass fraction polymer by $\phi_m(t_1)$. $\phi_m(t_1)$ can be considered as a coating property and is in principle independent from the time required to reach the end of the first drying stage.

During the first drying stage of a coating on wood, water or solvent will evaporate to the air and will be taken up into the wood. Later in the drying process, water or solvent originally taken up into the wood might evaporate again through the dried coating but this will take considerably longer. On a wooden substrate, the mass fraction polymer in the coating during the first drying stage is now given by:

$$\phi_m(t) = \frac{m_p}{m_p + m_o - At(q^a + q^w)} \tag{4.6}$$

q^w	:	water or solvent evaporation rate to wood	(kg m^{-2} s^{-1})
q^a	:	water or solvent evaporation rate to air	(kg m^{-2} s^{-1})

The evaporation rate to the air can be measured directly from the mass-loss during drying. This can most accurately be measured on an inert substrate like glass, but might also be measured from the evaporation rate to the air from a coating applied on wood if all water or solvent taken up into the wood is released after the end of the first drying stage. During the initial drying stage, evaporation rates of water or solvent to the air should be equal regardless of the fact whether the coating is applied on wood or glass because in both cases the evaporation occurs from a liquid reservoir inside the coating film.

The evaporation rate to the wood can not be measured directly. However on wood, the end of the first drying stage will be reached earlier because the evaporation occurs into two directions. The time when the first drying stage on wood ends, is denoted by t_1' with $t1' < t_1$ if $q^w > 0$. The mass fraction polymer corresponding to the end of the first drying stage is however independent of time or substrate and hence $\phi_m(t_1) = \phi_m(t_1')$. This means that:

$$\phi_m(t_1') = \phi_m(t_1) = \frac{m_p}{m_p + m_0 - t_1'A(q^a + q^w)} \Leftrightarrow q^w = \frac{m_p + m_0 - \dfrac{m_p}{\phi_m(t_1)}}{t_1'A} - q^a \tag{4.7}$$

The evaporation rate to the wood can be derived from *equation 4.7* by determining q^a from the evaporation rate to the air (on glass or wood). From the mass loss curves on glass the end of the initial drying period (t_1) is determined and the corresponding $\phi_m(t_1)$ can be calculated. Finally, t_1' follows from the end of the constant evaporation rate during the drying of the coating on wood.

If it is assumed that the evaporation rate of water or solvent to the wood, as derived from a film on the surface, is equal to the evaporation rate by the coating inside the capillary to the cell wall, the increase in mass fraction polymer inside the capillary can be calculated as a function of time. This assumption can be justified by the fact that the drying film is in direct contact with the wooden cell wall, just like the coating inside the wood capillaries. Evaporation of water to the surrounding air during capillary uptake might be considered as zero as long as the wood is in direct contact with the liquid reservoir. The mass fraction polymer ($\phi_{cm}(t)$) inside the cylindrical wood capillary is then given by:

$$\phi_{cm}(t) = \frac{m_p}{m_p + m_0 - q_w A_c t} = \frac{V\rho f}{V\rho - q_w A_c t} = \frac{0.5\, r\, \rho\, f}{0.5\, r\, \rho - q_w t} \tag{4.8}$$

$\phi_{cm}(t)$	:	mass fraction polymer inside wood capillary	(-)
V	:	volume of the liquid filled part of the capillary ($\pi r^2 h$)	(m^3)
A_c	:	contact area between liquid inside capillary and cell wall ($2\pi r h$)	(m^2)
f	:	mass fraction solid of the coating	(-)
ρ	:	density of the polymeric liquid	(kg m^{-3})

The density of the polymeric liquid in principle depends on the mass fraction polymer but might be considered constant as long as the density of polymer and water or solvent are approximately equal.

The relation between the relative viscosity of a dispersion, or a concentrated emulsion [28], and the volume fraction of polymer particles can be described by the equations of Mooney [29] (*equation 4.9a*), Dougherty and Krieger [30] (*equation 4.9b*) or Frankel and Acrivos [31] (*equation 4.9c*).

$$\ln\frac{\eta}{\eta_0} = \frac{2.5\phi}{1 - \phi/\phi_{max}} \;(4.9a); \quad \frac{\eta}{\eta_0} = \left(1 - \phi/\phi_{max}\right)^{-2.5\phi_{max}} \;(4.9b); \quad \frac{\eta}{\eta_0} = \frac{9}{8}\frac{(\phi/\phi_{max})^{1/3}}{1 - (\phi/\phi_{max})^{1/3}} \;(4.9c)$$

η	:	viscosity of the polymeric liquid	(Pa s)
η_0	:	viscosity of the continuous phase (water or solvent)	(Pa s)
ϕ	:	volume fraction of polymer	(-)
ϕ_{max}	:	volume fraction polymer at which the viscosity goes to infinity	(-)

The sharply increasing viscosity close to ϕ_{max} will very rapidly decrease the capillary penetration rate and will eventually limit the penetration.

For many latex or dispersion paints, the viscosity also depends on the applied shear rate, in particular if thickeners or pigments are added [32,33]. The shear rate at the wall of a cylindrical capillary during the rise of the liquid is given by *equation 4.10* as a function of the capillary radius and the rate and height of capillary rise [34].

$$\tau_w = \frac{3+b}{r}\left(\frac{dh}{dt}\right) \quad \text{with} \quad b = \frac{d\log(dh/dt)}{d\,\log((h_\infty - h)/h)} \tag{4.10}$$

τ_w	:	shear rate at the wall of the capillary	(s^{-1})
h_∞	:	equilibrium height of rise	(m)

The factor b can be determined from a plot of the rate of capillary rise against the fractional height of rise. For Newtonian liquids b was found to be one, whereas for pseudoplastic liquids b > 1. E.g. for a 4% solution of polystyrene in toluene b was found to be about 1.2 [34].

The aim of this work is to understand the penetration process of a polymer containing liquid into cell capillaries of wood. The factors that will influence the penetration rate, like

viscosity, wetting and liquid surface tension are studied as a function of increasing mass fraction polymer. From this information the maximum penetration depth was calculated and compared with the data obtained experimentally. The capillary penetration process has been studied with four different commercially used polymeric binders, intended for the use in wood primers. Additional work involved studies on the influence of addition of thickeners to the binders and the effect of surfactants on the capillary uptake of water.

4.2   Experimental

4.2.1   Materials
The following commercial polymeric binders were used:
- ACEMUL: an emulsion of acrylic binder in water, particle size was not specified.
- ACDIS: a waterborne acrylic dispersion with a monomodal particle size of about 50 nm.
- ALKEMUL: an alkyd resin emulsified in water with a weight averaged molecular weight of 50.000 g mol^{-1} and a particle size about 500 nm. The oil-length was about 63 %.
- SOLVALK: a solventborne alkyd dissolved in white-spirit with a weight averaged molecular weight of 109.000 g mol^{-1} and an oil-length of about 63 %.

The binders where first diluted to approximately the same solid matter content of 33 % with respectively demineralised water or white spirit. Detailed mass fractions are given in *table 4.2*.

From all four binders three additional samples with three increased levels of viscosity were prepared by carefully adding a suitable thickener until a viscosity of approximately 2, 13 and 60 Pa s was reached (as measured with a Haake-FW viscosity meter at 180 rotations per minute). The waterborne binders were thickened with associative thickeners in a concentration range between 30 and 90 g l^{-1}. The solventborne binder was thickened with a bentonite paste in a concentration range between 25 and 65 g l^{-1}. After addition of the thickeners, the viscosity of the samples was measured over a range of shear-rate. *Table 4.1* shows the viscosities of the unthickened and thickened binders at shear-rate between 0.1 and 1000 s^{-1}. The four levels of viscosity are indicated with the codes I,II,III and IV.

Table 4.1 Viscosities (Pa s) of the binders at different levels of thickening and shear rates.

Binder type	Viscosity-level	Shear rate (s^{-1})				
		0.1	1	10	100	1000
ACEMUL	I	-	-	0.007*	0.007	0.007
	II	-	-	0.013*	0.013	0.012
	III	203	32	5.3	1.0	-
	IV	2457	331	61	8.6	-
ACDIS	I	-	-	0.03*	0.03	0.02
	II	-	1.4	0.85	0.42	0.16
	III	17	7.6	2.6	0.75	0.21
	IV	275	38	6.9	1.5	0.35
ALKEMUL	I	-	-	0.005*	0.005*	0.005
	II	-	2.9	0.37	0.06	0.02
	III	-	-	1.4	0.20	0.05
	IV	222	39	8.5	2.0	0.45
SOLVALK	I	-	-	0.03*	0.03	0.03
	II	22	3.1	0.50	0.12	0.07
	III	177	25	3.3	0.58	0.22
	IV	1132	153	18	3.0	-

*: extrapolated data   -: no data available

Apart from the addition of thickeners, the change of viscosity was also measured with increasing mass fraction polymer. The samples with increased solid matter content were prepared by evaporating the water or white spirit very slowly to avoid formation of a skin on the surface. Suitable conditions for this were 23°C and 55% relative humidity for the first 24 hrs., followed by 24 to 72hrs. at 75 % relative humidity and finally at 95 % relative humidity depending on the desired level of concentration. The solid matter content of the coating was determined afterwards by drying for 1hr. at 125 °C according to ISO-standard 3251. The density of the binders was measured with a pyknometer at the lowest mass fraction and densities were calculated for increased mass fractions of polymer. The density ranged between 1018 and 1034 kg m^{-3} for the water based samples and between 865 and 892 kg m^{-3} for the solvent based products depending on the concentration.

Four commercially available surfactants in demineralised water were used to prepare the aqueous solutions with reduced surface tension. Fluorinated alkyl polyoxyethylene ethanols were used as non-ionic surfactants, fluorinated alkyl quaternary ammonium iodides were used as cationic surfactant, potassium fluoralkyl carboxylates and sodium dodecylsulfate were used as anionic surfactants. The surfactants were used at at least two concentrations: around the critical micelle concentration and at a level 10 times above that concentration. All concentration were expressed in percentage of mass of commercial surfactant per mass of total mixture.

Pre-dried pine sapwood *(Pinus sylvestris)* with an initial moisture content of 8.5-9 % and a density of 500 kg m^{-3} was used to study capillary uptake because this wood species is known to have a very high permeability. Dry-mass of the wood was determined by drying at 103 °C until a constant weight was reached.

4.2.2 Viscosity, wetting and surface tension measurements

The viscosities of the thickened samples were measured at shear-rates between 0.01 to 1000 s^{-1} with a Bohlin controlled stress rheometer with a coaxial cylinder at a temperature of 23 °C The viscosities of the concentrated polymeric liquids were measured with a Rheolyst AR 1000N rheometer equipped with a cone and plate at a controlled shear-rate between 0.1 and 100 s^{-1}. The sample compartment was sealed from the environment to avoid drying during the measurement. All measured data were averages of the viscosities obtained with increasing and decreasing shear-rate. In general, the differences between these measurements were very small or even absent.

Surface tensions of the liquids were measured with Wilhelmy-plate method according to DIN-standard 53914. The contact angles were measured from coating droplets deposited on the wood with a digital video contact angle measuring device (Digidrop from GBX, France). The measurements were taken on the tangential surface of the wood parallel to the grain. Contact angles were taken as soon as the angle changed at a constant rate, which means that equilibrium conditions were reached.

4.2.3. Evaporation measurements

The evaporation of water or white spirit from the coatings applied on glass plates and wood boards (half-tangential surface) was measured by recording the weight loss as a function of time, at an accuracy of 0.1 mg with maximum time intervals of 2 min, on a analytical balance with automated data acquisition. The evaporation studies were carried out in a climate chamber of 50 % RH and 23 °C with a slow internal air circulation. The samples were protected by the glass cover on the front and backside of the balance but openings at the sides and top were opened to ensure air-circulation. All measurements were continued for at least 10 hours, but in most cases only the evaporation data during the first hours were effectively used. The evaporation rates were obtained from two or three replicates. The total area for evaporation was 0.009 m^2 and an initial wet film-thickness of approximately 140 μm

was applied with a film-applicator. The averaged total amount of coating applied is given in *table 4.2*.

4.2.4   Capillary uptake

The capillary uptake of the binder into the wood was recorded from the increase in mass (0.1mg accuracy) as a function of time. Wood blocks with dimensions of 15 x 12.5 x 20 mm (height x width x length) were hanging under a microbalance and were carefully brought into contact with the liquid by raising the liquid container. After the desired contact time, the liquid was lowered until contact with the liquid was lost. The excess amount of binder present on the surface was removed and the weight determined. Thereafter this procedure was repeated for the next time interval. The weight was recorded after approximately 15, 30, 60, 600 and 1800 seconds. Initially, attempts were made to record the weight continuously but this was impossible because of the disturbing influence of forces due to wetting of the edges of the wood blocks.

By sealing the sides of the blocks it was ensured that the capillary uptake could only occur through the axial surface (end grain) of the wood, which was previously smoothed on a microtome to obtain well defined open ends of the wood capillaries. All measurements were made in air of 23 °C and 50 % relative humidity with the penetrating liquid stored in a thermostatic bath with an accuracy of 23 ± 0.1 °C. The presented data are an average of 3-5 individual determinations.

Table 4.2   Initial mass fraction polymer ($\phi(t_0)$) and average amount of coating used in evaporation studies.

Binder type	viscosity-level	ϕ (t_0)	mass applied on glass (g)	mass applied on wood (g)
ACDIS	I	0.334	1.54	0.86
ACEMUL	I	0.326	1.84	1.55
ALKEMUL	I	0.326	1.58	1.16
SOLVALK	I	0.367	0.80	0.76
ACDIS	IV	0.342	0.81	1.02
ACEMUL	IV	0.334	1.00	0.93
ALKEMUL	IV	0.330	0.82	1.09
SOLVALK	IV	0.410	0.71	1.16

4.3.   Results and discussion

4.3.1   Evaporation rates-mass fraction polymer

The evaporation rate was measured for all four binders at two levels of viscosity: without addition of thickener (I) and with the highest concentration of thickener (IV). To make samples with different initial weights or solids contents comparable, the evaporation is expressed as a fraction of the total amount of water or solvent initially present. These fractional evaporation curves are shown in *fig. 4.2*. The differences between the wood and glass substrates were evident. On glass, the total amount of water or solvent present, evaporated completely within one to two hours. If the waterborne binders were applied on wood, 40 to 60 percent of the water was initially stored in the wood and evaporated only very slowly to the air. It took about 20 hours before all the water present in the coating evaporated to the air again. The white spirit in the solventborne binders (SOLVALK) was released from the wood far more rapidly. The influence of the thickeners on the fractional evaporation rates was dependent on the type of polymer. For the ACDIS binder no differences on glass were

observed and evaporation from wood proceeded slightly faster with a thickened binder. In combination with the ACEMUL and ALKEMUL binder, the fractional evaporation with thickener was somewhat faster on glass and in the case of the ACEMUL also on wood. These differences might however be due to the fact that a slightly higher amount of coating was applied at the lower viscosity level which means that the fractional evaporation will be lower if the absolute evaporation rate is independent from film thickness during the initial drying stage. The fractional evaporation on wood of the SOLVALK with thickener was faster then without, which might be explained by the fact that less material had penetrated the wood, which will facilitate a faster evaporation.
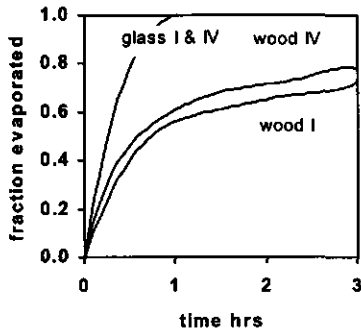
ACDIS   **ACEMUL**
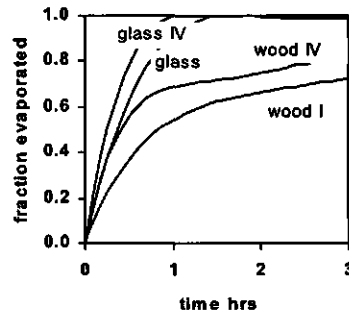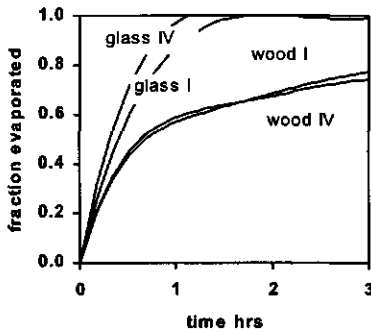
ALKEMUL   **SOLVALK**
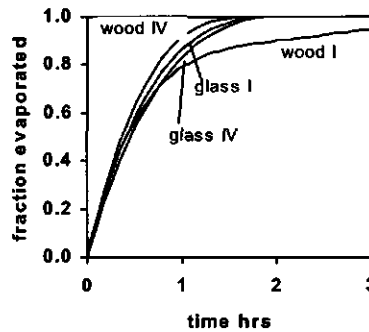
Figure 4.2   Fractional evaporation on glass and wood at viscosity level I and IV.

The evaporation rates during the first drying stage were determined from the linear part of a plot of mass loss against time for coatings applied on glass (denoted by q_{glass}^{air}) and on wood (denoted by q_{wood}^{air}). These data are given in *table 4.3*, typical mass loss – time plots are given in *fig. 4.3* and *4.4* for respectively the evaporation from glass and wood. The initial evaporation rate was approximately constant although in some case slight deviations from a straight line were observed which indicated slight changes in the evaporation rate during the initial stage. Nevertheless, the drying model described the experimental data fairly well, also for the alkyd emulsion (ALKEMUL) and solventborne alkyd binders (SOLVALK). From a

theoretical point of view, the initial evaporation rates to the air should be equal from coatings applied on glass or wood. In practice, some differences were observed but no consistent trend could be seen. With a wooden substrate, the constant rate period was shorter and subsequently the determination of the linear slope was less accurate. Therefore, the evaporation rates from glass were used to calculate the evaporation rate to the wood itself (q_w). The measured evaporation rates are comparable to data found in literature like $1.26\text{-}1.56 \times 10^{-5}$ kg m^{-2}s^{-1} [27], $1.1\text{-}3.4 \times 10^{-5}$ kg m^{-2}s^{-1} [35] and 6.67×10^{-5} kg m^{-2}s^{-1} [36] for various types of latex paints. Croll [26] reported values of 3.1, 3.5, 3.6 and 3.7×10^{-5} kg m^{-2}s^{-1} for the evaporation of water from respectively a latex, a paint, a titanium-dioxide slurry and pure water.

  The constant evaporation rate period on glass (t_1) lasted between 220 (ALKEMUL IV) and 900 (ACEMUL I) seconds, which was much shorter then the 4 hrs reported by Eckersley and Rudin [27] but in the same range as the results reported by Croll [26]. As expected the constant rate on wood (t_1') was considerable shorter which corresponded with the finding that the constant rate period decreased with film thickness [26]. On wood, the drying occurred to two sides, this can also be interpreted as a decrease of the effective film thickness. The mass fraction polymer corresponding to the end of the initial drying period was between 0.36 and 0.44 (see *table 4.3*) which was only slightly higher than the initial mass fraction polymer as given in *table 4.2*. The mass fraction polymer as a function of drying time is given in *fig.4.5*.
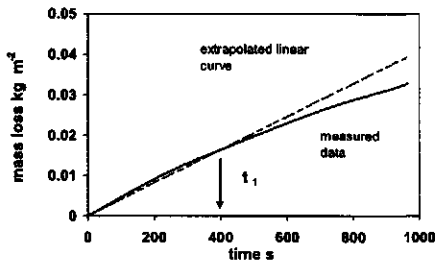
Figure 4.3
Mass-loss against drying time for ACDIS I on glass showing determination t_1.
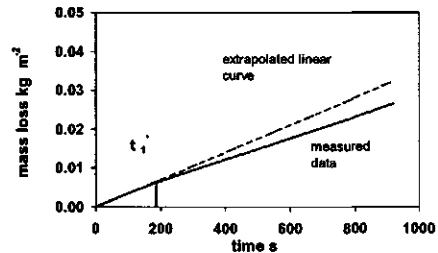
Figure 4.4
Mass-loss against drying time for ACDIS I on wood showing determination t_1'.

  The evaporation rates to wood (q^w) are given in *table 4.3* and were calculated according to *equation 4.7* With the unthickened binders, the evaporation to the wood is higher than to the air for the ACDIS and SOLVALK binder. Although with the latter, the white spirit was released from the wood much faster than the water as could be seen from the fractional evaporation plots (*fig. 4.2*). For the ACEMUL and ALKEMUL binder the evaporation to air and wood is about equal. Addition of a thickener reduced the evaporation to the wood considerably, which was mainly due to the shorter constant evaporation rate period and the lower corresponding mass fraction polymer. It might indicate also that the increase in viscosity, which will reduce the substrate penetration, had a marked effect on the amount of water or solvent transferred to the wood. The evaporation rate to the air, as measured most accurately on glass, was not much affected by the addition of thickener.
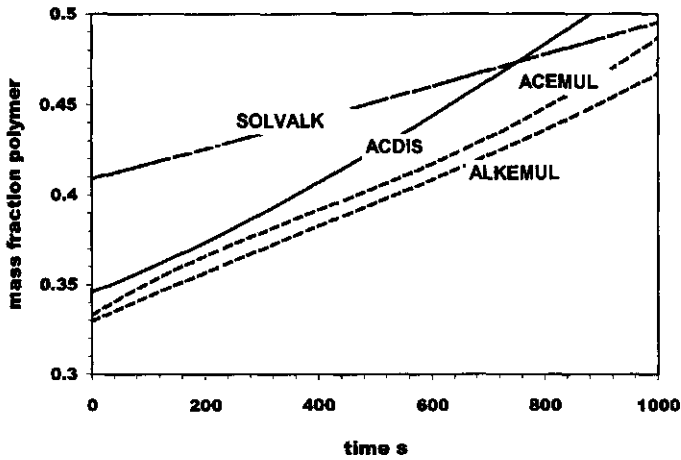
Figure 4.5 Mass fraction polymer as a function of drying time as determined on glass, viscosity level IV.

The mass fraction polymer inside a wood capillary as a function of time was calculated according to *equation 4.8* and is given in *fig.4.6* for the different binders for a capillary with a radius of 5 and 25 μm. The curves were extrapolated to higher mass fractions, mainly to show the differences clearly. In reality, some deviations might occur at high mass fraction because the evaporation rate will no longer be constant at high mass fractions. The influence of the evaporation rate to the wood and the capillary radius on the increase in mass fraction polymer can clearly be seen. For waterborne binders this is in good agreement with previous observations [1,18,37], where the deepest penetration was found in the widest capillaries. However, for solventborne binders the opposite was observed [37]. This might be an indication that for this binder *equation 4.3* was not valid all the time and that penetration was directly dependent on capillary pressure (*equation 4.2*) which predicts a deeper penetration with decreasing capillary radius.

Table 4.3 Evaporation data from binders applied on glass and wood.

Binder type	viscosity-level	q_{glass}^{air} (kg m^{-2}s^{-1})	q_{wood}^{air} (kg m^{-2}s^{-1})	t_1 (s)	ϕ_m (t$_1$)	t_1' (s)	q^{w*} (kg m^{-2}s^{-1})
ACDIS	I	4.10×10^{-5}	3.50×10^{-5}	400	0.40	220	8.71×10^{-5}
ACEMUL	I	3.35×10^{-5}	4.24×10^{-5}	900	0.42	680	3.31×10^{-5}
ALKEMUL	I	3.51×10^{-5}	5.04×10^{-5}	700	0.41	490	3.83×10^{-5}
SOLVALK	I	2.04×10^{-5}	3.54×10^{-5}	560	0.43	190	4.37×10^{-5}
ACDIS	IV	3.78×10^{-5}	3.16×10^{-5}	400	0.37	175	1.10×10^{-5}
ACEMUL	IV	3.95×10^{-5}	3.72×10^{-5}	550	0.38	290	0.21×10^{-5}
ALKEMUL	IV	3.47×10^{-5}	2.71×10^{-5}	220	0.36	200	1.27×10^{-5}
SOLVALK	IV	1.42×10^{-5}	2.09×10^{-5}	810	0.44	305	1.81×10^{-5}

*: determined on the basis of q_{glass}^{air} according to *equation 4.7*

4.3.2   Relation viscosity and polymer concentration

By careful evaporation of water or solvent, concentrated polymeric liquids up to 57 % solids were prepared from the polymeric binders without additional thickener. The viscosity was expressed relative to the viscosity of the continuous phase, which was 0.001 Pa s for the waterborne binders and 0.0012 Pa s for the solventborne binders. The change in relative viscosity with increasing mass fraction solids is given in the *fig. 4.7a* to *4.7d* for respectively the binders ACEMUL, ACDIS, ALKEMUL and SOLVALK. The viscosities are given at four shear rates of 0.1, 1, 10 and 100 s^{-1} respectively. The acrylic dispersion ACDIS showed a very sharp increase of the viscosity at higher mass fraction polymer, in particular at low shear rates. The viscosity of the acrylic emulsion (ACEMUL) also increased strongly with solid matter content but the dependence on shear rate was less pronounced. The viscosity of the alkyd emulsion (ALKEMUL) increased relatively slowly up to a mass fraction polymer of 0.55. Above this mass fraction, samples were not stable. During the viscosity measurement an instantaneous change for a liquid to a paste like structure occurred. Most likely, the shear forces applied on the liquid caused a phase inversion of an oil in water emulsion to a water in oil emulsion. According to literature [38], the drying and film formation of an alkyd emulsion involves such a change from a concentrated oil in water phase, through a metastable state into a water in oil emulsion. The latter phase will have a very high viscosity due to the high molecular weight of the alkyd resin. The solventborne alkyd resin (SOLVALK) showed the slowest increase in viscosity with mass fraction polymer and the increase at lower shear rates was independent from the mass fraction polymer.
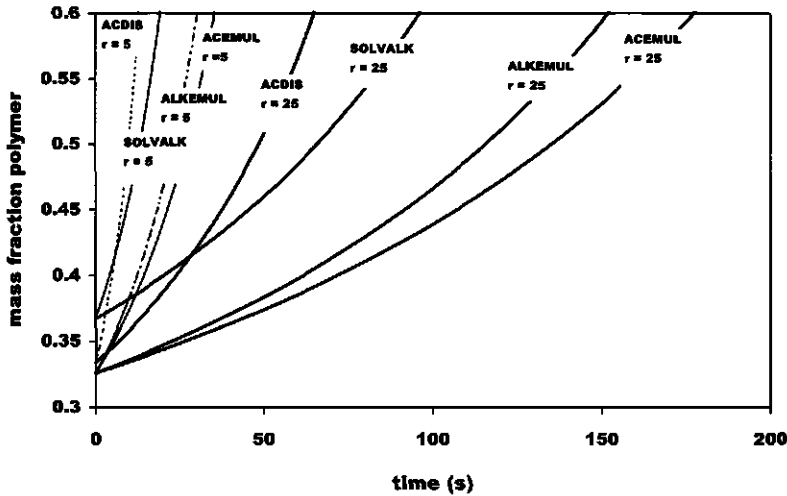
Figure 4.6   Increase in mass fraction polymer inside a wood capillary with a radius of 5 or 25 μm as a function of time, data are plotted for binders with the lowest initial viscosity (I).

The viscosity-mass fraction polymer relations were fitted by the following, semi-empirical relation with fit parameters c and d [39]:

$$\log\left(\frac{\eta}{\eta_0}\right) = \frac{\phi_m}{c - d\phi_m} \tag{4.11}$$

This is a modified version of *equation 4.9a* but based on mass fraction polymer and without the need to know the volume fraction polymer at infinite viscosity. *Equation 4.11* was preferred over *equations 9a* to *9c* because it fitted the measured data much more accurately with r-squares over 0.9. Fitted values of c and d are given in *table 4.4* including standard errors. The reason that the theoretical models from *equation 4.9* could not describe the measured data adequately might be twofold. Firstly, the polymer fraction on a volume basis had to be known whereas only the polymer fraction on a mass basis could be measured directly. A simple conversion into volumetric fractions based on liquid density was not realistic because it required knowledge about the volume to weight ratio, which will change upon drying due to polymer swelling and electrical double layer effects [36]. Secondly, the theoretical models required knowledge of the limiting polymer fraction ϕ_{max}, which should be determined from a plot of polymer fraction against reciprocal viscosity. This resulted in values with a large error, due to the absence of observations at very high and very low polymer fractions.

4.7 a
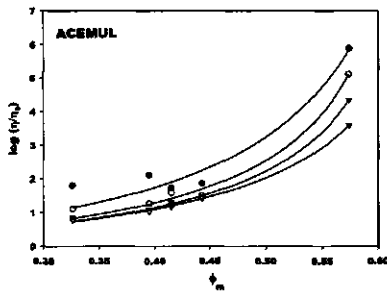
4.7 b
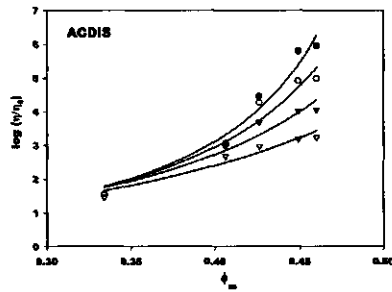
4.7 c
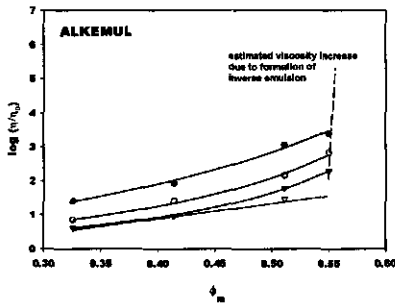
4.7 d
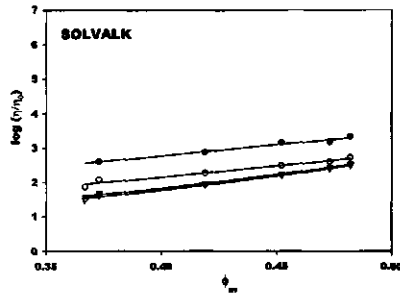
Figure 4.7   Relative viscosity of the binder as a function of solid matter content on mass basis. Shear rates: ● 0.1 s^{-1}; ○1 s^{-1}; ▼10 s^{-1}; ∇ 100 s^{-1}.

Table 4.4   Fit parameter for the relationship relative viscosity and mass fraction polymer.

Binder type:		Shear rate s^{-1}			
		0.1	1	10	100
ACEMUL	c:	0.529 (0.093)	0.761 (0.074)	0.845 (0.033)	0.830 (0.017)
	d:	0.751 (0.165)	1.130 (0.130)	1.242 (0.057)	1.169 (0.030)
ACDIS	c:	0.495 (0.092)	0.463 (0.065)	0.418 (0.068)	0.384 (0.061)
	d:	0.916 (0.206)	0.817 (0.147)	0.679 (0.155)	0.543 (0.141)
ALKEMUL	c:	0.352 (0.032)	0.661 (0.051)	0.977 (0.030)	0.830 (0.035)
	d:	0.351 (0.062)	0.840 (0.097)	1.340 (0.057)	0.934 (0.067)
SOLVALK	c:	0.134 (0.013)	0.224 (0.021)	0.361 (0.015)	0.353 (0.032)
	d:	0.025 (0.029)	0.094 (0.048)	0.394 (0.016)	0.417 (0.036)

Numbers in brackets are the standard errors of the fit parameters.

4.3.3   Relation polymer concentration and wetting

The capillary pressure, which is the driving force for the capillary penetration is directly proportional to the product of liquid surface tension and cosine of the contact angle between liquid and wood. Therefore, the surface tensions and the contact angles were measured as a function of polymer concentration. In principle, the contact angle should be determined from the meniscus of the wetting liquid inside the wood capillary, however, this was not experimentally possible. Therefore, the contact angle was measured from a droplet on the tangential surface of the wood. Equilibrium contact angles were used because these were least influenced by substrate penetration.

For the ALKEMUL and SOLVALK binders the surface tension remained constant with increasing solid matter content. The ACEMUL binder showed only a minor decrease in surface tension from 40 mN/m at a mass fraction of 0.33 to a value of 38 mN/m at a mass fraction of 0.44. The ACDIS binder had the strongest decrease in surface tension: from 33 mN/m at a mass fraction of 0.33 to a value of 24 mN/m at a mass fraction of 0.44. An increasing concentration of surfactant could explain the decreasing surface tension.

The wetting of the polymeric liquids decreased with increasing solid matter content. For the SOLVALK binder the contact angle increased from 16 ° at a mass fraction of 0.37 to an angle of 23 ° at a mass fraction of 0.48. For the ALKEMUL binder it changed from 7° at a mass fraction of 0.33 to 47° at a mass fraction of 0.51. For the ACEMUL binder the change was from 34° at a mass fraction of 0.33 to 64° at a mass fraction of 0.44. The contact angle of the ACDIS binder changed from 15° at a mass fraction of 0.33 to 103° at a mass fraction of 0.44. The latter represented a non-wetting case which meant that the capillary pressure was negative. Under these circumstances, the penetration of the coating in the wood will be limited by the absence of capillary pressure rather than the increase in viscosity. The lower contact angle with decreased liquid surface tension would normally not be expected and means that the interfacial tension (γ_{SL}) between binder and wood increased as follows from *equation 4.4* (note that γ_S will remain constant). The higher contact angle might be due to the increased viscosity, which could limit both the spreading and the mobility of surfactants. The relation between $\cos\theta \times \gamma_L$ and ϕ_m could be reasonably described by a linear trend that is given in *fig. 4.8* including individual data and regression equations.
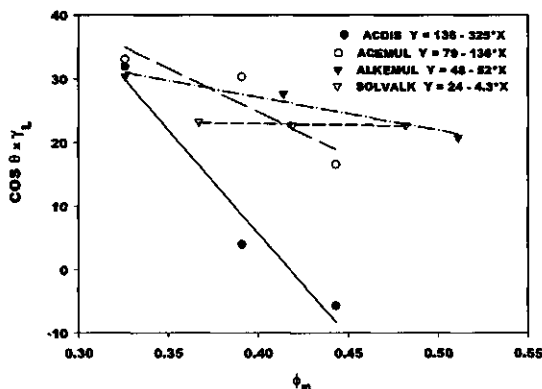
Figure 4.8   Cosine of the contact angle on wood times the liquid surface tension as a function of mass fraction polymer.

4.3.4. Capillary uptake of binder into wood

The capillary uptake into the axial direction the wood was determined for all binders at four different levels of thickener after a fixed time span of 30 minutes. The results are given in *table 4.5* in different ways. Firstly, as the total uptake of material (polymer and water or solvent) on both mass and volume basis. Secondly, as measured oven-dry weights of penetrated polymeric binder and thirdly on a theoretical oven-dry mass basis calculated from the uptake of total binder times its mass fraction solids. For the oven-dry cases, corrections for the impact of wood moisture content were made because the wood lost water during drying. The solid matter content was calculated from the mass of oven-dry binder in the wood divided by the amount of total uptake and compared with the solid matter content as determined according to ISO-3251.

The binders showed clear differences in capillary uptake of both total and dry material. The SOLVALK had the highest total uptake, followed by the ALKEMUL, ACEMUL and the ACDIS binders. The samples with increased thickener concentration and viscosity showed a decrease in total uptake. In case of the waterborne binders, the amount of dry polymer that penetrated into the wood was much lower than the amount that would be expected from the total uptake of material times its solid matter content. This proved that water was selectively removed from the waterborne binders during the capillary penetration, in particular with the ACDIS and ACEMUL samples and to a lesser extent also with the ALKEMUL binder. The difference in solid content between the liquid inside the wood and that of the bulk increased at higher levels of thickener. Most likely, the high viscosity prevented the capillary uptake of polymer whereas the water could still penetrate the wood.

The SOLVALK binder showed no indications of selective removal of solvent into the wooden cell wall during capillary penetration. The solid matter content of material in the wood and the bulk was identical within the limits of experimental error. On a volumetric basis, the uptake of white spirit was identical to that of the SOLVALK binder without thickener, whereas the uptake of water was four to ten times higher in comparison to the uptake of waterborne binders.

The rate of capillary uptake is given in *fig.4.9* for all four binders at the lowest and highest level of viscosity. Most of the material penetrated into the wood within the first

minute. In the later stage the increase was possibly limited to the uptake of water or organic solvent.

Table 4.5 Capillary uptake of binder into the axial directions of pine sapwood after a fixed time span of 30 minutes.

Binder type	Viscosity level	Total Uptake mass (g)	Total Uptake volume (ml)	Oven-dry mass (g) measured [1]	Oven-dry mass (g) calculated [2]	%-Solids in wood [3]	%-Solids [4]
ACEMUL	I	0.126	0.122	0.036	0.042	29	33
	II	0.129	0.125	0.040	0.043	31	33
	III	0.067	0.066	0.009	0.022	13	33
	IV	0.070	0.068	0.009	0.023	12	33
ACDIS	I	0.091	0.089	0.021	0.030	23	33
	II	0.078	0.077	0.013	0.026	17	33
	III	0.058	0.057	0.006	0.019	10	33
	IV	0.062	0.061	0.006	0.021	10	34
ALKEMUL	I	0.203	0.200	0.072	0.067	33	33
	II	0.119	0.117	0.041	0.039	34	33
	III	0.104	0.102	0.036	0.034	35	33
	IV	0.081	0.079	0.010	0.027	12	33
SOLVALK	I	0.360	0.416	0.144	0.130	40	36
	II	0.127	0.146	0.046	0.047	36	37
	III	0.107	0.121	0.040	0.042	37	39
	IV	0.050	0.056	0.020	0.020	40	41
Water		0.840	0.840	-	-	-	-
White spirit		0.330	0.420	-	-	-	-

1: oven-dry weight after penetration binder – oven-dry weight wood.
2: total mass uptake x % solids.
3: measured oven-dry mass divided by total mass uptake.
4: solid matter content determined by drying on inert substrate according to ISO 3251.

4.3.5   Modelling of the capillary penetration of binders into wood

The depth of penetration of the binder into the wood was calculated by a combination of the models for the mass fraction polymer inside a wood capillary (*equation 4.8*), the relation between mass fraction polymer and the viscosity at a shear rate of 0.1 s^{-1} (*equation 4.11*), cosθ x γ$_L$ as function of polymer fraction and the Washburn-equation for capillary rise (*equation 4.3*). The height of rise (*equation 4.12*) and rate of capillary rise (*equation 4.17*) were calculated as a function of time by a stepwise numerical calculation. The steps in time (Δt) used, ranged from 0.0001 s during the initial stage of capillary uptake to 10 s at the final stage.

$$\left(\frac{\Delta h}{\Delta t}\right)_t = \frac{2r(\cos\theta\,\gamma_L(\phi_m)) - \rho\,g\;h_t(r)^2}{8\eta(\phi_m)h_t} \qquad (4.12)$$

$$h_t = h_{t-1} + \left(\frac{\Delta h}{\Delta t}\right)_{t-1} x\;\Delta t \qquad (4.13)$$

The measured height of capillary rise was calculated from the measured weight increase as follows:

$$h_{meas} = \frac{m_{meas}}{\rho \, A_{eff}} \tag{4.14}$$

With m_{meas} as the total uptake on mass basis, ρ the density of the liquid and A_{eff} the effective area for capillary uptake which was calculated from [40]:

$$A_{eff} = A \, (1 - G(0.667 + 0.01u)) \tag{4.15}$$

In this case, for wood with a specific density[*] (G) of 0.50 and a wood moisture content (u) of 9 %, the ratio between A_{eff} and A was 0.62. Because the binder showed only a small change in density with increasing mass fraction polymer, the initial density values were used. An average value of 15 μm was used as the radius of the wood capillaries, which were assumed to be perfectly cylindrical.
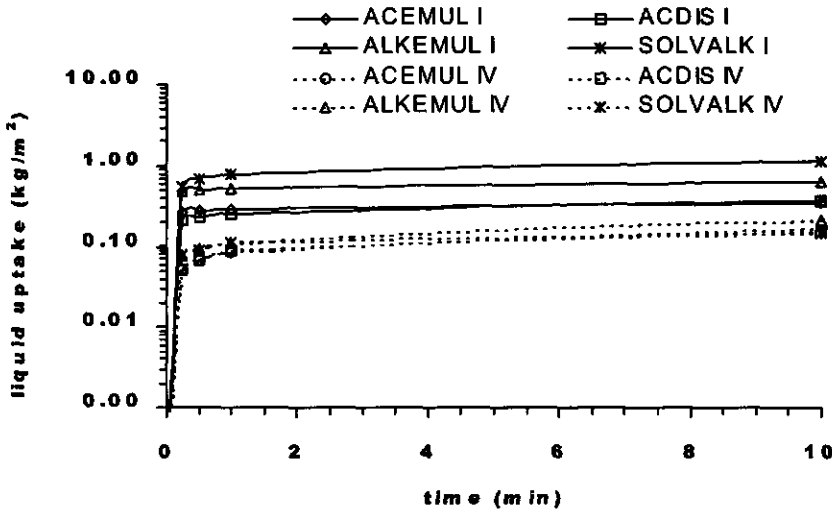
Figure 4.9   Uptake of liquid binder at viscosity levels I and IV as a function of time.

The model calculations predicted a limitation of the height of capillary rise by the increase of viscosity for the ACEMUL, ALKEMUL and SOLVALK binders, whereas the ACDIS binder was limited by zero capillary pressure and a sharp increase in viscosity at the same time. However, the maximum penetration depth was overestimated, most severely for the waterborne binders. The calculated depths for the ACDIS, ACEMUL, ALKEMUL and SOLVALK binders were respectively: 4.4 mm, 24 mm, 17 mm and 1.8 mm. The deviation between the measured and the calculated data might be explained by the fact that the limiting increase of the viscosity in the model calculation was reached much later than in reality. In order to adjust the model to the experimental data, the effective viscosity factor (E) was introduced to define the effective capillary viscosity (η'):

$$\eta' = E \, \eta \tag{4.16}$$

The experimental penetration data and the adjusted model predictions are given in *fig.4.10* The effective viscosity factors for the various binders were respectively 1.6 (SOLVALK), 150 (ACDIS), 400 (ALKEMUL) and 2700 (ACEMUL).

---

[*] Specific density is defined by the wood density (kg m^{-3}) devided by the density of water.

Most likely, the effective viscosity factor represents actually two phenomena. Firstly, the increase of the viscosity at shear rates below 0.1 s^{-1} in combination with a high mass fraction of polymer. It was estimated that with a high viscosity, and therefore a low rate of capillary rise, the shear rate applied on the penetrating binder would be below 0.1 s^{-1}. This effect will be most important for the ACEMUL and ACDIS binders, where the increase in viscosity at low shear rates was highest (see *fig. 4.7 a* and *b*). Secondly, the actual viscosity might be higher due to a faster transfer of water or solvent from liquid to cell wall. The data used in the model calculations originated from evaporation rate experiments that represented the transport in the bulk of the material. On a microscopic level, the loss of water or solvent from the penetrating liquid to the surrounding cell wall might happen faster. Furthermore, at the front of the penetrating binder, water or solvent will also evaporate to the air inside the capillary, this will cause an additional increase in solid matter content at the front of the penetrating liquid.
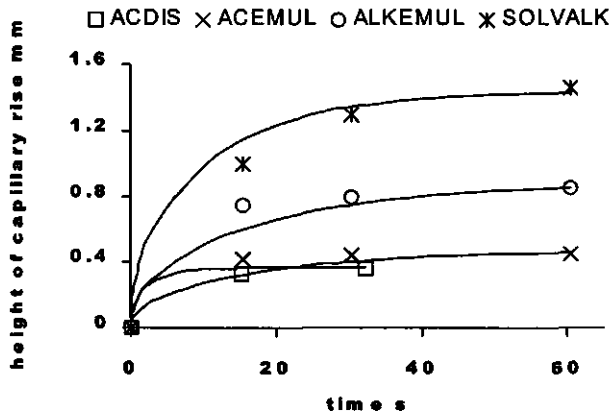
Figure 4.10   Experimental data and adjusted model calculations for height of capillary rise.

4.3.6   Influence of surfactants

Waterborne binders and coatings contain significant amounts of surfactants, which will lower the surface tension and might improve wetting. The uptake of distilled water into the wood containing different types of surfactant was tested at concentrations around and ten times above the critical micelle concentration (CMC). The gravimetric uptake of the anionic potassium fluoroalkyl carboxylate surfactant solutions is shown in *fig.4.11*. At all surfactant concentrations, the wood was wetted completely (contact angle was zero) and as predicted by the Washburn-equation (*equation 4.3*) under these circumstances the uptake was reduced with decreasing surface tension. Addition of surfactant did not caused a noticeable increase of the viscosity.

Increasing the surfactant concentration from 1 % (around the CMC) to 10 % caused an additional decrease in uptake although the surface tension of the liquid was not reduced any further. This might indicate that surfactant molecules were adsorbed at the wooden cell wall during the capillary penetration. Adsorption of surfactant to the cell wall will decrease the concentration inside the capillary and hence will increase the actual surface tension of the penetrating liquid at concentrations below or around the CMC. Far above the CMC, sufficient surfactant molecules will be present to compensate the loss due to adsorption at the cell wall and the surface tension of the liquid remains unaffected. Adsorption of surfactants at wood fibres was also reported in other studies on the wetting of wood [41].
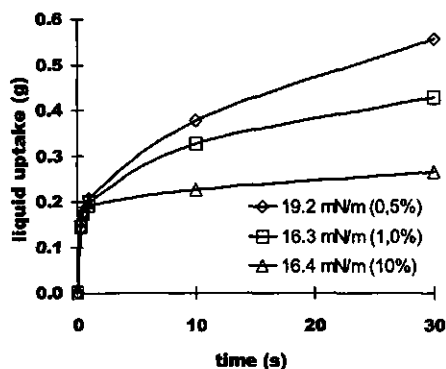
Figure 4.11
Influence of potassium fluoroalkyl carboxylkate surfactant concentration on capillary uptake of water.
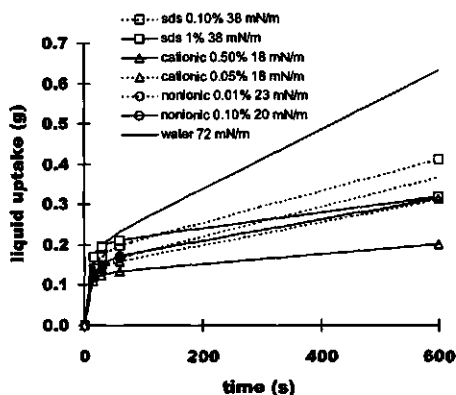
Figure 4.12
Influence surfactant type on capillary uptake of water. Concentrations are around and 10 x above the CMC.

The influence of surfactants types on the capillary uptake of water is given in *fig. 4.12*. All types of surfactant caused a reduction of the capillary uptake and a complete wetting of the wood. Regardless of the fact whether the surfactant was non-ionic, anionic or cationic, a lower uptake was found at a concentration ten times above the CMC. This indicated that different types of surfactants tested could be absorbed to the wood. Anionic surfactants solutions showed the highest uptake, followed by the nonionic surfactant. The solution containing the cationic surfactant had the lowest uptake.

4.4   Conclusions

This study has shown that during the drying and capillary penetration of coatings on wood, water or organic solvent was selectively transferred from the polymer containing liquid to the wood. This resulted in a more rapid increase in polymer concentration during drying on wood, in comparison to an inert substrate like glass. Inside a wood capillary, the polymer concentration increased because water entered the cell wall whereas polymer particles were too large to migrate into the cell wall. The evaporation rate to the wood was estimated from the constant evaporation rate period, the evaporation rate to the air and the mass fraction polymer at the end of the constant rate period. Depending on the binder type, the evaporation rate to the wood was equal or even higher than evaporation rate to the air. This was observed for both waterborne and solventborne binders but the solvent taken up into the wood was released again a lot faster. With the waterborne binders, the selective removal of water increased after addition of a thickener, this effect was absent with a solventborne binder.

The viscosity of the binders rapidly increased with mass fraction of polymer, in particular for the waterborne binders. For the ACDIS and ACEMUL binders, the increase in viscosity was much higher at low shear rates. For the ALKEMUL binder the viscosity was increased extremely as soon as a water in oil emulsion was formed. Because of the increasing polymer concentration, the viscosity of the binder appeared to be the limiting factor in the

capillary penetration of coatings into wood. Increasing the initial viscosity by addition of a thickener reduced the capillary uptake for all types of binder investigated.

The driving force for capillary penetration, which is the product of liquid surface tension and the cosine of the contact angle of the liquid on the wood, also decreased with increasing mass fraction polymer. This was due to decreased liquid surface tension and a poorer wetting that resulted in higher contact angles. This effect was strongest for the ACDIS and least important for the SOLVALK binder. Separate studies on the capillary uptake of water containing various types and concentrations of surfactants showed reduced capillary penetration with lower surface tension if the wetting of the wood was complete. A subsequent reduction of penetration at a surfactant concentration well above the critical micelle concentration indicated that adsorption of surfactants on the wooden cell wall took place. Surfactant adsorption will increase the actual liquid surface tension inside the capillary until there is sufficient surfactant to compensate the losses by adsorption.

The measured penetration of the binders into wood showed clear differences between binder types. The lowest penetration was observed for the acrylic dispersion (ACDIS) and emulsion (ACEMUL), the waterborne alkyd (ALKEMUL) showed deeper penetration and the solventborne alkyd (SOLVALK) penetrated deepest, which was in good agreement with previous findings. The maximum depth of capillary penetration was calculated from the Washburn-equation for capillary penetration taking into accounts the increasing viscosity and decreasing capillary pressure. In comparison to the experimental data, the maximum penetration was severely overestimated which indicated that in reality the viscosity increased much faster than could be predicted from evaporation rate measurements and the mass fraction-viscosity relationships. To adopt the model to the experimental data, the effective viscosity factor was introduced. The effective viscosity was about 1.6 (SOLVALK) to 2700 (ACEMUL) times higher than the viscosity with the highest mass fraction polymer, measured at a shear rate of 0.1 s^{-1}. This might be explained by a lower shear rate in practice or by a more rapid increase in mass fraction polymer, due to a faster drying on a micro-scale at the front of the penetrating binder. More detailed studies on the viscosity of concentrated dispersions or emulsions at high mass fractions and direct measurements of the solids content during capillary penetration will be needed to fully understand the capillary penetration of coatings into wood.

Finally, it can be concluded that to obtain a good penetration and pore filling of a coating on wood, the viscosity at very low shear rates and high mass fractions polymer is the most decisive factor. Addition of a thickener will reduce the penetrating capacity. Reducing the surface tension of the coating, if the wetting of the wood is already complete, will only decrease the penetration.

References

[1] **Meijer, M. de; Thurich, K.; Militz H.**; Comparative study on penetration characteristics of modern wood coatings, Wood Science and Technology, 32, 1998, 347-365.

[2]   **Scheikl, M.; Dunky, M.;** Measurement of dynamic and static contact angles on wood for the determination of its surface tension and the penetration of liquids into the wood surface, Holzforschung, 52, 1998, 89-94.

[3]   **Militz, H.; Peek, R-D.;** Möglichkeiten der Verbesserung einiger Eigenschaften von Pappelnholz durch Tränken mit wasserlöslichen Harzen, Material und Organismen, 28, 1993/94, 55-73.

[4]   **Banks, W.B.;** Water uptake by Scots Pine Sapwood, and its restriction by the use of water repellents, Wood Science and Technology, 7, 1971, 271-284.

[5]   **Loon, J. van;** The interactions between paint and surface, Journal of the Oil and Chemists Association, 49 (10), 1966, 844-867.

[6]   **Rødsrud, G.; Sutcliff, E.J.;** Alkyd emulsions-properties and application. Results from comparative investigations of penetration and ageing of alkyds, alkyd emulsions and acrylic dispersions, Surface Coatings International 77 (1), 1994, 7-16.

[7]   **Nussbaum, R.M.; Sutcliffe, E.J.; Hellgren, A.C.;** Microautoradiographic studies of the penetration of alkyd, alkyd emulsion and linseed oil coatings into wood, Journal of Coatings Technology, 70 (878), 1998, 49-57.

[8]   **Nussbaum, R.M.;** Penetration of water-borne alkyd emulsions and solvent-borne alkyds into wood, Holz als Roh- und Werkstoff, 52, 1994, 389-393.

[9]   **Dulien, F.A.L.; El-Sayed, M.S.; Batra, V.K.;** Rate of capillary rise in porous media with nonuniform pores, Journal of Colloid and Interface Science, 60 (3), 1977, 498-506.

[10]   **Marmur, A.;** Capillary rise and hysteresis in periodic porous media, Journal of Colloid and Interface Science, 129 (1), 1989, 278-285.

[11]   **Denesuk, M.; Smith, G.L.; Zelinski, B.J.J.; Kreidl, N.J.; Uhlmann, D.R.;** Capillary Penetration of Liquid Droplets into Porous Materials, Journal of Colloid and Interface Science, 158, 1993, 114-120.

[12]   **Borhan, A.; Rungta, K.K.;** An Experimental Study of the Radial Penetration of Liquids in Thin Porous Substrates, Journal of Colloid and Interface Science, 158, 1993, 403-411.

[13]   **Washburn, E.W.;** The dynamics of capillary flow, Physical Review, 17, 1921, 273-283.

[14]   **Tollenaar, D.;** Capillarity and wetting in paper structures: Properties of porous systems, In: Surfaces and Coatings related to paper and wood (Editors: Marchessault, R.H.; Skaar, C.), 1st Ed. Syracuse University Press, Syracuse, 1967, pp.196-197.

[15]   **Fengel, D.; Grosser, D.;** Holz, Morphologie und Eigenschaften. In: Ullmanns Encylopädie der Technischen Chemie, 4th Ed. Vol. 12 Verlag Chemie, Weinheim, 1976, pp. 669-679.

[16]   **Stamm, A.J.;** Passage of liquids, vapors, etc. through softwoods, U.S. Dept. Agr. Technical Bulletin, No. 929, 1946.

[17]   **Rijckaert, V.; Acker, J. van; Stevens, M.; Meijer, M. de; Militz, H.;** Quantitative analysis of the penetration of waterborne primers into wood by means of fluorescence microscopy, In: Advances in exterior wood coatings and CEN-standardisation, Proc. of PRA-Conference Brussels, 1998, paper 19.

[18]   **Meijer, M. de; Militz, H.; Thurich, K.;** Surface interactions between low VOC-coatings and wooden substrates, Proceedings of the XXIII Fatipec Congress Brussels, Volume C, 1996, 191-214.

[19]   **Kerr, A.J.; Goring, D.A.I.;** The role of hemicellulose in the delignification of wood, Canadian Journal of Chemistry, 53 (6), 1975, 952-959.

[20]   **Tarkow, H.; Feist, W.C.; Southerland, C.F.;** Interaction of wood with polymeric materials, penetration versus molecular size, Forest Products Journal, 16 (10), 1966, 61-65.

[21] **Coté, W.A.; Robison, R.G.**; A comparative study of wood, Journal of Paint Technology, 40 (525), 1968, 427-432.

[22] **Schneider, M.H.**; Scanning electron microscope study of a coating component deposited from solution into wood, Journal of the Oil and Chemists Association, 62, 1979, 441-444.

[23] **Schneider, M.H.; Sharp, A.R.**; A model for the uptake of linseed oil by wood, Journal of Coatings Technology, 54 (693), 1982, 91-96.

[24] **Vanderhoff, J.W.; Bradford, E.B.; Carrington, W.K.**; The transport of water through latex films, Journal of Polymer Science, 41, 1973, 155-174.

[25] **Croll, S.G.**; Drying of latex paint, Journal of Coatings Technology, 58 (734),1986, 41-49

[26] **Croll, S.G.**; Heat and mass transfer in latex paints during drying, Journal of Coatings Technology, 59 (751), 1987, 81-92.

[27] **Eckersley, S.T.; Rudin, A.**; Drying behaviour of acrylic latexes, Progress in Organic Coatings, 23, 1994, 384-402.

[28] **Sherman, P.**; Rheological properties of emulsions, In: Encyclopedia of emulsion technology (Ed. Becher, P.) Vol 1. Marcel Dekker, New York Basel Hong Kong, 1983, pp. 403-437.

[29] **Mooney, M.**; Journal of Colloid Science, 6, 1951, 162.

[30] **Dougherty, T.J.; Krieger, I.**; Advances in Colloid and Interface Science, 3, 1972, 111.

[31] **Frankel, N.A.; Acrivos, A.**; Chemical Engineering Science, 22, 1967, 847.

[32] **Janssen, J.W.; Blom, C.; Mellema, J.**; The flow curves of latex dispersions with added thickener (In Dutch), Verfkroniek 61 (6), 1988, 254-258.

[33] **Janssen, J.W.; Blom, C.; Mellema, J.**; The flow curves of latex dispersions with added pigment and thickener (In Dutch), Verfkroniek, 62 (7/8), 1989, 283-293.

[34] **Kissling, R. L.; Gross, P.H.**; Capillary behaviour of viscous liquids, Journal of Physical Chemistry, 74 (2), 1970, 318-326.

[35] **Dillon, P.W.**; Application of critical relative humidity, an evaporation analog of azeotropy, to the drying of water-borne coatings, Journal of Coatings Technology, 49 (634), 1977, 38-49.

[36] **Löfflath, F.; Gebhard, M.**; Rheological changes during the drying of a waterborne latex coating, Journal of Coatings Technology, 69 (867), 1997, 55-66.

[37] **Meijer, M. de; Thurich, K.; Militz, H.**; Quantitative measurements of capillary coating penetration in relation to wood and coating properties, accepted for Wood Science and Technology, 1999.

[38] **Beetsma, J.**; Alkyd paints: from the ease of organic solvents to the difficulties of water, XXIIth Fatipec Conference Budapest Vol. 2, 1994, 157-167.

[39] **Patton, T.C.**; Paint Flow and Pigment Dispersion: A Rheological Approach to Coating and Ink Technology, 2nd ed. John Wiley and Sons, New York, Chichester, Brisbane, Toronto, Singapore,1979, pp. 99.

[40] **Siau, J.F.**; Transport Processes in Wood. Springer, Berlin, Heidelberg, New York, Tokyo , 1984, pp29.

[41] **Deng, Y.; Abazeri, M.**; Contact angle measurement of wood fibers in surfactant and polymer solutions, Wood and Fiber Science, 30 (2), 1998, 155-164.

5. Surface energy determinations of wood: a comparison of methods and wood species[*]

Summary

The Lifshitz- van der Waals, acid-base and total surface free energies of various wood species were calculated from contact angle measurements. For spruce *(Picea abies)* and meranti *(Shorea spp.)* the following three methods were compared: capillary rise in wood powder columns (based on the Washburn equation), dynamic contact angle measurements (according to the Wilhelmy-plate principle) and sessile drop measurements along and across the grain of the wood. The capillary rise method was limited to non-swelling solvents, which means that only the Lifshitz-van der Waals component could be measured. With the dynamic contact angle measurement the wettability during the first immersion was decreased compared to the sessile drop. This was probably due to reduced capillary penetration but with the second immersion the presence of an adsorbed solvent layer increased the wettability and hence effected the surface energy data. The sessile drop measurements were highly dependent on the direction of measurement. Increasing wood moisture content decreased the Lifshitz- van der Waals component and increased the basic surface energy parameter of the wood. All of the wood species tested were characterised as having low energy surfaces with a dominant Lifshitz-van der Waals component. Measurement of acid and base parameters of wood surfaces seemed not to be very reliable because of its strong dependence on the measuring conditions. With respect to this, it should be noted that thermodynamic equilibrium conditions assumed by Young's equation are generally not fulfilled with wood surfaces because of chemical heterogeneity, surface roughness and the adsorption of the test solvent.

[*]   **Mari de Meijer, Sander Haemers, Wiro Cobben, Holger Militz**
        In preparation for publication.

5.1   Introduction

Studies have indicated that data on surface energy of wood could be used to predict and understand the wettability of wood by various liquids like coatings and glues [1-6]. Contact angle and surface energy data also allow the calculation of theoretical work of adhesion values across an interface between wood and another material [7], or can be used to assess changes in chemical composition of the surface after various treatments [8-10], weathering [11] or ageing [12,13] of wood. Measurement of surface energies for wood has received ongoing attention in recent decades, following the general theoretical developments in this field. The earliest research [14,15] was based on measuring critical surface tensions (γ_c) [43], later followed by measurements of polar (γ^P) and disperse (γ^D) or non-polar energy components of the surface energy according to either the geometric [44] or harmonic mean [22] methods [1,16-18, 39]. More recently, the Lifshitz-van-der-Waals (γ^{LW}) and (Lewis) acid-base components (γ^{AB}) [45] were used to measure the surface free energy [18-19]. Here the total surface free energy is the sum of the Lifshitz-van der Waals and the combined acid (γ^+) and base (γ^-) components. In the definition provided by Lewis, the acidity of a surface is determined by the possibility to accept electrons or donate protons. The basicity is controlled by the ability to donate electrons and accept protons. The acid-base interaction does include hydrogen bonding.

The methods used to determine surface energies of wood are generally based on static contact angle measurements of sessile drops or dynamic contact angle measurements (Wilhelmy plate) [20]. It should also be emphasised that all these methods are based on Young's equation:

$$\gamma_s = \gamma_{sl} + \gamma_l \cos \theta \tag{5.1}$$

where γ is the surface tension (in mN m^{-1} or mJ m^{-2}) of the solid (s), the solid-liquid (sl) and the liquid (l) interface respectively. In principle Young's equation assumes that the entire system is at thermodynamic equilibrium and that the solid surface is chemically homogeneous, flat and not influenced by chemical interaction or adsorption of the liquid to the surface. An overview of the literature on surface energy data obtained for various wood species and methods is given in *table 5.1*. The critical surface tension of most wood species lies within a relatively narrow range of 40 to 55 mJ m^{-2}, although the wood species vary in chemical composition and the different researchers used various sets of test liquids. The total surface free energy based on polar and dispersive components shows a larger variation and is generally higher than the critical surface tensions. The magnitude of the polar and dispersive components is highly variable. None of the components seem to be consistently dominant. Even for one specific wood species, the values are highly variable. For example, the polar surface energy of beech ranges between 19.6 and 53.1 mJ m^{-2} and the dispersive component ranges between 6.9 and 32.1 mJ m^{-2}. The calculation method also has a strong impact on the results; data obtained by geometric mean methods [21] are generally higher than those calculated from the harmonic mean equation [22]. With the Lifshitz-van der Waals approach, the total surface free energy is much lower, generally below or similar to the critical surface tension. The surface free energy is primarily composed of the Lifshitz-van der Waals component, but most wood species also show a significant base parameter with only a very low acidic parameter.

Apart from differences in calculation methods, a large part of the variation between different observations might be explained by the complex nature of the wood surface with respect to contact angle measurements. Firstly, wood is porous which causes a continuous decrease in contact angle with sessile drop measurements due to capillary penetration into the wood structure [23-25]. Secondly the wood structure causes surface roughness. As a

Table 5.1   Overview of literature data for the surface free energy of wood (mJ m^{-2}).

Wood species	Type of measurement	γ_c	γ^P	γ^D	γ^{S1}	γ^{LW}	γ^+	γ^-	γ^{AB}	γ^{S2}	Ref.
Ash	Wilhelmy plate	42.9	85.16	2.68	87.8	42.6	0.00	67.35	0.60	43.2	[18]
Ash	Wilhelmy plate		60.15	13.87	74.0						[18]
Aspen	Wilhelmy plate		13.2	41.8	55*	45.0	0.02	12.64	0.91	45.9	[30][7]
Beech	sessile drop		19.18	31.88	50.0						[23]
Beech	sessile drop[3]		45.53	24.48	68.8						[23]
Beech	sessile drop	50.6	53.1	6.9	60						[1]
Cherry	Wilhelmy plate	48.1	38.1	16.19	54.3	47.5	0.42	28.00	6.84	54.3	[18]
Cherry	Wilhelmy plate		35.1	20.09	55.2*						[18]
Douglas fir	Wilhelmy plate		11.8	36.2	48*	38.7	2.86	3.29	6.13	44.8	[30][7]
Douglas fir	sessile drop	52.8	19.2	28.8	48*						[16]
Douglas fir	sessile drop		11.5	37.5	49						[12]
Maple	Wilhelmy plate	46.8	56.07	8.77	64.8	45.5	0.46	33.19	7.85	53.3	[18]
Maple	Wilhelmy plate		40.93	20.13	61.1*						[18]
Maple	Wilhelmy plate	42	16.4	40.2	56.6*	43.2	0.71	13.29	6.15	49.4	[30][7]
Pine [4]	sessile drop					40.7	1.73	8.41	7.63	48.3	[19]
Pine [4]	Wilhelmy plate					38.9	0.05	17.33	1.86	40.8	[19]
Pine [5]	sessile drop	50.9	83.4	0.4	83.8						[1]
Pine [6]	sessile drop	54.3	68.1	3	71.1						[1]
Poplar	sessile drop	53.1	28.5	25.2	53.7						[1]
Red Maple	sessile drop		72.7	3.9	76.6	45.5	0.02	57.01	2.14	47.7	[39]
Red oak	Wilhelmy plate	46.8	42.2	10.4	52.6*	39.7	0.46	37.74	8.30	48.0	[18]
Red oak	Wilhelmy plate		35.04	16.87	51.9*						[18]
Redwood	sessile drop	57	31.5	22.7	54.2*						[12]
Spruce	Wilhelmy plate	45	16.5	45	61.5*	49.4	0.81	11.35	6.06	55.5	[30][7]
Spruce [5]	sessile drop	51.8	71.6	2	73.6						[1]
Spruce [6]	sessile drop	53.2	41.9	13.9	55.8						[1]
Walnut	Wilhelmy plate	10.8	86.14	1.28	87.4	37.9	0.09	58.93	4.63	42.6	[18]
White oak	Wilhelmy plate	31.4	41.65	5.29	46.9	34.0	0.39	22.80	5.98	40.0	[18]
White oak	Wilhelmy plate		38.31	8.59	46.9*						[18]

[1] $\gamma^S = \gamma^P + \gamma^D$
[2] $\gamma^S = \gamma^{LW} + \gamma^{AB}$
[3] adjusted to ideal surface
[4] measured parallel to the grain of the wood
[5] earlywood area's
[6] latewood area's
[7] data calculated from contact angles reported
* calculated by the harmonic mean method [22], otherwise geometric mean is used.

consequence liquid spreading is more pronounced perpendicular than parallel to the orientation of the wood cells [19,20] and the roughness of the surface will affect the measured contact angle data [26,27]. Differences in spreading between the smoother latewood area's and the more rough and porous earlywood areas were also observed by various authors [1,15].

Another complicating factor is the chemical heterogeneity of the wood surface. Apart from its major constituent's cellulose (40-50%)[1], hemicellulose (15-25%)[1] and lignin (20-35%)[1] wood can also contain 5-15 % of material consisting of a wide range of terpenoid, fatty acid or polyphenolic substances. These so-called extractives can have a strong negative impact on the wettability of wood surfaces [28]. Available data on isolated wood components show that for cellulose γ^{LW}= 44 mJ m^{-2}, γ^{AB}= 17.2 mJ m^{-2}, γ^{+}= 1.62 mJ m^{-2}, γ^{-}= 17.2 mJ m^{-2} and for arabinogalactan (hemicellulose) γ^{LW}= 37.6 mJ m^{-2}, γ^{AB}= 12.6 mJ m^{-2}, γ^{+}= 0.75 mJ m^{-2}, γ^{-}= 53.1 mJ m^{-2} [34]. For extracted lignin it is reported that γ^{AB}= 10-13 mJ m^{-2} and γ^{D}= 45-50 mJ m^{-2} [46]. Because the cell wall components are not distributed evenly within the cell walls, a spreading liquid will encounter differences in the chemical composition of the surface depending whether its on the outside, inside or cross-section of the wooden cell wall. Furthermore water adsorbed onto the cell wall will always be present in significant amounts; the exact amount will, however, differ depending on the wood species and the relative humidity of the environment. Liquids used for the contact angle measurements will also be adsorbed onto the wooden surface and might even diffuse into it. This means that a thin layer of liquid vapour will be present in front of the spreading liquid.

The objective of this study is to compare different methods for the measurement of contact angles on wood, to measure surface free energy data for several wood species under similar conditions and to study the impact of moisture and test solvent adsorption on the wood.

5.2   Experimental

Three different methods were employed to measure the contact angles on wood. The first one was based on the direct measurement of the contact angle of a spreading droplet **(sessile drop)** of approximately 20 μl on wood. The spreading of the droplet was recorded on videotape at a magnification of about 40 x and contact angles were measured afterwards according to a method described in literature [29]. Because the surface structure of the wood can have a serious influence on the contact angle [19], both measurements along and across the direction of the wood grain were taken for the wood species spruce *(Picea abies)*, pine sapwood *(Pinus sylvestris)* and dark red meranti *(Shorea spp.)* (density approximately 650 kg m^{-3}). Only measurements along the grain were obtained for the other wood species: framiré *(Terminalia ivorensis)*, white fir *(Abies alba)*, oregon pine *(Pseudostuga menziesii)*, western red cedar *(Thuja plicata)*, padouk *(Pterocarpus indica)*, white meranti *(Shorea spp.)* (density approximately 550 kg m^{-3}), iroko *(Chlorophora excelsa)*, pine heartwood *(Pinus sylvestris)* and thermally treated or acetylated pine sapwood. The partial penetration of the liquid caused a continuous decrease of the contact angle in the initial observation period and an increase in the radius of the droplet base. Taking into account the previous observations of Liptáková *et al* [23], the contact angle was measured when the radius of the droplet no longer increased. This can be considered to be at equilibrium. Because of the liquid penetration into the substrate, only advancing contact angles were used for the sessile drop measurements. Samples were stored and measured at a relative humidity of 65 % and a temperature of 21 °C.

The second method was based on **dynamic contact angle** measurements [20,30]. Thin slices of wood were planed to dimensions of 30 x 10 x 0.8 mm (length x width x thickness). The end grain of the wood was sealed with a 2-pack epoxy sealant to avoid capillary uptake of

---

[1] Mass fraction, ranges depending on wood species.

the test liquid. The samples were hung under an analytical balance (accuracy of 0.1 mg) to measure the wetting forces. The wood was brought into contact with the test liquids at a speed of 150 μm s^{-1} with a total immersion depth of approximately 15 mm. All measurements were made with the grain parallel to the direction of immersion. The contact angle was obtained from the measured forces according to the following equation:

$$F = \gamma_L\, P \cos\theta - \rho_L g A d \qquad (5.2)$$

where F is the measured force (N), γ_L the surface tension of the liquid (mJ m^{-2}), P the perimeter of the sample (m) , θ the contact angle (°) between liquid and wood, ρ_L the density of the liquid (kg m^{-3}), g the gravitational constant (m^2 s^{-1}), A the cross sectional area of the sample (m^2) and d the depth of immersion (m). The first part on the right hand side of *equation 5.2* is the actual wetting force, the second part is the buoyancy counter force which can be eliminated by extrapolation of the force to zero immersion depth (see *fig.5.2*). The perimeter of each individual sample was determined from the forces measured with cyclohexane which completely wetted the wood and hence cos θ =1. With the dynamic contact angle measurements both advancing and receding contact angles were obtained. Additionally, the samples were immersed in the liquid twice immediately after each other, to study the effects of liquid adsorption on the surface. The samples were brought into contact with the liquids in the following order: cyclohexane, diiodomethane, formamide and finally distilled water. After every immersion, the remaining solvent was removed by drying in a vacuum-oven at 100 mPa and 30 °C followed dry reclimatisation at 50 % relative humidity and 23 °C until at least 99 % of the initial weight was regained. To check the influence of potential surface modification by the various liquids, additional experiments were made where only one solvent was used.

With the third method, contact angle data were obtained from wood that was ground to a fine powder to control the effects of surface roughness and capillary penetration. The method was based on the Washburn equation [31,32] for **capillary rise** of a liquid in the following form:

$$h^2 = (t\, R\, \gamma_L \cos\theta)/2\eta \qquad (5.3)$$

where h is height of capillary rise (m), t the time (s), R the effective capillary radius (m) and η the liquid viscosity (Pa s). The wood powder was packed in a glass column with a glass filter at the bottom and the weight increase after contact with the liquid was recorded against time using an underweighing balance. *Equation 5.3* was rewritten to:

$$\cos\theta = (\Delta m^2/\Delta t) \times (2\eta / (\gamma_L\, \rho^2 C)) \qquad (5.4)$$

where m is the mass of the liquid taken up by the column (kg) and C the column constant (m^5) which also contains the effective capillary radius amongst the cross-sectional area of the column and the pore radius of the glass filter. C was determined from the rate of rise of cyclohexane, which wets the column completely and does not swell the wood. Wood swelling has to be avoided in this case because it would change the effective capillary radius between the wood particles. The wood was ground in a centrifugal mill under dry ice to avoid excessive heating and sieved to fractions smaller than 63 μm or between 63 and 106 μm. Samples were stored at 60 °C for at least 5 days to obtain a moisture content of about 4 % and allowed to cool down to a temperature of 20 °C just prior to the measurements. The temperature of the test liquid was controlled at 20 °C ($\pm$0.2) °C to avoid changing the viscosity.

All probe liquids were of at least 99 % purity and were stored under an anhydrous atmosphere to avoid contamination by water. The relevant physical data and surface tension data are given in *table 5.2*. Wood samples were industrially pre-dried from fresh state and subsequently stored at 65 % RH or 50 % RH (temperature of 22$\pm$3 °C). After preparing the

final surface, samples were stored for at least one week to avoid changes in wettability that might occur during the first 3 days [13]. For studies on the influence of wood moisture content, wood was stored at relative humidities of respectively 33, 60 and 94 %.

Table 5.2   Physical data and surface tensions of liquids used at a temperature of 20 °C

Liquid	Density kg / m³	Viscosity mPa s	γ_L mJ m⁻²	γ^{LW} mJ m⁻²	γ^+ mJ m⁻²	γ^- mJ m⁻²	γ^{AB} mJ m⁻²
Diiodomethane	3325	2.8	50.8	50.8	0	0	0
Water	1000	1.00	72.8	21.8	25.5	25.5	51.0
Formamide	799	1.02	58	39	2.28	39.6	19
Cyclohexane	799	1.02	25.2	25.2	0	0	0
Toluene	867	0.59	28.5	28.5	0	2.3	0
Methanol	792	0.60	22.6	18.2	-	-	4.3

Surface tension data obtained from [34].

Surface free energy components were calculated from the contact angles of diiodomethane, formamide and water according to *equations 5.6-5.9*, which are all based on [33]:

$$0.5\gamma_1(1+\cos\theta) = \sqrt{(\gamma_s^{LW}\gamma_1^{LW})} + \sqrt{(\gamma_s^-\gamma_1^+)} + \sqrt{(\gamma_s^+\gamma_1^-)} \qquad (5.5)$$

The Lifshitz-van der Waals component of the surface free energy (γ_s^{LW}) was obtained from the contact angle of diiodomethane (denoted 1) by:

$$\gamma_s^{LW} = 0.25\,\gamma_1^{LW}\,(1+\cos\theta)^2 \qquad (5.6)$$

With the known γ_s^{LW} component, the acid (γ_s^+) and base (γ_s^-) parameters of the surface energy can be calculated from the contact angles of water (denoted 2) and formamide (denoted 3):

$$\sqrt{\gamma_s^+} = (AF-BD)/(CF-CE) \text{ and } \sqrt{\gamma_s^-} = (BC-AE)/(CF-CE)$$

$$A = \gamma_2\,(1+\cos\theta) - 2\,\sqrt{(\gamma_s^{LW}\gamma_2^{LW})} \text{ and } B = \gamma_3\,(1+\cos\theta) - 2\,\sqrt{(\gamma_s^{LW}\gamma_3^{LW})}$$

$$C = 2\sqrt{\gamma_2^-} \quad D = 2\sqrt{\gamma_2^+} \quad E = 2\sqrt{\gamma_3^-} \quad F = 2\sqrt{\gamma_3^+} \qquad (5.7)$$

The total acid-base component to the surface energy (γ_s^{AB}) is given by:

$$\gamma_s^{AB} = 2\,\sqrt{\gamma_s^+}\,\sqrt{\gamma_s^-} \qquad (5.8)$$

The total surface free energy of the wood (γ_s) is given by:

$$\gamma_s = \gamma_s^{LW} + \gamma_s^{AB} \qquad (5.9)$$

5.3   Results and discussions

5.3.1   Capillary rise in wood powder columns

Some results of the squared mass increase by capillary rise of the liquid against time are shown in *fig.5.1*. The linear part of the slope was used to calculate the column constant or $\cos\theta$. Deviations at the beginning and end were respectively due to initial turbulence [32] and slow filling of closed capillaries respectively [31]. Cyclohexane and methanol, which both wetted the wood completely, were compared to assess the influence of swelling of the wood particles on the column constant. Cyclohexane is a non-swelling solvent where as methanol

lets the wood swell to almost the same extent as water [35-37]. *Table 5.3* shows the column constant as a function of test liquid, particle size and wood species. The differences between cyclohexane and toluene, which is also a non-swelling solvent, showed that other solvent properties also affected the rate of capillary rise. Probably, diffusion of solvent molecules into the wood particles affected the rate constant of capillary rise.

Table 5.3   Column constant obtained using different materials and liquids

Liquid type	Wood species	Particle size (μm)	Column constant x 10^{-15} (m^5)
cyclohexane	spruce	63-106	2.71 ± 0.98
cyclohexane	spruce	< 63	2.22 ± 0.09
methanol	spruce	< 63	1.42 ± 0.10
toluene	spruce	< 63	1.75 ± 0.10
cyclohexane	meranti	63-106	2.47 ± 0.29

As expected the particle size and the wood species had a considerable influence on the column constant. It should be noted that the wood particles were highly hetero-disperse and contained still fractions of wood fibres, which can be considered as micro-capillaries. The finer fractions gave more reliable results, probably because the influence of wetting of the wall of the glass sample holder was reduced. Loosely and densely packed columns were compared, the latter showed internal cracks due to contraction during drying of the cyclohexane. For this reason, loosely packing of the powder was preferred if repetitive wetting of the column was needed. The error between the six repeated wettings using cyclohexane was only 5 %. With ongoing repetition, a slight decrease in column constant was observed which was probably due to setting of the wood powder. Extraction of soluble wood material by the cyclohexane did not play a significant role because wood pre-extracted with cyclohexane yielded the same column constants as native wood.
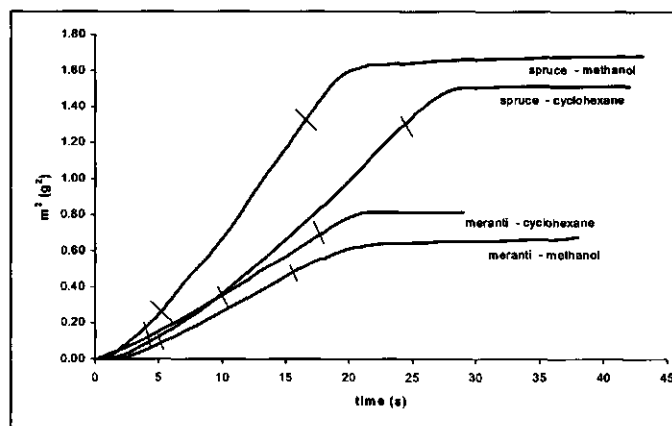
Figure 5.1   Squared mass increase during capillary uptake in column with wood powders (0.06-0.1μm fraction). Markers indicate the range used to calculate the slope of the lines.

Table 5.4 shows the different contact angles for diiodomethane obtained by the capillary rise method. The contact angles were considerably higher then those reported in literature obtained by alternative methods. The error within one type of sample was only 5 to 7 % for spruce but was 19 % for meranti. However, the impact of particle size and packing density was more important. In principle, the column constant should account for these factors, but apparently there is a specific interaction between the type of solvent and the wood powder structure. The Lifshitz-van der Waals component of the surface free energy of spruce, based on these contact angle data, ranged between 18.8 and 25.6 mJ m^{-2}; whereas for meranti it was 22.7 mJ m^{-2}. These values are lower than those reported in literature. Since the variability of this method is in the same range as for other types of measurements and because of the expected problems related to swelling of the wood powder with water or formamide no further acidic or base parameters were obtained.

Table 5.4   Contact angle of diiodomethane obtained by the capillary rise method

Wood species	Particle size (μm)	Powder packing	Cos θ	θ °
spruce	63-106	dense	0.370 ± 0.021	68.3
spruce	63-106	loose	0.216 ± 0.014	77.5
spruce	< 63	dense	0.420 ± 0.011	65.2
meranti	63-106	loose	0.336 ± 0.064	70.4

5.3.2   Dynamic contact angle measurements

The contact angles obtained by this method are given in *table 5.5* for spruce and meranti. Advancing and receding contact angles during both the first and second immersion are presented. Generally, the advancing contact angles were larger than the receding ones. Water on meranti even exhibited a non-wetting behaviour, which could also be seen from the non-wetting meniscus around the sample. During the second immersion, the advancing contact angle was much lower, whereas the receding angle was not much affected which means that the contact angle hysteresis was reduced. On meranti, the advancing angle during the second immersion was still larger than the receding one. Remarkably on spruce during the second immersion, the receding contact angle with water or formamide was larger than the advancing one. Similar effects were reported by Shen *et al* [19] who observed decreasing advancing and increasing receding contact angles upon increasing water absorption time prior to measurement.

Additional information about the wetting process could be obtained from the curves of the wetting force against immersion depth. A few typical examples are given in *figures 5.2* to *5.5*. With cyclohexane used to determine the sample perimeter, straight lines were observed in all cases for both spruce and meranti which means that there was not much interaction between liquid and wood. With water, the advancing curves during the first immersion showed a lot of variation, which can be caused by surface roughness effects, or absorption of liquid [20]. Chemical heterogeneity of the surface can also cause variation in the wetting force similar to surface roughness as was demonstrated in studies with contaminated smooth surfaces [38]. With diiodomethane and formamide a slight fluctuation in the first advancing profile was seen but to a far lesser extent then for water. To check the potential influence of cyclohexane, samples that were first exposed to test liquids followed by cyclohexane and vice versa were compared but no differences in the wetting profile or contact angle were seen. From the measurements with cyclohexane the perimeter of the samples was calculated

according to *equation 5.2*. By comparing the measured (P) and the gross perimeter (P_g) as derived from the dimensions of the sample, the actual surface roughness (P/P_g) was calculated. The surface roughness was 1.07 for spruce and 1.13 for meranti.

Table 5.5   Contact angles and surface free energies obtained by dynamic measurements

	Contact angle °*			Surface free energy (mJ m^{-2})				
	diiodo-methane	formamide	water	γ_s^{LW}	γ_s^+	γ_s^-	γ_s^{AB**}	γ_s***
Spruce								
1st advancing	37.1 ± 1.6	49.4 ± 1.8	68.1 ± 1.8	41.0	0.15	12.8	2.80	43.8
1st receding	25.6 ± 2.3	49.4 ± 2.2	46.5 ± 2.7	45.9	0.49	43.6	(-) 9.29	36.6 (55.2)
2nd advancing	22.6 ± 2.2	47.3 ± 2.8	36.4 ± 1.9	47.0	0.77	57.0	(-) 13.28	33.7 (60.2)
2nd receding	20.0 ± 3.2	49.5 ± 1.6	44.5 ± 2.8	47.8	0.82	47.1	(-) 12.42	35.3 (60.2)
Meranti								
1st advancing	55.5 ± 1.6	66.1 ± 0.9	104 ± 2.3	31.2	1.30	0.74	(-) 1.96	29.2 (33.1)
1st receding	21.5 ± 4.1	44.9 ± 0.8	33.3 ± 2.3	47.3	0.63	58.7	(-) 12.15	35.2 (59.5)
2nd advancing	23.5 ± 2.2	45.5 ± 0.8	37.2 ± 1.5	46.7	0.50	53.8	(-) 10.33	36.3 (57.0)
2nd receding	17.8 ± 2.2	45.2 ± 1.2	32.9 ± 2.1	48.4	0.81	59.7	(-) 13.91	34.5 (62.3)

*   Including 95 % confidence limits
**   Negative sign between brackets indicate presence of a negative value of $\sqrt{\gamma_s^+}$ or $\sqrt{\gamma_s^-}$
***   Data between brackets are based on a positive acid-base interaction.

Table 5.6   Contact angles and surface free energies from sessile drops measured along and across the grain.

	Contact angle °*			Surface free energy (mJ m^{-2})				
	diiodo-methane	Formamide	water	γ_s^{LW}	γ_s^+	γ_s^-	γ_s^{AB}	γ_s
Spruce								
Along	33.3 ± 1.4	25.4 ± 2.4	54.1 ± 1.7	42.6	1.7	16.7	10.8	53.3
Across	52.5 ± 1.7	37.2 ± 1.9	83.3 ± 1.9	32.9	6.4	0.05	1.1	34.0
Meranti								
Along	50.8 ± 2.0	55.4 ± 4.6	84.6 ± 2.3	33.8	1.3	1.92	3.1	36.9
Across	64.2 ± 2.2	70.3 ± 3.2	98.9 ± 1.9	26.2	1.0	0.13	0.7	26.9
Pine sapwood								
Along	41.1 ± 1.4	22.3 ± 2.6	50.3 ± 2.0	39.1	2.6	19.6	14.2	53.3
Across	61.4 ± 1.6	33.4 ± 3.0	67.7 ± 2.2	27.8	7.0	5.88	12.8	40.6

*   Including 95 % confidence limits

Figure 5.2   Wetting profile of water on meranti during the first and second immersion with dynamic contact angle measurements.

Figure 5.3   Wetting profile of diiodomethane on meranti during the first and second immersion with dynamic contact angle measurements.
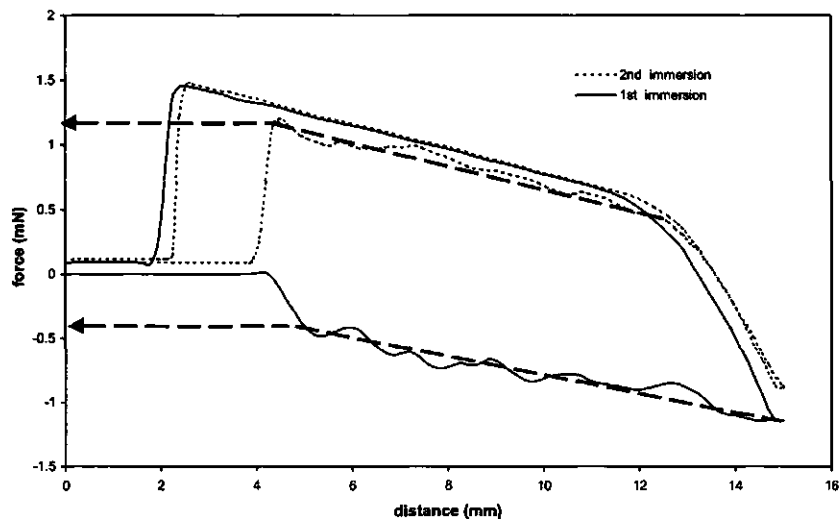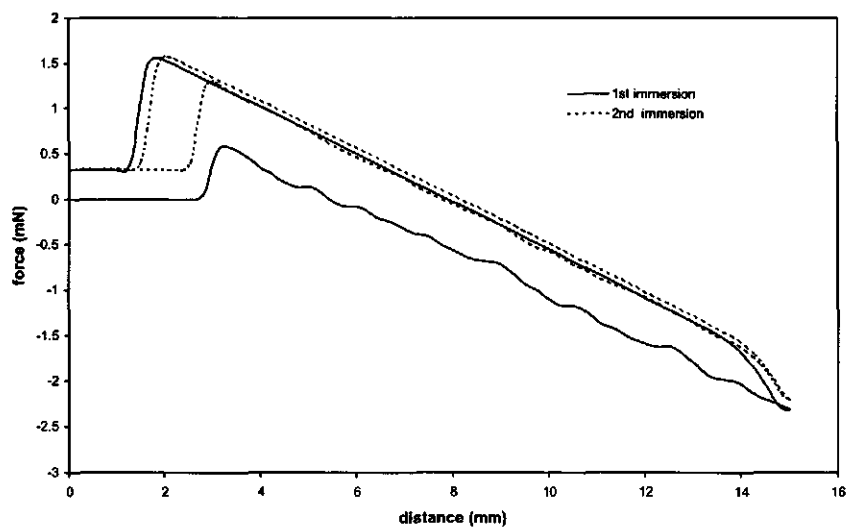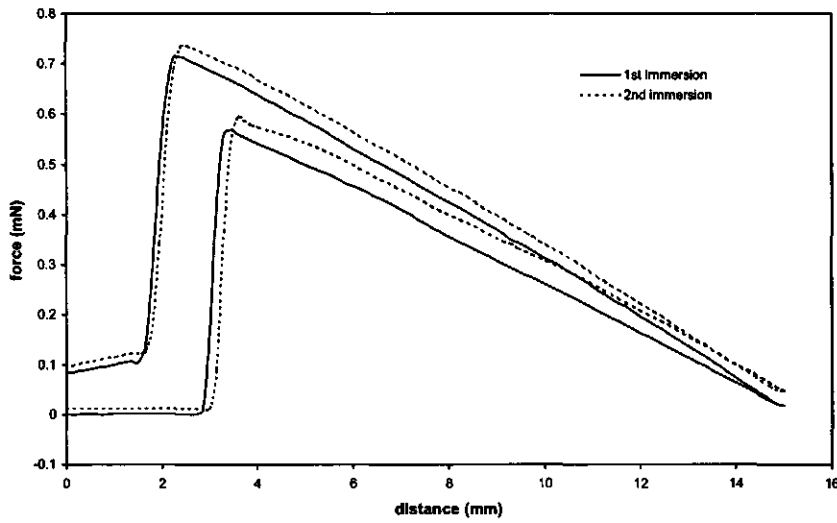
Figure 5.4   Wetting profile of cyclohexane on meranti during the first and second immersion with dynamic contact angle measurements.
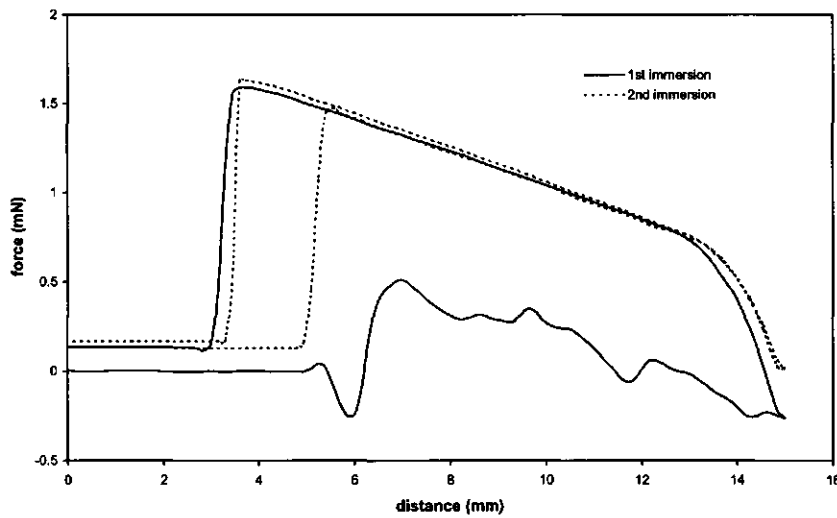

Figure 5.5   Wetting profile of water on spruce during the first and second immersion with dynamic contact angle measurements

Surface free energy data are also given in *table 5.5*. The Lifshitz-van der Waals fraction ranged between 45 and 48 mJ m^{-2} for the receding or second advancing data. The first advancing contact angle gave somewhat lower values, 41 and 31 mJ m^{-2} for spruce and meranti respectively. All results were generally comparable with data obtained by the dynamic contact angle measurements reported in the literature [18,30,39]. The acidic parameters were very low in all cases, and were similar to most other findings in literature (see *table 5.1*). The base parameters obtained from the advancing contact angle measurements during the first immersion were also low but much higher values were obtained from the other measurements. During both the first receding and with the second immersion it might be assumed that a molecular layer of the test liquid was still present on the surface of the wood. This means that only the first advancing contract angle can be considered as representing the true wetting process [45].

With the calculation of the total acid-base parameters at the wood surface, a problem arose with respect to negative square roots. Except for the advancing contact angle measurements on spruce all calculations according to *equation 5.7* yielded negative square roots for either $\sqrt{\gamma_s^-}$ (1st advancing data on meranti) or negative $\sqrt{\gamma_s^+}$ (all others). Good [33] discussed the aspect of negative square roots and dismissed negative values of $\sqrt{\gamma_s^-}$ as artefacts. Whether or not this was true in this case is questionable, because the negative $\sqrt{\gamma_s^-}$ was due to the very high contact angle of water, which was real, keeping in mind the non-wetting meniscus. The negative root of $\sqrt{\gamma_s^+}$ might be interpreted as a negative contribution to the total surface tension [33]. If only one square root is negative, the total acid-base component is negative. This logically reduces the total surface energy as is shown in *table 5.5*. The numbers in brackets show the values if all of the data were assumed to be positive. The total energy of 43.8 mJ m^{-2} for spruce (advancing) was rather close to the data obtained by Mantanis and Young [30] for spruce and by Shen *et al* [19] for pine.

5.3.3   Sessile drop measurements

Contact angles on spruce, pine sapwood and meranti were measured both parallel and perpendicular to the grain of the wood (see *table 5.6*). Wetting along the direction of the wood fibres was much better than across the fibre direction, as was also reported by Shen *et al* [19]. This might be caused by the higher surface roughness encountered by the liquid during spreading across the grain and the possibility of penetration into open ends of wood capillaries at the surface, which might enhance the spreading in the parallel direction [23,25]. Furthermore, chemical heterogeneity might be different in both directions since in the perpendicular direction more cell wall middle lamella, with a higher lignin content [42], have to be crossed. The difference in the contact angle across and along the grain also had a strong effect on the surface free energy. The total surface energy measured along the grain was higher than across, due to the higher Lifshitz-van der Waals and acid-base interactions. With respect to the acid and base parameters, the results were quite confusing. In particular for spruce and pine sapwood the dominant parameter along the grain was basic whereas across the grain acid components were dominant. If this is true it would mean that along the fibre direction mainly proton accepting (basic) groups are present and across the grain proton donating (acid) groups prevail. Further research on the chemical composition of wood surfaces seems necessary to check whether this is real or whether the differences are an artefact due to different response of the liquids to surface roughness or capillary penetration. It was also remarkable that contact angles measured for the sessile drops along the grain were lower in comparison to the data from the dynamic measurements during the first immersion. This contradicts to findings reported for pine [19]. No negative square roots were observed for sessile drop measurements.

Table 5.7   Contact angles and surface free energies from sessile drops measured along the grain. Variations within and in between different wood species.

Wood species	Sample*	Contact angle °**			Surface free energy (mJ m^{-2})				
		Diiodo-methane	Water	Formamide	γ_s^{LW}	γ_s^{+}	γ_s^{-}	γ_s^{AB}	γ_s
Framiré	1A	33 ± 2	62 ± 4	39 ± 2	43	0.6	14.0	6.0	49
	1B	28 ± 1	68 ± 2	35 ± 3	45	1.2	6.5	5.6	51
	2A	31 ± 2	59 ± 2	41 ± 3	44	0.3	18.5	4.5	48
	2B	29 ± 2	56 ± 4	38 ± 2	45	0.3	20.5	4.6	49
Abies Alba	1A	17 ± 3	58 ± 2	29 ± 3	49	0.7	13.6	6.3	55
	1B	16 ± 3	59 ± 2	26 ± 2	49	0.9	12.4	6.7	56
	2A	21 ± 3	64 ± 3	54 ± 5	47	0.4	21.6	-5.8	53
	2B	24 ± 2	58 ± 2	36 ± 2	47	0.3	17.0	4.7	51
Oregon Pine	1A	14 ± 1	78 ± 2	36 ± 2	49	1.2	1.4	2.6	52
	1B	14 ± 1	72 ± 2	30 ± 4	49	1.5	2.9	4.2	53
Western Red	1A	27 ± 2	79 ± 2	32 ± 3	46	2.6	0.6	2.5	48
Cedar	1B	22 ± 2	69 ± 2	28 ± 3	47	1.7	4.7	5.7	53
Padouk	1A	39 ± 3	62 ± 4	51 ± 3	40	0.0	21.5	1.2	41
	1B	37 ± 2	60 ± 2	47 ± 2	41	0.1	21.2	2.5	44
	2A	36 ± 2	60 ± 2	48 ± 2	42	0.0	21.4	1.8	43
	2B	37 ± 3	67 ± 2	48 ± 3	41	0.2	13.5	3.2	44
White	1A	26 ± 2	60 ± 2	34 ± 3	46	0.7	13.6	6.1	52
meranti	1B	38 ± 2	58 ± 4	46 ± 3	40	0.1	22.8	3.3	44
	2A	34 ± 2	63 ± 2	42 ± 3	42	0.4	14.9	5.0	47
	2B	37 ± 2	60 ± 3	49 ± 3	41	0.0	23.3	0.9	42
Iroko	1A	30 ± 2	72 ± 2	48 ± 2	44	0.2	8.1	2.5	47
	1B	36 ± 3	64 ± 2	49 ± 3	42	0.1	16.7	2.2	44
Pine	1A	22 ± 3	64 ± 2	21 ± 2	47	2.1	6.7	7.5	55
Heartwood	1B	19 ± 2	66 ± 2	23 ± 2	48	2.0	5.6	6.7	55
Acetylated	1A	20 ± 2	57 ± 2	32 ± 3	48	0.5	16.6	5.6	53
Pine §	1B	21 ± 2	54 ± 3	28 ± 2	48	0.7	18.1	6.9	54
Thermal ‡	1A	11 ± 2	61 ± 2	30 ± 3	50	0.6	11.4	5.2	55
Treated wood	1B	12 ± 1	51 ± 3	29 ± 2	50	0.3	21.8	4.9	55

*   Samples 1 and 2 refer to woods from different origin, A and B are replicates taken from the same log.

**   With 95% confidence limits; n ranges between 15 and 30.

§   Acetylated according to procedure described in ref. [40].

‡   Thermal treatment described in ref. [41].

To determine the variability in wettability and surface energy between wood species and within individual wood species, a large number of samples were tested by measuring the contact angle along the grain which seemed to be the most reliable method; results are given in *table 5.7*. In general, the variability within one wood species was of the same order as the experimental error, even if the boards originated from different logs. The only exception to this was found for *Abies alba* where the two logs exhibited clear differences in wettability by diiodomethane and formamide. This was also the only case were a negative $\sqrt{\gamma_s^+}$ existed.

The Lifshitz-van der Waals components dominated the surface energies for all of the wood species and the variations between the different wood species were relatively small. The same applied to the total surface energy data that were in close agreement to most of the data reported in literature. In comparison to the surface energies derived from polar and disperse components, the Lifshitz-van der Waals acid-base approach yielded lower surface energy values which were closer to the critical surface tension data of wood. The surfaces of the tropical hardwood species like Framiré, Padouk, White Meranti, Iroko and the softwood *Abies alba* had hardly any acid parameter; the dark red meranti was an exception to this. The other untreated softwood surfaces were slightly more acidic. In this respect, it was remarkable that the thermal treated and acetylated pine wood showed a reduction in proton donating capacity. Due to the replacement of hydroxyl groups by the acetyl groups in acetylated wood a more acidic character would be expected. A possible explanation for this unexpected behaviour might be the removal of resinous acids during the acetylation or the thermal treatment [41].

Table 5.8   Influence of moisture on the contact angle and surface energy

Wood species	RH %*	Contact angle °**			Surface free energy (mJ m^{-2})				
		Diiodo-methane	Water	Formamide	γ_s^{LW}	γ_s^+	γ_s^-	γ_s^{AB}	γ_s
spruce	33	34 ± 1	50 ± 1	27 ± 2	42	1.31	21.7	10.7	53
	60	34 ± 1	46 ± 1	32 ± 1	42	0.59	29.9	8.4	51
	94	38 ± 1	46 ± 1	45 ± 1	40	0.00	40.1	0.7	41
meranti	33	45 ± 2	82 ± 2	54 ± 3	37	0.64	3.31	2.9	40
	60	51 ± 2	85 ± 2	56 ± 5	34	1.25	1.92	3.1	37
	94	52 ± 1	84 ± 2	82 ± 1	33	2.17	16.5	-12.0	21

*   Relative humidity during storage of wood before measurement.
**   With 95% confidence limits; n ranges between 40 and 60. Angles measured along the grain.

5.3.4   Influence of moisture

Because wood is a hygroscopic material moisture will always be present on the surface. In order to study this effect samples were stored at relative humidities of 33 %, 60 % and 94 % to reach wood moisture contents of approximately 7 %, 12 % and 25 %. The results are presented in *table 5.8*. For diiodomethane and formamide, the wettability decreased with increasing moisture content. In case of water on spruce, a slightly improved wettability was observed going from 33 to 60 % RH but this effect was absent for meranti. Scheikl and Dunky [1] also studied the influence of the wood moisture content on wetting by water but could not find consistent trends.

Increasing concentrations of water at the surface slightly decreased the Lifshitz-van der Waals components and the total surface tension. The most pronounced effect was seen for the acid-base parameters. For spruce the presence of water decreased the acid and increased the base parameters of the wood. With meranti at 94 % RH both an increase in acid and base

properties of the surface was observed. At 94 % RH a negative $\sqrt{\gamma_s^+}$ was found, leading to a negative contribution by the acid-base component to the total surface free energy.

5.4   Conclusions

Independent of the measurement techniques used, all of the wood surfaces proved to have low surface energies, typically between 30 and 50 mJ m^{-2}. The electromagnetic Lifshitz-van der Waals component was the major component in the surface free energy of wood. The total surface free energy of wood obtained by the Lifshitz –van der Waals acid-base approach yielded a lower surface energy than that obtained by measuring polar-disperse components and was also closer to the critical surface tension. The acid-base component of the surface energy of wood was small and under certain circumstances even negative. Values of the separate acid and base parameters appeared to be highly sensitive to measuring conditions; in particular the acid parameters showed high fluctuations. It should be emphasised that an inherent difference in sensitivity exists between the acid and base surface energy with respect to small changes in contact angle. To illustrate this both parameters are plotted in *figures 5.6* and *5.7* as a function of the contact angle of water and formamide. With a few exceptions the base parameter is dominant on wood surfaces. This might reflect the true chemical composition of the wood surfaces but criticisms on the calculation methods for the Lifshitz-van der Waals theory, as proposed by van Oss, Good and Chaudhury [33, 34, 45], have shown that the split up of water into equal acid and base parameters results in a large base parameter for most surfaces [47].
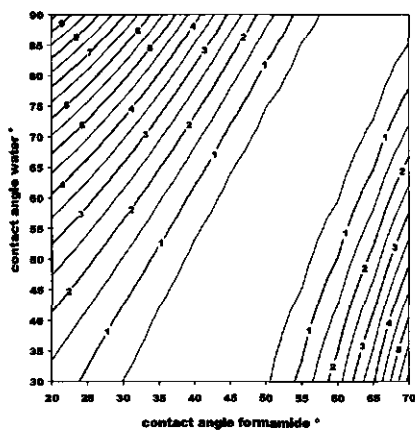
Figure 5.6
Acid part of surface parameter (mJ m^{-2}) as a function of the contact angles of water and formamide with the contact angle of diiodomethane fixed at 40 °.
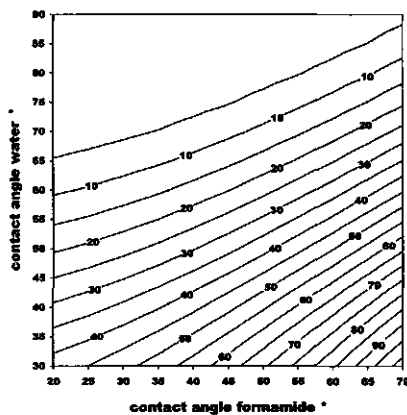
Figure 5. 7
Base part of surface parameter (mJ m^{-2}) as a function of the contact angles of water and formamide with the contact angle of diiodomethane fixed at 40 °.

The determination of contact angles by capillary rise measurements in wood powder columns is limited to the measurement of the Lifshitz-van der Waals component because non swelling solvents are needed, which exclude the measurement of acid and base parameters. The γ_s^{LW} obtained is lower than with other techniques, indicating that there might be a difference in chemical surface composition between solid and powdered wood. Dynamic

[36] **Guyer, V.L.; Hossfeld, R.L.**; Interactions of methanol-water binary solutions with wood, Holzforschung, 44, 1990, 157-161.

[37] **Rosen, H.N.**; Interaction of alcohol and organic acids with wood, Wood Science, 10 (3), 1978, 151-157.

[38] **Davies, J.; Nunnerly, C.S.; Brisley, A.C.; Edwards, J.C.; Finlayson, S.D.**; Use of dynamic contact angle profile analysis in studying the kinetics of protein removal from steel, glass, polytetrafluoroethylene, polypropylene, ethylenepropylene rubber, and silicone surfaces, Journal of Colloid and Interface Science, 182, 1996, 437-443.

[39] **Maldas, D.C.; Kamdem, D.P.**; Surface tension and wettability of CCA-treated red maple, Wood and Fiber Science, 30 (4), 1998, 368-373.

[40] **Beckers, E.P.J.; Militz, H.**; Process of acetylating solid wood, European Patent Application 0680810A1.

[41] **Tjeerdsma, B.F.; Boonstra, M.; Pizzi, A.; Tekely, P.; Militz, H.**; Characterisation of thermally modified wood: molecular reasons for wood performance improvement, Holz als Roh- und Werkstoff, 56, 1998, 149-153.

[42] **Fengel, D.; Wegener, G.**; Wood, Chemistry, Ultrastructure, Reactions, Berlin New York, 1989.

[43] **Zisman, W.A.**; Surface energetics of wetting spreading and adhesion, Journal of Paint Technology, 44 (564), 1972, 42-57.

[44] **Girifalco, L.A.; Good, R.J.**; A theory for the estimation of surface and interfacial energies I. Derivation and application to interfacial tension, Journal of Physical Chemistry, 61, 1957, 904.

[45] **Van Oss, C.J.; Chaudhury, M.K.; Good, R.J.**; Interfacial Lifshitz –van der Waals and polar interactions in macroscopic systems, Chemical Review, 88, 1988, 927-941.

[46] **Shen, W.; Parker, I.H.; Sheng, Y.G.**; The effects of surface extractives and lignin on the surface energy of eucalypt kraft pulp fibres, Journal of Adhesion Science and Technology, 12 (2), 1998, 161-174.

[47] **Volpe, C.D.; Siboni, S.**; Some reflections on acid-base solid surface free energy theories, Journal of Colloid and Interface Science, 195, 1997, 121-136.

6.   Wet Adhesion of Low-VOC Coatings on Wood; A Quantitative Analysis[*]

Summary

Adhesion of coatings on wood is most critical under wet conditions. However, the mechanisms controlling the adhesion are not well understood. Therefore, a quantitative analysis of coating adhesion on wood is needed. A new technique is presented to measure the wet adhesion quantitatively, based on measuring the forces needed to peel the coating from the wood with a tape. Differences in peel forces corresponded to areas in the wood with a lower or a higher degree of coating penetration. Coatings with better penetration and substrate wetting showed an improved adhesion and the better adhering coatings had an increased level of cohesive failure in the coating. Chemical analysis of the air-faced and wood-faced side of the coatings showed differences in chemical composition. The stored strain energy due to internal hygroscopic stress could reduce the actual level of adhesion significantly. Surface energy effects did not contribute to reduced adhesion after exposure to water. The interfacial work of adhesion between coating and wood was very much lower than the measured force and lacked correlation with measured differences in adhesion. Therefore, it can be concluded that mechanical anchoring plays a dominant role in obtaining good adhesion of a coating on wood.

[*]   **Mari de Meijer, Holger Militz**
Submitted to Progress in Organic Coatings

6.1   Introduction

In order to fulfil its protective and aesthetic functions, a coating should adhere well to its substrate for a long period. The adhesion should also be maintained at high moisture contents at the interface between coating and wood, which can either be induced by the presence of liquid water or high relative humidity (RH). This so-called wet adhesion is generally lower in comparison to the adhesion measured at standard conditions in the range between 50 and 65 % RH [1-3]. Depending on the formulation, the adhesion of waterborne coatings can be more sensitive to high moisture levels in comparison to traditional solventborne types [4-7]. Because of an increased use of waterborne coatings, a better understanding of the mechanisms controlling the adhesion of coatings on wood is desired.

The general mechanisms governing adhesion phenomena are reviewed in many papers [8-14]. Those aspects particular relevant to the adhesion of wood will be discussed briefly. Wood has a rough surface [15] and a porous structure [16] with a typical porosity of 55-70 % depending on specific gravity and moisture content [17,18]. As a consequence, good surface wetting and capillary penetration is generally considered to be a prerequisite for good adhesion of a coating. It increases the contact area between the substrate and the adhering material and reduces the concentration of stresses on specific loci during adhesion measurement [8].

Many researchers have shown that substrate penetration varies with the type of coating applied [19-21]. In softwoods grown in temperate climates, clear differences exist between penetration in the wider (diameter 16-60 μm) earlywood cells (tracheids) formed during spring and more narrow (diameter 6-25 μm) latewood cells formed during summer [22-25]. Furthermore the angle between the length axis of the wood cells and the surface influences the number of pores at the surface and thus the potential for capillary penetration [25].

Some workers [26,27] have suggested that there is no relation between adhesion and penetration. However, there are many studies on both adhesion of glues [28,29] and coatings [30-32], in which differences in adhesion between early- and latewood areas correspond to varying degrees of substrate penetration. Normally the adhesion strength is higher in the earlywood, which corresponds with its deeper penetration. Adhesion is only higher in the less penetrated latewood cells, if the wood is preweathered before application of the coating. This can be explained by the fact the unprotected earlywood degraded faster during weathering which lead to a weaker bond strength [33]. Richter *et al* [34] reported increased adhesion strength of a coating with increasing surface roughness. From the results mentioned, it can be assumed that mechanical anchoring plays an important role in the adhesion of coatings to wood.

Apart from mechanical interlocking, surface energy aspects and molecular interactions between coating and substrate are important in achieving good adhesion. The first approach to this was made by Zisman [35] through the concept of critical surface tension. The critical surface tension of wood lies around 50 mN m^{-1} [36-38] but can be strongly influenced by the way it is determined [38]. The surface energy concepts of Fowkes [39], Owens-Wendt [40] and Wu [41] in terms of dispersion and polar, or non-dispersion forces has also been applied to wooden surfaces. The surface free energy of softwoods ranged between 48 and 61 mJ m^{-2} with a polar fraction of 25 to 40 % [36,42]. The more recent theory of van Oss *et al* [43] separates into Lifshitz van der Waals (LW) forces and Lewis acids (electron acceptor) and base (electron donor) (AB) interactions, which include hydrogen bonding. On softwood surfaces the Lifshitz van der Waals forces are dominant (γ^{LW} approx. 40-50 mJ m^{-2}) in comparison to acid-base interactions (γ^{AB} approx. 5-8 mJ m^{-2}) [44,45]. To our knowledge no specific studies on the above mentioned molecular interactions between coatings and wood are published so far.

Interdiffusion of polymer chain segments or molecular entanglements might also contribute to adhesion between two polymeric phases [12, 46]. Theoretically, this could also happen at the interface of the coating polymer and the lignin, hemicellulose or cellulose polymers in the wooden cell wall. In practice however, this is extremely unlikely due to two factors. Firstly, the pore size in wooden cell walls ranges from 0.1 to 1 nm [47]. This means that dispersion or emulsion particles would be too large to enter the cell wall. Studies with polyethylene glycol indicated that penetration in water saturated cell walls only occurred if the molecular weight was below 3100 g mol^{-1} [48]. Secondly, intermolecular diffusion should take place above the glass transition temperature. Most of the wood polymers are in the glassy region: the T_g of lignin ranges between 80 °C (wet) and 200 °C (dry); the T_g of hemicellulose is between 0 °C (wet) and 180 °C (dry); cellulose has a (theoretical) T_g >>200°C [49].

The weak boundary layer theory [50] explains the loss of adhesion as a failure in an intermediate molecular layer between adhesive and adherent. This molecular layer consists of low molecular weight impurities of various origins, including water. This theory has never been verified for wood, but it is known that low molecular weight extractives can easily migrate to the surface and might reduce adhesion [51]. Also lower molecular weight fractions in the coating (e.g. surfactants, thickeners or coalescing agents) can influence wet adhesion [52] because they might cause a weak boundary layer.

Another important aspect in the evaluation of measured adhesion forces is the development of internal stresses in the coating, which can lower the actually measured adhesion force due to stored strain energy [53-55]. The internal stress within the coating can originate from three sources: stresses due to solidification during film formation; thermal stress due to differences in thermal expansion coefficients between coating and substrate, or hygroscopic stress due to differences in hygroscopic swelling and shrinkage between coating and substrate. The remaining residual stress can be different from the initial stress because of stress-relaxation in the coating [56-58].

Frequently used techniques to measure the adhesion of a coating on wood are: the axial pull-off test with a dolly glued on the coating (ISO 4624) [1,59,60]; shear measurements in torque mode [2,31,61] or block-shear tests [62] and the semi-quantitative x-cut or cross hedge (ISO 2409 or ASTM D3359). The first two methods are often difficult to interpret because cohesional failure can occur in the coating, glue or wood. These are often combined within one fractured surface. Furthermore, the measured force is influenced by the stress-distribution under the dolly and the method of cutting the coating around the stamp [63,64]. The third method suffers from reduced reproducibility due to manual influences during the application and removal of the tape and the visual assessment of the removed coating area. Several attempts have been made to improve the reproducibility by mechanising or automating the various actions [65-67]. Although adhesion measurements by peeling of coatings with pressure-sensitive tape in a tensile testing machine are successfully used on metals [68] and glass [69] this technique has not been applied to wood. Only peel test with cheesecloth glued to the wood with the liquid paint has been reported with limited success [34].

The objective of the work presented was to develop a method to measure quantitatively the adhesion between a coating and wood, in such a way that the measured adhesion strength can be further analysed. Special attention has been given to the relation between adhesion strength, surface free energy or work of adhesion and the microscopic structure of the wood. This gives the opportunity to understand whether the adhesion of the coating is improved by penetration into the substrate.

6.2   Experimental

6.2.1   Wood and coating materials

Two wood species were used in this study: spruce (*Picea abies*) with an average density of 480 kg m^{-3} and pine sapwood (*Pinus sylvestris*) with an average density of 470 kg m^{-3}. The wood was cut and planed into boards with the convex side of the annual rings parallel to the test surface. Growth-ring width was between 2 and 6 mm and the wood was conditioned to an initial moisture content of around 14 %.

Six model coatings based on commercially available polymeric binders were used in this study. All coatings were pigmented with titanium dioxide to a pigment volume concentration of about 17 %. *Table 6.1* provides a brief overview of their characteristics. From previous studies [24,25], it is known that there is a wide variation of penetration into the substrate. Mechanical properties of the coatings were characterised by the measurement of modulus of elasticity, tensile strength, yield strength and elongation at yield and break, both at 65 % RH (dry) and after immersion in water (see *table 6.2*).

Table 6.1   Characteristics of coatings used

Code	Binder type	Wood penetration	Surface tension N m^{-1} (a)	Viscosity Pa s at 1 s^{-1}	Viscosity Pa s 100 at 1 s^{-1}	Density kg m^{-3} (b)
Ac1	acrylic dispersion	very limited	39.3	15.20	3.58	1282
Ac2	acrylic emulsion 1	very limited	32.4	4.17	1.98	1250
Ac3	acrylic emulsion 2	very limited	35.8	19.10	4.09	1253
WBA	alkyd emulsion	moderate	39.2	2.90	0.29	1243
HSA	high solid alkyd	very deep	30.3	6.97	6.97	1160
SBA	solvent borne alkyd	deep	28.2	1.61	1.64	1386

a: of liquid coating measured according to DIN 53419
b: measured according to ISO 8130

6.2.2   Peel experiments

The adhesion measurements are based on peeling the coating from the wood. This was done by applying a pressure sensitive tape with a width of 20 mm on a coated wood sample; comparable to the well known tape-test (ASTM D3359). Contrary to this test method, the tape was not removed by hand but in a tensile-testing machine in order to measure the force against the peel-length. The tape was peeled at a rate of 30 mm min^{-1}, at an angle of 180 °, which was the easiest angle to maintain constant during the experiment. Preliminary experiments showed that using this peel rate gave the most reliable results. This method is only successful if the adhesive tape adheres better to the coating than the coating adheres to the wood. So the pressure-sensitive tape with the strongest adhesion was selected first.

From a large number of commercial products, the tape 3M no. 396 was found most suitable. This pressure sensitive tape consists of a polyester backing with a rubber glue. On aluminium, this tape had an adhesion strength of 600 N/m. The tape was applied by hand followed by pressing it to the coating with a wheel with a fixed weight. In order to avoid peeling beyond the area of the tape, incisions through the coating were made directly adjacent

to the tape. A V-shaped incision was made in the coating under the tape, to have a fixed starting point for delamination between coating and wood. Before application of the tape, the coating was cleaned with a 10 % ammonia-solution.
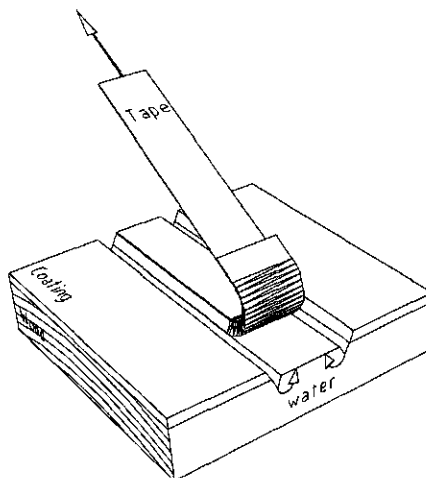
Figure 6.1 Peel-test sample design.

The interface between coating and wood was wetted from two grooves on both sides of the test area (*fig.6.1*). Through this uncoated grooves the water could rapidly penetrate the wood through the axial grain. An additional advantage of this approach was that the coating surface remained dry, which prevented a weaker adhesion of the tape. If the wood was wetted by liquid water, the wood-moisture content directly under the coating was around 30 % for pine sapwood and around 25 % for spruce. If the wetting was done by vapour (98 % relative humidity chamber), a wood moisture content of about 25 % was reached. Depending on the wood species and coating type, it took 1 to 7 days to reach the moisture contents mentioned.

6.2.3 Contact angle measurements and surface characterisation

Advancing contact angles (sessile drops) of the liquid coating on the wood were measured by a video-technique [70] to assess the wetting of substrates. It is known that contact angles on wood can differ on radial or tangential surfaces [71] and early- or latewood bands [29,37]. So these were measured separately. Measurements were also taken parallel and perpendicular to the grain, because liquids do not spread uniformly into all directions of the wood. Contact angles were measured at equilibrium. It was assumed that the equilibrium was reached as soon as the rate of change of the contact angle became constant. All changes at a constant rate are assumed to be due to capillary penetration into the wood [72].

Advancing contact angles of water, diiodomethane and formamide (all reagent grade) were measured on both wood (parallel and perpendicular to the grain) and on the air-faced and the wood-faced side (after detachment) of the coatings. The Lifshitz-van der Waals (γ^{LW}), acid (γ^{+}) and base (γ^{-}) solid surface (γ_s) free energy parameters were calculated according to the method described by Good [73]. Polar (γ^{P}) and non-polar or disperse (γ^{D}) surface energies were calculated according to Owens-Wendt [40, 74].

Table 6.3   Equilibrium contact angles (°) of liquid coating on wood

Wood species	Surface type	Position growth-ring	Orientation measurement	Coating type					
				Ac1	Ac2	Ac3	WBA	HSA	SBA
spruce	radial	EW/LW	along	83	81	78	58	20	40
			across	95	98	95	79	29	55
	tangential	EW/LW	along	80	79	55	42	17	45
			across	96	107	79	65	33	57
pine sapwood	radial	EW/LW	along	74	72	70	45	22	40
			across	93	106	96	64	35	54
	tangential	EW	along	71	82	78	48	24	44
			across	80	95	93	70	30	52
		LW	along	80	85	85	71	24	51
			across	90	99	95	78	33	58

EW: earlywood   LW: latewood   EW/ LW: mixed early- and latewood

Figure 6.2 Microscopic image (SEM) showing influence of wood structure on the spreading of the coating droplet. Insert at higher magnification shows substrate penetration in the spreading liquid front.

6.3.2   Peel strength adhesion

Initially, the tape peel-test was applied on both dry and wet samples but only the latter appeared to be successful because of the much lower adhesion of the coating to the wood. On dry wood, the adhesion of the coating on the wood was too strong, resulting in failure between coating and tape. Some attempts were made to glue the tape to the wood with a solvent-free epoxy glue but these were unsuccessful. Additional dolly pull-off tests confirmed the strong adhesion between coating and wood under dry conditions, since most of the failure was cohesive within the wood.

On wet wood, the adhesion between tape and coating was mostly strong enough to measure the adhesion between coating and wood. A typical plot of peel-force against peeled distance is shown in *fig.6.3*. The adhesion force (F) is expressed as measured force in Newton's (N), divided by the width (w) of the tape in metres (m). This is equal to energy per unit area ($J m^{-2}$) because J= N.m. By using this unit, measured adhesion can be expressed in the same units as the interfacial work of adhesion.
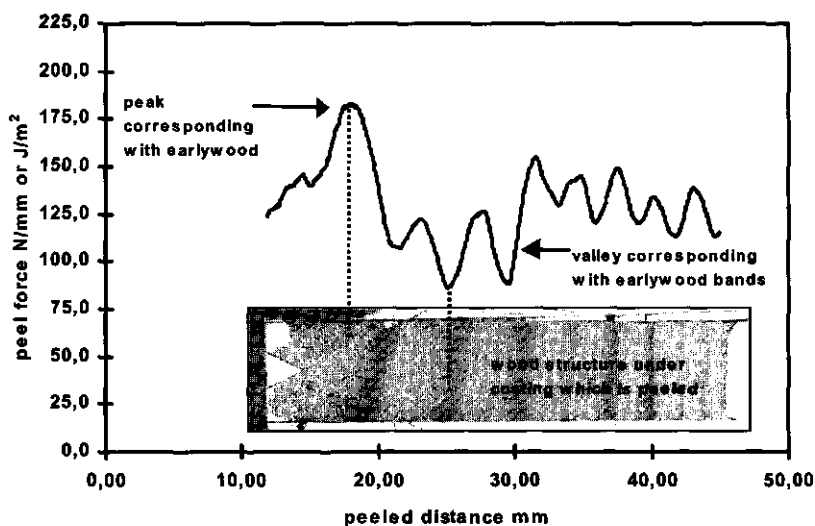
Figure 6.3   Adhesion as a function of peeled distance on pine sapwood, inserted photo
shows the corresponding early- and latewood zones.

With all measurements, typical increasing and decreasing peel forces were observed. If the peeled distances were compared with the structure of the wood, it was evident that the highest peel forces corresponded with the earlywood zones and that the lowest peel forces with the latewood zones. Several experiments, in which the orientation and width of growth rings was varied, showed corresponding changes in peel forces. If the same test was performed on a flat metal surface, no fluctuating peel forces were seen. In the earlywood zone, coating penetration was deeper in comparison to the latewood zone, where penetration of the coating was absent or reduced [20,22,25,27]. *Fig.6.4* shows a typical example to demonstrate this. Surface roughness in early- and latewood was also different as can be seen from *fig.6.5*.
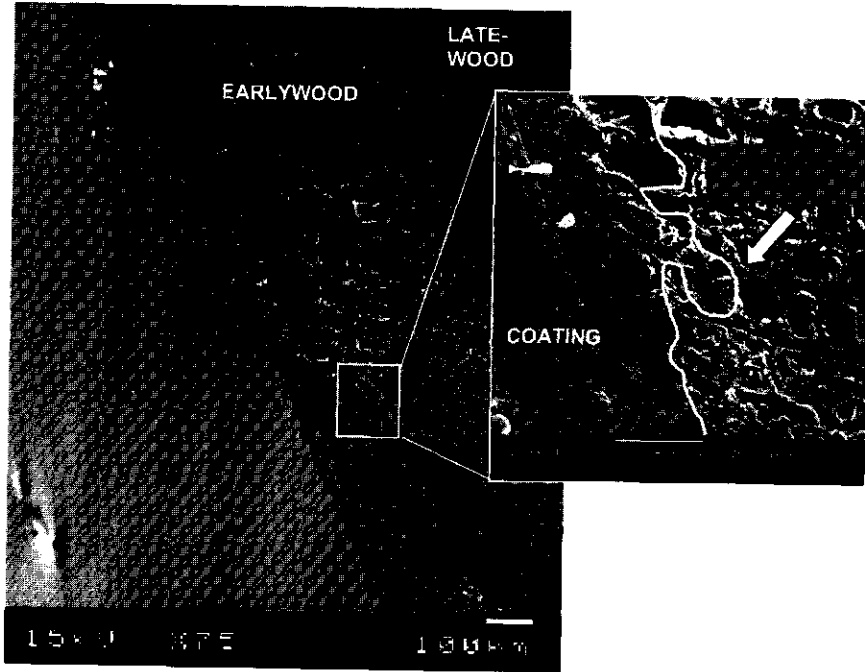
Figure 6.4 Difference in penetration between early- and latewood (SEM-micrograph).
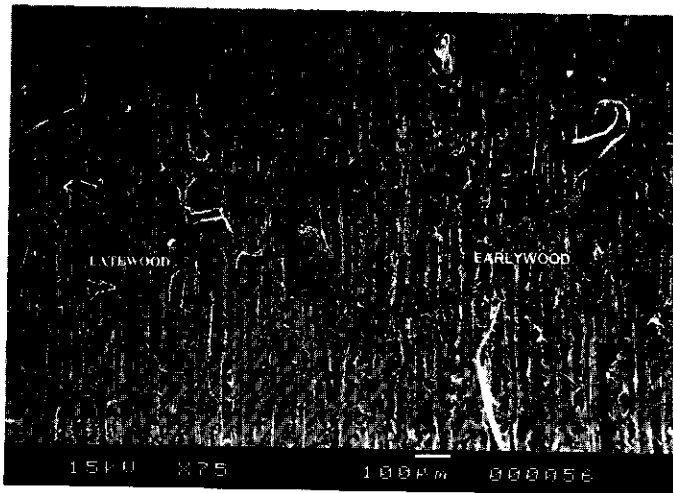
Figure 6.5 Wood surface showing differences in surface roughness between earlywood (right) and latewood (left) (SEM-micrograph).

In most cases, two measurements on each sample were made. The number of replicates for every combination of coating type and wood species ranged between 3 and 8. The largest number of useful measurements was obtained for the acrylic coatings (Ac1 to Ac3). For the waterborne alkyd (WBA) and especially the solventborne (SBA) and high solid (HSA) failure between the coating and the tape occurred more often than for the other

coatings. This reduced the number of useful measurements obtained. As a consequence, the data measured for these coatings represents the areas with the weakest adhesion. An overview of the reproducibility within (error bars) and between samples is given in *fig.6.6* for coating Ac1 on pine sapwood. Although there is some variation between replicates, the test was sufficiently reliable to distinguish the level of adhesion between the different coatings. The differences between early- and latewood peel forces were quite consistent in all cases.

The measured peel forces of all six coatings tested on pine sapwood and exposed to liquid water are given in *fig.6.7*. All three acrylic (Ac1-Ac3) coatings showed similar adhesion values and differences between early and latewood were also comparable. The adhesion to the earlywood was in most cases 50 percent higher than to the latewood. Adhesion of the waterborne alkyd coating (WBA) was somewhat higher in comparison to Ac1–Ac3, in particular in the earlywood. Adhesion of the SBA and HSA paint was the highest, adhesion on the earlywood was 2.5 to 3.4 times higher than on the latewood. All these differences were in very good agreement with differences in penetration between coatings, and between early- and latewood.
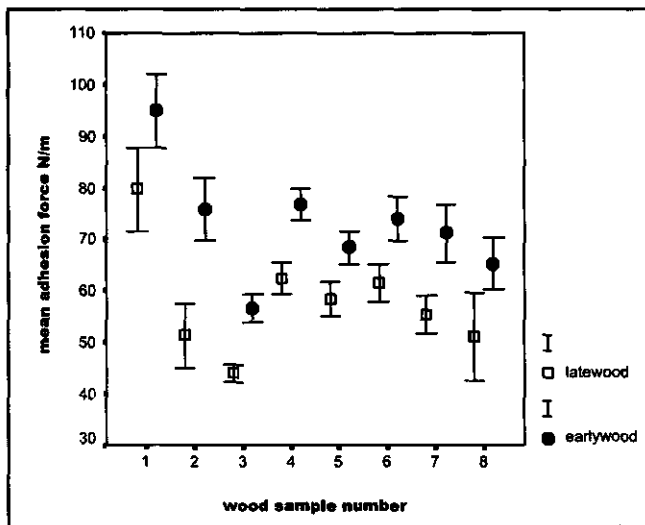
Figure 6.6   Wet-adhesion of coating Ac1 on 8 different pine sapwood panels exposed to liquid water.
Error bars indicate variation within the sample (95% confidence limits).

The wet-adhesion values of coatings Ac1 to Ac3 on both pine sapwood and spruce are shown in *fig.6.8*. No serious differences between these two wood species were found for these three coatings, only coating Ac1 had a slightly higher adhesion on spruce. The adhesion on spruce was higher than on pine with the WBA, HSA and SBA coatings, because the tape could not remove the coating from the spruce samples. This might have been caused by somewhat lower wood moisture content on spruce.

The differences between pine sapwood samples exposed to liquid water and water vapour are given in *fig.6.9*. Only results for the acrylic coatings can be presented, because with the other coatings failure between coating and tape occurred. This clearly indicated a better adhesion of the WBA, HSA and SBA coating after exposure to vapour. The adhesion of the acrylic coatings was very much higher if the samples were exposed to water vapour. Apparently the presence of liquid water at the wood coating interface reduced the adhesion
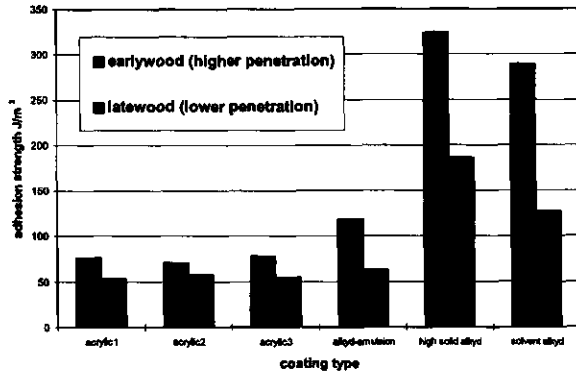
Figure 6.7   Wet-adhesion on pine sapwood after exposure to liquid water.
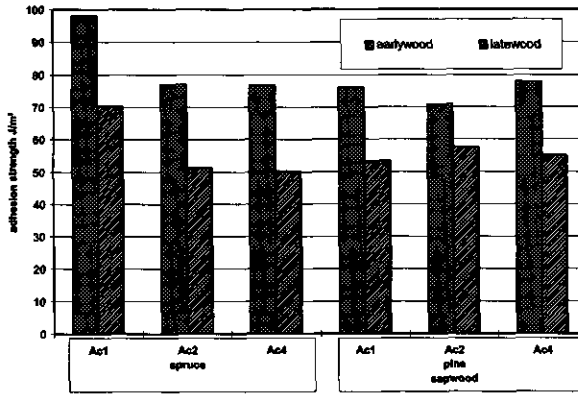
Figure 6.8   Wet-adhesion on early- and latewood of pine and spruce after exposure to liquid water.
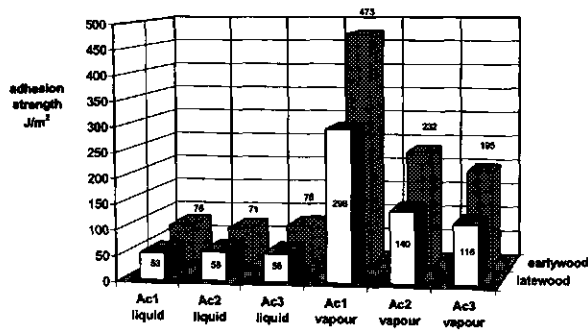
Figure 6.9   Difference in wet-adhesion between pine sapwood samples exposed to liquid water and water vapour (98% RH).

strength further, although the wood moisture content was only slightly lower (25-28 % instead of 30-32 %). After exposure to water vapour, larger differences between acrylic coatings and between early- and latewood were observed.

In order to make the measured peel forces comparable to the work of adhesion determined by other means, the work of peeling (W^P) had to be determined. The work of peeling is a function of the measured force per unit area of tape-width (F/ w), the peel angle (θ), the modulus of elasticity of the coating (E) and the coating thickness (c) [14]. The work of peeling is given in *table 6.6*.

$$W^P = \left(\frac{F}{w}\right)(1-\cos\theta) + \frac{\left(\frac{F}{w}\right)^2}{2cE} \qquad (6.5)$$

Table 6.4   Contact angles and surface free energies of coatings and wood

|			contact angles °			surface energy mJ m^{-2}						
			Diiodo-methane	Distilled Water	For-mamide	γ_s^{LW}	γ_s^+	γ_s^-	γ_s a	γ_s^D	γ_s^P	γ_s b
Coating: Air-faced		Ac1	48	73	61	35	0.01	13.5	36	28	8.6	37
		Ac2	47	68	64	36	0.29	24.5	41	25	12.2	37
		Ac3	49	55	53	35	0.02	33.6	36	23	21.8	45
		WBA	41	64	42	39	0.86	13.6	46	33	12.5	46
		HSA	53	80	77	32	0.95	17.6	41	23	6.8	30
		SBA	48	77	46	36	1.99	3.8	41	34	6.2	40
	Wood-faced	Ac1	50	78	74	34	0.85	17.8	42	25	6.9	32
		Ac2	46	77	64	37	0.03	11.4	38	30	6.3	36
		Ac3	46	48	58	37	0.47	50.6	46	21	26.3	47
		WBA	36	85	53	41	0.58	1.20	43	41	1.8	43
		HSA	-	-	-	-	-	-	-	-	-	-
		SBA	50	88	73	34	0.17	5.92	36	29	2.4	31
Wood	Along	spruce	34	54	25	43	1.72	16.8	53	35	17.2	52
		pine sapw.	41	50	22	39	2.57	19.7	53	32	21.4	53
	Across	spruce	53	83	37	33	6.29	0.1	35	37	4.0	41
		pine sapw.	61	68	33	28	7.07	5.9	41	27	14.4	41

a $\gamma_s = \gamma_{LW} + 2\sqrt{\gamma_s^+}\sqrt{\gamma_s^-}$ b $\gamma_s = \gamma_s^D + \gamma_s^P$

6.3.3   Analysis of fractured surfaces

After removal of the coating from the wood, the detached surfaces of wood and coating were examined by scanning electron microscopy. On the wood face of the coating clear imprints of the wood structure were visible. Parts of the coatings were clearly torn out of the wood cells as can be seen in *fig.6.10*. Some wood cell fragments like loose fibrils were
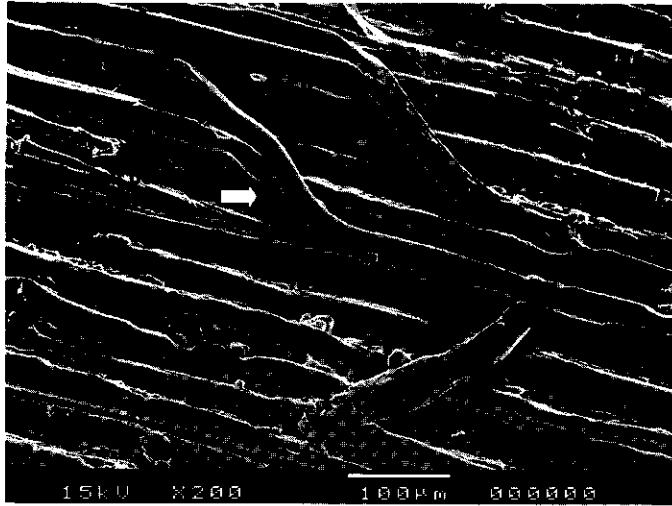
Figure 6.10   SEM image of WBA-coating detached from the wood,
                       note coating materials torn out of the wood.
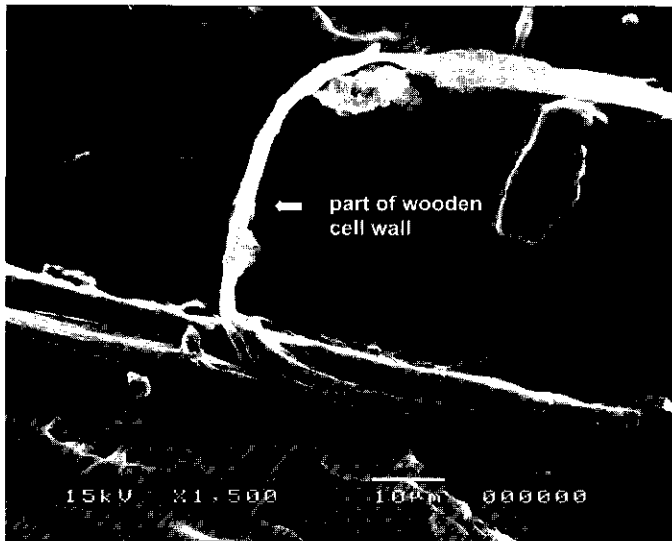
Figure 6.11   SEM image of loose wood fibrils present at the detached coating side

also observed in the coating (see *fig.6.11*), but true parts of the tracheid wall (as observed by
Bardage and Bjurman [2]) could not be found. At magnifications of 10,000 x or more, a fine
course structure was visible on the coating; this was most likely due to the pigment particles.
Fractured pieces of coating material were observed in the wood, especially with the better
adhering HSA and SBA coatings. Cohesive failure of the coating was observed in two ways.
Firstly as true cohesive failure with the coating being still in its original position in the wood
(fig.6.12), and secondly as cohesive failure after the coating had been partly torn out of the

wood *(fig.6.13)*. The imprints of the pit-membranes present in the wooden cell walls (see *fig.6.13)*, showed that the coating had perfectly wetted the fine structure of the cell wall.
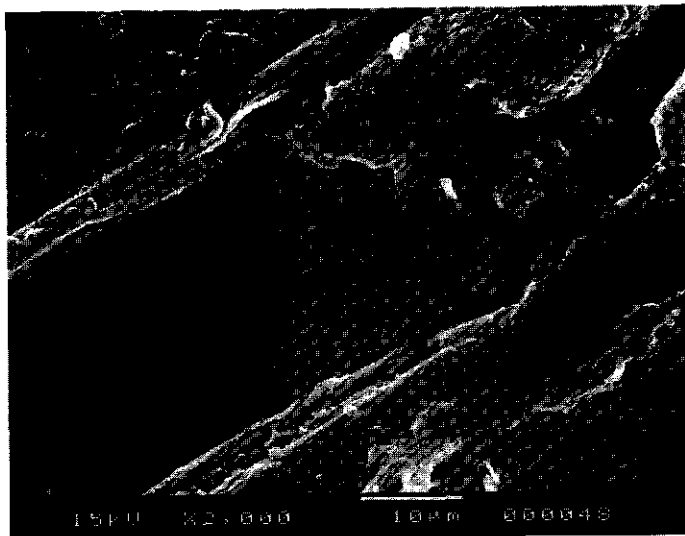
Figure 6.12 SEM image of cohesive failure with the coating (HSA) still in its original position in the wood.
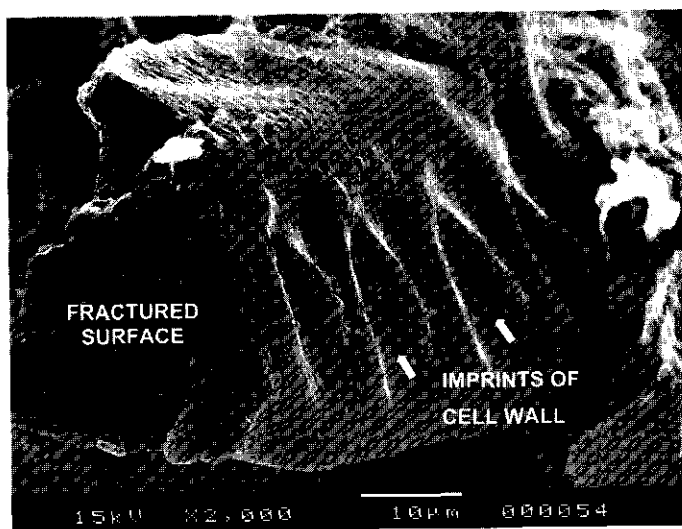
Figure 6.13 SEM image of cohesive failure after the coating (SBA) has been partly torn out of the wood.

Diffuse reflectance infrared spectra of the wood-faced and air-faced surfaces of the coating showed two main differences. Firstly, the titanium-dioxide peak around 800 cm^{-1} was always higher at the air-faced surface. Secondly, the spectra of the wood-faced surfaces of the coatings clear showed features of the spectra of the pure binder, absent in the spectra of the

air-faced surfaces (see *fig.6.14* as an example). This was most clearly seen in the range between 1500 and 1680 cm^{-1} (typical for C=C stretch in double bonds [78]), where the binder and wood-faced side of the coating showed specific peaks and valleys whereas the air-faced side of the coating only showed a broad shoulder. The infrared spectra suggested the existence of a binder-enriched layer close to the surface. This was also observed with TiO$_2$ pigmented paints based on various binders and applied on metal surface [79].

Diffuse reflectance infrared spectra of the wood under the peeled coating were compared to spectra of wood that had never been painted. No differences were observed except with the HSA coating as is shown in *fig.6.15*. Here the wood spectrum showed many features specific for the coating like strong absorbency around 850 cm^{-1} (TiO$_2$). In combination with the SEM-analysis, it was evident that the HSA showed significant failure within the wood, in particular in the earlywood zones.
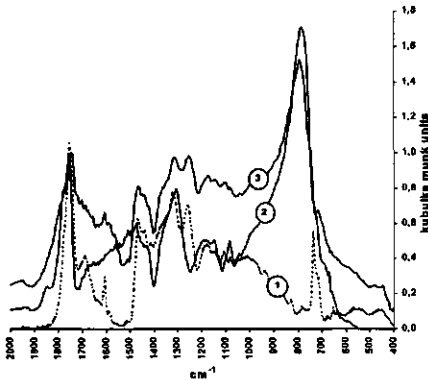
Figure 6.14
Diffuse reflectance infrared spectra of pure binder (1), wood-faced coating surface (2) and air-faced coating surface (3) of the WBA-coating
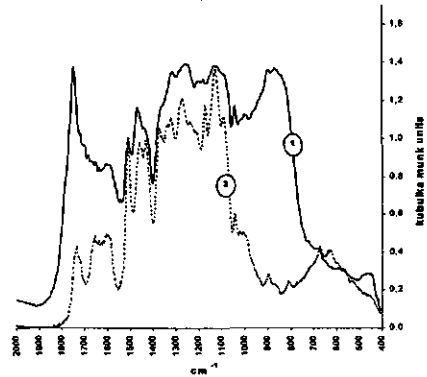
Figure 6.15
Diffuse reflectance infrared spectra of the wood after peeling of the HSA coating (1) and uncoated wood (2).

Differences in the chemical composition of the surfaces were further evaluated by measurement of contact angles with three different probes (diiodomethane, formamide and water) which were used subsequently to calculate the surface free energies. *Table 6.4* shows these data for both air-faced and wood-faced coating surfaces and the wood itself. Contact angles on the wood-faced surface of the HSA coating could not be determined because of a large amount of cracks and wood fibres. The Lifshitz-van-der-Waals interactions were most dominant on both coating and wood. In comparison to the coatings, wood had a much stronger acidic character. On the air-faced side of the coating all coatings except SBA, had a strong base parameter and only a small acid parameter. The ratio between the parameters of the coatings was of about the same order as those reported by Osterwold and Armbruster [80]. On the wood faced side, the Lifshitz-van-der-Waals interactions were only slightly affected. However, acid and base parameters both decreased and increased depending on the coating type. It was difficult to judge to what extent this was due to changes in chemical composition in the surface, because the wood-faced side of the coating was very rough due to the imprints of the wood. Surface roughness effect had a strong influence on acid-base parameters as could be seen from the large differences between the wood data measured along and across the grain. The measurements along the grain seemed the most realistic ones, because they would

be least effected by roughness and by sharp edges. The data presented for the wood-faced side of the coating were the ones measured along the grain of the imprint of the wood structure.

Both the coating and the wood had a strong disperse components in the surface free energy. The polar components was more variable, the wood (if measured along the grain) and coatings Ac2, Ac3 and WBA also had a substantial polar component. Comparing wood-faced and air-faced sides of the coating, the disperse component was not much affected but the polar component decreased except for coating Ac3.

6.3.4   Interfacial work of adhesion

From the surface free energies of both coating (γ_c) and wood (γ_w), the work of adhesion (W^a_{cw}) between the two phases was calculated according to the following equation [73] using Lifshitz-van der Waals-acid-base parameters:

$$W^a_{cw} = \gamma_C + \gamma_W - \gamma_{CW} \tag{6.6}$$

$$W^a_{cw} = 2\left(\sqrt{\gamma_c^{LW}\gamma_w^{LW}} + \sqrt{\gamma_c^+\gamma_w^-} + \sqrt{\gamma_c^-\gamma_w^+}\right) \tag{6.7}$$

Table 6.6 gives the interfacial work of adhesion between coating and wood calculated according to this equation. The measured differences in interfacial energy did not reflect the adhesion differences between the coatings.

The interfacial work of adhesion after exposure to water (W^a_{wet}) was obtained from the interfacial energies between coating-water (γ_{CL}), wood - water (γ_{WL}) and coating – wood (γ_{CW}) as follows:

$$W^a_{wet} = \gamma_{CL} + \gamma_{WL} - \gamma_{CW} \tag{6.8}$$

If the surface energy is expressed in terms of Lifshitz-van der Waals and acid-base interactions, W^a_{wet} can be obtained from the following equation [43,75] in which γ_L refers to water:

$$\begin{aligned} W^a_{wet} = &-2\,(\sqrt{\gamma_L^{LW}} - \sqrt{\gamma_W^{LW}})(\sqrt{\gamma_C^{LW}} - \sqrt{\gamma_L^{LW}}) \\ &-2\left[\sqrt{\gamma_L^+}\left(\sqrt{\gamma_W^-} + \sqrt{\gamma_C^-} - \sqrt{\gamma_L^-}\right) + \sqrt{\gamma_L^-}\left(\sqrt{\gamma_W^+} + \sqrt{\gamma_C^+} - \sqrt{\gamma_L^+}\right) - \sqrt{\gamma_W^+\gamma_C^-} - \sqrt{\gamma_W^-\gamma_C^+}\right] \end{aligned} \tag{6.9}$$

The work of adhesion with polar and disperse components ($W_{wet}^{a\,DP}$) in the presence of water was calculated according to *equation 6.8*. The geometric mean method was used to calculate the polar and disperse interactions between coating, wood and water as it is shown in *equation 6. 10.*

$$\gamma_{CL} = \gamma_C + \gamma_L - 2\sqrt{\gamma_C^D\gamma_L^D} - 2\sqrt{\gamma_C^P\gamma_L^P}\;; \quad \gamma_{WL} = \gamma_W + \gamma_L - 2\sqrt{\gamma_W^D\gamma_L^D} - 2\sqrt{\gamma_W^P\gamma_L^P}\;;$$

$$\gamma_{CW} = \gamma_C + \gamma_W - 2\sqrt{\gamma_C^D\gamma_W^D} - 2\sqrt{\gamma_C^P\gamma_W^P} \tag{6.10}$$

Inserting *equation 6.10* into *6.8* gives:

$$W_{wet}^{a\,DP} = 2\,(\gamma_L - \sqrt{\gamma_C^D\gamma_L^D} - \sqrt{\gamma_C^P\gamma_L^P} - \sqrt{\gamma_W^D\gamma_L^D} - \sqrt{\gamma_W^P\gamma_L^P} + \sqrt{\gamma_C^D\gamma_W^D} + \sqrt{\gamma_C^P\gamma_W^P}) \tag{6.11}$$

The calculated work of adhesion after exposure to water (W^a_{wet}) is given in *table 6.5*. Calculations are based on the surface energies given in *table 6.4*. The data of the air faced side of the coating and the wood data obtained along the grain were used because these data were most reliable. Regardless of the type of coating or the method of calculation, the work of adhesion was always positive, which meant that the reduction in adhesion strength was not due to surface energy effects.

Table 6.5   Interfacial work of adhesion between coating and wood after exposure to water

Coating:	$W^{a\,LW\text{-}AB}_{wet}$ (mJ m^{-2})	$W^{a\,DP}_{wet}$ (mJ m^{-2})
Ac1	19.6	84.0
Ac2	10.4	82.3
Ac3	4.7	79.2
WBA	19.4	82.9
HSA	14.1	84.4
SBA	29.9	85.6

The following data for water were used (mJ m^{-2}):

$$\gamma^{LW}\ 21.8;\ \gamma^{+}\ 25.5;\ \gamma^{-}\ 25.5;\ \gamma^{D}\ 21.8;\ \gamma^{P}\ 51.0$$

Table 6.6   Quantitative analysis of the factors influencing adhesion for coatings on pine sapwood exposed to liquid water. W is expressed in J m^{-2} ; A is dimensionless.

Coating:	Measured work of peeling (W^P)		Elastic strain Energy (β)	Interfacial work of adhesion W$^a_{cw}$	A (W^P/ W$^a_{cw}$)		Work of cohesive coating failure W^c
	EW	LW			EW	LW	
Ac1	152	107	0.087	28	1750	1226	3.3
Ac2	142	115	0.096	12341	1477	1202	2.6
Ac3	156	110	0.094	7415	1660	1172	2.9
WBA	238	126	0.098	25	2425	1290	5.8
HSA	682	200	0.093	74	7334	2152	22.4
SBA	580	255	0.093	96	6240	2744	60.5

6.3.5   Internal stress

The maximum volumetric swelling of the coatings and pine sapwood between 65 % RH and immersion in liquid water is given in *fig.6.16*. The alkyd based coatings clearly swelled less than the wood whereas the acrylic coatings swelled more than the wood. In particular Ac2 and Ac3 showed a very high swelling. The stored elastic energy due to internal strain from differential swelling between coating and wood was calculated according to *equation 6.4* and is given in *table 6.6*. The stored strain energy due to internal strain in the coatings Ac1, WBA, SBA and HSA was below the adhesion values measured. This was, however, not the case for the coatings Ac 2 and Ac 3, which had a very high stored elastic strain energy because the swelling of the coating was much higher than that of the wooden substrate. It should also be noted that, the differences between coatings Ac1 to Ac3 exposed to water vapour, were fairly consistent with the differences in the hygroscopic stress. The coating with the lowest stress (Ac1) showed a much better adhesion than the ones with the higher internal hygroscopic stress (Ac2 and Ac3).

The development and stress relaxation was measured directly; results are given in *fig.6. 17*. The results should, however, be judged only in a qualitative way because variation between samples was very large (co-variation up to 70%). The strong variation was most

likely due to blistering of the coating on the metal strips during immersion in water. Nevertheless, some interesting trends were observed. Coatings Ac2 and Ac3 showed the highest swelling stresses in liquid water in accordance with the direct swelling measurements, the developed stress only relaxed slowly. The other coatings showed a negative internal stress, which indicated contraction of the coating. This could be due to film formation or extraction of materials during immersion in water [55]. Coating WBA showed a typical behaviour, directly after immersion a positive stress developed (swelling) followed by a decrease to negative values. This was probably due to extraction of hydrophilic materials because similar changes in weight were observed during immersion of the WBA coatings. At 65 or 94 % RH, no significant stress was developed except for coating SBA.
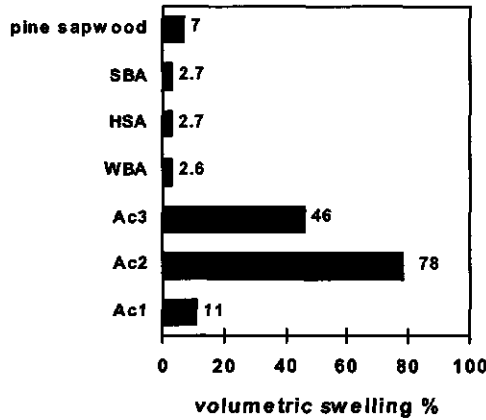

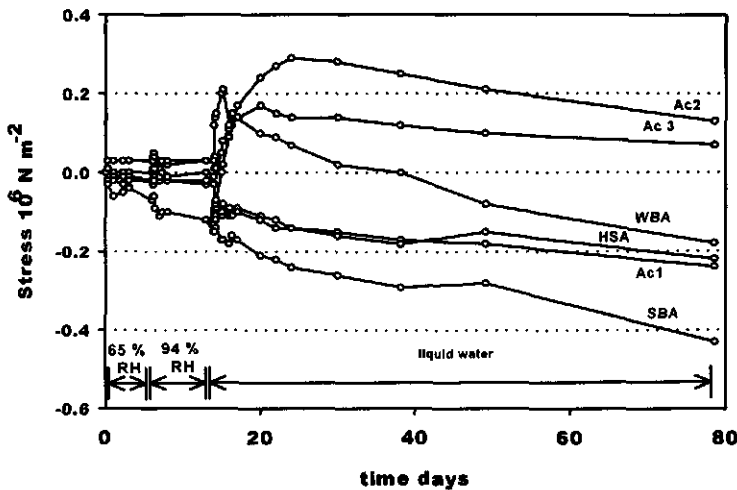**Figure 6.16**   Maximum volumetric swelling of coatings and wood from 65 % RH to liquid water

Figure 6.17   Development of internal stress in coatings

6.4   Discussion

The measured peel work of adhesion (W^p) is a function of: interfacial work of adhesion (W^a_{CW}) calculated from *equation 6.7*, work expanded in plastic deformation during peeling (W^d) and elastic energy stored in the coating because of internal strain (β). The relationship between these parameters is given by the following equation:

$$W^p = W^a_{CW} + W^d - \beta \tag{6.12}$$

The work expanded in plastic deformation was neglected in this study, because the forces used to peel the coating from the wood were clearly below the range where these coatings started to deform plastically. The plastic deformation of the coatings started at forces of 2.6 N mm^{-2} or higher whereas the force applied on the cross section of the coating was approximately 0.4 N mm^{-2} (acrylic coatings) to 2.1 N mm^{-2} (solvent borne alkyd).

From the results it was obvious that *equation 6.12* can not hold because $\beta >> W^a_{CW}$ which theoretically means that the coating should have detached spontaneously ($W^p<0$). There are three possible reasons why this did not occur. Firstly the hygroscopic stress might have relaxed very rapidly before the adhesion measurements were made. Secondly, it should be noted that the hygroscopic stress was calculated from the maximum swelling of the coating, which could be considerably higher than the swelling obtained during the test. Thirdly, a spontaneous detachment of the coating could be prevented by mechanical anchoring of the coating into the substrate.

The partial cohesive failure of the coating might also have had an influence on the measured strength. The work of cohesive failure (W^c) tensile with a cleavage stress (σ_t) in a bond during peeling at an angle of 180 ° is given by [81]:

$$W^c = \frac{\sigma_t^2 c}{4E} \tag{6.13}$$

Using the tensile strength and the E-modulus of the coating given in *table 6.2*, and an average coating thickness of 140 µm the work of cohesive failure was calculated. The work of cohesive failure based on wet strength properties is given in *table 6.6*. For the waterborne coatings, the work of cohesion was negligible. For the SBA or HSA it accounted for 3 to 10 % of the measured peel strength.

Neglecting the stored strain energy, an anchoring factor (A) can be introduced by writing:

$$A = \frac{W^p}{W^a_{CW}} \tag{6.14}$$

The calculated A-values are given in *table 6.6* for both early- and latewood adhesion and ranked between 1200 – 2700 in less penetrated latewood cells to 1500-7300 in deeper penetrated earlywood cells depending on coating type. The value of A might reflect two factors, the first is the increase in contact area on a microscopic level between coating and wood and the second is a hooking or anchoring effect. Image analysis of the wood-coating interface showed an increase in the true contact area between the coating and the wood by a factor of 1.1 in the latewood and a factor of 1.5 in the earlywood. These factors are low in comparison to the magnitude of A. This indicates that hooking or anchoring might be the more important factor.

Some of the results are still difficult to explain, although most of the factors that might influence measured adhesion data have been quantified. The penetration of the WBA coating in the outer wood cells was not much lower than for the SBA but the latter showed a much stronger adhesion. Also, the differences between the coatings in penetration of the latewood zones are rather small and do not seem to completely justify the large differences in measured

adhesion. An answer to these questions might come from the theory of weak boundary layers. Fractions of polymeric binder might cause weak boundaries because of their preferential accumulation in the wood-coating interface. Surfactants, present in high concentrations in all four waterborne coatings, could have negatively affected the adhesion because they act as loci of failure [69,82] or might cause electrostatic repulsion in the presence of water [43].

Water might contribute to the formation of a weak boundary layer as well if it accumulates in the coating-substrate interface [83]. This might even cause differences in adhesion between early- and latewood adhesion because differences in wood moisture content exist between these area's [84,85]. Wood moisture content in the earlywood zones would have been higher than in the latewood zones which causes higher swelling. Differences in swelling between early- and latewood could also be influenced by the angle between growth-rings and the surface of the wood [86-87]. Both facts might lead to differences in stored strain energy on a microscopic level.

6.5   Conclusions

With the newly developed tape peel method, adhesion of coatings on wood could be measured up to adhesion forces of 300 to 400 J m^{-2}. By comparing peel-strength with the wood microstructure, differences in adhesion within one growth-ring of the wood were observed. Adhesion was clearly higher in the deeper penetrated earlywood cells in comparison to the less penetrated latewood cells and differences in adhesion increased with better penetration and wetting.

For the coatings studied, the method was limited to the measurement of wet adhesion, which was very much lower compared to the dry adhesion. The six coatings studied showed very clear differences in wet adhesion strength. The adhesion of the acrylic coatings was the lowest, followed by the alkyd emulsion and the highest adhesion was found for the solventborne or high solid alkyd paints. Water vapour reduced the adhesion strength, but the reduction was the strongest with liquid water.

Differences between pine sapwood and spruce were small and seemed only to be related to differences in wood moisture content. The critical moisture content in the interface lies around 25 % for the acrylic coating and around 30 % for the other coatings. A thermodynamic evaluation of the work of adhesion after exposure to water showed no reasons for reduced adhesion. The lower wet adhesion can partially be explained by the stored strain energy due to internal stresses. The poorest adhesion was observed if the swelling of the coating was very much higher than the swelling of the wood. Weak boundary layers might also contribute to the decreased adhesion.

Analysis of the fractured surfaces showed that partially cohesive failure had taken place in the coating. Cohesive failure was higher with the better adhering HSA and SBA paints. The calculated contribution of the cohesive failure to the measured work of adhesion was only in the range of 3-10 %. Analysis of the fractured surface by infrared analysis and contact angle measurements showed differences between the air-faced and wood-faced side of the coating. The wood-faced side of the coating seemed to be enriched in polymeric material.

The measured work of peel adhesion was about 1200 to 7300 times larger than the interfacial work of adhesion between the coating and the wood. The differences in adhesion between the coatings did not correlate with the differences in interfacial adhesion but did show a good correlation with differences in penetration and wetting. This confirms that coating adhesion is strongly related to the penetration of a coating into wood. Firstly by mechanical anchoring or hooking and secondly by increasing the contact area between wood and coating on a micro level. The hygroscopic stored strain energy in coatings exposed to moisture was much higher than the interfacial work of adhesion, which only emphasised the importance of mechanical adhesion.

To obtain good adhesion of a coating to wood there are two critical factors. Firstly, the coating should wet the wood cells properly and to a certain extent penetrate into the open pores in the earlywood. Secondly, the hygroscopic expansion should be equal to that of the wood to minimise internal stress in the coating. To understand the adhesion of a coating on wood in more detail, an improved knowledge on microscopic moisture accumulation at the wood-coating interface and the chemical composition of the wood-faced side of the coating is desirable.

Acknowledgements

References

[1]   **Jansen, M.L.**; Performance testing of exterior wood primers, Journal of the Oil and Colour Chemists Association, 5, 1986, 117-128.
[2]   **Bardage, S. L.; Bjurman, J.**; Adhesion of waterborne paints to wood, Journal of Coatings Technology, 70 (878), 1998, 39-47.
[3]   **Ahola, P.**; Adhesion between paints and wooden substrates: effects on pre-treatment and weathering of wood, Materials and structures, 28, 1995, 350-356.
[4]   **Hora, G.; Belz, A.; Kruse D.; Avarlik A.**; New approach to investigate the suitability of coatings for stable end-use conditions, In: Advances in exterior wood coatings and CEN-standardisation, Proceedings of PRA-Conference Brussels, 1998, paper 2.
[5]   **Rijckaert, V.; van Acker, J.; Stevens, M.; Meijer, M. de; Militz, H.**; Quantitative analysis of the penetration of waterborne primers into wood by means of fluoresence microscopy, In: Advances in exterior wood coatings and CEN-standardisation, Proceedings of PRA-Conference Brussels, 1998, paper 19.
[6]   **Bosschaart-Thurich, K.; Pathak, U.; Berkhout, L.**; Advances in waterborne coatings for joinery, In: Advances in exterior wood coatings and CEN-standardisation, Proceedings of PRA-Conference Brussels, 1998, paper 26.
[7]   **Meijer, M. de; Militz, H.**; Wet adhesion measurements of wood coatings, Holz als Roh- und Werkstoff, 56, 1998, 306.
[8]   **Collett, B.M.**; A review of surface and interfacial adhesion and interfacial adhesion in wood science and related fields, Wood Science and Technology, 6, 1972, 1-42.
[9]   **Good, R.J.**; On the definition of adhesion, Journal of Adhesion, 8, 1976, 1-9.
[10] **Mittal, K.L.**; The role of the interface in adhesion phenomena, Polymer Engineering and Science, 17 (7), 1977, 467-473.
[11] **Wake, W.C.**; Theories of adhesion and uses of adhesives: a review, Polymer, 19, 1978, 291-309.
[12] **Allen, K.W.**; A review of contemporary views of theories of adhesion, Journal of Adhesion, 21, 1987, 261-277.
[13] **Pizzi, A.**; Non-mathematical review of adhesion theories as regards their applicability to wood, Holzforschung Holzverwertung, 44, 1992, 62-97
[14] **Prosser, J.L.**; Adhesion of coatings theory and practice, PRA Teddington, 1993.

[15] **Richter, K.; Feist, W.C.; Knaebe, M.T.**; The effect of surface roughness on the performance of finishes. Part 1, Roughness characterisation and stain performance, Forest Products Journal, 45 (7/8), 1995, 91-97.

[16] **Coté, W.A.**; Wood as a substrate for coatings, Journal of Coatings Technology, 55 (699), 1983, 25-35.

[17] **Kollmann, F.F.P.; Coté, W.A.**; Principles of wood science and technology Vol. I, Springer, Berlin, Heidelberg, New York, Tokyo, 1984, pp. 162.

[18] **Siau, J.F.**; Transport processes in wood, Springer, Berlin, Heidelberg, New York, Tokyo, 1984, pp. 142.

[19] **Rødsrud, G.; Sutcliff, E.J.**; Alkyd emulsions-properties and application. Results from comparative investigations of penetration and ageing of alkyds, alkyd emulsions and acrylic dispersions, Surface Coatings International, 77 (1), 1994, 7-16.

[20] **Nussbaum, R.M.; Sutcliffe, E.J.; Hellgren, A.C.**; Microautoradiographic studies of the penetration of alkyd, alkyd emulsion and linseed oil coatings into wood , Journal of Coatings Technology, 70 (878), 1998, 49-57.

[21] **Rijckaert, V.; Acker, J. van; Stevens, M.; Meijer, de M.; Militz, H.**; Quantitative assessment of the penetration of water-borne and solvent-borne wood coatings in Scots pine sapwood, accepted for Holz als Roh- und Werkstoff, 1999.

[22] **Wagenführ, R.; Scheiber, C.**; Holzatlas, VEB Fachbuchverlag Leipzig, 1985, pp 656-665.

[23] **Nussbaum, R.M.**; Penetration of water-borne alkyd emulsions and solvent-borne alkyds into wood, Holz als Roh- und Werkstoff 52, 1994, 389-393.

[24] **Meijer, de M.; Militz, H.; Thurich, K.**; Surface interactions between low voc-coatings and wooden substrates, Proceedings of XXIII Fatipec Con. Vol. C., 1996, 191-214.

[25] **Meijer, M. de; Thurich, K.; Militz, H.**; Comparative study on penetration characteristics of modern wood coatings, Wood Science and Technology, 32, 1998, 347-365.

[26] **Gray, R.V.**; The wetting, adhesion and penetration of surface coatings on wood, Journal of The Oil and Colour Chemists Association, 44 (11), 1961, 756-786.

[27] **Loon, J. van**; The interactions between paint and surface, Journal of The Oil and Colour Chemists Association, 49 (10), 1966, 844-867.

[28] **Marian, J.E.; Stumbo, D.A.; Maxey, C.W.**; Surface texture of wood as related to glue-joint strength, Forest Products Journal, 8 (12), 1958, 345-351.

[29] **Hse, C.Y.**; Gluability of southern pine earlywood and latewood, Forest Products Journal, 18 (12), 1958, 32-36.

[30] **Ward, R.J.; Coté, W.A.; Day, A.C.**; The wood substrate-coating interface, Journal of Paint Technology and Engineering, 36 (477), 1964, 1091-1098.

[31] **Ahola, P.**; Adhesion between paint and wood substrate, Journal of The Oil and Colour Chemists Association, 74 (5), 1991, 173-176.

[32] **Williams, R.S.; Feist, W.C.**; Durability of paint or solid-color stain applied to preweathered wood, Forest Products Journal, 43 (1), 1993, 8-14.

[33] **Thay, P.D.; Evans, P.D.**; The adhesion of an acrylic primer to weathered radiata pine surfaces, Wood and Fiber Science 30 (2), 1998, 198-204.

[34] **Richter, K.; Feist, W.C.; Knaebe, M.T.**; The effect of surface roughness on the performance of finishes, Research report 115/31, Swiss Federal Laboratories for Materials Testing and Research, Dübendorf, Switzerland, 1994.

[35] **Zisman, W.A.**; Surface energetics of wetting spreading and adhesion, Journal of Paint Technology, 44 (564), 1972, 42-57.

[36] **Nguyen, T.; Johns, W.E.**; Polar and dispersion force contributions to the total surface free energy of wood, Wood Science and Technology, 12, 1978, 63-74.

[37] **Scheikl, M.; Dunky, M.**; Measurement of dynamic and static contact angles on wood for the determination of its surface tension and the penetration of liquids into the wood surface, Holzforschung 52, 1998, 89-94.

[38] **Gray, V.R.**; The wettability of wood, Forest Prod. Journal 12 (9), 1962, 452-461.

[39] **Fowkes, F.M.**, Attractive forces and interfaces, Industrial Engineering Chemistry, 56 (12), 1964, 40-52.

[40] **Owens, C.K.; Wendt, K.C.**; Estimation of the surface free energy of polymers, Journal Applied Polymer Science, 12, 1969, 1741-1747.

[41] **Wu, S.**; Calculation of interfacial tension in polymer systems, Journal Polymer Science Part C, 34, 1971, 19-30.

[42] **Mantanis, G.I.; Young, R.A.**; Wetting of Wood, Wood Science and Technology, 31, 1997, 339-353.

[43] **van Oss, C.J.; Chaudhury, M.K.; Good, R.J.**; Interfacial Lifshitz van der Waals and polar interactions in macroscopic systems, Chemical Review, 88, 1988, 927-941.

[44] **Gardner, D.J.**; Application of the Lifshitz-van der Waals acid-base approach to determine wood surface tension components, Wood and Fiber Science, 28 (4), 1996, 422-428.

[45] **Shen, Q.; Nylund, J.; Rosenholm, J.B.**; Estimation of the surface energy and acid-base properties of wood by means of wetting method, Holzforschung, 52, 1998, 521-529.

[46] **Raghava, R.S.; Smith, R.S.**; Adhesion through molecular entanglements in polymer interfaces, Journal of Polymer Science: Part B: Polymer Physics 27, 1989, 2525-2551.

[47] **Kerr, A.J.; Goring, D.A.I.**; The role of hemicellulose in the delignification of wood, Canadian Journal of Chemistry, 53 (6), 1975, 952-959.

[48] **Tarkow, H.; Feist, W.C.; Southerland, C.F.**; Interaction of wood with polymeric materials, penetration versus molecular size, Forest Prod. Journal, 16 (10), 1966, 61-65.

[49] **Olsson, A-M.; Salmén, L.**; Humidity and temperature affecting hemicellulose softening in wood, Proceedings Int. Conf. On Wood-Water Relations, COST E8, Copenhagen, 1997, 269-279.

[50] **Bikerman, J.J.**; Causes of poor adhesion: Weak boundary layer, Industrial Engineering Chemistry, 59 (9), 1967, 40-44.

[51] **Nussbaum, R.M.**; The critical time limit to avoid natural surface inactivation of spruce surfaces (Picea Abies) intended for painting and gluing, Holz als Roh- und Werkstoff, 53, 1995, 384.

[52] **Kambanis, S.M.; Chip, G.**; Polymer and paint properties affecting wet adhesion, Journal of Coatings Technology, 53 (682), 1981, 57-64.

[53] **Croll, S.G.**, Adhesion loss due to internal strain, Journal of Coatings Technology, 52, (665), 1980, 35-43.

[54] **Perera, D.Y.**; On adhesion and stress in organic coatings, Progress in Organic Coatings, 28, 1996, 21-23.

[55] **Negele, O.; Funke, W.**; Internal stress and wet adhesion of organic coatings, Progress in Organic Coatings, 28, 1996, 285-289.

[56] **Perera, D.Y.**; Stress Phenomena in organic coatings, In: Paint and coating testing manual (Ed. Koleske, J.V.) ASTM Manual Series MNL 17, 1995, 585-599.

[57] **Croll, S.G.**; Internal strain in solvent-cast coatings, Journal of Coatings Technology, 51 (648), 1979, 64-68.

[58] **Perera, D.Y.; Vanden Eynde, D.**; Moisture and temperature induced stresses (hygrothermal stresses) in organic coatings, Journal of Coatings Technology, 59, 748, 1987, 55-63.

[59] **Underhaug,A.; Lund, T.J.; Kleive, K.**; Wood protection - the interaction between substrate and product and the influence on durability, Journal of the Oil and Colour Chemists Association, (11), 1983, 345-350.

[60] **Jaic, M.; Zivanovic, R.**; The influence of the ratio of the polyurethane coating components on the quality of finished wood surface, Holz als Roh- und Werkstoff, 55, 1997, 319-322.

[61] **Boxall, J.**; Exterior wood finishes: performance testing by accelerated natural weathering, Journal of the Oil and Colour Chemists Association, 67 (2), 1984, 40-44.

[62] **Williams, R.S.; Plantinga, P.L.; Feist, W.C.**; Photodegradation of wood affects paints adhesion, Forest Products Journal, 40 (1), 1990, 45-49.

[63] **Hopma, P.C.**; The direct pull-off test, Journal of the Oil and Colour Chemists Association, 67 (7), 1984, 179-184.

[64] **Sickfeld, J.**; Experimental aspects of adhesion testing, Journal of the Oil and Colour Chemists Association, 61, (8), 1978, 292-298

[65] **Naslund, G.E.; Hallberg, B.O.**; New tool for measuring adhesion of coatings to wood, Forest Products Journal, 9(1), 1959, 23-26.

[66] **Hemmelrath, M.; Funke, W.**; Bestimmung der Nasshaftung von organischen Beschichtungen, XIX Fatipec Conference, Vol. 4, 1988, 137-153.

[67] **Evans, P.D.; Thay, P.D. Schmalzl, K.J.**; Degradation of wood surfaces during natural weathering. Effects on lignin and cellulose and on the adhesion of acrylic latex primers, Wood Science and Technology, 30, 1966, 411-422.

[68] **Barbehön, J.**; Haffestigkeit reproduzierbar prüfen, Metalloberfläche, 46 (12), 1996, 546-552.

[69] **Kientz, E.; Charmeau, J.Y.; Holl, Y.; Nanse, G.**; Adhesion of latex films. Part I Poly(2-ethyl-hexyl methacrylate) on glass, Journal Adhesion Science and Technology, 10 (8), 1996, 745-759.

[70] **Kalnins, M.A.; Katzenberger, C.; Schmieding, S.A.; Brooks, J.K.**; Contact angle measurement on wood using videotape technique, Journal of Colloid and Interface Science, 125 (1), 1988, 344-346.

[71] **Liptáková, E.; Kúdela, J.**; Analysis of the Wood-Wetting Process, Holzforschung, 48 1994, 139-144.

[72] **Nussbaum, R.M.**; Natural wood surface inactivation evaluated by contact angle measurements, submitted to Holzforschung, 1998.

[73] **Good, R.J.**; Contact angle, wetting, and adhesion: a critical review, In: Contact angle, wettability and adhesion (Ed. Mittal, K.L.), 1993, 3-36.

[74] **van Oss, C.J.**; Acid-base interfacial interactions in aqueous media, Colloids and Surfaces A: Physicochemical and Engineering Aspects, 78, 1993, 1-49.

[75] **Perera, D.Y.; Eynde, D. Van den**; Considerations on a cantilever (beam) method for measuring the internal stress in organic coatings, Journal of Coatings Technology, 53 (677), 1981, 39-44.

[76] **Potente, H.; Krüger, R.**; Bedeutung polarer und disperser Oberflächenspannungsanteile von Plastomeren und Beschichtungstoffen für die Haftfestigkeit von Verbundsystemen, Farbe und Lack, 84 (2), 1978, 72-75.

[77] **Huh, C.; Mason, S.G.**; Effects of surface roughness on wetting (theoretical), Journal of Colloid and Interface Science, 60 (1), 1977, 11-38.

[78] **Socrates, G.**; Infrared characteristics groups frequencies, John Wiley and Sons Chicester, 1980, 85 p.

[79] **Roche, A. A.; Dole, P.; Bouzziri, M.**; Measurements of the practical adhesion of paint coatings to metallic sheets by pull-off and three-point flexure tests, Journal of Adhesion Science and Technology, 8 (6), 1994, 587-609.

[80] **Osterwold, M.; Armbruster, K.**; Correlation between surface tension and physical paint properties, XXIV Fatipec Conference, Vol. A. Interlaken, 1998, 37-47.

[81] **Kinloch, A.J.**; The science of adhesion. Part 2, Mechanics and mechanisms of failure, Journal of Materials Science, 17, 1982, 617-651.

[82] **Charmeau, J.Y.; Kientz, E.; Holl, Y.**; Adhesion of latex films; influence of surfactants, Progress in Organic Coatings, 27, 1996, 87-93.
[83] **Nguyen, T.; Byrd, E.; Bentz, D.; Lin, C.**; In situ measurement of water at the organic coating / substrate interface, Progress in Organic Coatings, 27, 1996, 181-193.
[84] **Arfvidsson, J.; Lindgren, O.; Wiberg, P.**; The development of a moisture sorption model to predict moisture distribution within solid wood, Proceedings Int. Conf. On Wood-Water Relations, COST E8, Copenhagen, 1997, 107-120.
[85] **Nicholls, C.**; NMR for non-destructive wood moisture content measurements, Workshop on wood and lumber scanning, Skellfteå, Sweden, 1992, 43-48.
[86] **Browne, F.L.**; Swelling of springwood and summerwood in softwood, Forest Products Journal, 1957, 416-424.
[87] **Ellwood, E.L.; Wilcox, W.W.**; The shrinkage of cell walls and cell cavities in wood microsections, Forest Products Journal, 1962, 235-242.

7. Sorption Behaviour and Dimensional Changes of Wood-Coating Composites[*]

Summary

The moisture related properties of wood-coating composites have been studied to evaluate the influence of coating penetration on the protection of wood against moisture. Pine sapwood samples were vacuum-impregnated with 7 pigmented and unpigmented coatings, both water and solvent borne. The retention and void filling of the coating have been determined. After drying, the samples were exposed to relative humidities between 33 and 98 % and to liquid water and equilibrium moisture content and dimensional changes were measured. The rate of swelling and moisture sorption has been measured, the latter was also used to calculate diffusion coefficients. The sorption isotherms were analysed by the Hailwood-Horrobin equation. In order to obtain additional information on the hygroscopicity of coatings, similar measurement were made on free coating films.

The void filling of wood with coating material has the strongest impact on the uptake of liquid water. A limited reduction was observed for the equilibrium moisture content, the diffusion coefficient during adsorption and the rate of dimensional change. No influence on the equilibrium swelling have been found but the shrinkage during desorption was however often slightly increased for the wood-coating composites.

The limited impact of the penetrated coating on moisture related properties can to a large extent be explained by the low void filling after drying (20 -60 %) and the relatively high moisture sorption and swelling of the coating film itself. In general, it can be concluded that the moisture protection of penetrated coating material is low in comparison to coating applied as a film on the surface of wood.

7.1   Introduction

The protection of wood against liquid water and water vapour is one of the most important functions of a coating for exterior use. The reduction of wood moisture content should prevent the wood from cracking and decay by fungi. This aspect has become even more important with the introduction of waterborne coatings, which usually have a higher water permeability. Research on the permeability of various waterborne and other types of wood coatings has been carried out during recent years [1-7]. All these studies are dealing with the permeability of a coating applied as a film on the surface of the wood. Far less is known about the moisture related properties of the outer wood cells if they are filled with a penetrating coating.

Schneider [8,9] studied the hygroscopicity and the diffusion of water in wood impregnated with linseed oil. Moisture diffusion rates and equilibrium moisture content were found to be reduced with increasing linseed oil content. Additional information about the hygroscopic nature of wood impregnated with polymers is available from various studies on bulking or dimensional stabilisation of wood. Militz and Peek [10] studied poplar, impregnated with polymers comparable to those used as binders in coatings, like waterborne acrylic dispersions, waterborne alkyd-emulsions and air-drying alkyd resins dissolved in methoxy-propanol. Most of these chemicals reduced the water sorption and the dimensional changes of wood.

The polymers used in other studies are often based on the same monomers as those used in coating binders, but have a smaller molecular size or volume because they are intended to penetrate the transient capillaries in the wood cell wall. Dimensional stability of basswood and Eastern white pine, immersed with a water-dilutable air-curable alkyd-resin, was studied by Smulski and Côté [11]. Initially, a moderate reduction of swelling was observed, but this effect was lost after leaching. Treatments of basswood with various mixtures of waterborne polymers and cosolvents [12] caused only a small reduction of shrinkage. Kabir *et al* [12] used, among other chemicals, a 7% solution of an acrylic polymer and a combination of water dilutable alkyd resin (5%) and butyl carbitol (20%) to stabilise Southern yellow pine. Both chemicals caused certain water repellence, but only the acrylic resin caused a small reduction of swelling (Anti-Shrink-Efficiency of 13%). Ellis [13] treated maple, red oak and Southern pine with various acrylate monomers followed by an in situ polymerisation. For most of the acrylates, no permanent reduction in swelling was found.

The objective of this research is to measure the water sorption, diffusion rates and subsequent dimensional changes of wood cells which are filled with a coating, which will be further referred to as "wood-coating composites". A better knowledge of the moisture content and the dimensional changes of wood-coating composites will help to judge the usefulness of improving the penetration characteristics of wood primers. Furthermore, a better understanding of the dimensional changes in the wood-coating interface will facilitate the research on development of stress and cracking in topcoats. Finally, knowledge about the moisture content in wood-coating composites can help to understand the susceptibility of coatings to biological degradation like mould-growth and blue-stain in service.

7.2   Materials and Methods

Seven different model coatings with known formulations have been used in this study. The selection was based on penetration characteristics determined in previous research [14]. Four unpigmented (denoted with U) coatings have been used: a waterborne acrylic dispersion (WAD-U), an alkyd emulsion (WBA-U), a high solid alkyd resin with a reactive solvent (HSA-U) and a traditional solventborne alkyd (SBA-U). The formulation of the unpigmented coatings consisted only of the commercial binder and either water or white spirit as diluent.

To facilitate drying a siccative mixture was added in case of the alkyd resins and coalescent in case of the acrylic dispersion. Opaque paints (denoted with P), pigmented with titanium dioxide to a pigment volume concentration of about 17 %, were also included for the alkyd emulsion (WBA-P), high solid alkyd (HSA-P) and solventborne alkyd (SBA-P). A pigmented acrylic dispersion was not used, because of its very limited penetration into the wood. An overview of the properties of the coatings is given in *table 7.1*. All coatings contained about 5 % of the fluorochrome Rhodamine B for examination of the penetration with a fluorescent microscope after treatment. Preliminary tests with a binder containing a covalently bond anthracene fluorochrome showed no significant separation of the Rhodamine B from the polymer solution. All tests were made on Nordic grown, industrially pre-dried, defect free pine sapwood *(Pinus sylvestris)* with a density of 546 to 580 kg m^{-3} and a growth-ring width of 2 to 5 mm.

Table 7.1 Physical properties of the coatings tested

	density [a] kg.m^{-3}	mass % solids [b]	volume % solids [c]	water-vapour transmission rate [d] kg.m^{-2}.h
WBA-P	1250	56	45	10.60
HSA-P	1395	88	91	1.31
SBA-P	1133	67	44	0.69
WAD-U	1046	48	41	3.63
WBA-U	1033	61	40	1.51
HSA-U	979	94	64	1.34
SBA-U	910	45	35	1.03

a: determined according to ISO-2811
b: determined according to ISO-3251
c: determined according to IS0-3233
d: determined according to ASTM-1653 in range: 98-65% RH

If the coatings used in this study are applied on surfaces along the grain of the wood, the penetration is mostly limited to depth of 3 to 15 cells away from the surface [14]. Therefore, in practice sorption and dimensional changes in the wood-coating composites will take place in very small areas of less then a square millimetre. Because measurement of dimensional change and moisture content on such small areas is beyond the possibility of existing measuring equipment, the following alternative approach was used.

Small blocks of 33 x 33 x 4 mm (radial x tangential x longitudinal direction) were impregnated by an overnight vacuum of 0.01 bar, subsequent immersion by the coating whilst maintaining vacuum, followed by an overnight pressure treatment at 7 bar under a nitrogen atmosphere to avoid oxidative drying of the coating during impregnation. After treatment, samples were wiped free from coating on the surface and allowed to dry at room temperature for several days. The samples originated from four different areas in one piece of wood. To reduce the disturbing influence of variation inside the wood, treatments and replications were allocated within a blocked experiment. Eight to ten replicates have been used for most measurement. For measurements on the coating itself, free films were prepared on plastic sheets from which the coating was removed after drying.
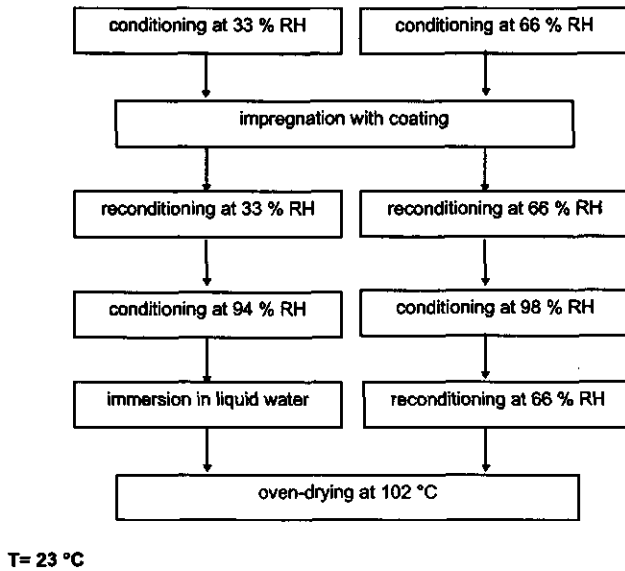
Figure 7.1   Environmental conditions used during the experiments

Climatisation of the samples at various relative humidities was done in boxes over corresponding saturated salt solutions at a temperature of 23 °C. An overview of the environmental conditions used during the experiments is given in *fig.7.1*. Weight changes were recorded to an accuracy of 1 mg. Dimensions of the wood-coating composites were measured by either discrete measurements with a digital thickness gauge with an accuracy of 1µm, or continuously in a swellograph with an accuracy of 10 µm. All samples were oven-dried (103 ± 2 °C) afterwards to determine dry-mass. Dimensional changes in the free coating film were determined by calculating the volume from the mass of displaced water, whilst submersing the film in water hanging under an analytical balance in analogy to the ISO 3233 standard. According to this standard, the volume of the coating is calculated according to the following formula. The time for submersing the film to determine volume (V) is only a few seconds, therefore the uptake of water during this determination can be neglected in comparison to the uptake of moisture during climatisation.

$$V = \frac{\left(m_{air} - m_{liquid}\right)}{\rho_{water}} \tag{7.1}$$

With: m_{air} being the mass of the coating in air, m_{liquid} being the mass of the coating while submersed in water and ρ_{water} is the density of the water. The distribution of the coating material within the wood has been evaluated by light, fluorescence- and scanning electron microscopy.

7.3   Results and Discussion

7.3.1   Coating impregnation

The coatings have been impregnated into wood which has been climatised at 33 % relative humidity to a moisture content of about 11 % and into wood which has been climatised at 66 % relative humidity to a moisture content of about 14 %. Somewhat higher quantities of coating could be impregnated in the wood samples with the lower moisture content. The uptake on a mass basis, retention and fractional void filling data are given in *table 7.2*. The fractional void filling (F_{vf}) of the wet coating is calculated according to the following procedure described by Siau [15], in which the porosity of wood is expressed as a function of specific gravity of the wood (G) and the wood moisture content (u).

$$F_{vf} = \frac{w_{coating}}{\rho_{coating} V_{wood} \cdot (1 - G(0.667 + 0.01u))} \tag{7.2}$$

With: $w_{coating}$ is the weight of the coating taken up by the wood with volume V_{wood} ; $\rho_{coating}$ is the density of the liquid coating. The void filling of the dry coating is obtained by multiplying the void filling of the wet coating with the volume based solid matter content of the coating.

Table 7.2   Uptake, retention and fractional void filling of the wood-coating composites

	climatised at 33 % RH				climatised at 66 % RH			
	mass-uptake	retention	void filling	void filling	mass-uptake	retention	void filling	void filling
	$kg_{coating}$/ kg_{wood}	$kg_{coating}$ m^{-3}	wet coating	dry coating	$kg_{coating}$/ kg_{wood}	$kg_{coating}$ m^{-3}	wet coating	dry coating
WBA-P	1.5	876	0.78	0.35	1.3	729	0.66	0.29
HSA-P	1.5	870	0.70	0.63	1.3	717	0.58	0.53
SBA-P	1.1	658	0.65	0.28	1.0	541	0.54	0.23
WAD-U	1.2	669	0.71	0.29	1.0	553	0.60	0.25
WBA-U	1.3	766	0.83	0.33	1.2	638	0.70	0.28
HSA-U	1.0	591	0.67	0.43	0.9	496	0.57	0.36
SBA-U	1.0	566	0.69	0.24	0.9	468	0.58	0.20

Although the fractional void filling by the liquid coating is fairly high, the remaining void filling after drying is rather low, due the decrease in volume of the coating after drying. An exception to that is observed for the high solid coatings which have a dry fractional void filling of 0.4 to 0.6, due to the higher percentage solids on a volumetric basis. The microscopic examination of the samples showed that the coating has penetrated into the centre of the samples. Nevertheless, many lumina are not filled (see *fig.7.2*) which is consistent with the relatively low dry fractional void filling. The coating has mostly wetted the cell wall well, but occasionally small cavities between coating and cell wall are observed (see *fig. 7.3*). No signs of cell wall penetration by the coating were observed.

Figure 7.2   SEM-microphotograph of pine sapwood impregnated with WAD300-U
                        at a magnification of 200X.

Figure 7.3   SEM-microphotograph of pine sapwood impregnated with HSA-P at a
                        magnification of 1500 X.

7.3.2   Moisture sorption

The equilibrium moisture content (mass of water as percentage of dry mass of the sample) of the wood-coating composite at relative humidities of 33, 66, 94 and 98 % is shown in *fig.7.4* Depending on the type of sample, it took 6000 to 20,000 minutes to reach equilibrium. Most of the wood-coating composites show lower equilibrium moisture content in comparison to the control at relative humidities up to 94%. At a relative humidity of 98 %, the moisture content in the wood-coating composites increases to a higher level, which is closer to that of untreated wood. An unexpected behaviour has been observed for the unpigmented solvent borne alkyd SBA-U, which showed very high equilibrium moisture content. The equilibrium moisture content of the wood filled with unpigmented solvent borne alkyd resin is higher as for the wood and the resin separately. Apparently, the presence of the alkyd resin inside the wood facilitates the adsorption of water molecules. The increase in moisture content during immersion in liquid water of the samples previously climatised at 94 % relative humidity, is given in *fig.7.5*. The filling of the wood with coating material appears to be very effective in repelling the uptake of liquid water far above fibre saturation point. The reduction in moisture content in the wood-coating composites is permanent because lower equilibrium values are reached. This is most likely the result of filling voids inside the wood with coating material, which reduces the space available for liquid water. The very strong reduction by the HSA-P and HSA-U is supporting this idea because these products have the highest void filling by dry coating material.
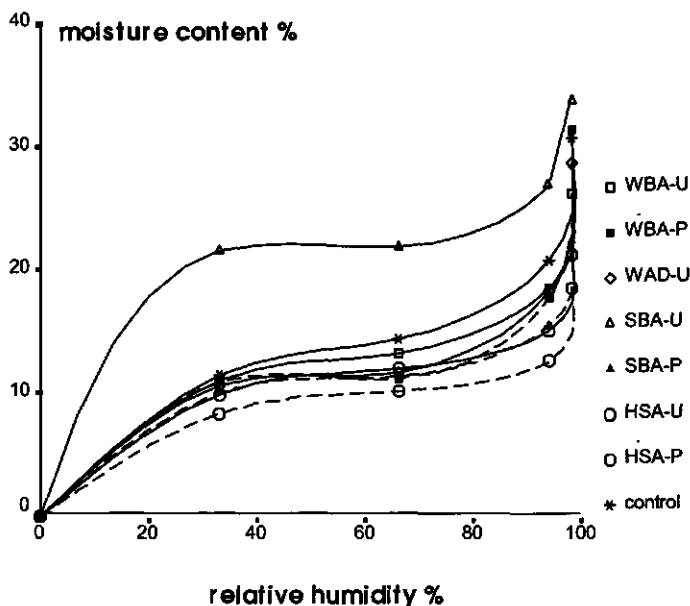
Figure 7.4   Moisture content of the wood-coating composites at various relative humidities
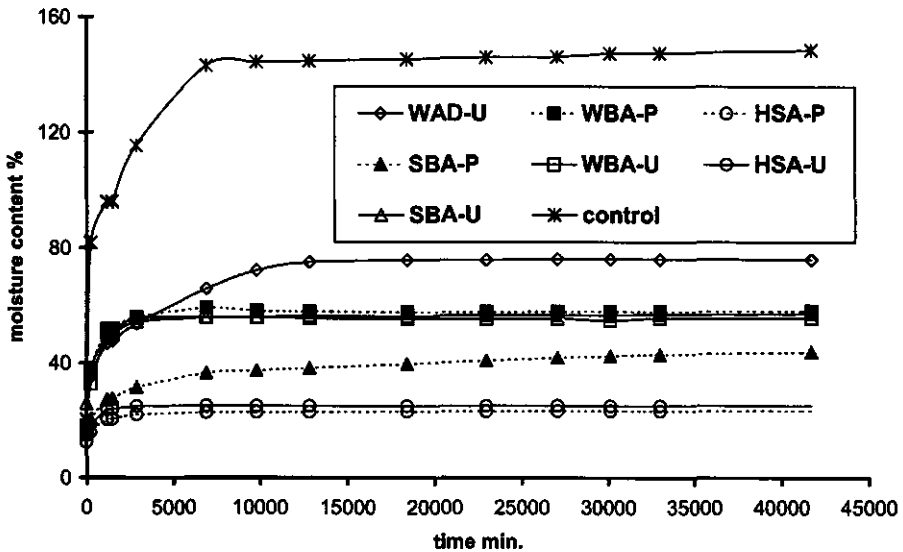
Figure 7.5   Increase in moisture content of samples (previously climatised at 94 % RH) during immersion in liquid water.

The equilibrium moisture content of free coating films has also been determined at the same relative humidities and after immersion in liquid water. The results belonging to this experiment are given in *table* 7.3 Within the studied range of 66 to 98 % relative humidity, the moisture content of the coating itself is actual constant, excluding some variation due to experimental errors. After immersion in liquid water, the moisture content increased strongly. The unpigmented acrylic coating WAD-U showed an increase in moisture content at already lower relative humidities, with an extremely high uptake of liquid water.

Table 7.3   Equilibrium moisture content of free coating films

	relative humidity %					liquid		
	33			**94**			**water**	
WBA-P	10.3	±	1.9	10.9	±	1.5	15.2	±	1.3
HSA-P	4.9	±	0.2	5.2	±	0.2	9.8	±	0.2
SBA-P	4.7	±	0.2	4.8	±	0.1	13.9	±	0.2
WAD-U	3.3	±	0.2	6.2	±	0.2	65.7	±	4.8
WBA-U	15.6	±	0.6	14.7	±	0.5	20.2	±	0.6
HSA-U	16.6	±	0.9	17.2	±	0.9	27.7	±	1.0
SBA-U	12.3	±	1.2	11.8	±	0.2	24.6	±	1.1

The sorption data of the wood-coating composites have been fitted by the Hailwood-Horrobin equation [16,17] following the procedure described by Yasuda *et al* [18]. Fit parameters (A, B, C) and equilibrium constants are given in *table 7.4* together with the r^2. K_1 is the equilibrium constant between the free dissolved (capillary condensed) water in the solid material (either wood or coating) and the hydrate (surface bound) water. K_2 is the equilibrium constant between the dissolved water and the external vapour pressure. W is the molecular weight of the polymer substance necessary to associate with one molecular weight of water.

Table 7.4 Calculated values of A, B, C, K_1, K_2 and W belonging to the Hailwood-Horrobin equation

	r^2	A	B	$C.10^{-3}$	K_1	K_2	W
WAD-U	0.83	4.377	0.297	2.159	1.10	66.922	11080
WBA-P	0.80	5.69	0.346	2.539	1.10	63.829	13697
HSA-P	0.73	2.444	0.244	1.601	1.13	76.099	7135
SBA-P	0.80	3.313	0.256	1.749	1.11	68.897	8678
WBA-U	0.81	2.364	0.209	1.425	1.12	73.345	6618
HSA-U	0.78	1.999	0.204	1.331	1.13	76.655	5884
SBA-U	0.93	1.586	0.117	0.706	1.12	63.114	3814
control	0.76	2.039	0.194	1.383	1.12	77.737	6055

The Hailwood-Horrobin equation fits the experimental data reasonably well with r^2 values of 0.72 or higher. K_1 is clearly increased in case of the HSA-P and HSA-U, which means an increase in the amount of free dissolved water and decreased in case of WAD-U and WBA-P, which means an increase in surface bound water. The equilibrium between dissolved water and the external vapour pressure (K_2) is hardly influenced by the coating treatment except for SBA-U. The values of W are somewhat increased, again apart from the SBA-U coating. Hailwood-Horrobin fit parameters obtained by Hartley and Schneider [17] for wood-polymer composites of sugar maple also showed an increase of K_1 and W. K_2 did not showed a consistent change because it increased with certain treatment and decreased for others.

7.3.3 Moisture diffusion coefficients
Diffusion coefficients are calculated from the sorption-data in the range of 66-98 % RH and 98-66% RH. The calculation is based on Fick's second law for unsteady-state diffusion [19]. Furthermore, it is assumed that at the surface of the sample, the equilibrium moisture content between sample and surrounding air is reached instantaneously. The initial moisture content is assumed to be equally distributed at the start of the sorption experiment. For the vapour adsorption, the initial rate of sorption is used to calculate the diffusion coefficient according to the equation given by Siau [15].

$$\left[\overline{E}\right]^2 = \left[\frac{u_t - u_0}{u_\infty - u_0}\right]^2 = \frac{5.10\, t\, D}{L^2} \tag{7.3}$$

With: u_t is the moisture content at time t, u_0 the initial moisture content and u_∞ the moisture at equilibrium (infinite time). D is the diffusion coefficient that is assumed to be concentration independent and L is the thickness of the sample. By plotting $\overline{E}^2$ against t, the diffusion coefficient can be determined from the linear part of the slope. An example of such a plot is given in *fig.7.6*.
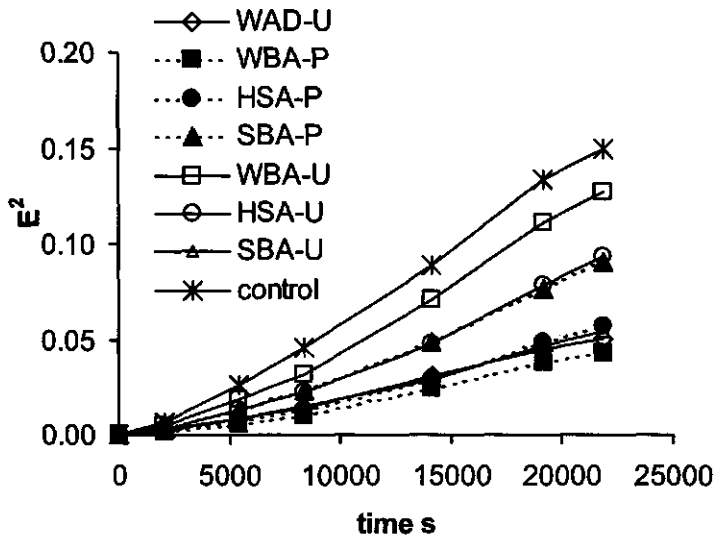
Figure 7.6   Plot of E^2 against time used to calculate the diffusion coefficient for moisture absorption from the slopes of the lines

Equation 3 can only be used to calculate the diffusion coefficient from the initial rate of sorption, or in other words if $\bar{E}$ is smaller than 0.6 [15] In the desorption experiments the initial desorption proceeds rather fast which has lead to an insufficient number of observations being available in the initial desorption stage. Therefore the diffusion coefficient were calculated from the final rate of desorption given by the following equation [19].

$$\frac{d}{dt}\left\{\ln\left(u_{t=0} - u_{t=\infty}\right)\right\} = -\frac{D\pi^2}{L^2} \tag{7.4}$$

The diffusion coefficient can now be obtained from the slope in a plot of $\ln\left(u_{t=0} - u_{t=\infty}\right)$ against t. Diffusion coefficients of the free coating films are obtained from the measurements of the water-vapour transmission rates (F) given in *table 7.1*, the film thickness (l) and the equilibrium water concentration on both sides of the film (C_1 and C_2), using the following equation [19] for steady-state diffusion.

$$F = D \left(C_1 - C_2\right) / 1 \tag{7.5}$$

The calculated diffusion coefficients for the wood coatings composites and the free coatings films are given in *table 7.5*.

Table 7.5.   Moisture diffusion coefficients of wood-coating composites and free
coating films

Diffusion coefficients $m^2 s^{-1} . 10^{-12}$

	Wood-coating composites [a]							
RH - change	WBA-P	HSA-P	SBA-P	WAD-U	WBA-U	HSA-U	SBA-U	control
66-98 %	4.6 ± 1.3	5.5 ± 0.5	7.8 ± 1.3	5.0 ± 1.0	11.0 ± 1.4	6.5 ± 0.8	4.8 ± 0.6	13.6 ± 1.8
98-66 %	7.5 ± 3.5	6.8 ± 2.0	6.3 ± 2.0	7.4 ± 2.8	6.8 ± 1.7	7.6 ± 2.5	5.6 ± 1.9	9.0 ± 4.9
	Free coating films							
98-66 %	27.0	8.5	1.3	4.6	4.4	3.9	1.9	-

a: including 95 % confidence

The impregnation of the wood with a coating reduces of the moisture diffusion coefficient slightly. However in comparison to the reduction achieved by a coating film applied on the outside of the wood, the reduction is only very limited. The diffusion coefficients from the desorption experiments are somewhat higher than those from the adsorption experiments. During desorption the influence of the coating material on the moisture diffusion is even further reduced. The moisture diffusion coefficients of the wood-coating composites ranged between 4.6 to 11.0 x 10^{-12} $m^2 s^{-1}$. This is comparable to the diffusion coefficients of 0.546 to 24.95 x 10^{-12} $m^2 s^{-1}$ reported by Hartley and Schneider [17] for wood polymer composites of sugar maple. Somewhat higher values have been reported in other studies. Schneider [9] measured a transverse diffusion coefficient of 53 x 10^{-12} $m^2 s^{-1}$ for *Picea glauca* that was filled with linseed oil to a concentration of 40 % and diffusion coefficients between 33.3 and 38.5 x 10^{-12} $m^2 s^{-1}$ for sugar maple filled with a methyl methacrylate like polymer [20].

The diffusion coefficients of the free coating films are slightly lower in comparison to the data of the wood-coating composites. The correlation between moisture diffusion coefficient and water vapour transmission rate seems low, but this can largely be explained by differences in water uptake in the film. For example, the relatively high water-vapour transmission for the WAD-U is not reflected in the diffusion coefficient because of the higher moisture content in the coating, which reduces the concentration gradient. Only the free film of WBA-P shows an exceptional high vapour transmission and diffusion. Because this is not reflected in the data of the wood-coating composite, the free film may have had some microscopic defects like entrapped air-inclusions that could have increased the water transmission rates. Differences between coatings are very small and the ranking order is not consistent for adsorption, desorption or free film diffusion. Therefore, it is questionable whether differences in diffusion coefficients between coatings are significant, also because confidence limits of the diffusion coefficients are relatively large.

7.3.4 Dimensional changes
The dimensional changes and Anti-Shrink-Efficiencies (ASE) at different equilibrium moisture contents are given in *table 7.7*. The ASE is defined by the following formula:

$$ASE = \frac{dimensions_{untreated} - dimensions_{treated}}{dimensions_{untreated}} \times 100 \% \qquad (7.6)$$

The wood-coating composites do not show a reduction in equilibrium shrinkage or swelling at any of relative-humidity steps studied. Often the dimensional change is slightly increased as can be seen from the negative ASE.

The small or negative effect on equilibrium dimensional change is consistent with findings of Ellis [21], Kabir *et al.* [12] and the results of Smulski and Côté [11] after leaching. In a study on poplar, a higher reduction in ASE was found, in particular for the alkyd-resins studied [10]. This can possibly be explained by different treatment conditions and mainly by different curing conditions at higher temperatures. However, in the study of Militz and Peek [10] also a strong reduction in ASE was observed after leaching the samples.

The ratio between tangential and radial swelling is only seriously affected for the WBA-P samples because the radial swelling is reduced with no reduction or even a small increase in tangential swelling. The wood coating composites show a higher increase in tangential shrinkage compared to radial shrinkage. Therefore, the T/R-ratio is often increased during shrinkage. This can be explained by the presence of coating material in ray-cells, which affects only the radial movement of the wood [12].

A possible reason for the small or negative impact of the coating impregnation on the dimensional stability of wood could be the swelling of the coating material itself. Therefore the volumetric swelling of free coating film itself has been determined and the results are given in *table 7.6*. In many cases, the swelling of the free coating film is low, even below the detection limits of the method used. With the exception of the WAD-U, the coating swells less or equally to the wood. However the very high swelling of the WAD-U films, up to 43 % in liquid water, does not cause an additional swelling of the wood. This indicates that the wooden cell wall is still controlling the actual swelling within the wood-coating composite. The swelling of the free coating film is of the same order of magnitude as the swelling data reported by Nakato [22] but mostly lower as the ones reported by Browne [23]. The coatings used in these studies however differ in chemical composition from the ones used in this work.

Table 7.6   Volumetric swelling of free coating films

	66% - 98%	94% -liquid
WBA-P	2.2 ± 0.3	-
HSA-P	1.5 ± 0.1	0.6 ± 0.1
SBA-P	-	-
WAD-U	8.1 ± 0.4	41.2 ± 4.4
WBA-U	2.5 ± 0.7	-
HSA-U	3.4 ± 1.5	-
SBA-U	1.8 ± 0.3	3.8 ± 0.5

-    : not detectable
average values with 95 % confidence limits

Table 7.7   Equilibrium dimensional changes of wood-coating composites

| RH-step | Code | dimensional change % [a] | | | ASE % [b] | |
		Radial	Tangential	T/R-ratio	Radial	Tangential
33 % - 94 %	WBA-P	0.9 ± 0.4	2.8 ± 0.4	3.0	28	-9
	HSA-P	1.3 ± 0.4	2.7 ± 0.3	2.1	-5	-3
	SBA-P	1.2 ± 0.3	2.5 ± 0.3	2.0	-13	2
	WAD-U	1.2 ± 0.4	2.9 ± 0.5	2.5	2	-12
	WBA-U	1.0 ± 0.3	2.5 ± 0.3	2.5	4	-1
	HSA-U	1.2 ± 0,4	2.8 ± 0.3	2.2	-2	-8
	SBA-U	1.1 ± 0.3	2.4 ± 0.3	2.2	10	8
	Control	1.2 ± 0.3	2.6 ± 0.4	2.1		
94 % - liquid	WBA-P	1.2 ± 0.6	3.7 ± 1.3	3.1	25	6
	HSA-P	1.5 ± 0.6	3.9 ± 1.3	2.6	11	-1
	SBA-P	1.6 ± 0.6	3.9 ± 0.7	2,4	18	8
	WAD-U	2.0 ± 1.0	4.5 ± 1.3	2.3	2	1
	WBA-U	1.3 ± 0.6	3.8 ± 0.8	2.9	30	10
	HSA-U	1.9 ± 0.8	4.6 ± 1.0	2.5	0	-10
	SBA-U	1.8 ± 0.7	4.3 ± 1.0	2.4	9	-1
	Control	1.6 ± 0.6	4.0 ± 0.9	2.5		
65 % - 98 %	WBA-P	1.0 ± 0.5	3.7 ± 0.7	3.7	39	-7
	HSA-P	1.4 ± 0.6	3.4 ± 0.5	2.4	9	0
	SBA-P	1.7 ± 0.7	3.7 ± 0.6	2.2	-7	-8
	WAD-U	1.4 ± 0.8	3.2 ± 0.7	2.2	17	10
	WBA-U	1.2 ± 0.6	3.8 ± 0.7	3.1	10	-14
	HSA-U	1.5 ± 0.5	3.6 ± 0.7	2.5	4	-4
	SBA-U	1.5 ± 0.6	3.3 ± 0.8	2.2	5	6
	Control	1.6 ± 0.6	3.5 ± 0.7	2.2		
98 % - 65 %	WBA-P	1.2 ± 0.6	4.1 ± 0.7	3.5	5	-37
	HSA-P	1.1 ± 0.6	3.6 ± 0.4	3.4	-21	-40
	SBA-P	1.5 ± 0.7	3.9 ± 0.7	2.6	-32	-48
	WAD-U	0.6 ± 0.0	2.3 ± 0.3	3.7	11	0
	WBA-U	1.2 ± 0.7	3.8 ± 0.9	3.2	-3	-26
	HSA-U	1.3 ± 0.6	3.3 ± 0.9	2.6	-11	-21
	SBA-U	1.7 ± 0.8	4.6 ± 1.1	2.8	-36	-59
	Control	0.9 ± 0.5	2.6 ± 0.7	2.7		

a: Average value with 95 % confidence limits
b: ASE is calculated from control corresponding to the same sample block

The influence of the coating impregnation on the rate of dimensional change from 66-98-66 % RH has been studied as well. *Fig.7.7* shows the fractional swelling (swelling at time t relative to the equilibrium swelling). The wood-coating composites do show a reduction in swelling rate, in particular for the HSA-U and HSA-P samples. In the desorption range no reduction in shrinkage rate has been observed.
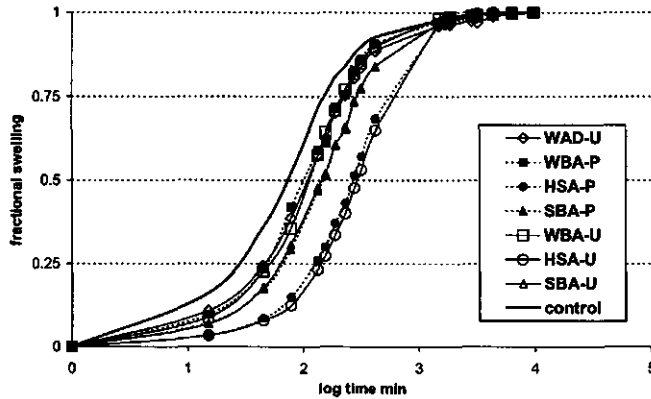

Figure 7.7 Fractional tangential swelling rate from 66 - 98 % RH against logarithmic time

7.4   Conclusions

For the coatings used in this study, the filling of the void volume of the wood with coating material has only a limited impact on moisture sorption behaviour and dimensional change. The highest reductions in hygroscopicity are found for the uptake of liquid water above the fibre saturation point of the wood. With respect to the equilibrium moisture content, diffusion coefficient and swelling rate, only a small reduction is observed for the wood-coating composites in comparison to the untreated pine sapwood.

The limited impact on the moisture related properties of the wood-coating composites could be explained by two reasons. Firstly, after drying of the coating only 20 to 60 % of the void volume is effectively filled with coating material due to the strong decrease in volume of the coating upon drying. Secondly the coating material itself is also hydrophilic and tends to swell under certain circumstances although the coating transmits and absorbs less water than wood does.

In comparison to the influence of a coating applied as a film on the outside of wood, the reduction of sorption behaviour, moisture diffusion and dimensional change by the coating material penetrated into the wood is only very limited. Practically, only a serious impact of coating penetration on the reduction of liquid water uptake can be expected. This does however not mean that coating penetration is not important, because adhesion can still be improved [24].

References

[1] **Ahola P.; Derbyshire, H; Hora, G.; Meijer, M.de**; Water protection of wooden window joinery painted with low organic solvent content paints with known composition, Holz Roh- Werkstoff,57,1999,45-50.

[2] **Ekstedt, J.**; Moisture Dynamic Assessment of Coatings for Exterior Wood, Licentiate thesis, Kungl Tekniska Högskolan, Stockholm,1995.

[3] **Rødsrud, G.; Sutcliffe, J.E.**; Alkyd emulsions - properties and application. Results from comparative investigations of penetration and ageing of alkyds, alkyd emulsions and acrylic dispersions. Presentation held at the 14th Congress of the Federation of Scandinavian, Paint & Varnish Technologists-Copenhagen, 1993.

[4] **Hora, G.; Böttcher, P.**; Beurteilung des Feuchteschutzes von Holzanstrichen, Farbe und Lack, 11, 1993, 924-928.

[5] **Ahola, P.**; Moisture transport in wood coated with joinery paints, Holz Roh-Werkstoff, 49, 1991, 428-432.

[6] **Linden, J.A. van de; Oort, P.**; Water permeability, comparison of methods and paint systems, Proceedings XXII, Fatipec Conference, Budapest, Hungaria, 1994.

[7] **Teichgräber, R.**; Measurement and evaluation of the interactions between paint systems, wood, species and climate, Holz Roh- Werkstoff 31, 1973, 127-132.

[8] **Schneider, M.H.**; a. Hygroscopicity of wood impregnated with linseed oil, Wood Science Technology, 14, 1980, 107-114.

[9] **Schneider, M.H.**; b. Model for moisture diffusion through wood containing linseed oil, Wood Science, 12 (4), 1980, 207-213.

[10] **Militz, H.; Peek, R.-D.**; Möglichkeiten der Verbesserung einiger Eigenschaften von Pappelholz durch Tränken mit wasserlöslichen Harzen, Material und Organismen, 28 (1), 1993, 55-73.

[11] **Smulski, S.; Côté, W.A.**; Penetration of wood by a water-borne alkyd resin, Wood Science Technology, 18, 1984, 59-75.

[12] **Kabir, A.F.R.;Nicholas, D.D.; Vasishth, R.C.; Barnes, H.M.**; Laboratory methods to predict the weathering characteristics of wood, Holzforschung 46 (5), 1992, 395-401.

[13] **Smith, W.B.; Côté,W.A.; Siau, J.F.; Vasishth, R.C.**; Interactions between water-borne polymer systems and the wood cell wall, Journal of Coatings Technology, 57 (729), 1985, 27-35.

[14] **Meijer, M.de; Thurich, K.; Militz H.**; Comparative study on penetration characteristics of modern wood coatings, Wood Science and Technology, 32, 1998, 347-365.

[15] **Siau, J.F.**; Transport Processes in Wood (Springer Series in Wood Science), Springer, Berlin Heidelberg New York Tokyo, 29, 1984, 186.

[16] **Spalt, H.A.**; The fundamentals of water vapour sorption by wood, Forest Products Journal, 8 (10), 1058, 288-295.

[17] **Hartley, I.D.; Schneider, M.J**; Water vapour diffusion and adsorption characteristics of sugar maple (Acer saccharum, Marsh.) wood polymer composites, Wood Science and Technology, 27, 1993, 421-427.

[18] **Yasuda, R.; Minato, K.; Norimoto, M.**; Moisture adsorption thermodynamics of chemically modified wood, Holzforschung. 49, 1995, 548-554.

[19] **Crank, J.**; The mathematics of diffusion 2nd edition, Oxford University Press, Oxford, 1975 44, 48, 246.

[20]   **Schneider, M.H.; Brebner, K.I.; Hartley, I.D**.; Swelling of a cell lumen filled and a cell lumen bulked wood polymer composite in water, Wood and Fiber Science, 23 (2), 1991, 165-172.

[21]   **Ellis, D.W.**; Moisture sorption and swelling of wood-polymer composites, Wood and Fiber Science, 23 (3), 1994, 333-341.

[22]   **Nakato, K.; Shiraishi, N.; Kadita, H**.; On the adsorption of water, swelling and internal strain of paint film painted on wood, Mokuzai Gakkaishi, 9, 1963, 217-224.

[23]   **Browne, F.L.**; Swelling of paint films in water, II Adsorption and volumetric swelling of bound and free films before and after weathering, Journal of Forest Products and. Soc. 1954, 391-400.

[24]   **Meijer, M.de; Militz, H**.; Adhesion of Low-VOC Coatings on Wood. A Quantitative Analysis. Proceedings XXIV, Fatipec Conference, Interlaken, Switzerland, 1998.

8. MOISTURE TRANSPORT IN COATED WOOD
Part 1: Analysis of sorption rates and moisture content profiles in Spruce during liquid water uptake [*]

Summary

The sorption of liquid water in coated spruce was determined by measuring the change in the overall moisture content of the wood as a function of time, and by determination of the moisture content profiles after various time intervals. The coatings studied included a solventborne alkyd coating and two waterborne acrylic coatings with different layer thickness. Uncoated wood was used as a reference.

The measured data were analysed according to different models, which were based on capillary flow or on diffusion with a constant or a changing surface concentration. The apparent diffusion coefficients based on sorption rates ranged between 7.65 and 98.16 x 10^{-11} m s^{-2} depending on the surface treatment. These diffusivities were however, not suitable to predict the moisture content profiles in the coated wood, which showed a strong increase close to the surface.

The most accurate prediction of the moisture content profile was based on the changing surface concentration and the diffusion coefficient from sorption data of uncoated wood. In general, diffusion seemed to be the most important factor in the transport of water. Capillary flow of water only influenced the sorption very close to the surface of the wood. This aspect became more important for uncoated wood.

8.1 Introduction

In order to avoid the emission of volatile organic components during the application of coatings, the use of waterborne coatings gained importance in the decoration and protection of wood. Although waterborne coatings showed a large variation in water-permeability depending on their formulation [1], in general the resistance against transport of moisture was lower in comparison to solventborne coatings. This prompted to a large number of research activities during the last decades, evaluating the permeability of free coating films, water absorption and desorption rates of coated wood and moisture content in outdoor weathering trials [2-10]. In general the results of these studies showed that the average moisture content for wood coated with waterborne coatings was higher than for wood coated with solventborne coatings. It was also found that fluctuations in wood moisture content during the year increased with a higher coating permeability. On the other hand, as long as the end-grains were properly protected [11-13] and the coatings film maintained its integrity [7], the observed average wood moisture contents were in general below the point of about 20 to 25 % moisture content where risk of decay by fungi can be expected.

However, most of these results deal with average moisture content data and far less information was available on the distribution of moisture within the wood. Ekstedt [5] studied the moisture distribution in coated wood by means of microdensitometry and X-ray CT-tomography. His results showed sharp increases in the moisture content at the surface of the wood after exposure to water. Furthermore, the moisture distribution was influenced by the development of cracks and blue-stain at the surface. In a study on the moisture balance in painted wood panelling, Hjort [3] observed moisture contents of over 40 % at the surface of spruce coated with a waterborne acrylic coating after exposure to 97.6 % relative humidity. Both observations showed that at the surface of coated wood relatively high moisture contents could be reached. These high moisture contents might lead to rapid swelling of the wood at the surface which could cause stresses in the coating film which eventually might lead to coating failure. The high moisture contents at the wood surface could also create favourable conditions for the growth of blue-stains and moulds [14].

The first objective of the present work was to measure the moisture content distribution of the wood as a function of coating permeability after long term exposure to liquid water. The second objective was to determine the driving forces for the moisture transport, which could be diffusion, capillary uptake or a combination of these two phenomena. In this case, the exposure of the coated wood to liquid water was preferred over the exposure to high relative humidity, because constant moisture concentrations were more easily maintained with liquid water. Also, in practice the wood would absorb significant amount of liquid water from rain or dew [15].

8.2 Theory

In general terms, the increase in moisture content of coated wood as a function of time is controlled by the moisture flux into the coating and the wood, which is proportional to the driving force times a conductance factor [16,17]. Excluding any thermally induced phenomena, the following two physical processes can cause a moisture flux into either coating or wood:
1. Adsorption of water molecules to available molecular sites like hydroxyl groups present in both the wood and the organic material in the coating. The absorption of water molecules to wood or coating can also cause a change in the diffusion resistance making the diffusion coefficients of the wood or the coatings concentration dependent [8, 18, 23].
2. Diffusion of water molecules through the air-filled lumina of the wood and as bound water diffusion through cell walls and pit membranes [19] provided the wood moisture content is below the fibre saturation point. In coatings diffusion takes place through the free volumes of coating polymers or along particle interfaces and surfactant in case of latex paints [20, 21].

The general form of Ficks law for unsteady state diffusion in one direction is governed by:

$$\frac{\partial(u)}{\partial t} = ID \frac{\partial^2(u)}{\partial x^2} \tag{8.1}$$

In the case of diffusion in a plane sheet with an uniform initial concentration distribution, a constant diffusion coefficient and a constant concentration at the boundary of the sample, the following solution of *equation 8.1* applies [22]:

$$E = \frac{M_t}{M_\infty} = \frac{u - u_0}{u_\infty - u_0} = 1 - \sum_{n=0}^{\infty} \frac{8}{(2n+1)^2 \pi^2} \exp\{-ID(2n+1)^2 \pi^2 t / 4l^2\} \tag{8.2}$$

The diffusion coefficient can be obtained from plot of E against the square root of time [23]:

$$ID = \frac{l^2}{5.1} \left(\frac{dE}{d\sqrt{t}} \right)^2 \tag{8.3}$$

The specific length for diffusion is two times the sample thickness for unidirectional diffusion. It should be noted that the diffusion coefficient obtained in this way should actually be called an apparent diffusion coefficient because it can be influenced by non-Fickian types of diffusion [26]. If the moisture content at the boundary is constant, the moisture content as a function of position in a semi-infinite medium is given by [22]:

$$u = u_{x=0} - (u_{x=0} - u_0)\mathrm{erf}\left(\frac{x}{\sqrt{4IDt}} \right) \tag{8.4}$$

If the moisture content at the boundary is changing linearly with time the following equation can be used to predict the moisture content profile [22]:

$$u = u_0 + q\,t\left[\left(1 + \frac{x^2}{2\,ID\,t}\right)\left(1 - \mathrm{erf}\left(\frac{x}{2\sqrt{ID\,t}}\right)\right) - \frac{x}{\sqrt{\pi\,ID\,t}}\,e^{\left(\frac{-x^2}{4\,IDt}\right)} \right] \tag{8.5}$$

With boundary conditions:

$$u = u_0, \qquad x > 0, \qquad t = 0$$
$$u = u_0 + q\,\sqrt{t}, \qquad x = 0, \qquad t > 0$$

3. Liquid flow through wood or coating capillaries with the capillary pressure as driving force. Although a coating might seem to be a non-porous material, on a microscale various pores with different sizes can exist. Apart from capillary liquid flow, the very small capillaries can also cause Knudsen diffusion or slip flow resulting in faster diffusion than normal [25]. Nevertheless, it can be expected that the coating will strongly reduce the rate of liquid water flow by blocking the wood capillaries on the surface. Capillary liquid flow will be governed by Darcy's law for liquid flow and the expression for capillary pressure:

$$\frac{dV_1}{dt} = \frac{K\,A\,\Delta P}{\eta\,x} \qquad\qquad \Delta P = \frac{2\gamma\cos\theta}{r} \tag{8.6}$$

Combining these equations and expressing the water uptake in terms of fractional void filling of the wood gives [23]:

$$F = \frac{w_l}{\rho\, V_w\, v_a} = \sqrt{\frac{4\,K\,\gamma_1 \cos\theta\, t}{\eta_1\, v_a\, L^2\, r}} \tag{8.7}$$

Equation 8.7 shows that the liquid water uptake is controlled by the permeability, effective capillary radius and the degree of wetting of the wood and the coating. Indeed Hora [26] found positive correlations between contact angles of water on coated wood and the water absorption rates.

8.3   Experimental

Industrially pre-dried, Nordic grown, defect free Spruce *(Picea abies Karst.)* with a density of about 450 kg m^{-3} and an initial wood moisture content between 11 % and 13 % was used in the experiments. The average width of the growth-rings was around 2 mm. All measurements were carried out in duplicate with one set of samples taken out of one wood beam (referred to as Sample 1) and another set originating from a second beam (referred to as Sample 2). Each set consisted of 24 wood blocks with a size of 110 x 65 x 80 mm. The set of samples was grouped into four blocks with different surface treatment. Each group contained six samples used for different water absorption times. An overview of the sampling structure is given in *fig. 8.1.*
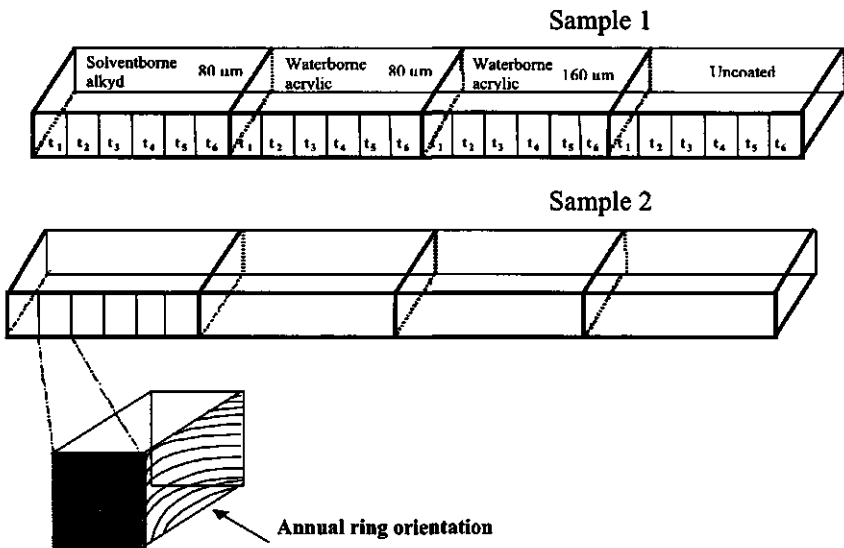
Figure 8.1   Sampling structure of the two wood-blocks.

One radial surface was treated with one of the three coatings tested or left untreated in case of the uncoated reference sample. All other sides were treated with a 2-pack polyurethane coating with a very low moisture permeability to ensure one-dimensional moisture movement. The test coatings were: a white pigmented opaque solventborne alkyd paint with a dry film-thickness of 80 μm applied in two layers, a white pigmented opaque waterborne acrylic paint with a dry film-thickness of 80 μm applied in two layers and the same acrylic paint with a dry film-thickness of 160 μm applied in four layers. All coating were commercial products intended

to be used as wood primers. Application of the paint was done by brush followed by a drying period of several weeks at ambient conditions.

The wood was exposed to moisture by hanging the samples with the test face in liquid water at a temperature of about 23 °C. Average wood moisture contents were determined by frequently weighing the sample to an accuracy 0.01 g. After time durations of 72, 240, 408, 576, 1100 and 1683 hours, samples were taken out of the test and sawn into 11 slices of about 10 mm thickness to measure the moisture profile. Immediately after sawing the weights of the slices were recorded to an accuracy of 0.01 g and dried at 103 ±2 °C to determine the dry-mass. The thickness of the slices was also measured with a digital thickness gauge (accuracy of 0.01 mm) to determine the exact position in the wood block.

8.4   Results and discussion

The overall wood moisture contents of the different wood blocks are shown in *fig. 8.2* as a function of sorption-time. Because samples were withdrawn during the test for the determination of the moisture content profile, the number of observations decreased with time. After 1700 hours the moisture content of the wooden blocks coated with the solventborne coating was between 15% and 18%. After the same duration the wood coated with a waterborne acrylic coating had a moisture content between 18% and 23% with a coating thickness of 80 μm and between 17% and 23% with a coating thickness of 160 μm. The uncoated blocks exhibited a much faster increase in wood moisture content up to 20 % or 30 %. In all cases the blocks from Sample 1 exhibited a faster water adsorption in comparison to those originating from Sample 2. Because both samples were taken from different logs, this difference would be the result of a variation in permeability of the wood. The variation between samples from the same log were quite small as could be seen from the variation in moisture content between the various measurements during the initial stage of water adsorption.

None of the samples reached a true equilibrium moisture content within the time-span studied. There were two possible reasons for this. Firstly in most cases the fibre saturation point was not yet reached and secondly liquid water uptake was still ongoing beyond the fibre saturation point. Apparent moisture diffusion coefficients were calculated from a plot of the increase in dimensionless concentration against square root of time according to *equation 8.3*. The final equilibrium moisture content (u_∞) was set to 30 %, corresponding to the equilibrium moisture content at 100 % relative humidity as it was found in separate measurements and data provided in literature [27]. The moisture diffusion data are provided in *table 8.1* including the 95 % confidence limits. In order to separate the moisture diffusivity in the wood from the resistance of the coating against moisture diffusion the following resistance factor was calculated:

$$k = \frac{ID^{*}_{coated\,wood}}{ID^{*}_{uncoated\,wood}} \tag{8.8}$$

There was a consistent reduction in moisture diffusivity by the coating, depending both on the coating type and the film thickness. Typically reductions by a factor of 0.08 to 0.4 were achieved.

The diffusion coefficients for the uncoated wood were in the same order of magnitude as the ones found by Fakhouri *et al* [28] for the absorption of liquid water in spruce. In comparison to the results of Wädso [29] obtained for vapour diffusion in spruce, the measured data were a factor 10 to 30 larger. This might be explained by the faster moisture transport with liquid water.
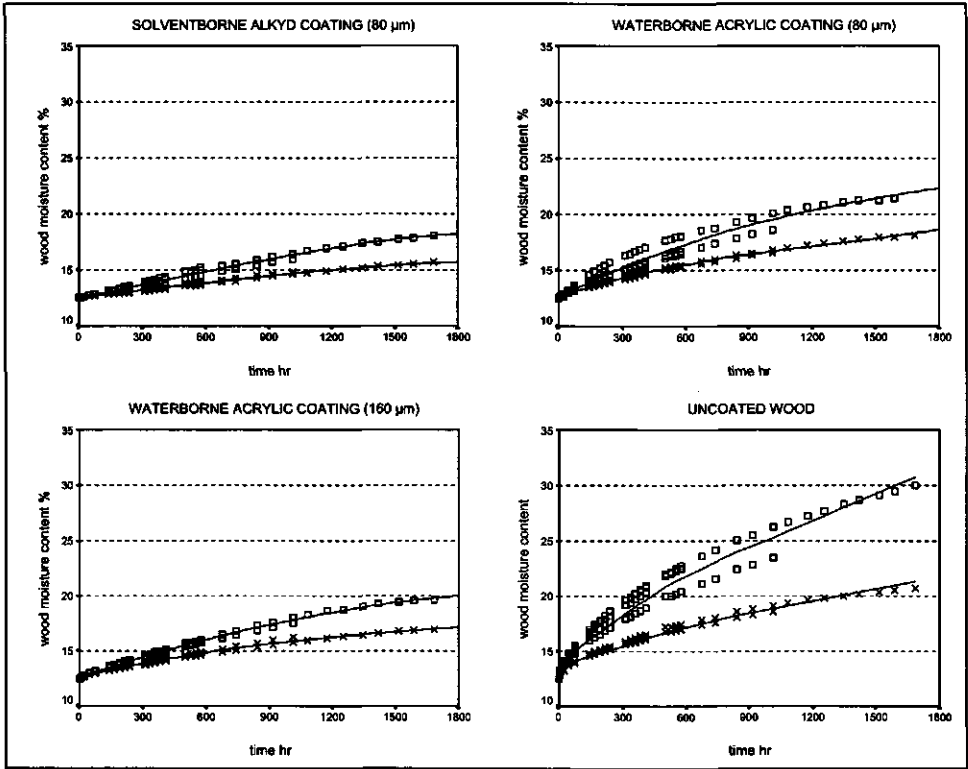
Figure 8.2   Increase of the wood moisture content during sorption of liquid water.

Table 8.1   Apparent diffusion coefficients and diffusion resistance factors

$$ID \; m \; s^{-2} \cdot 10^{-11}$$

Sample	Coating	lower 95 % limit	average	upper 95 % limit	k
1	solventborne alkyd 80 μm	7.46	8.41	9.43	0.086
	waterborne acrylic 80 μm	23.55	25.88	28.29	0.264
	waterborne acrylic 160 μm	15.51	16.92	18.38	0.172
	uncoated	92.78	98.16	103.56	-
2	solventborne alkyd 80 μm	2.45	2.75	3.07	0.088
	waterborne acrylic 80 μm	11.80	12.48	13.18	0.400
	waterborne acrylic 160 μm	7.14	7.65	8.17	0.245
	uncoated	30.41	31.23	32.05	-

The moisture content profiles obtained for different sorption times gave very valuable additional information about the moisture transport process. For all samples a clear decrease in moisture content could be seen with increasing distance away from the surface exposed to water.

Close to the exposed surface the wood moisture content was fairly high. After 1700 hours all coated samples from the first group (Sample 1) had moisture contents of 25 % or more. The samples from the second group (Sample 2) also showed an increase up to 20% or 25%, which was consistent with the lower overall moisture content. All the uncoated samples had a wood moisture content far above the fibre-saturation-point close to the surface.

The measured concentration profiles were compared with the theoretical predictions given by *equation 8.4* and *8.5*. Therefore the following two questions had to be answered. Firstly whether the surface concentration (x=0) could be considered as constant and secondly, which value of the diffusion coefficient should be used, namely the ones obtained from the coated or the uncoated samples.

Only the concentration profiles for the uncoated samples could be reasonably well described with a constant surface concentration (*equation 8.4*) which was assumed to be 30 %. The results given in *fig. 8.3* and *8.4* show both measured and calculated data. Only at moisture contents clearly above the fibre-saturation-point, the model could not predict the measured data. This was logical because here the capillary liquid flow was the main type of water transport process instead of moisture diffusion. The assumption of a constant surface concentration (*equation 8.4*) was incorrect for the coated wood as is clearly shown in *fig. 8.5*. For coated wood the moisture content at short distances (x < 20 mm) was overestimated whereas at longer distances (x > 50 mm) the moisture content was underestimated.

Table 8.2   Rate of change of the wood moisture content at the surface

Sample	Coating	k s^{-1} · 10^{-6}	r^2
1	solventborne alkyd 80 μm	5.80	0.963
	waterborne acrylic 80 μm	8.16	0.943
	waterborne acrylic 160 μm	5.40	0.884
	uncoated	32.34	0.970
2	solventborne alkyd 80 μm	4.38	0.927
	waterborne acrylic 80 μm	6.18	0.621
	waterborne acrylic 160 μm	4.98	0.998
	uncoated	10.17	0.863

For an accurate prediction of the moisture content profiles by *equation 8.5*, the rate of moisture content change at the surface had to be estimated. This was done by extrapolating the measured concentration profiles to x = 0. The rate of change appeared to be fairly linearly dependent on time. In *table 8.2* the rate of moisture content change at the surface is given including the r^2 data. The rate of change was both dependent on the type of coating and the permeability of the wood.

The measured moisture content profiles were fitted by *equation 8.5* in two ways: firstly by using the diffusion coefficient obtained from the sorption rates of the coated wood blocks and secondly by using the diffusion coefficient of the uncoated wood. For the solventborne alkyd coating both fits are given in *fig. 8.6* and *8.7* respectively. The profiles calculated with the apparent diffusion coefficient of the coated wood strongly underestimated the measured values, in particular after longer sorption times. A good prediction of the data was found if the apparent diffusion coefficients of the uncoated wood were used. This is actually quite logical because the diffusivity of the moisture in the wood was in principal not influenced by the presence of a coating. The coating caused a lower moisture content at the surface and a decrease of the in

going moisture flux. This model could also predict the moisture content profiles for the other coatings as is shown in *fig. 8.8* and *8.9*. The strongest deviations of the measured data from the model were found at the higher concentrations at the surface after longer sorption times. This was probably due to the fact that at this stage capillary water flow contributed significantly to the sorption process. The model with changing surface concentration was also applied to the uncoated samples but this resulted in a severe overestimation of the moisture content profiles. This is because of the fact that the rapid change in wood moisture content at the surface of the uncoated wood is controlled by capillary sorption instead of moisture diffusion.
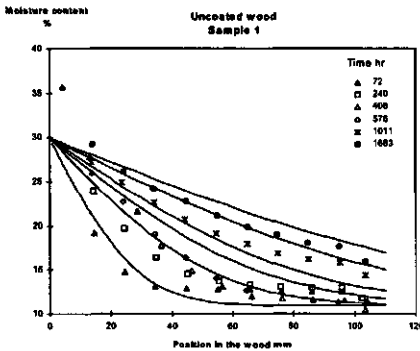
Figure 8.3
Measured (symbols) and calculated (lines) moisture content profiles of uncoated wood Sample 1.
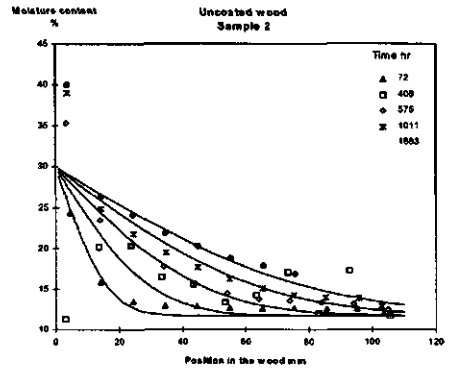
Figure 8.4
Measured (symbols) and calculated (lines) moisture content profiles of uncoated wood. Sample 2.

Figure 8.5
Measured (symbols) data and calculated (lines) moisture content profiles of Sample 1 with solvent borne alkyd coating assuming a constant surface concentration (u $_{x=0}$) according to *equation 8.4*.
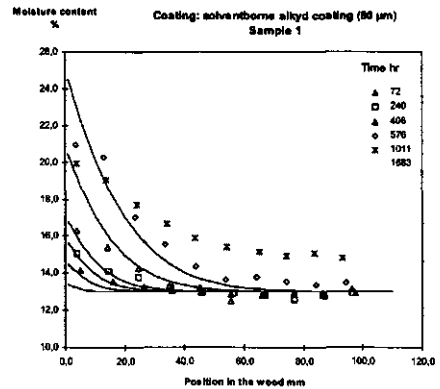
Figure 8.6
Measured (symbols) data and calculated(lines) moisture content profiles of Sample 1 with solvent borne alkyd coating assuming a changing moisture content at the surface according to *equation 8.5* (u$_{x=0}$) and using the ID from the sorption of coated wood (ID = 7.46. 10^{-11} m.s^{-2}).
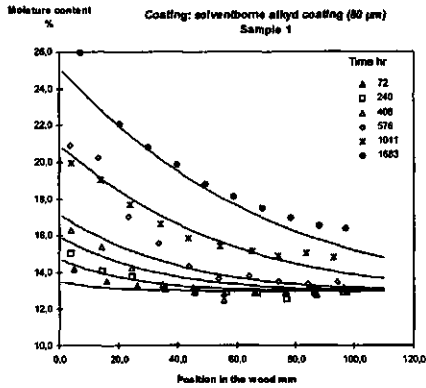
Figure 8.7
Measured (symbols) data and calculated
(lines) moisture content profiles of Sample 1
with solvent borne alkyd coating assuming
a changing moisture content at the surface
($u_{x=0}$) according to *equation 8.5* and using the
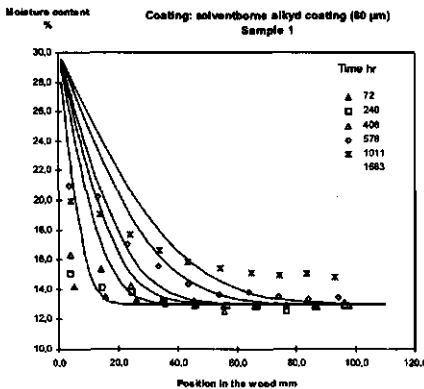ID from the sorption of uncoated wood
(ID= 92.78 . 10^{-11} m.s^{-2}).
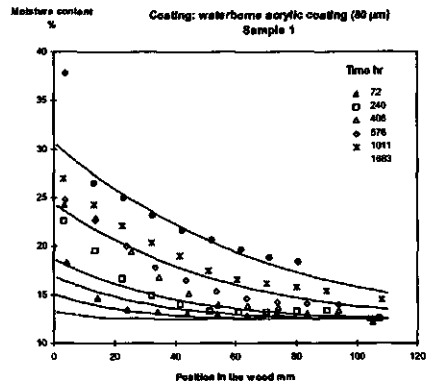
Figure 8.8
Measured (symbols) data and calculated
(lines) moisture content profiles of Sample 1
with waterborne acrylic coating (80μm)
assuming a changing moisture content at the
surface ($u_{x=0}$) according to *equation 8.5* and
using the ID from the sorption of uncoated
wood (ID= 92.78 . 10^{-11} m.s^{-2}).

A comparison of the moisture content profiles of samples with different surface treatments but approximately the same overall wood moisture contents is given in *fig. 8.10*. A moisture content of 19 % was reached for the uncoated sample 1 within 240 hours. This took 1683 hours for the wood coated with the solventborne alkyd and for the waterborne acrylic this moisture content was reached within 1011 hours. The moisture content profiles for both coated samples with the same overall moisture content were almost identical. The moisture content for the uncoated sample was quite different, close to the surface the moisture content was higher but deeper in the wood the moisture content was lower in comparison to the coated wood.
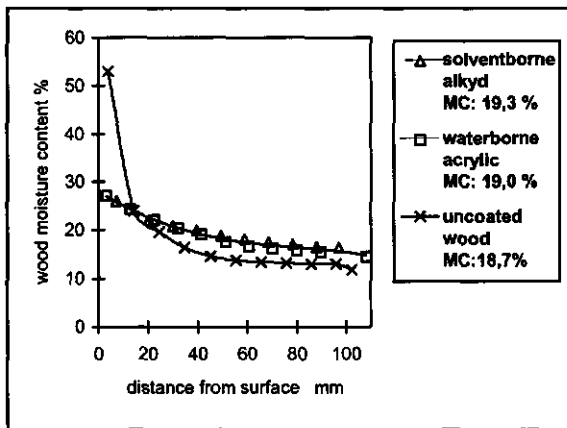
Figure 8.10   Moisture content profiles of Samples with the same overall moisture content, surface treatment and sorption times differ.

The influence of capillary water uptake was evaluated on the basis of *equation 8.7* by plotting the following variables which should result in a linear relationship:

F   against $\sqrt{\dfrac{t}{v_a}}$

The porosity of the wood was calculated from the following relationship [23]:

$$v_a = 1 - G\,(0.667 + 0.01u) \qquad \text{with} \qquad G = \frac{m_{OD}}{V_w\,\rho_1} \tag{8.9}$$
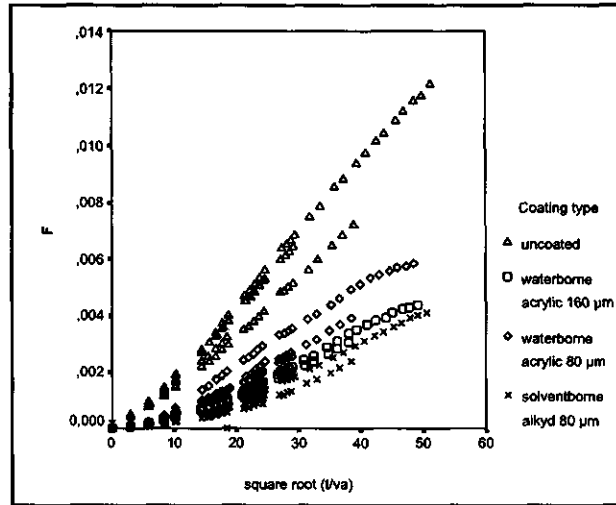
Figure 8.11   Plot of the fractional void filling of liquid water in Sample 1 against $\sqrt{(t/v_a)}$.

Fig. 8.11 shows the plot of the above mentioned variables for Sample 1. The overall fractional void filling of the wood was restricted to 1.2 % for the uncoated wood. A linear relationship was only observed for the uncoated wood at longer sorption times. This was in good agreement with the moisture content profiles which showed void filling above the fibre saturation point at this stage. The coated samples did not show a true linear relationship, which indicated that moisture diffusion was the main transport process in these cases instead of capillary uptake.

8.5   Conclusions

As expected, the results of this study clearly showed that a coating had a strong influence on the sorption process of liquid water into wood. The degree of reduction of moisture sorption depended on the coating type and the film thickness. The moisture content profile in the wood was also influenced by the presence of a coating. In comparison to uncoated wood, the change in moisture content within the wood was levelled off. The coating type had no influence on the shape of the moisture content profile as long as the overall moisture content was equal.

The liquid water sorption process in uncoated wood was a combined effect of diffusion and capillary water uptake. If a coating was present at the surface, the capillary water uptake is almost completely excluded. This is in agreement with earlier findings on wood which was filled with coating material [2].

Apparent diffusion coefficients obtained from sorption rates of coated wood were useful in quantifying the reduction of the sorption rate. They could not, however, be treated as true diffusion coefficients because they failed to predict the moisture content profiles accurately. The

moisture content profiles in coated wood can best be modelled by using a model which takes into account a changing wood moisture content at the surface in combination with diffusivities obtained from uncoated wood. The influence of the coating has to be incorporated by its impact on the rate of moisture content change at the surface rather than by the change in apparent diffusion coefficient.

Uncoated wood can be reasonably well described by a model with a fixed concentration at the surface. Only very high moisture contents close to the surface are not well predicted, because capillary liquid uptake is the main driving force under these circumstances. The importance of capillary liquid flow in uncoated wood after relatively long sorption times was confirmed by analysing the fractional void filling as a function of time.

Finally, it should be mentioned that the results presented here are intended to be used to analyse laboratory studies on moisture sorption in coated wood. Care has to be taken before using them to predict real life situations because there the surface will never be exposed to liquid water for such a long time. Changes in the surface conditions by lower relative humidity or surface heating due to solar irradiation will complicate the entire moisture transport process including the moisture content profiles inside the wood.

Acknowledgements

References

[1]   **Ahola, P.; Derbyshire, H.; Hora, G.; Meijer, M. de;** Water protection of wooden window joinery painted with low organic solvent content paints with known composition,. Holz als Roh- und Werkstoff, 57, 1999, 45-50.

[2]   **Meijer, M. de; Militz, H.;** Sorption Behaviour and Dimensional Changes in Wood-Coating Composites, 5th Conference on Wood-Coatings-Moisture, Espoo Finland, 1998.

[3]   **Hjort, S.;** Moisture Balance in Painted Wood Panelling, Publication P-97-5 Chalmers University of Technology Department of Building Materials, Göteborg, 1997.

[4]   **Albas, B.P.; van Londen, A.M.;** Comparative testing of the performance of several types of coating systems for the protection of wooden window frames, Surface Coatings International, 79, 1998, 555-572.

[5]   **Ekstedt, J.;** Moisture dynamic assessment of coatings for exterior wood, Licentiate Thesis, Kungliga Tekniska Högskolan, Stockholm, 1995.

[6]   **Hora, G.; Böttcher, P.;** Beurteilung des Feuchteschutzes von Holzaußenanstrichen, Vergleich von dynamischer Randwinkelmessung und Bestimmung des Wasseraufnahmekoeffizienten, Farbe und Lack (11), 1993, 924-928.

[7]   **Ahola, P.;** Moisture transport in wood coated with joinery paints, Holz als Roh- und Werkstoff, 49, 1991, 428-432.

[8]   **Huldén, M.; Hansen, C.M.;** Water permeation in coatings, Progress in Organic Coatings, 13, 1985, 171-194.

[9]   **Böttcher, P.;** Zum Verhalten unterschiedlich feuchtedurchlässiger Anstriche auf einigen einheimischen Holzarten bei natürlicher Bewitterung, Holz als Roh- und Werkstoff, 33, 1975, 116-120.

[10]   **Teichgräber, R.;** Measurement and Evaluation of the Interactions between Paint Systems, Wood Species and Climate, Holz als Roh- und Werkstoff, 31, 1973, 127-132.

[11]   **Boxall, J.;** Factory-applied finishes for timber joinery; an evaluation, Journal of the Oil and Colour Chemists Association, 75 (8), 1992, 284-292.

[12]   **Miller, E.R.; Boxall, J.**; The effectiveness of end-grain sealers in improving paint performance on softwood joinery, Holz als Roh- und Werkstoff, 42, 1984, 27-34.

[13]   **Miller, E.R.; Boxall, J.**; The effectiveness of end-grain sealers in improving paint performance on softwood joinery. L-joint results after 4-year natural weathering, Holz als Roh- und Werkstoff, 45, 1987, 69-74.

[14]   **Viitanen, H.**; Factors effecting the development of mould and brown rot decay in wooden material and wood structures, Effect of humidity, temperature and exposure time. Dissertation Swedish University of Agricultural Sciences, Uppsala, 1996.

[15]   **Sell, J.**; Untersuchungen zur Optimierung des Oberflächenschutzes von Holzbauteilen, Teil 1: Bewitterungsversuche mit Fensterrahmen-Abschnitten, Holz als Roh- und Werkstoff, 40, 1982, 225-232.

[16]   **Perrera, D.Y.**; Hygric aspects of coated porous building materials, Progress in Organic Coatings, 8, 1980, 183-206.

[17]   **El Kouali, M.; Vergnaud, J.M.**; Modelling the process of absorption and desorption of water above and below the fiber saturation point, Wood Science and Technology, 25, 1991, 327-339.

[18]   **Crank, J.; Park, G.S.**; Diffusion in polymers, Academic Press, New York London, 1968.

[19]   **Stamm, A.J.**; Combined bound-water and water-vapour diffusion into sitka spruce, Forest Products Journal, 10, 1960, 644-648.

[20]   **Richard, J.; Mignaud, C.; Wong, K.**; Water vapour permeability, diffusion and solubility in latex films, Polymer International, 30, 1993, 431-439.

[21]   **Roulstone, B.J.; Wilkinson, M.C.; Hearn, J.**; Studies on polymer latex films: II Effect of surfactants on the water vapour permeability of polymer latex films, Polymer International, 27, 1992, 43-50.

[22]   **Crank, J.**; The mathematics of diffusion 2nd ed., Oxford University press, Oxford, 1975.

[23]   **Siau, J.F.**; Transport Processes in Wood (Springer Series in Wood Science), Springer, Berlin Heidelberg, New York, Tokyo, 1984.

[24]   **Wadsö, L.**; Unsteady-state water vapour adsorption in wood: an experimental study, Wood and Fiber Science, 26, 1994, 36-50.

[25]   **Lindberg, H.; Grahn, J.**; The coalesence and quality of latex paint films, 5th Conference on Wood-Coatings-Moisture, Espoo Finland, 1998.

[26]   **Hora, G.**; The dynamic contact angle: a characteristic to predict the lifetime of a wood topcoat, Journal of Coatings Technology, 66, 1994, 55-59.

[27]   **Rijsdijk, J.F.; Laming, P.B.**; Physical and related properties of 145 timbers. Information for practice, Kluwer Academic Publishers, Dordrecht, Boston, London, 1994.

[28]   **Fakhouri, B.; Mounji, H.; Vergnaud, J.M.**; Comparison of the Absorption and Desorption of Water Between Scots Pine and Spruce after Submersion in Water, Holzforschung, 47, 1993, 271-277.

[29]   **Wadsö, L.**, Measurements of water vapour sorption in wood. Part 2 Results, Wood Science and Technology, 28, 1993, 59-65.

Nomenclature

u	wood moisture content	(mass-mass$_{oven-dry}$) / mass$_{oven-dry}$ x 100%.
u$_\infty$	final equilibrium wood moisture content	(mass-mass$_{oven-dry}$) / mass$_{oven-dry}$ x 100%.
u$_0$	initial wood moisture content	(mass-mass$_{oven-dry}$) / mass$_{oven-dry}$ x 100%.
u$_{x=0}$	wood moisture content at the boundary	(mass-mass$_{oven-dry}$) / mass$_{oven-dry}$ x 100%.
M$_t$	total amounts of absorbed moisture at time t	kg
M$_\infty$	total amounts of absorbed moisture at equilibrium	kg
ID	moisture diffusion coefficient	m^2 s^{-1}
ID$^*_{coated\ wood}$	apparent diffusion coefficient for coated wood	m^2 s^{-1}
ID$^*_{uncoated\ wood}$	apparent diffusion coefficient for uncoated wood	m^2 s^{-1}
t	time	s
x	position in the sample	m
E	dimensionless moisture concentration	-
q	rate of wood moisture content change at x=0	s^{-1}
l	specific length = 2x sample thickness	m
V$_l$	volume of adsorbed liquid	m^3
K	permeability constant	m^2
L	thickness of the sample	m
A	surface area	m^2
ΔP	capillary pressure difference	N m^{-2}
η$_l$	viscosity of liquid (water)	N s m^{-2}
γ$_l$	surface tension of liquid (water)	N m^{-1}
θ	contact angle of liquid (water)	°
r	capillary radius	m
F	fractional void filling of the wood by liquid	-
w$_l$	weight of adsorbed liquid	kg
ρ$_l$	density of liquid (water)	kg m^{-3}
V$_w$	volume of the wood	m^3
v$_a$	porosity of the wood	-
k	diffusion resistance factor	-
G	specific gravity	-
m$_{OD}$	ovendry weight of the sample	kg

9 MOISTURE TRANSPORT IN COATED WOOD
Part 2: Influence of coating type, film thickness, wood species, temperature and moisture gradient on kinetics of sorption and dimensional change[*]

Summary

The sorption of moisture by spruce and meranti coated with both waterborne and solventborne coatings was studied during controlled conditions. Experimental variables included: coating film thickness, temperature and gradients in relative humidity (33 – 98, 65-98 or 33-75 %) or exposure to liquid water. Changes in moisture content of the wood and the tangential or the radial dimensions were recorded as a function of time.

Apparent moisture diffusion coefficients were calculated from the initial slope of the fractional weight increase following Fick's second law for unsteady state conditions. The apparent moisture diffusion coefficients were clearly influenced by both coating and wood species. The fastest moisture adsorption was observed for uncoated spruce which could be explained by the rapid capillary uptake of water. Moisture diffusion in coated samples of spruce or with coated or uncoated meranti was much lower. With the exception of liquid water, moisture diffusion during desorption was faster than during adsorption. The measured moisture diffusion coefficients should be considered as apparent because they were dependent on the initial and final moisture content. Moisture diffusion was found to be strongly dependent on temperature with activation energies between 55 - 76 kJ mol^{-1}.

The rate of dimensional change was described by a two-parameter asymptotic regression model that included one constant for the rate of dimensional change and an asymptotic constant given by the dimensions at equilibrium wood moisture content as an asymptote. The differences in rate constant were influenced by the same factors as those for moisture diffusion. The correlation between rate constant and moisture diffusion coefficient was good except for very high moisture diffusion coefficients that were controlled by capillary water uptake.

9.1   Introduction

Reduction of the rate and magnitude of changes in moisture content of the wood is one of the primary functions of a coating that has to protect wood during outdoor weathering. The introduction of waterborne coatings has generally led to an increased movement of moisture through the coating film [1-4]. In many circumstances, this will result in faster, larger and more frequent fluctuations in wood moisture content.

Previous research on the mechanisms governing moisture transport like diffusion and capillary sorption are discussed in more detail in the first part of this paper [2]. In this second paper the following aspects of moisture protection by a coating are studied:
  – differences between the uptake of water in the vapour and liquid state,
  – two wood species, spruce and meranti are compared,
  – influence of the coating film thickness,
  – temperature influences on moisture transport in coated wood.

The moisture protection by the coating is evaluated in two ways: firstly by the measurement of the sorption rate and the calculation of apparent moisture diffusion coefficients, and secondly by the determination of the rate of dimensional change in both the radial and tangential directions.

An improved knowledge about the rate of both moisture adsorption and desorption and their subsequent impact on the dimensional changes of the wood will help in understanding and predicting the performance of coated wood in practice. The equilibrium wood moisture content is not influenced by the coating, but many studies on outdoor weathering of wood, have shown reductions in moisture content or dimensional change if a coating is present [4, 5-10]. The observed reductions can be explained by the fact that the coating reduces the rate of moisture transport induced by a change in the environmental conditions like relative humidity, solar irradiation or rain. Because in an outdoor environment, steady state conditions are never reached, the reduction in sorption rate actually means a permanent reduction in average moisture content or dimensions.

Dimensional changes can influence performance of both the coating and the wooden construction itself. The difference in hygroscopic expansion between coating and substrate can cause internal stress inside the coating [11] which can lead to cracking [12]. The reduction in differences in moisture content within the wood and its subsequent dimensional change improves the performance of glued-laminated wood [13]. Finally a limitation of the dimensional movement of wood is needed to prevent jamming of windows and doors [14].

9.2   Materials and methods

Nordic grown spruce *(Picea abies Karst.)* with an average density of 483 kg m^{-3} and dark red meranti *(Shorea spp.)* with an average density of 685 kg m^{-3} were used. All of the samples were industrially pre-dried to a moisture content of around 16 %. Samples with dimensions of 40 x 40 x 37 mm (width x thickness x length) were sawn out of one board. To guarantee clearly defined radial and tangential surfaces the samples had their growth rings parallel to one surface. Only for the studies on the influence of temperature, smaller samples (dimensions of 24 x 24 x 22 mm) were used to obtain equilibrium conditions more quickly. Conditioning of the samples was done over saturated salt solutions to reach relative humidities (RH) of 33 % (MgCl$_2$.6H$_2$O), 65 % (NaNO$_2$) and over distilled water (to reach 98 % RH) at a temperature of 23°C. Liquid water uptake was determined by immersion in liquid tap water. Sorption studies at different temperatures were performed over solutions of saturated NaCl which gives a relative humidity of 79 % to 73 % in the temperature range between 5 and 55 °C. Changes in the moisture content of the wood were determined by

weighing to an accuracy of 0.01 g. Dimensional changes were measured at four locations on two sides of the sample (radial or tangential) with a digital thickness gauge to an accuracy of 0.001 mm. All of the data presented are average values based on at least three replicates. Two types of white pigmented commercial wood coatings were used: one solvent borne alkyd and one waterborne acrylic dispersion. Application was done by brush in two to four layers depending on dry film thickness which ranged between 60 and 180 μm. Axial surfaces of the wood were sealed with three layers of a very moisture tight two-pack polyurethane coating. An overview of the entire experimental set-up is provided in *fig. 9.1.*
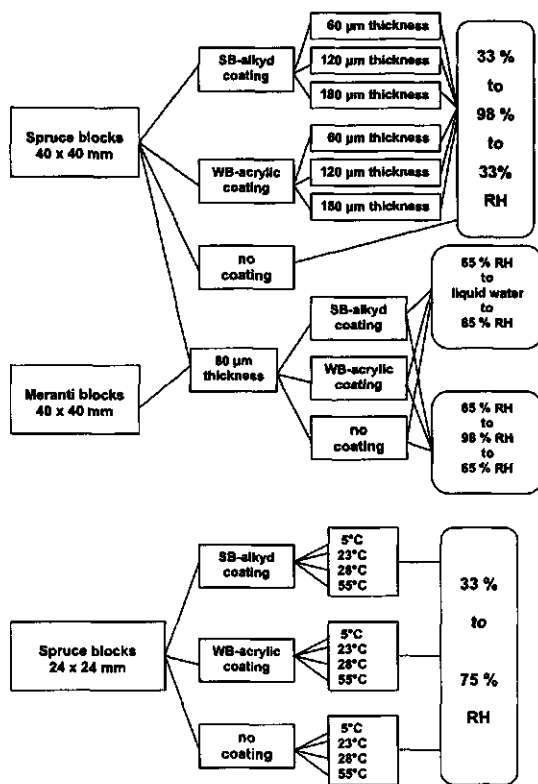
Figure 9.1.   Schematic overview of experimental set-up.

9.3.   Results and discussion

9.3.1   Moisture sorption and diffusion coefficients

From the plots of increase or decrease in moisture content with time the apparent diffusion coefficients were calculated according to the procedure given by Siau [15]. The dimensionless moisture concentration was calculated according to the following formula.

$$E_{4-\text{sided}} = \left[\frac{u_t - u_0}{u_\infty - u_0} \right] \tag{9.1}$$

The dimensionless concentration from the block shaped samples was based on 4-sided diffusion into a square block. Most analytical solutions of Fick's second law, from which diffusion coefficients can be derived, are based on parallel-shaped bodies with diffusion into only two directions. Siau [15] described the following way to transform the dimensionless concentration from a 4-sided sorption experiment into one, which can be treated as being based on parallel-shaped bodies. Identical diffusion rates in the radial and tangential directions were assumed. This seemed a reasonable assumption taking into account the relatively small differences in the radial and tangential diffusion mentioned in previous studies {16, 17].

$$1- E_{4\text{-sided}} = (1- E_{2\text{-sided}})^2 \tag{9.2}$$

As long as $E < 0.6$ the diffusion coefficient could now be derived from the slope of E against the square root of time using the following equation.

$$ID^* = \left(\frac{d\left\{ 1 - \sqrt{(1 - E_{4-\text{sided}})} \right\}}{d\sqrt{t}} \right)^2 \times \left(\frac{l^2}{5.10} \right) \tag{9.3}$$

The diffusion coefficient derived in this way should be considered as an apparent diffusion coefficient because it is known from previous research [17, 18] that diffusion is often influenced by non-Fickian behaviour. This was also the case in the present experiments as could be seen in the deviations from a straight line shown in *fig. 9.2*. The linear parts of the curves were used to calculate diffusion coefficients. The non-Fickian behaviour could be partly explained by the fact that capillary water uptake played a role in cases where the samples were exposed to liquid water, in particularly for uncoated wood [2].
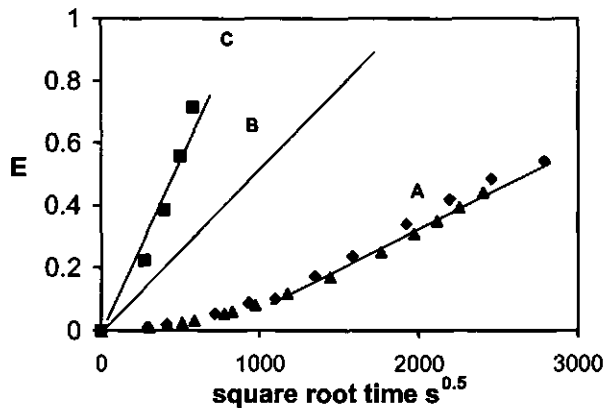
Figure 9.2   Plot of dimensionless moisture concentration against square root of time
                   A: delayed initial sorption; B: fast initial sorption; C: pure Fickian sorption.

A special problem arose, if the equilibrium moisture content had to be determined for samples immersed in liquid water. As could be seen from *fig. 9.3*, equilibrium was not reached within even 160 days. However, after twenty days any increase in wood moisture content did not give an additional change in dimensions. This clearly indicated that the fibre saturation point was reached and any further increase in wood moisture content would be due to the capillary uptake of water in the cell lumina. Therefore, the moisture content of the

wood at the point of maximum swelling was taken as the equilibrium moisture content in calculations of diffusion coefficients.
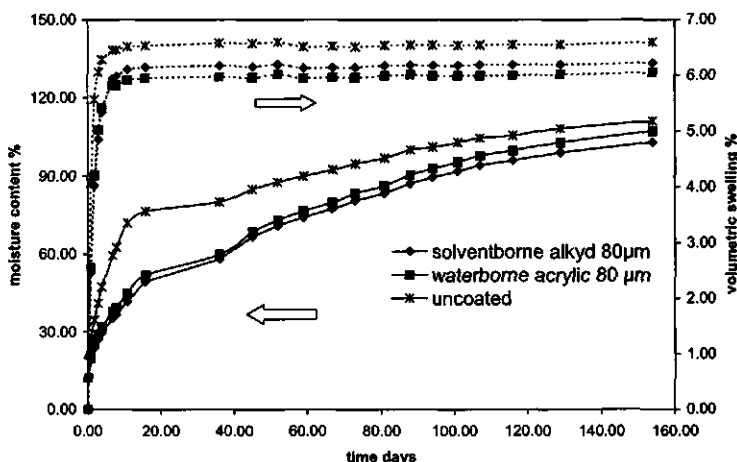
Figure 9.3 Increase in moisture content and swelling of spruce samples immersed in water.

Fig. 9.4 and 9.5 show the dependence of the apparent diffusion coefficient on coating film thickness during respectively adsorption in the range 33-98 % RH and desorption in the range of 98-33 % RH respectively.
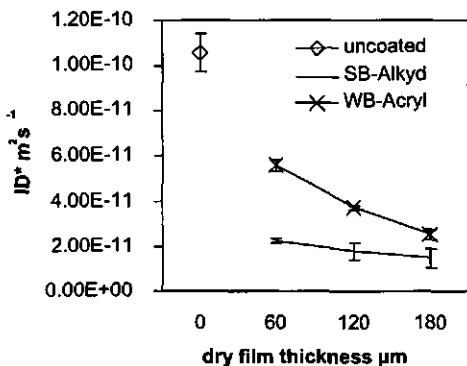
Figure 9.4
Apparent diffusion coefficients as a function of film thickness obtained from moisture adsorption measurements in the range 33-98 % RH.
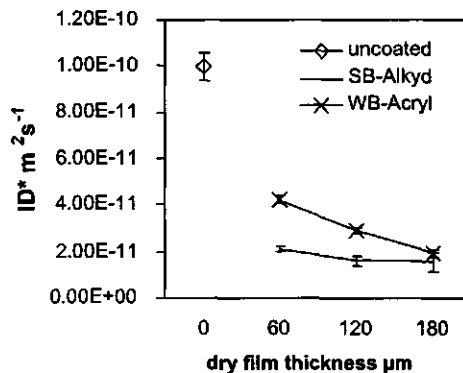
Figure 9.5
Apparent diffusion coefficients as a function of film thickness obtained from moisture desorption measurements in the range 98-33% RH.

The film thickness had an influence on the diffusion coefficient but it was limited in comparison to the type of coating. The strongest influence of film thickness was observed for the waterborne acrylic dispersion during moisture adsorption. Comparing diffusion coefficients for adsorption and desorption experiments, the uncoated samples and the ones

with a solventborne coating gave more or less similar results. However, the waterborne acrylic coatings showed a slightly higher diffusion coefficient during adsorption in the range of 33-98 % RH.

Table 9.1 Diffusion coefficient obtained for different wood species, moisture gradient and coatings.

wood	exposure	uncoated			SB-Alkyd			WB-Acryl		
					ID* m s^{-2} * 10^{-10}					
spruce	65%-98%	1.35	±	0.06	1.10	±	0.06	1.35	±	0.04
	65%-liquid	13.14	±	5.45	4.03	±	0.68	3.73	±	0.46
	98-65%	4.37	±	0.21	2.48	±	0.23	2.39	±	0.16
	liquid-65%	4.04	±	0.20	2.29	±	0.22	2.22	±	0.15
meranti	65%-98%	0.30	±	0.01	0.12	±	0.00	0.23	±	0.01
	65%-liquid	1.14	±	0.11	0.15	±	0.01	0.31	±	0.02
	98-65%	0.90	±	0.04	0.27	±	0.01	0.45	±	0.01
	liquid-65%	1.21	±	0.03	0.14	±	0.01	0.21	±	0.01

Table 9.1 gives the apparent diffusion coefficients of spruce and meranti for sorption of liquid water and water vapour in the range of 65-98 % RH. Water transport was clearly lower for meranti compared to spruce which reflected the differences in permeability between these two species. With the exception of spruce exposed to liquid water, moisture diffusion proceeded faster during desorption than during adsorption. The very high moisture diffusion coefficients obtained with liquid water on spruce can be explained by the capillary uptake of water [19]. As it was expected from many previous observations [1,5,3], water transport through the waterborne acrylic coatings was faster in comparison to the solventborne alkyd coating.

The apparent diffusion coefficients for liquid water uptake of uncoated wood are slightly higher in comparison to the results obtained for earlier findings [2]. It should, however, be noted that in this case both radial and tangential surfaces are exposed to water, whereas in the previous study the main area of exposure was the tangential surface. A second factor that might attribute to the difference in diffusion coefficient, was the size of the sample which considerably larger in the previous experiment. Fakhouri *et al* [20] reports diffusion coefficient of respectively $4*10^{-9}$ m^2 s^{-1} (radial) and $3*10^{-9}$ m^2 s^{-1} (tangential) for the transport of liquid water into wood.

9.3.2 Influence of temperature on moisture diffusion

Apparent diffusion coefficients were measured at temperatures of 5, 23, 28 and 55 °C for spruce without a coating and with a solventborne alkyd or a waterborne acrylic coating (film thickness of 80µm). The equilibrium moisture content was calculated as a function of temperature. From the diffusion coefficients the activation energies were calculated according to the Arrhenius equation:

$$ID = ID_0 \, e^{\frac{-Ea}{RT}}$$

(9.4)

Table 9.2 Diffusion coefficients and equilibrium moisture content (EMC) at 75 % RH as a function of temperature; activation energies of diffusion

	ID* $m^2 s^{-1}$ * 10^{-10}			
T °C	SB-alkyd	WB-Acryl	Uncoated	EMC %
5	0.27	0.68	4.53	13.6
23	1.66	2.20	9.92	12.3
28	3.41	5.59	23.12	11.8
55	39.60	50.37	163.73	9.8
E kJ mol^{-1}	76.1	66.5	55.7	
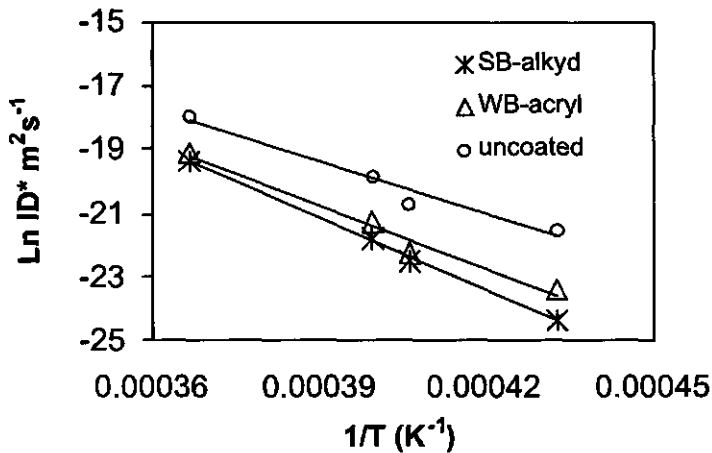
Figure 9.6 Plot of diffusion coefficient against reciprocal absolute temperature to obtain activation energies from the slope of the line.

The activation energy can be obtained from the slope if the diffusion coefficient is plotted against the reciprocal absolute temperature. *Fig. 9.6* shows this plot, all other results are given in *table 9.2*. The moisture diffusion of the wood was strongly increased with temperature, which was to be expected from previously reported research [21-24]. The temperature dependence of the moisture diffusion was somewhat reduced if a coating was applied but is still clearly present. This corresponded with findings in literature [19, 25]. This might indicate that the moisture movement through the coating was less sensitive to temperature, which could also be seen from the increased activation energies.

The calculated activation energies of the diffusion coefficients were somewhat higher than those mentioned in literature. Mantanis *et al* [26] mentioned activation energies in the range of 32.2 to 50.2 kJ mol^{-1} for diffusion in uncoated wood. Richard *et al* [27] reported activation energies of 35.2 kJ mol^{-1} for diffusion of water vapour into carboxylated styrene-butadiene copolymer latexes.

The decrease in equilibrium moisture content with increasing temperature was to be expected [16, 28]. The lower equilibrium moisture content would have indirectly also effected the measured diffusion coefficient. If the initial sample temperature was lower than the

temperature during sorption, the same amount of adsorbed water would have given a higher diffusion coefficient because the fractional moisture uptake was increased due to the reduction of the maximum amount of adsorbed water. If the test temperature was below the pre-conditioning temperature, the opposite would happen which leads to a lower diffusion coefficient.

9.3.3 Modelling of dimensional change

Below the fibre saturation point, the rate of shrinkage or swelling can be expected to be directly proportional to respectively moisture adsorption and desorption. Stamm [16] even derived moisture diffusion data from swelling data. The rate of dimensional change can be described by the initial linear rate [22] or by a two-parameter asymptotic regression model [29]. The latter approach was used to describe the dimensional movement of the wood.

$$y = y_{max}(1 - e^{-kt})$$ (9.5)

By rewriting *equation 9.5* to the following one, k could be obtained from a linear regression:

$$\ln(1 - \frac{y}{y_{max}}) = -kt$$ (9.6)

The shrinkage rate was expressed on the basis of the maximum swelling data (y_{max}) and the final dimensions after shrinkage (y_{min}):

$$\ln \frac{(y - y_{min})}{(y_{max} - y_{min})} = -kt$$ (9.7)

The time needed to reach 50 % of the equilibrium dimensions was defined by:

$$t_{0.5} = \frac{-\ln(1 - 0.5)}{k} = \frac{0.6932}{k}$$ (9.8)

The data obtained from the model given in *equation 9.5* to *9.8* are provided in *table 9.3*. The model fitted the observed experimental data well as could be seen from the high values of r^2. *Fig. 9.7* shows both the experimental and model radial swelling data of meranti in the range of 66-98 % RH. The dimensional changes correlated well with the diffusion coefficients as can be seen in *fig. 9.8*. Deviations were only observed for very high moisture diffusion coefficients obtained with the uptake of liquid water. This can be explained by the fact that with liquid water sorption the moisture content in the outer cells might rise above the fibre saturation point where no additional contribution to swelling was made [30, 31].

The time needed to reach 50 % of the maximum dimensions ($t_{0.5}$) was between 1 (uncoated) and 25 days for spruce depending on the presence of a coating. For meranti, the swelling rate was much lower, the half time to swell ranged between 6 and 86 days. The strong reduction in swelling rate of the coated samples explains why during outdoor weathering, where steady-state conditions do not exist, the coating gives a permanent reduction in the dimensions of the wood [5, 32]. The swelling rate was slightly higher in the radial direction. This was caused by the fact that the swelling rate was calculated from the ratio between actual and maximum swelling. Therefore, the higher maximum swelling in tangential direction reduced the rate of swelling.

Table 9.3   Data obtained from modelling the dimensional changes.

wood	exposure	coating	film thickness (μm)	radial k (days^{-1})	$t_{0.5}$ (days)	$y_{max/min}$ %	r^2	tangential k (days^{-1})	$t_{0.5}$ (days)	$y_{max/min}$ %	r^2
spruce	33-98	none	0	0.19	3.6	2.7	0.99	0.17	4.1	4.5	0.99
		SB-Alkyd	60	0.04	15.5	2.5	0.98	0.03	20.9	3.9	0.99
			120	0.04	19.0	2.7	0.99	0.03	23.0	4.4	1.00
			180	0.03	20.7	2.7	0.99	0.03	25.4	4.2	1.00
		WB-Acryl	60	0.10	7.1	3.1	0.99	0.11	6.5	5.3	0.97
			120	0.07	9.5	2.9	0.99	0.07	9.5	5.0	0.99
			180	0.06	11.8	2.1	0.99	0.06	12.2	4.7	0.98
	65-98	none	0	0.31	2.2	1.7	1.00	0.20	3.5	3.9	0.97
		SB-Alkyd	80	0.18	3.9	1.5	1.00	0.14	5.1	3.6	1.00
		WB-Acryl	80	0.23	3.0	1.5	1.00	0.16	4.3	3.6	1.00
	65-liquid	none	0	1.20	0.6	1.8	0.99	0.39	1.8	4.1	0.85
		SB-Alkyd	80	0.59	1.2	1.6	1.00	0.33	2.1	3.8	0.93
		WB-Acryl	80	0.70	1.0	1.7	1.00	0.34	2.0	3.9	0.93
	98-65	none	0	0.28	2.5	0.3	0.92	0.26	2.7	0.4	0.89
		SB-Alkyd	80	0.26	2.6	0.2	0.96	0.25	2.7	0.3	0.95
		WB-Acryl	80	0.28	2.5	0.2	0.98	0.26	2.6	0.3	0.96
	liquid-65%	none	0	0.28	2.5	0.3	0.95	0.29	2.4	0.5	0.94
		SB-Alkyd	80	0.18	3.9	0.2	0.95	0.20	3.5	0.4	0.95
		WB-Acryl	80	0.19	3.7	0.1	0.96	0.21	3.3	0.3	0.96
meranti	65-98	none	0	0.08	8.5	1.5	0.97	0.03	21.7	4.2	0.95
		SB-Alkyd	80	0.03	23.3	1.5	0.91	0.02	27.9	4.1	0.99
		WB-Acryl	80	0.06	12.2	1.5	0.96	0.03	23.8	4.1	0.97
	65-liquid	none	0	0.11	6.4	1.5	0.99	0.09	7.9	4.3	0.98
		SB-Alkyd	80	0.04	16.0	1.5	0.97	0.04	18.8	4.3	0.88
		WB-Acryl	80	0.07	10.4	1.5	0.97	0.06	11.6	4.1	0.95
	98-65	none	0	0.05	14.2	0.5	0.98	0.05	13.6	1.4	0.99
		SB-Alkyd	80	0.02	39.2	0.5	0.98	0.02	44.1	1.4	0.98
		WB-Acryl	80	0.03	26.5	0.5	0.99	0.03	25.9	1.4	1.00
	liquid-65%	none	0	0.04	16.0	0.4	0.87	0.03	22.0	1.4	0.91
		SB-Alkyd	80	0.01	86.2	0.4	0.79	0.01	79.3	1.4	0.93
		WB-Acryl	80	0.01	50.5	0.4	0.83	0.01	48.6	1.4	0.92
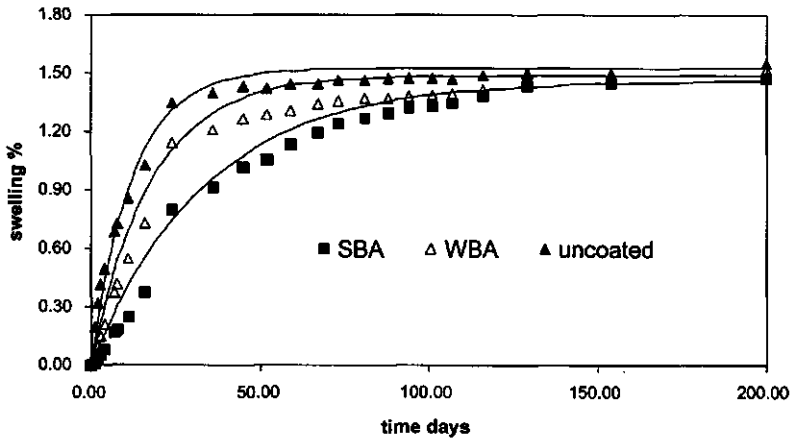
Figure 9.7 Radial swelling of meranti samples in the range of 66-98 % RH. Dots represent measured data, lines are fitted according to *equation 9.4*.
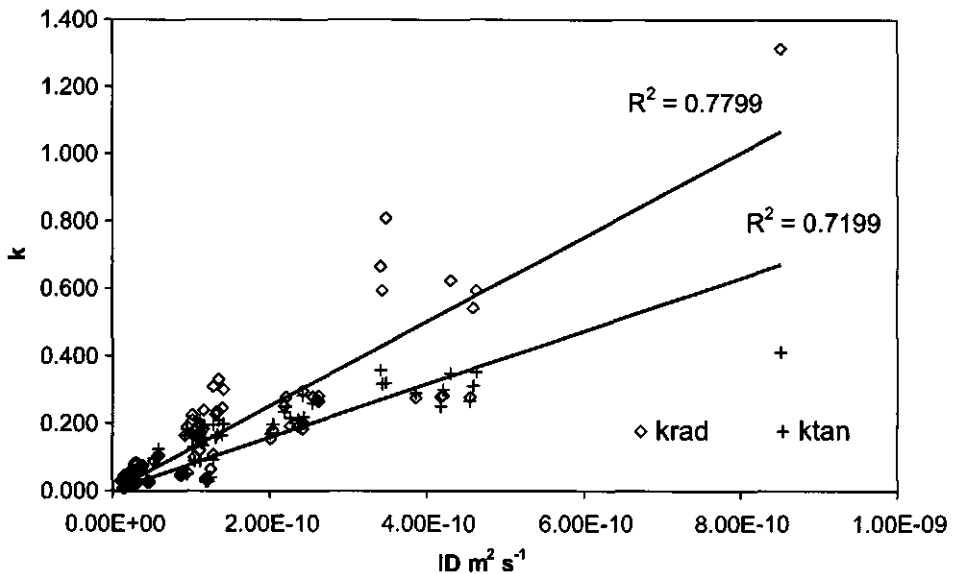
Figure 9.8 Correlation between apparent diffusion coefficients and the rate of dimensional change.

The equilibrium dimensions were hardly influenced by the presence of the coating, which is logical, because the equilibrium moisture content was not changed. The only exception was for the spruce samples, where a somewhat higher variation in equilibrium dimensions was observed. This was most likely due to errors in the measurements of dimensions caused by

uneven surfaces due to raising of latewood bands during swelling of the wood. The equilibrium dimensions after desorption were clearly above the dimensions before start of the moisture adsorption. This can be easily explained by the hysteresis in moisture sorption. The hysteresis effects were in the range of 0.2 to 1.4 percentage in dimensional change, which was in good agreement with the data given by [33].

9.4. Conclusions

The apparent diffusion coefficients obtained in the experiments discussed give valuable information about the influence of wood species, coating type and coating thickness on the rate of moisture sorption. In general, the highest sorption rates were found for uncoated wood, followed by wood coated with a waterborne acrylic coating whereas the slowest sorption is obtained with the solventborne alkyd. Moisture diffusion in spruce proceeded much faster in comparison to meranti. These findings correspond well with results from studies where the moisture content in the coated wood was monitored in practice [3, 5, 6, 19, 34].

Increased temperature lead to faster moisture diffusion which compliments the findings that darker coloured paints give rise to faster fluctuations in moisture contents in the wood [35, 36] or higher fluctuations in dimensional change [9]. The coating film thickness had only a limited influence on the moisture diffusion which means that that a higher permeability of coatings can not easily be compensated by a higher film thickness.

Comparing the diffusion rate for adsorption and desorption, the latter was higher, except for adsorption of liquid water on spruce. This can easily be explained by the important role of capillary water uptake [2]. The large difference in liquid water sorption versus the lower desorption supports the practical knowledge that water accumulation in wooden joinery is almost always related to fast adsorption of liquid water.

The moisture diffusion coefficients obtained should be considered apparent diffusion coefficients, which means that their absolute values can be strongly influenced by the conditions during which they were obtained. There were several indications that Fickian diffusion was not always valid. The initial fractional sorption curves did not always follow a straight line from the origin. This can indicate the influence of a surface resistance effect [18].

Furthermore, the diffusion coefficients depended on the initial and final relative humidities used during the measurement. Comparing diffusion coefficient for spruce from the range 33-98 % RH (initial moisture content: 7%) and 65-98 % (initial moisture content: 12 %), the latter were considerably higher, in particular for the coated samples. The diffusion coefficients from the smaller sized samples tested in the range of 33-75 % RH were a factor 5 to 10 higher then those from the range 33-98%. The sample size was not likely to be responsible for this, because Rosen [37] reported that higher apparent diffusion coefficients were produced with thicker samples. Differences in moisture content prior and during the sorption process seemed to be a more likely explanation. Stamm [16] and Avramidis and Siau [21] reported increasing diffusion coefficients with increasing moisture content which might explain the differences between 65-98 and 33-98 % RH. Wadsö [17] reported lower diffusion coefficients for the step 75-84 % RH in comparison to 54-75 %. Droin *et al* [38] also mentioned decreasing diffusion coefficients with increasing initial moisture content. According to Siau [15], the bound water diffusion in the cell wall was positively correlated to moisture content whereas the vapour diffusion in the lumina was negatively correlated. Differences in the prevailing process might explain the conflicting results mentioned.

The applied two-parameter asymptotic regression model described the actual data well. The rate constants for dimensional change showed the same dependence on wood species, coating type and moisture gradients as the moisture diffusion coefficients. The correlation between these two parameters was quite good, except with the very high diffusion

coefficients observed with liquid water sorption. This indicated that water uptake above the fibre saturation range was taking place under these circumstances.

Acknowledgements

References

[1]   **Ahola, P.; Derbyshire, H.; Hora, G.; Meijer, M. de**; Water protection of wooden window joinery painted with low organic solvent content paints with known composition, Holz als Roh- und Werkstoff, 57, 1999, 45-50.

[2]   **Meijer, M. de; Militz,H.**; Moisture transport in coated wood Part 1: Analysis of sorption rates and moisture content profiles in spruce during liquid water uptake. Accepted for Holz als Roh- und Werkstoff, 1999.

[3]   **van Linden, J.A.; Oort, P.**; Water permeability: comparison of methods and paint systems. XXII Fatipec Conference Budapest, IV, 1994, 135-148.

[4]   **Böttcher, P.**; Zum Verhalten unterschiedlich feuchtedurchlässiger Anstriche auf einigen einheimischen Holzarten bei natürlicher Bewitterung, Holz als Roh- und Werkstoff (33), 1975, 116-120.

[5]   **Meijer, M. de; Creemers, J.G.M.; Cobben, W.N.H.**; Interrelationships between the performance of low-voc wood coatings and the dimensional changes of the wood substrate, Advances in exterior wood coatings and CEN standardisation PRA-conference Brussels, paper 9, 1998a.

[6]   **Meijer, M. de; Creemers, J.G.M.; Cobben, W.N.H.; Ahola,P**; Influence of a dipping preservative treatment on the performance of wood finished with waterborne coatings. IRG/WP 98-40121 Maastricht , The Netherlands, 1998b.

[7]   **Roux, M.L.; Wozniak, E.; Miller, E.R.; Boxall, J.; Böttcher, P.; Kropf, F.; Sell, J.**; Natural weathering of various surface coatings on five species at four european sites, Holz als Roh- und Werkstoff, 46, 1988, 165-170.

[8]   **Sell, J.**; Untersuchungen zur Optimierung des Oberflächenschutzes von Holzbauteilen, Teil 1: Bewitterungsversuche mit Fensterrahmen-Abschnitten, Holz als Roh- und Werkstoff, 40, 1982, 225-232.

[9]   **Sell, J.**; Physikalische Vorgänge in Wetterbeanspruchten Holzbauteilen Fensterrahmen, Holz als Roh- und Werkstoff, 43, 1985, 259-267.

[10]   **Teichgräber, R.**; Measurement and Evaluation of the Interactions between Paint Systems, Wood Species and Climate, Holz als Roh- und Werkstoff, 31, 1973, 127-132.

[11]   **Perera, D.Y.; Van den Eynde, D.**; Moisture and temperature induced stresses (hygrothermal stresses) in organic coatings, Journal of Coatings Technology, 59 (748), 1987, 55-63.

[12]   **Floyd, F.L.**; Predictive model for cracking of latex paints applied to exterior wood surfaces, Journal. of Coatings Technology, 55 (696), 1983, 73-80.

[13]   **Turkulin, H.**; Dauerhaftigkeit von lamellierten Holzfensterprofilen Feuchteverlauf und Formstabilität, Holz als Roh- und Werkstoff, 50, 1992, 347-352.

[14]   **Graystone, J.**; Moisture transport through wood coatings: the unanswered questions. Advances in exterior wood coatings and CEN standardisation PRA-conference Brussels, paper 6, 1998.

[15]   **Siau, J.F.**; Transport Processes in Wood (Springer Series in Wood Science), Springer, Berlin Heidelberg New York Tokyo, 1984, 29,186.

[16]   **Stamm, A.J.**; Bound water diffusion into wood across-the-fiber directions, Forest Products Journal, 10, 1960, 524-528.

[17]   **Wadsö, L.**; Unsteady-state water vapour adsorption in wood: an experimental study, Wood and Fiber Science, 26, 1994, 36-50.

[18]   **Absezt, I.; Koponen, S.**; Fundamental diffusion behaviour of wood, International conference on wood-water relations Cost Action E8 Copenhagen Denmark, 1997.

[19]   **Huldén, M.; Hansen, C.M.**; Water permeation in coatings, Progress in Organic Coatings,13, 1985, 171-194.

[20]   **Fakhouri, B.; Mounji, H.; Vergnaud, J.M.**; Comparison of the absorption and desorption of water between scots pine and spruce after submersion in water, Holzforschung, 47, 1993, 271-277.

[21]   **Avramidis, S.; Siau J.F.**; An investigation of the external and internal resistance to moisture diffusion in wood, Wood Science and Technology, 21, 1987, 249-256.

[22]   **Walker, I.K.**; Changes of bound water in wood Non Fickian changes of weight at 25 °C. New Zealand, Journal of Science, 20, 1977, 3-10.

[23]   **Bramhall, G.**; Fick's law and bound water diffusion, Wood Science, 8 (3), 1976, 153-161.

[24]   **Stamm, A.J.**; Diffusion and penetration mechanism of liquids into wood, Pulp and paper magazine of Canada, 1953. 54-63.

[25]   **Yaseen, M.; Funke, W.**; Journal of the Oil Colour Chemist Association, 61, 1978, 284.

[26]   **Mantanis, G.I.; Young, R.A.; Rowell, R.M.**; Swelling of wood Part 1 Swelling in water, Wood Science and Technology, 28, 1994, 119-134.

[27]   **Richard,J.; Mignaud, C.; Wong, K.**; Water vapour permeability, diffusion and solubility in latex films, Polymer International, 30, 1993, 431-439.

[28]   **Choong, E.T.**; Movement of moisture through softwood in the hygroscopic range, Forest Products Journal, 1963, 489-498.

[29]   **Rypstra, T.**; Analytical techniques for evaluation of wood and wood finishes during weathering, PhD-thesis, University of Stellenbosch South-Africa, 1995, pp. 243.

[30]   **Keylwerth, R.**; Untersuchungen über freie und behinderte Quellung I Freie Quellung, Holz als Roh- und Werkstoff, 20 (7), 1962, 252-259.

[31]   **Noack, D.; Schwab, E.; Bartz, A.**; Characteristics for a judgement of the sorption and swelling behaviour of wood, Wood Science and Technology, 7, 1973, 218-236.

[32]   **Kiguchi, M.; Suzuki, M.; Imamura, Y.**; Weatherability of exterior wood coatings in Japan, Advances in exterior wood coatings and CEN standardisation PRA-conference Brussels, paper 12, 1998.

[33]   **Rijsdijk, J.F.; Laming, P.B.**; Physical and related properties of 145 timbers Information for practice, Kluwer Academic Publishers, Dordrecht, Boston, London, 1994.

[34]   **Samuelsen, B.**; Exterior high performance wood coatings systems. Advances in exterior wood coatings and CEN standardisation PRA-conference Brussels, paper 8, 1998.

[35]   **Schultz, H.; Böttcher, P.; Neigenfind, W.**; Effect of some paints and colours on the moisture conditions of naturally weathered wood specimens, Holz als Roh- und Werkstoff, 31 (3), 1973, 132-137.

[36]   **Janotta, O.**; Der Einfluss des Farbtones und der Wasserdampfdurchlässigkeit von Anstrichmitteln auf die Feuchtigkeitsverteilung im Holz. Auswirkungen auf die Kondenswasserbildung an Holzverbundfenstern, Holzforschung und Holzverwertung, 31 (3), 1979, 45-59.

[37] **Rosen, H.N.**; The influence of external resistance on moisture adsorption rates in wood, Wood and Fiber, 10 (3), 1978: 218-228.

[38] **Droin, A.; Taverdet, J.L.; Vergnaud, J.M.**; Modeling the kinetics of moisture adsorption by wood, Wood Science and Technology, 22, 1988, 11-20.

Nomenclature

u	Wood moisture content	$(mass-mass_{oven-dry}) / mass_{oven-dry} \times 100\%$.
u_∞	Final equilibrium wood moisture content	$(mass-mass_{oven-dry}) / mass_{oven-dry} \times 100\%$.
u_0	Initial wood moisture content	$(mass-mass_{oven-dry}) / mass_{oven-dry} \times 100\%$.
$u_{x=0}$	Wood moisture content at the boundary	$(mass-mass_{oven-dry}) / mass_{oven-dry} \times 100\%$.
ID^*	Apparent moisture diffusion coefficient	$m^2 s^{-1}$
t	Time	s or days
$E_{4-sided}$	Dimensionless moisture concentration for four sided diffusion in a square block	-
$E_{2-sided}$	Dimensionless moisture concentration for two sided diffusion in a parallel plate	-
l	Specific length = 2x sample thickness	m
y	Dimensional change %	-
y_{max}	Equilibrium dimensions after swelling	m
y_{min}	Equilibrium dimension after shrinkage	m
k	rate constant	s^{-1}
$t_{0.5}$	time to reach 50 % of maximum dimensions	days
Ea	Activation energy	$kJ\ mol^{-1}$

10. GENERAL DISCUSSION AND CONCLUSIONS

In this thesis several aspects of the interactions between wood, in particular softwoods, and low-VOC coatings have been studied and discussed in comparison to the behaviour of traditional solventborne alkyd coatings. The work focuses on how the properties of coatings and wood might affect phenomena occurring at the interface between the materials. The studied aspects included the substrate penetration and wetting, the adhesion of coatings to wood, the moisture sorption and the dimensional changes. The aim is to find ways in which these aspects might be used to predict, understand and further optimise the durability of exterior wood coatings and wooden joinery as a whole. In this respect, it should, however, be emphasised that the service life of wood during exterior use not only depends on the coating but on many other factors like exposure conditions and substrate design as well (see *chapter 1.2*).

10.1 Penetration of coatings into wooden substrates

The microscopic studies presented in *chapter 2* showed that penetration of a coating into wood is both controlled by the ability of the coating to flow into the capillaries present in the wood and by the number of open pores present at the surface. The lowest penetration was observed for the waterborne acrylic dispersion followed by the alkyd emulsions, solventborne alkyds and high solid alkyds. Addition of pigment or thickener strongly reduced the penetration. This is in good agreement with results reported in other studies on the penetrating capacity of waterborne acrylic dispersions and alkyd emulsions coatings on wood [1,2,3]. In softwoods, the penetration of a coating is mainly limited to the outer tracheids and the rays. This pattern was also observed in several previous studies with spruce and pine sapwood [1,4]. If the penetration of a coating exceeds the length of a single cell element, the permeability of the wood has an influence on the depth of penetration as well. With the studied softwoods, this was directly related to the permeability of the pits between ray cells and tracheids or combinations of these cell elements because the cell wall itself is impermeable to binders or pigments.

The polymeric binders and pigments used in coatings are very small (typical radius below 400 nm) in comparison to the radius of a tracheid (5-30 μm) but are still far too large to penetrate the micro-pores in the cell wall which have a size of 0.1-1nm [5]. In previous studies [6,7] it was observed that a coating or larger polymer can not penetrate the cell wall. During the flow of a coating through pits, the particle size might have an influence since size exclusion effects and particle agglomeration around pit membranes were observed. In *chapter 2*, a flow model is described that gives the possible penetration pathways of a coating in relation to the anatomical structure of softwoods. The studies for meranti *(Shorea spp.)* showed that the penetration was limited to the flow of the coating into vessels and rays. To extend this flow model to hardwoods, studies with more permeable hardwood species would be required.

In *chapters 3* and *4*, the capillary penetration has been quantified in three different ways: firstly by measuring the maximum depth of coating penetration in the axial direction after drying, secondly by measuring the volumetric uptake from combined measurements of contact angle, height and diameter of droplets and thirdly by gravimetric measurements. The static measurement of final penetration depth on a microscopic level has the advantage of giving an accurate penetration depth of the coating in relation to capillary radius. The other two methods only give information on a macroscopic scale but can measure the rate of capillary penetration.

The capillary flow model developed by Washburn [8] can relate, at least qualitatively, most of the phenomena observed in the penetration process. In this model, the capillary pressure is the driving force for the penetration but the flow rate is also influenced by the viscosity of the penetrating liquid. The rate of capillary rise is proportional to the surface tension of the liquid, the cosine of the contact angle and the radius of the capillary and is inversely proportional to the viscosity and the height of rise (excluding gravity induced factors).

In *chapter 4*, it was shown that during capillary uptake the solid matter content of the coating increases due to the selective uptake of water or organic solvent into the cell wall. The influence of the uptake of water into the cell wall could also be seen from the deeper penetration with higher wood moisture content (*paragraph 3.3.4*). This causes an increase in viscosity of the coating, which becomes the limiting factor in the penetration of a coating into wood. Additionally the capillary pressure will also drop with increasing solid matter content. How fast this limiting level is reached largely depends on the nature of the polymeric binder. Binders based on emulsions or dispersions reach an almost infinitely high viscosity at solid matter contents of 60 % or less. Binders based on solutions (in this thesis limited to solventborne polymers) retain a relatively low viscosity at higher concentrations. The penetration of an alkyd based binder is reduced in the presence of a catalyst for oxidative drying (*chapter 2*). This indicates that cross-linking of the polymer network also contributes to the viscosity increase during capillary uptake, although this will occur at a much slower rate than the increase in solid matter content. The increase in viscosity at low shear rates, as observed for most of the binders studied, also reduces the penetration because it can be estimated that shear rates during the flow into the wood are low (0.1 s^{-1} or less). Additionally, the low viscosity of dispersions and emulsions at higher shear rates requires the use of thickeners to obtain an acceptable application viscosity. This however has an adverse effect on the penetration capacity of the coating.

Decreased penetration with a reduction of liquid surface tension, whilst maintaining a complete wetting of the substrate is predicted by the Washburn model and has been demonstrated experimentally in studies with increasing surfactant concentration in water. The increased reduction of penetration at surfactant concentrations above the critical micelle concentration (where the surface tension no longer decreases) suggests that surfactants might be adsorbed at the wooden cell wall. This behaviour seems to be independent of the type of surfactant.

The proportionality between the capillary radius and the maximum penetration depth has been confirmed for most of the coatings studied but some striking contradictory cases were observed for the deep penetrating unpigmented high solid and solventborne alkyd coatings. It is not fully understood why the smallest capillaries showed the deepest penetration in those cases. Possibly, the viscosity is no longer a limiting factors under these conditions, which make an alternative model applicable in which the penetration depth is inversely proportional to capillary radius. Further refinement of the flow model is also needed to predict the maximum penetration depth quantitatively. Even if all relevant parameters for the Washburn model are known from direct or indirect measurements (see *chapter 4*), a viscosity correction factor is needed to fit the model to the measured data. Direct measurement of the flow rate of a coating in a single capillary in combination with the in situ measurement of solids content might be able to resolve these questions.

If penetration of the coating into the wood is a desired property, the following practical recommendations can be given. Firstly, the increase of the viscosity at high solid matter content and low shear rates should be as limited as possible. This is in conflict with the rheological properties of dispersions or emulsions that show a rapid viscosity increase with increased volume fraction of particles and at the same time low viscosity at lower volume fractions, requiring thickeners for high shear applications like spraying and brushing. This

suggests that those low-shear application techniques like dipping or flow coating (sprinkling of paint) are preferable. Specific modification of the associative thickeners might also contribute to the desired behaviour of higher viscosity at low solids content and high shear rates without a very rapid increase in viscosity at higher solid contents as was demonstrated recently [9]. Secondly, for an optimum penetration the surfactant concentration should be limited to the levels needed to obtain complete wetting because an excess amount of surfactant will only lower the liquid surface tension and hence the capillary uptake.

10.2   Adhesion and surface free energy

The surface energy was characterised in *chapter 5* using contact angle measurements followed by the calculation of the Lifshitz-van der Waals, acid-base and total surface free energy components according to the theory of van Oss, Chaudhury and Good [10,11]. The total surface free energy of wood ranges between 35 and 55 mJ m^{-2} with a dominant Lifshitz-van der Waals component and only a small (and for special cases even negative) acid-base contribution. The acid and base parameters showed less consistent results as they depended on the method of measurement. For most wood species, the base parameter is significantly larger than the acid parameter if measured along the grain of the wood. If measurements are taken across the grain, the acid parameter is dominant. The reason for this phenomena, also observed by others [12], is not clear but might be related to chemical heterogeneity, surface roughness or capillary penetration. Adsorbed molecular layers of test solvent or water also have a strong influence on the measured contact angle.

In *chapter 5*, three different methods to measure the contact angles of liquids on wood were compared. The capillary rise method appeared to be of limited use because it can not deal with a swelling solvent like water. The dynamic contact angle measurements (Wilhelmy-plate principle) can give very valuable information about advancing and receding contact angles and its relation to surface roughness. By comparing data from the first and second immersion, solvent absorption effects could be studied. The contact angle measurements from droplets are the easiest to perform and do not require an additional measurement of the sample perimeter. However, with all of the methods the results should be interpreted with care because the basic assumptions in the Young's equation like absence of roughness, chemical purity and no solvent absorption at the surface are generally not fulfilled. This might also explain the large differences in results obtained in different studies as it was summarised in *paragraph 5.1*.

The adhesion of a coating was measured quantitatively using a newly developed method, based on measurement of the forces needed to peel the coating from the wood by means of a pressure sensitive tape attached to a tensile testing machine (see *chapter 6*). Adhesion forces up to approximately 350 J m^{-2} can be measured due to the limited adhesion of the coating to the tape. For the coatings studied, it means that only adhesion on wood with a high moisture content (25-30 % in the interface) could be measured. This so-called wet-adhesion is, however, found to be most critical in practice and reduced adhesion at high moisture content has been reported previously [13,14].

The observed adhesion differences between early- and latewood zones clearly correspond to differences in substrate penetration. Differences between coatings are considerable, the lowest values (around 50 J m^{-2}) are found for adhesion of the least penetrating acrylic coatings on latewood; the highest values are observed for the adhesion of deep penetrating high solid paints on the earlywood (above 300 J m^{-2}). Adhesion differences between early- and latewood have not been described for coatings so far but is known to occur for glues [15]. The measured work of adhesion has been analysed by the contribution of the interfacial work of adhesion and the negative contribution due to stored elastic strain

energy as it was proposed by Perera [16]. The stored elastic strain energy, as it was calculated from stresses due to the swelling differences between coating and wood, can reach very high values that even exceed the actually measured adhesion data. In those cases, the adhesion will only be based on mechanical anchoring. Very high levels of stored strain energy are reached if the coating swells much more than the wood. Volumetric swelling between 10 to 70 % was observed for the acrylic coatings with swelling of about 2.7 % for the alkyd coatings (solvent- and waterborne). The higher adhesion in the presence of water vapour instead of liquid water seems also to be related to differences in swelling stresses.

From the Lifshitz-van der Waals and acid-base parameters of both coating and wood the interfacial work of adhesion has been calculated [10,11]. Also, in the presence of water as a third phase, the total interaction between the interfaces remains attractive. The magnitude of the interfacial forces is very much lower than the measured adhesion data and no rank correlation between interfacial and measured adhesion was observed. This emphasises the importance of increased surface area and mechanical anchoring for obtaining good adhesion.

Analysis of the fractured surfaces showed that partially cohesive failure had occurred, mainly in the deeply penetrated parts of the coating. Furthermore, differences in the chemical surface composition were observed between the wood and air faced sides of the coating. Surfactant adsorption on to the wood as observed during penetration studies (*chapter 4*) might have also affected adhesion, because the potential negative influence of surfactants on adhesion as was demonstrated in studies on the adhesion of latex on glass [17] and for the adhesion of waterborne alkyd and acrylic paints on wood [18].

To summarise, it can be stated that in order to obtain good adhesion of a coating on wood, a good wetting and a certain amount of substrate penetration are required. To maintain good adhesion at high moisture contents, the elastic strain energy originating from hygroscopic stress should be minimised. This means that dimensional changes of both coating and wood should match each other as closely as possible although some difference will always remain because of the different shrinkage and swelling of wood in the radial and tangential directions.

10.3 Moisture sorption and dimensional changes

The protection against moisture and dimensional changes was evaluated in several ways. The studies with the coating present inside the pores of the wood (*chapter 7*), showed that a penetrated coating is far less effective in protection against water in comparison to a coating applied as a film on the surface as was described in *chapter 8* and *9*. The filling of the wood pores with a coating only prevented the capillary uptake of liquid water to a large extent. Moisture vapour diffusion, equilibrium moisture content and swelling or shrinkage are only slightly affected. Other studies with wood that was impregnated with polymeric material also report a relatively strong impact on liquid water repellency but no or limited impact on dimensional change [19,20]. This can be explained by the fact that the coating itself also adsorbs a significant amount of water and sometimes exhibited considerable swelling itself. Furthermore, due to shrinkage upon drying, the final void filling of the wood is relatively low. Nevertheless, several studies have shown a positive influence of a water-repellent pre-treatment on coating durability [21, 22, 23]. This might indicate that uptake of liquid water has a more pronounced impact on coating failure than the changes in relative humidity.

The measured moisture content profiles (*chapter 8*) gave valuable information about the actual moisture transport processes in coated and uncoated wood. For uncoated wood in direct contact with water, both diffusion and capillary water uptake takes place. The latter is mainly responsible for the high moisture content at the surface. In coated wood, the moisture transport is mainly diffusion controlled. Apparent moisture diffusion coefficients obtained

from sorption rates of coated wood samples are not suitable to predict the moisture content profiles. The values actually measured can be far more accurately predicted if the apparent diffusion coefficients of the wood itself are used and the influence of the coating is taken into account by a change in moisture content at the surface.

The apparent moisture diffusion coefficients derived from coated samples in *chapter 9* are useful to evaluate the influence of coating type, film thickness, temperature and wood species (spruce and meranti). They should, however, not be considered as representing the diffusion process inside the wood as was explained in *chapter 8*. If moisture diffusion coefficients are obtained from tests with the samples immersed in liquid water both true vapour diffusion and capillary flow are incorporated in the apparent moisture diffusion coefficients. In *chapter 9* it was demonstrated that apart from the permeability of the coating itself, the wood species, the temperature and the coating thickness have a marked influence on the moisture diffusion rates. The impact of coating thickness is, however, not large enough to easily compensate for differences in moisture permeability between coatings by the application of thicker coatings. With vapour diffusion, desorption proceeds faster than adsorption. With liquid water, the (capillary) uptake proceeds much faster than the release by vapour diffusion, in particular with spruce. The employed two parameter regression model developed by Rypstra [24], was found to be suitable to describe the rates of dimensional change, which were closely related to the apparent moisture diffusion coefficients.

The moisture sorption measurements described are mainly intended to understand the basic phenomena of moisture transport in coated wood. Practical situations are far more complex because boundary conditions are continuously changing. This will have a significant influence on the actual moisture content and its distributions as was demonstrated in studies by Derbyshire and Robson [25] and Bancken and Frencken [26].

10.4 Concluding remarks

Finally some general differences and similarities between waterborne and solventborne (including high solid alkyds) coatings will be addressed. With respect to capillary flow of a coating into wood, the nature of the carrier medium appeared to be a dominant factor. Dispersing or emulsifying the polymeric binder in an aqueous environment has a strong impact on its rheological behaviour. In combination with the surfactants applied, this has an adverse impact on the penetrating capacity of a coating into the wood. The reduced penetration, in combination with high hygroscopic stresses observed in some acrylic coatings, is mainly responsible for the reduced wet adhesion of waterborne coatings in comparison to the solventborne counterparts.

The moisture permeability of waterborne coatings is higher than for solventborne ones. This has already been demonstrated in various studies [27,28,29] but was confirmed again. On the other hand, moisture content levels that are a risk for wood decay (above 20 %) are reached only after very long periods of continuous exposure to moisture that will never be observed in practice. This means that if decay in wooden joinery occurs, this will be due to other factors than the coating permeability like e.g. rapid water entry through unprotected end grains. In this sense, waterborne coatings will not differ from solventborne ones.

It has also been shown that moisture sorption and swelling of the coating itself is often only slightly lower than for wood, sometimes the swelling is even far exceeded. This fact can bring new insights towards the stresses and coating failures during exterior exposures. The stored strain energy concept [16] from *chapter 6* might also be used to understand stress in exterior wood coatings in terms of differences in hygroscopic expansion between the coating and the wood. This concept might be used to understand the origin of coating failure during exterior exposure better.

References

[1]   **Nussbaum, R.M.**; Penetration of water-borne alkyd emulsions and solvent-borne alkyds into wood, Holz als Roh- und Werkstoff, 52, 1994, 389-393.

[2]   **Rødsrud, G.; Sutcliff, E.J.**; Alkyd emulsions-properties and application. Results from comparative investigations of penetration and ageing of alkyds, alkyd emulsions and acrylic dispersions, Surface Coatings International, 77 (1), 1994, 7-16.

[3]   **Nussbaum, R.M.; Sutcliffe, E.J.; Hellgren, A.C.**; Microautoradiographic studies of the penetration of alkyd, alkyd emulsion and linseed oil coatings into wood, Journal of Coatings Technology, 70 (878), 1998, 49-57.

[4]   **Loon, J. van**; The interactions between paint and surface, Journal of the Oil and Colour Chemists Association, 49 (10), 1966, 844-867.

[5]   **Kerr, A.J.; Goring, D.A.I.**; The role of hemicellulose in the delignification of wood, Canadian Journal of Chemistry, 53 (6), 1975, 952-959.

[6]   **Côté, W.A.; Robison, R.G.**; A comparative study of wood, Journal of Paint Technology, 40 (545), 1968, 427-432.

[7]   **Tarkow, H.; Feist, W.C.; Southerland, C.F.**; Interaction of wood with polymeric materials, penetration versus molecular size, Forest Products Journal, 16 (10), 1966, 61-65.

[8]   **Washburn, E.W.**; The dynamics of capillary flow, Physical Review, 17, 1921, 273-283.

[9]   **Reuvers, A.J.**; Control of rheology of water-borne paints using associative thickeners, accepted for Progress in Organic Coatings, 1999.

[10]   **Good, R.J.**; Contact angle, wetting and adhesion: a critical review, In: Contact angle, wettability and adhesion, Ed. K.L. Mittal, 1993, pp. 3-36.

[11]   **van Oss, C.J.; Chaudhury, M.K.; Good, R.J.**; Interfacial Lifshitz-van der Waals and polar interactions in macroscopic systems, Chemical Review, 88, 1988, 927-941.

[12]   **Shen, Q.; Nylund, J.; Rosenholm, J.B.**; Estimation of the surface energy and acid-base properties of wood by means of wetting method, Holzforschung, 52, 1998, 422-428.

[13]   **Jansen, M.L.**; Performance testing of exterior wood primers, Journal of the Oil and Colour Chemists Association, 69 (5), 1986, 117-128.

[14]   **Ahola, P.**; Adhesion between paints and wooden substrates: effects of pre-treatments and weathering of wood, Materials and Structures, 28, 1995, 350-356.

[15]   **Hse, C.Y.**; Gluability of southern pine earlywood and latewood, Forest Products Journal, 18 (12), 1968, 32-36.

[16]   **Perera, D.Y.**; On adhesion and stress in organic coatings, Progress in Organic Coatings, 28, 1996, 21-23.

[17]   **Gerin, P.A.; Grohens, Y.; Schirrer, R.; Holl, Y.**; Adhesion of latex films. Part IV. Dominating interfacial effect of the surfactant, Journal of Adhesion Science and Technology, 13 (2), 1999, 217-236.

[18]   **Bardage, S.L.; Bjurman, J.**; Adhesion of waterborne paints to wood, Journal of Coatings Technology, 70 (878), 1998, 39-47.

[19]   **Kabir, A.F.R.; Nicholas, D.D.; Vasishth, R.C.; Barnes, H.M.**; Laboratory methods to predict the weathering characteristics of wood, Holzforschung, 46 (5), 1992, 395-401.

[20]   **Smulski, S.; Côté, W.A.**; Penetration of wood by a water-borne alkyd resin, Wood Science and Technology, 18, 1984, 59-75.

[21]   **Bravery, A.F.; Miller, E.R.**; The role of pre-treatment in the finishing of exterior softwood, BWPA Annual Convention, 1980.

[22] **Feist, W.C.**; Weathering performance of painted wood pre-treated with water repellent preservatives, Forest Products Journal, 40 (7/8), 1990, 21-26.

[23] **Meijer, M. de; Creemers, J.; Cobben, W.; Ahola, P.**; Influence of a dipping preservative treatment on the performance of wood finished with waterborne coatings, The Int. Res. Group on Wood Preserv., Stockholm, Doc. No. IRG/WP 98-40121,1998.

[24] **Rypstra, T.**; Analytical techniques for evaluation of wood and wood finishes during weathering, PhD-thesis, University of Stellenbosch, 1995, pp. 243.

[25] **Derbyshire, H.; Robson, D. J.**; Moisture conditions in coated exterior wood. Part 4: Theoretical basis for observed behaviour. A computer modelling study. Holz als Roh- und Werkstoff, 57(2), 1999,105-113,.

[26] **Bancken, E.J.L.; Frencken, M.**; Modelling and measurement of moisture transport in coating-protected wood, PRA 7th Asia Pacific Conference, paper 19, 1997.

[27] **Ahola, P.; Derbyshire, H.; Hora, G.; Meijer, M. de**, Water protection of wooden joinery painted with low organic solvent content paints with known composition, Holz als Roh- und Werkstoff, 57,1999, 45-50.

[28] **Ahola, P.**; Moisture transport in wood coated with joinery paints, Holz als Roh- und Werkstoff, 49, 1991, 428-432.

[29] **Linden, J.A. van; Oort, P.**; Water permeability: comparison of methods and paint systems, XXII Fatipec Conference Budapest, IV, 1994,135-148.

ANNEX I   List of abbreviations

AB:	acid-base
Ac 1:	acrylic dispersion coating type 1
Ac 2:	acrylic emulsion coating type 2
Ac 3:	acrylic emulsion coating type 3
ACDIS:	acrylic dispersion
ACEMUL:	acrylic emulsion
ALKEMUL:	alkyd emulsion
D:	disperse
HSA:	high solid alkyd
L:	liquid
LW:	Lifshitz-van der Waals
Mn:	number averaged molecular weight
Mw:	weight averaged molecular weight
n:	number of observations
OPS:	Organo Psycho Syndrome
P:	pigmented
P:	polar
RH:	relative humidity
S:	solid
SB:	solventborne
SBA:	solventborne alkyd
SEM:	scanning electron microscopy
SOLVALK:	solventborne alkyd
TiO_2:	titanium dioxide
U:	unpigmented
UV:	ultraviolet
VOC:	Volatile Organic Compound
WAD100:	waterborne acrylic dispersion with a particle size of about 100 nm
WAD300:	waterborne acrylic dispersion with a particle size of about 300 nm
WB:	waterborne
WBA:	waterborne alkyd emulsion

ANNEX II Coating formulations

The formulations of the coatings used in chapter 2,3,6 and 7 is given below in weight percentage.

Pigmented paints:

	WAD 300	WAD100		WBA
water	2,50	2,50	water	12,18
preservative	0,10	0,10	dispersing agent	2,38
defoamer	0,30	0,30	pigment wetting agent	0,50
propylenglycol	2,50	2,50	stabiliser	0,99
pigment wetting agent	1,00	1,00	Ti-O$_2$ pigment	23,82
Ti-O$_2$ pigment	24,00	24,00	defoamer	0,10
water	1,00	1,00	WBA-binder	44,39
WAD 300-binder	58,60	-	dryer*	0,50
WAD 100-binder	-	62,73	water	14,06
coalescent	1,50	1,50	thickener	1,09
defoamer	0,10	0,10		
thickener	1,72	0,46		
water	6,68	3,81		

	HSA			SBA
HSA-binder	23,12		SBA-binder	39,46
Ti-O$_2$ pigment	40,90		Ti-O$_2$ pigment	25,51
HSA-binder	23,12		white spirit	9,91
dryer*	6,89		SBA-binder	5,97
solvent	5,34		dryer*	3,31
anti-skinning agent	0,62		anti-skinning agent	0,50
			white spirit	15,33

	Ac 1			Ac 2 / 3
water	0.34		wetting agent	5.71
preservative	2.00		cosolvent	0.90
defoamer	0.10		water	0.50
cosolvent	0.30		defoamer	0.50
pigment wetting agent	2.50		TiO2-pigment	22.72
Ti-O$_2$ pigment	24.00		preservative	0.10
water	1.00		Ac2 or Ac 3 binder	62.96
Ac 1 binder	64.00		cosolvent	1.00
coalescent	1.50		thickener type A	4.50
defoamer	0.10		water	1.10
thickener	4.16			

Binder solutions:

	WAD300	WAD100	WBA	HSA	SBA
WAD 300-binder	63,0	-	-	-	-
WAD 100-binder	-	67,0	-	-	-
WBA-binder	-	-	60,0	-	-
HSA-binder	-	-	-	82,0	-
SBA-binder	-	-	-	-	62,0
water	36,0	32,0	37,5	-	-
white spirit	-	-	-	14,0	35,0
coalescent	1,0	1,0	-	-	-
dryer*	-	-	2,5	4,0	3,0

*:   Mass percentage dryer (siccative) is expressed on the basis of total products, containing 5 to 15 % active ingredient.

CURRICULUM VITAE

Mari de Meijer werd op 20 april 1967 geboren te Rijswijk Z.H. Na het behalen van zijn VWO-diploma aan het Christelijk Lyceum Delft studeerde hij Bosbouw aan de Landbouwuniversiteit Wageningen. Deze studie ronde hij in 1992 af met als specialisatie Bosprodukten. Tijdens deze studie volgde hij afstudeervakken in de richtingen bosprodukten, proceskunde en bedrijfskunde en liep hij stage bij het laboratorium van een papierfabriek in de Verenigde Staten. In 1996 ronde hij met succes de postacademische opleiding Coatingtechnologie van Stichting Polymeer Technologie Nederland af.

Van 1992 tot 1993 was hij werkzaam als toegevoegd onderzoeker bij de Landbouwuniversiteit Wageningen, vakgroep Bosbouw, sectie Houtkunde. Vanaf 1994 is hij werkzaam bij SHR Houtresearch te Wageningen als onderzoeker op het gebied van coatings voor de toepassing op hout. Het in dit proefschrift beschreven onderzoek voerde hij in deze hoedanigheid uit. Sinds 1997 heeft hij de leiding van de Sectie Coatings van het gelijknamige instituut.

PUBLICATIONS

Meijer, M. de; Zwan, R. P., van der; Militz, H.;Unsteady-State Diffusion of Methanol in Douglas-fir Heartwood at High Temperatures, Holzforschung, 50 (2), 1996, 135-143.

Meijer, M. de; Thurich, K.; Militz, H.; Comparative Study on Penetration Chararacteristics of Modern Wood Coatings, Wood Science and Technology 32, 1998, 347-365.

Meijer, M. de; Militz, H.; Wet adhesion measurements of wood coatings, Holz als Roh- und Werkstoff, 56, 1998, 306.

Ahola, P.; Derbyshire, H.; Hora, G.; Meijer, M. de; Water protection of wooden window joinery painted with low organic solvent content paints with known composition. Part 1: Results of interlaboratory tests, Holz als Roh-und Werkstoff, 57, 1999, 45-50.

Beckers, E.P.J.; Meijer, M. de; Militz, H.; Stevens, M., Performance of Finishes on Wood that is Chemically Modified by Acetylation, Journal of Coatings Technology, 70 (878), 1998, 59-67.

Meijer, M. de; Militz, H.; Sorption behaviour and dimensional changes of wood-coating composites, Holzforschung, 53, 1999, 553-560.

Meijer, M. de; Militz, H.; Moisture transport in coated wood. Part 1: Analysis of sorption rates and moisture content profiles is Spruce during liquid water uptake, accepted for Holz als Roh- und Werkstoff.

Meijer, M. de; Militz, H., Moisture transport in coated wood. Part 2: Influence of coating type, film thickness, wood species, temperature and moisture gradient on kinetics of sorption and dimensional change, accepted for Holz als Roh und Werkstoff.

Meijer, M. de; Creemers, J.G.M.; Cobben, W.N.; Interrelationships between the Performance of low-VOC Wood Coatings and the Dimensional Changes of the Wooden Substrate, accepted for Surface Coatings International.

Meijer, M. de; Militz, H.; Quantitative measurements of capillary penetration in relation to wood and coating properties, accepted for Wood Science and Technology.

Rijckaert, V.; Stevens, M.; Acker, J. van; Meijer, de M.; Militz, H.; Quantitative assesment of the penetration of water-borne and solvent-borne wood coatings in Scots pine sapwood, accepted for Holz als Roh- und Werkstoff.